

The Pennsylvania State University
The Graduate School
Department of Crop and Soil Sciences

**COUPLING DISSOLVED ORGANIC CARBON AND HYDROPEDOLOGY IN
THE SHALE HILLS CRITICAL ZONE OBSERVATORY**

A Dissertation in

Soil Science

by

Danielle M. Andrews

© 2011 Danielle M. Andrews

Submitted in Partial Fulfillment
of the Requirements
for the Degree of

Doctor of Philosophy

May 2011

The dissertation of Danielle M. Andrews was reviewed and approved* by the following:

Henry Lin
Associate Professor of Hydropedology/ Soil Hydrology
Dissertation Advisor
Chair of Committee

Jason Kaye
Assistant Professor of Soil Biogeochemistry

Susan Brantley
Distinguished Professor of Geosciences

Kamini Singha
Assistant Professor of Geosciences

Michael Gooseff
Assistant Professor of Civil Engineering

David Sylvia
Professor of Soil Microbiology
Head of the Department of Crop and Soil Sciences

*Signatures are on file in the Graduate School

ABSTRACT

During the last three decades, significant progress has been made in understanding the dynamics of dissolved organic carbon (DOC) in both terrestrial and aquatic ecosystems. However, while considerable research has focused on the concentrations and fluxes of DOC, predictive models have had limited success because the factors that control the spatiotemporal trends of DOC under field conditions remain debatable. The overall objective of this dissertation was to use DOC to couple hydrogeology (integration of pedology and hydrology to better understand soil-water interactions at multiple scales) and biogeochemistry in an attempt to understand the factors that control DOC at different spatiotemporal scales at the Shale Hills Critical Zone Observatory (CZO).

Specifically, a field scale research project was initiated to: (1) investigate the impact of combined soil and landscape features on the spatial variability of soil organic carbon (SOC) storage and soil pore water DOC concentration, (2) evaluate the influence of precipitation, discharge, and temperature on stream water DOC concentration and export, (3) investigate how soil and landscape features combined influence C and nitrogen (N) concentrations along two contrasting hillslopes (swale versus planar hillslopes), (4) assess the importance of DOC and pH in controlling metal concentrations, and (5) examine soil redox potential (Eh) dynamics along two transects (hillslope and valley floor) using automated and continuous (10-minute interval) monitoring.

Results showed that in the two north-facing slopes investigated, average soil pore water DOC concentrations were noticeably higher along the swale (range: 5 – 25 mg/L)

as compared to the planar hillslope (range: 5 – 15 mg/L). Elevated soil pore water DOC at the soil-bedrock interface at the ridgetop and at the Bw-Bt horizon interface at the valley floor are consistent with transport-driven “hot spots” (solute concentrations are >20 % than in surrounding areas) of soil pore water DOC at these restrictive interfaces. Swales appeared to be hot spots for C storage and DOC export. Clay content was the single best predictor of SOC storage, explaining > 70 % of SOC storage variability within the catchment. Stream water DOC (range: 0.6 – 28.6 mg/L) was significantly correlated to stream discharge and water temperature, reflecting combined controls of flushing (linked to discharge) and biological activity (related to temperature). Transport-driven “hot moments” (short periods during which solute concentrations are significantly greater than that during the intervening time) of stream water DOC were observed during the periods of snowmelt and late summer/early fall wet-up, which contributed to ~55% of DOC exported.

Results for objective (3) showed that along both hillslopes, SOC (0.1 to 3.0 %) and TN (0.1 to 0.2 %) exponentially decreased with increasing soil depth, with a 60 % decrease across the A - B soil horizon interface. Soil pore water DOC also exponentially decreased with soil depth for both hillslopes, while nitrate (NO_3^- , range of 0.01 to 8.7 mg/L) did not show an obvious exponential decrease within the soil profile. Soil pore water DOC (but not NO_3^-) concentrations were significantly correlated to soil pore water pH, SOC, soil TN, C:N ratio. However, soil pore water concentrations of DOC and NO_3^- were consistently elevated at restrictive soil horizon interfaces. Elevated concentrations of stream water DOC and NO_3^- (range of 0.0 to 2.4 mg/L) during snowmelt and rainfall

events during the early fall period are consistent with flushing of shallow soil pore waters (high concentrations) to the stream during those times.

This study also found that soil pore water concentrations of DOC, and total Al (range of 0.01 – 0.72 mg/L), Fe (range of 0.01 – 3.86 mg/L), and Mn (range of 0.01 – 10.49 mg/L) generally decreased with increasing soil depth, while pH slightly increased with depth. This depth distribution was especially evident in the swale where soils are much thicker and thus an exponential decline with depth was observed. Regardless of landscape position and soil depth, the variability in soil pore water metal concentrations was best predicted by the combined effect of soil pore water DOC and pH ($R^2 = 0.76$). Stream water DOC and total metal concentrations (Al: range of 0.01 – 0.15 mg/L, Fe: range of 0.01 – 5.99 mg/L, and Mn: range of 0.01 – 3.79 mg/L) were synchronized in this catchment during the late summer/early fall wet up period such that elevated stream water concentrations of both DOC and metals (especially Fe and Mn) were observed. These results are consistent with DOC and metals being strongly correlated in this acidic forested ecosystem. Moreover, results are consistent with the inference that DOC will significantly facilitate metal transport in catchments impacted by acid deposition.

Furthermore, the 6- months monitoring of soil Eh showed a range of -240 to +750 mV from April to October 2010. A combination of landscape position, soil depth, and season explained 72% of soil Eh variability within the catchment. Soil Eh varied with topographic position where the ridgetop site was strongly oxidized (> 400 mV), while the valley floor was in general moderately to strongly reduced (< 200 mV). Differences in soil Eh at each landscape position reflected variability due to seasonal differences in soil moisture, soil temperature, and water table levels, which combined, explained 20 to 90 %

of soil Eh variation. This study demonstrated that spatiotemporal variation in soil Eh in upland forested ecosystems is best interpreted in conjunction with landscape position, soil depth, and seasonal differences in soil temperature, soil moisture, and water table level, rather than water table levels only as observed in wet/anaerobic environments.

The overall findings of this dissertation demonstrated that explicit consideration of both soil physiochemical properties and hydrological characteristics can elucidate the main factors that are consistently correlated to DOC spatiotemporal patterns. Results provided a better link between hillslope soil pore water DOC and stream water DOC. Preferential flow pathways along restrictive soil horizon interfaces are associated with elevated soil pore water concentrations which is likely the major contributor to the elevated stream water concentrations during snowmelt and the late summer/early fall wet-up period, as groundwater and rainfall concentrations are very low.

TABLE OF CONTENTS

LIST OF FIGURES	x
LIST OF TABLES	xvii
ACKNOWLEDGEMENTS	xix
Chapter 1 Coupling Hydropedology and Biogeochemistry in the Shale Hills	
Critical Zone Observatory – a dissolved organic carbon perspective	1
Introduction	1
References	7
Chapter 2 Dissolved Organic Carbon Export and Soil Carbon Storage in the Shale Hills Critical Zone Observatory	13
Abstract	13
Introduction	14
Materials and Methods	19
Site description	19
Study design and data collections	20
Laboratory analyses	22
Calculations of SOC storage, DOC export, and precipitation indices	23
Soil organic carbon (SOC) storage	23
Dissolved organic carbon (DOC) export	24
Precipitation indices	24
Statistical analyses	25
Results and Discussion	27
Catchment SOC storage and its influencing factors	27
DOC in soil pore water and stream water and their influencing factors	29
Soil pore water	29
Stream water	30
Hot spots and hot moments of DOC export and SOC storage	33
Summary and Conclusions	36
References	38
Chapter 3 Dissolved Organic Carbon and Nitrate Patterns along Two Contrasting Hillslopes in the Shale Hills Critical Zone Observatory	61
Abstract	61
Introduction	62

Materials and Methods.....	65
Site description and soils.....	65
Soil and water sampling.....	67
Laboratory analyses.....	69
Data analysis.....	70
Results and Discussion.....	70
Spatial and temporal variability of C and N.....	70
Spatial variability of DOC and NO ₃ ⁻ in soil waters along contrasting hillslopes.....	71
Temporal variability of DOC and NO ₃ ⁻ in soil, stream- and ground water.....	74
Influence of soil properties on DOC and NO ₃ ⁻	77
Summary and Conclusions.....	81
References.....	83
Chapter 4 Control of DOC and pH on Spatio-temporal Concentrations of Al, Fe, and Mn in Soil Pore Water and Stream Water in the Shale Hills Critical Zone Observatory.....	103
Abstract.....	103
Introduction.....	104
Materials and Methods.....	107
Site description.....	107
Study design and data collections.....	108
Laboratory analyses.....	110
Statistical analyses.....	110
Results and Discussion.....	112
Spatial patterns of Al, Fe, and Mn in soil pore water.....	112
Seasonal patterns of metals in soil pore water and stream water.....	114
Relationships of pH and DOC with metal concentrations in soil pore water and stream water.....	116
pH and metal interactions in soil pore water and stream water.....	117
DOC and metal interactions in soil pore water and stream water.....	118
Summary and Conclusions.....	120
References.....	122
Chapter 5 Spatiotemporal Patterns of Soil Redox Potential in relation to Soil Moisture, Temperature, and Water Table in the Shale Hills Critical Zone Observatory.....	138
Abstract.....	138
Introduction.....	139
Materials and Methods.....	143
Site description.....	143

Study design and data collection	144
Soil water sample collection and lab analyses	147
Soil Eh data corrections and analyses	148
Soil Eh data corrections	148
Statistical analyses	148
Results and Discussion.....	150
Variability between replicates	150
Spatial patterns of soil Eh	151
Soil profile pattern of soil Eh.....	151
Hillslope and catchment patterns of soil Eh	153
Temporal patterns of soil Eh	154
Factors controlling soil Eh.....	155
Soil Eh impacts on soil pore water chemistry	157
Summary and Conclusions.....	160
References	162
Chapter 6 Summary and Future Needs.....	191
References	196
Appendix A Soil Profile Properties	199
Appendix B Original organic matter (OM), and soil pore water and stream water dissolved organic carbon (DOC) data for the Shale Hills Critical Zone Observatory	201
Appendix C First Approximation of the Carbon Budget for Shale Hills	213
Appendix D Redox Probes.....	218

LIST OF FIGURES

Figure 1-1: Framework for dissertation research	11
Figure 1-2: Schematic diagram of hypothesized hillslope water and solute transport in the Shale Hills CZO (Modified from Lin et al., 2006). Three typical soil profiles are shown along the hillslope and dashed arrows indicate potential lateral flow pathways while block arrows represent solute concentration and transport.....	12
Figure 2-1: Map of the Shale Hills CZO in central Pennsylvania and the location of the hillslope transects monitored (Jin et al., 2010). Red dashed lines represent the swale and planar transects; green boxes represent the ridgetop, midslope, and valley floor positions (SPRT – planar hillslope ridgetop, SPMS – planar hillslope midslope, SPVF – planar hillslope valley floor position, SSRT – swale ridgetop, SSMS – swale midslope, and SSVF – swale valley floor)	46
Figure 2-2: Soil organic matter (SOM) concentration (% by weight) in relation to soil organic carbon (SOC) concentration (% by weight) for 61 soil samples from the Shale Hills	47
Figure 2-3: Interpolated maps of soil organic carbon (SOC) concentration (% by weight) in the A and B soil horizons, respectively, and SOC storage (g/cm^2) within $\leq 1.1\text{-m}$ solum based on 56 sampling sites shown on each map	48
Figure 2-4: Vertical distribution of soil organic carbon (SOC) concentration (% by weight) for the ridgetop, midslope, and valley floor in the north-facing swale (a) and planar hillslope (b). Inset in (a) shows the swale data for the same soil depth as the planar hillslope	49
Figure 2-5: Soil organic carbon (SOC) storage within $\leq 1.1\text{-m}$ solum as a function of landform unit (RT – ridgetop, planar hillslope, swale, VF – valley floor) and aspect (VF – valley floor, SF – south-facing slope, NF – north-facing slope) based on 56 sampling sites	50
Figure 2-6: Soil organic carbon (SOC) storage for the Shale Hills catchment within $\leq 1.1\text{-m}$ solum ($N = 56$) plotted as a function of (a) clay amount (within $\leq 1.1\text{-m}$ solum), (b) slope, (c) depth to bedrock, (d) topographic wetness index, and (e) elevation.....	51

- Figure 2-7: Soil pore water DOC concentration for the swale transect (y-axis) versus the planar hillslope transect (x-axis) at similar soil depths for all landscape positions investigated in this study from Aug. 2007 to Oct. 2009 (RT: ridgetop; MS: midslope; VF: valley floor) 52
- Figure 2-8: Depth function of (a) soil pore water DOC concentration (mean and standard deviation for the period from Aug. 2007 to Oct. 2009), with fitted dashed curves showing the exponential decline with depth, and (b) soil clay content (% by weight). Upper panel is for the swale transect and the lower panel for the planar hillslope transect 53
- Figure 2-9: Time series data from May 2008 to Oct. 2010 for daily stream water DOC concentration (red dots), precipitation (black bar), discharge (blue line), air temperature (gray line), and stream water temperature (green line) (n = 353 for daily stream water DOC, with no samples collected during the summers of 2008 and 2010 due to no flow conditions and during the winters due to frozen conditions). Gray bars represent summer no flow periods and brown bars represent winter periods. The pink dashed line is groundwater DOC concentration (averaging 1.4 ± 0.5 mg/L) for this time period 54
- Figure 2-10: Daily stream water DOC concentration plotted as a function of (a) stream discharge and (b) stream water temperature for the period from May 2008 to May 2010 (n = 353, with no samples collected during the summers of 2008 and 2010 due to no flow conditions and during the winters due to frozen conditions). Only 2009 has a complete dataset for the entire year. Fitting equation is for the entire dataset from May 2008 to May 2010 55
- Figure 2-11: Illustration showing transport-driven hot spots and hot moments (modified from Harms and Grimm, 2008): Transport-driven hot spots are zones with elevated (> 20% increase) concentrations and/or fluxes compared to surrounding areas. Transport-driven hot moments are short periods (< 20% of total time period considered) during which solute concentrations (and/or fluxes) are elevated compared to the rest of the time period 56
- Figure 3-1: Map of the Shale Hills Critical Zone Observatory. Red dashed lines represent the swale and planar transects, green boxes represent the ridgetop, midslope, and valley floor positions, blue and purple dots at the west end of catchment represents the stream and groundwater collection points, respectively 90
- Figure 3-2: Vertical soil profile distribution of dissolved organic carbon (DOC) concentrations in soil pore water for the planar (left panel) and swale (right panel) hillslopes at the ridgetop (A, D), midslope (B, E) and the valley floor (C, F) (n = 29 sampling dates from 2007 to 2009) 91

- Figure 3-3: Vertical soil profile distribution of nitrate (NO_3^-) concentrations in soil pore water for planar (left panel) and swale (right panel) hillslopes at the ridgetop (A, D), midslope (B, E) and the valley floor (C, F) ($n = 29$ sampling dates from 2007 to 2009) 92
- Figure 3-4: Comparison of dissolved organic carbon (DOC) (upper) and nitrate (NO_3^-) (lower) concentrations in soil pore water for planar (x-axis) and swale (y-axis) hillslopes for all landscape positions at similar depths..... 93
- Figure 3-5: Relationship between dissolved organic carbon (DOC) and nitrate (NO_3^-) concentrations for all soil pore water samples from 2007 to 2009 for the planar and swale hillslopes 94
- Figure 3-6: Average of weekly soil pore water dissolved organic carbon (DOC) concentrations for spring and fall for different depths at the ridgetop (A, D), midslope (B, E), and valley floor (C, F) sites for the planar (left panel) and swale (right panel) hillslopes from 2008 to 2009..... 95
- Figure 3-7: Average of weekly soil pore water nitrate (NO_3^-) concentrations for the spring and fall for different depths at the ridgetop (A, D), midslope (B, E), and valley floor (C, F) for the planar (left panel) and swale (right panel) hillslopes from 2008 to 2009..... 96
- Figure 3-8: Temporal trends of dissolved organic carbon (DOC) and nitrate (NO_3^-) concentrations in the headwater stream from 2008 to 2009. Dashed line represents the average groundwater DOC concentration during this period (1.4 ± 0.5 mg/L), and dotted line represents the average groundwater NO_3^- concentration during this period (0.02 ± 0.02 mg/L). Black bars represent rainfall. Brown and gray bars represent the dry summer and frozen winter periods respectively during which no samples were collected 97
- Figure 3-9: Vertical soil profile moisture content for (a) the planar and (b) swale hillslopes in different landscape positions (mean \pm SD, $n = 30$ sampling dates from 2007 to 2009) 98
- Figure 3-10: Vertical soil profile distribution of total carbon (TC), total nitrogen (TN), and C:N for the planar (upper panel) and swale (lower panel) hillslopes at different landscape positions in the Shale Hills Critical Zone Observatory 99
- Figure 3-11: Relationship between soil pore water dissolved organic carbon (DOC) concentration (concentrations for each lysimeter are averaged over time from April 2008 to November 2009) and (a) soil organic carbon (TC) ($p < 0.001$; $R^2 = 0.60$), (b) soil total nitrogen (TN) ($p < 0.001$; $R^2 = 0.59$), and (c) soil C:N ratio ($p < 0.05$; $R^2 = 0.47$)..... 100

- Figure 3-12: Relationship between soil pore water nitrate (NO_3^-) concentration (concentrations for each lysimeter are averaged over time from April 2008 to November 2009) and (a) soil organic carbon (TC) ($p > 0.05$; $R^2 = 0.05$) (b) soil total nitrogen (TN) ($p > 0.05$; $R^2 = 0.05$), and (c) soil C:N ratio ($p > 0.05$; $R^2 = 0.03$)..... 101
- Figure 4-1: Map of the Shale Hills CZO in central Pennsylvania and the location of the hillslope transects monitored (Jin et al., 2010). Red dashed lines represent the swale and planar transects; green boxes represent the ridgetop, midslope, and valley floor positions (SPRT – planar hillslope ridgetop, SPMS – planar hillslope midslope, SPVF – planar hillslope valley floor position, SSRT – swale ridgetop, SSMS – swale midslope, and SSVF – swale valley floor) 126
- Figure 4-2a: Depth profiles of soil pore water concentrations of total Al (a), Fe (b), and Mn (c) (mean and standard from Aug. 2007 to Oct. 2009, $n = \sim 20$ sample dates). Upper panel is for the planar hillslope transect and the lower panel for the swale transect..... 127
- Figure 4-2b: Depth profiles of soil pore water concentrations of DOC (left panel) and pH (right panel) (mean and standard deviation from Aug. 2007 to Oct. 2009, $n = \sim 20$ sample dates). Upper panel is for the planar hillslope transect and the lower panel for the swale transect..... 128
- Figure 4-3: Soil pore water concentrations of total Al, Fe, and Mn (mean and standard deviation from Aug. 2007 to Oct. 2009, $n = 294$ and 191 lysimeter samples for the swale and planar hillslopes respectively) as a function of landscape position. Different letters indicate significant difference between each landscape position for swale versus planar hillslope for total Al, Fe, and Mn concentrations. SSRT represents swale ridgetop, SSMS - swale midslope, SSVF - swale valley floor, SPRT - planar ridgetop, SPMS - planar midslope, and SPVF - planar valley floor..... 129
- Figure 4-4: Time series data from May 2008 to Oct. 2009 for daily stream water concentrations of DOC, total Al, total Fe, and total Mn, along with precipitation (black bar) and stream discharge ($n = 300$ for daily stream water DOC and total metal, with no samples collected during the summer of 2008 due to no flow condition and during the winters due to frozen condition). Gray bars represent summer or winter periods during which no samples were collected 130
- Figure 4-5a: Soil pore water total metal concentration (Al + Fe + Mn) as a function of soil pore water pH and DOC based on a total of 725 soil pore water samples (from all three landscape positions and all soil depths) collected during the time period of Aug. 2007 to Oct. 2009 131

- Figure 4-5b:** Soil pore water total metal concentration (Al + Fe + Mn) as a function of soil pore water pH and DOC for the three landscape positions: (a) ridgetop (RT), (b) midslope (MS), and (c) valley floor (VF) and for the three soil depths: (d) topsoil (< 30cm), (e) middle (30-50cm), and (f) bottom (>50cm). The data were combined for both the swale and planar hillslopes for the time period from Aug. 2007 to Oct. 2009 132
- Figure 4-6:** Average soil pore water total Al (a), Fe (b), Mn (c), and DOC (d) concentrations plotted as a function of average soil pore water pH. Average values (n = 33) were calculated for each soil depth at all six landscape positions for both the swale and planar hillslopes over the time period from Aug. 2007 to Oct. 2009..... 133
- Figure 4-7:** Average soil pore water total Al (a), Fe (b), and Mn (c) concentration plotted as a function of average soil pore water DOC. Average values (n = 33) were calculated for each soil depth at all six landscape positions for both the swale and planar hillslopes over the time period from Aug. 2007 to Oct. 2009 134
- Figure 5-1:** Map of the Shale Hills CZO in central Pennsylvania and the location of the monitoring sites along the hillslope and valley floor transects 167
- Figure 5-2:** Example of variability between the replicated redox probes (n = 3) at the A, B and C soil horizons (ridgetop (upper panel) and valley floor 2 (lower panel)) 168
- Figure 5-3:** Distribution of soil redox potential (Eh) values collected between Apr. and Oct. 2010 (no data for valley floor sites 3 and 4 from 5/7/10 to 6/24/10 and the shoulder slope from 6/17/10 to 6/25/10 and 9/20/10 to 10/12/10 due to equipment malfunction) for the seven monitoring sites(hillslope transect – left panel; valley floor transect – right panel). Valley floor site 2 is duplicated as it is located along both transects. 169
- Figure 5-4a:** Soil redox potential (Eh) for the A, B and C horizons at the seven monitoring sites (hillslope transect – left panel; valley floor transect – right panel) from Apr. to Oct. 2010 (no data for valley floor sites 3 and 4 from 5/7/10 to 6/24/10 and the shoulder slope from 6/17/10 to 6/25/10 and 9/20/10 to 10/12/10 due to equipment malfunction). Valley floor site 2 is duplicated as it is located along both transects. Different letters indicate significant difference between soil horizons Eh. Soil Eh values are grouped into oxidizing (>400 mV), weakly reducing (+200 to +400 mV), moderately reducing (-100 to +200 mV), or strongly reducing (<-100 mV)..... 170
- Figure 5-4b:** Soil temperature for the A, B and C horizons of the seven monitoring sites (hillslope transect – left panel; valley floor transect – right panel) from Apr. to Oct. 2010. Valley floor site 2 is duplicated as it is located

- along both transects. (*Data for Valley Floor 4 are from Jul. 2010 to Oct. 2010 and no data for Valley Floor 3*)..... 171
- Figure 5-4c:** Soil moisture content for the A, B and C horizons of the seven monitoring sites (hillslope transect – left panel; valley floor transect – right panel) from Apr. to Oct. 2010. Valley floor site 2 is duplicated as it is located along both transects. (*Data for Valley Floor 4 are from Jul. 2010 to Oct. 2010; no data for Valley Floor 3*) 172
- Figure 5-5:** Time series of soil redox potential (Eh) measurements, along with soil temperature, volumetric soil moisture content and water table height from Apr. to Oct. 2010 in the seven monitoring sites. Blue line represents A horizon, pink line represents B horizon, green line represents C horizon, and black bars represent rainfall. Gray bars represent the period when Eh data were not collected due to equipment malfunction. *Note: no soil temperature and moisture content data for the valley floor 3, and data for the valley floor 4 were from Jul. 2010 to Oct. 2010* 173
- Figure 5-6:** Frequency (% of time) of oxidation and reduction at different landscape positions for the A, B, and C horizons during spring, summer, and fall (April to October 2010). Soil redox (Eh) condition is grouped into oxidizing (>400 mV), weakly reducing (+200 to +400 mV), moderately reducing (-100 to +200 mV), or strongly reducing (<-100 mV)..... 176
- Figure 5-7:** Response of soil redox potential (Eh) to rainfall events at the seven monitoring sites (hillslope transect – left panel; valley floor transect – right panel) from Apr. to Oct. 2010. Brown arrows indicate obvious drop in soil Eh due to rainfall events, black dashed arrows indicate a drop in soil Eh as water table level rises regardless of the size of the rainfall event, gray dotted line indicates division into the different seasons (spring, summer, fall), and the gray bar represents the period when Eh data were not collected due to equipment malfunction. 178
- Figure 5-8a:** Average daily soil redox potential (Eh) plotted as a function of soil temperature for the soil horizons of A (left panel), B (middle panel), and C (right panel) during the spring, summer, and fall periods (Apr. to Oct. 2010). No data for Valley Floor 3 and no spring data for Valley Floor 4..... 179
- Figure 5-8b:** Average daily soil redox potential (Eh) plotted as a function of soil moisture for the soil horizons of A (left panel), B (middle panel), and C (right panel) during the spring, summer and fall periods (Apr. to Oct. 2010). No data for Valley Floor 3 and no spring data for Valley Floor 4..... 181
- Figure 5-9:** An example of soil redox potential (Eh) as a function of soil moisture content for the A (left panel) and B (right panel) soil horizons during a storm event (35 mm) that occurred on June 8th 2010 (7am to 10pm). Black arrows

indicate when the rainfall event started (A) and ended (B). Solid green line represents general soil Eh pattern and brown arrow depicts soil moisture content at which soil Eh drops. No data for Valley Floor 3 and 4 183

Figure 5-10: Depth function of soil redox potential (Eh) (mean and standard deviation for the period from Apr. to Oct. 2010) and soil pore water dissolved organic carbon (DOC), nitrate (NO_3^-), total iron (Fe) and total manganese (Mn) concentrations (mean and standard deviation for the period from Aug. 2007 to Oct. 2009) at valley floor sites 3 and 4 185

Figure 6-1: Conceptual diagram of overall dissertation findings. Solute transport along the swale is shown. Solute transport along the planar hillslope was similar to the swale except that concentrations were lower. Dashed arrows indicate potential lateral flow pathways while block arrows represent solute concentration and transport 198

LIST OF TABLES

Table 2-1: Dissolved organic carbon (DOC) concentrations and fluxes in precipitation, throughfall, soil pore water, and stream water for various temperate forested catchments in Northeastern USA and Canada.	57
Table 2-2: Analysis of variance of soil organic carbon (SOC) storage for the top ≤ 1.1 m solum, showing the effects of soil horizon (A and B horizons), landform unit (ridgetop, valley floor, swale, planar hillslope), aspect (south- and north-facing slopes), and their interactions. The <i>F</i> value is the test statistic used to determine whether the sample means are within the sampling variability of each other, and <i>p</i> value is the statistical significance level.	59
Table 2-3: Analysis of variance of soil pore water dissolved organic carbon (DOC) concentrations, showing the effects of landscape position, soil depth, season, and their interactions. The <i>F</i> value is the test statistic used to determine whether the sample means are within the sampling variability of each other, and <i>p</i> value is the statistical significance level.	60
Table 3-1: General soil properties for the swale and planar hillslopes in the Shale Hills Critical Zone Observatory	102
Table 4-1: Analysis of variance of soil pore water concentrations of total metal (Al + Fe + Mn), showing the effects of landscape position, soil depth, season, and their interactions. The <i>F</i> value is the test statistic used to determine whether the sample means are within the sampling variability of each other, and <i>p</i> value is the statistical significance level.....	135
Table 4-2: Average \pm standard deviation and range (in parenthesis) of DOC:metal ratios for the soil pore water of the swale and planar hillslopes investigated at the Shale Hills Critical Zone Observatory from 2007 to 2009	136
Table 5-1: Redox potential (Eh) range in soils showing microbial metabolism process and electron acceptor (after DeLaune and Reddy, 2005).....	186
Table 5-2: Basic soil characteristics for the seven sites monitored at the Shale Hills CZO.....	187
Table 5-3: Depth of sensor installation for the seven monitoring sites at the Shale Hills CZO.....	188
Table 5-4: Analysis of variance of soil redox potential (Eh) showing the effects of soil horizon (A, B, and C horizons), landscape position (ridgetop, shoulder slope, midslope, valley floor), season, and their interactions. The <i>F</i> value is	

the test statistic used to determine whether the sample means are within the sampling variability of each other, and p value is the statistical significance level..... 189

Table 5-5: Multiple regression table showing influence of soil moisture, temperature, and water table height on soil redox potential (Eh) for the A, B and C horizons at the seven monitoring sites. The R^2 value is the proportion of variability in a data set that is accounted for by the statistical model, and p value is the statistical significance level.... 190

ACKNOWLEDGEMENTS

I would like to thank my advisor, Dr. Henry Lin, for his guidance as well as the opportunities he provided me with during my Ph.D. journey. His perspective kept me continuously motivated during this process. I would also like to thank the rest of my committee: Dr. Susan Brantley, Dr. Kamini Singha, Dr. Jason Kaye, and Dr. Michael Gooseff, for all their helpful suggestions and encouragement throughout this process. Their knowledge sometimes intimidated me but their collegiality always reassured me. I would also like to thank Dr. Lin's Hydropedology lab group, Dr. Brantley's lab group (especially Dr. Lixin Jin), Dr. Boyer's lab group, and Dr. Ephraim Govere for insightful conversations and assistance with field and lab work. Many thanks to my family and friends for without their patience, love, support, and encouragement, this would have been difficult to complete. I would also like to express gratitude for fellowships received from Penn State's Graduate School (Robert W. Graham Endowed Fellowship) and Penn State's College of Agricultural Sciences (Alex and Jesse Black Graduate Fellowship). This research was funded in part by the National Science Foundation under Grants No. EAR-0725019 and No. CHE-0431328, the United States Department of Agriculture National Research Initiative (grant # 2002-35102-12547) and the United States Department of Agriculture Higher Education Challenge Program (grant # 2006-38411-17202).

Chapter 1

Coupling Hydrogeology and Biogeochemistry in the Shale Hills Critical Zone Observatory – a dissolved organic carbon perspective

Introduction

Advanced understanding of the integration of the carbon (C), nitrogen (N), and water cycles is one of the eight grand challenges to environmental science (Lohse et al., 2008). Furthermore, catchments provide a natural spatial field within which the coupling of these cycles can be studied, as catchments link the atmosphere, soils, groundwater and streams (Lohse et al., 2008). In particular, C has long been of interest because it gives an indication of ecosystem health, links energy and nutrient budgets, and facilitates transport of both soluble and insoluble constituents, all of which are of fundamental interest in watershed biogeochemistry.

This dissertation research represents the first record of C for the Shale Hills Critical Zone Observatory (CZO), in central Pennsylvania. The Shale Hills CZO is one of six CZOs funded by the National Science Foundation to study chemical, physical, and biological interactions in the critical zone. The critical zone is the area between the top of the vegetation and the lower boundary of groundwater. One of the four questions driving research at the Shale Hills CZO is “What processes and factors control carbon over different spatial and temporal scales?”

To tackle this question, my overall objective was to use dissolved organic carbon (DOC) to couple hydrogeology (integration of pedology and hydrology to better understand soil-water interactions at multiple scales) and biogeochemistry in an attempt to understand the factors that control DOC at different spatial and temporal scales in the Shale Hills CZO (Figure 1-1). Dissolved organic carbon was chosen to conduct this research for several reasons including:

- Provides a direct link between land and water ecosystems via the hydrologic cycle and therefore has the ability to link the water and C cycles (e.g. Neill et al., 2006; Lohse et al., 2008)
- Much remains to be understood about the factors that control the spatiotemporal patterns of DOC (e.g. Kalbitz and Kaiser, 2008; Lohse et al., 2008; Turgeon and Courchesne, 2008)
- Plays an important role in the acid-base chemistry of acid sensitive systems and affects complexation, solubility, and metal mobility (e.g. Hornberger et al., 1994; Inamdar and Mitchell, 2008; Futter and de Wit, 2008)
- Growing concerns about climate change has evoked interest in the role of DOC in the global C balance (Kalbitz and Kaiser, 2008)

To achieve my objective, I embarked upon a field scale research project and worked within a variety of spatial and temporal scales. This dissertation includes four field research projects that are described in Chapters 2-5.

The objectives of Chapter 2 were to: (1) investigate the impact of combined soil and landscape features on the spatial variability of soil organic C (SOC) storage and soil pore water DOC concentration in the Shale Hills CZO and (2) evaluate the influence of

precipitation, discharge, and temperature on stream water DOC concentration and export. Specifically, the factors influencing DOC export and SOC storage along different soil-landform units (especially swales versus planar hillslopes) were evaluated. The primary hypotheses were that SOC storage will be significantly different along swales versus planar hillslopes because of differences in soil thickness, soil moisture, vegetation, and slope, and the export of DOC in the stream water of the CZO is strongly correlated to climate variables (mainly rainfall, discharge, and temperature).

The objective of Chapter 3 was to characterize the spatial and temporal patterns of C (in particular DOC) and N (in particular nitrate (NO_3^-)) in the Shale Hills CZO. Our objective was to investigate how soil and landscape features combined influence C and N concentrations along two contrasting hillslopes (swale versus planar hillslopes). Different landscape positions (ridgetop, midslope, and valley floor) along both hillslopes, together with various soil properties (depth, texture, SOC, total N, C:N ratio, pH, and moisture content), were analyzed to examine how they influence DOC and NO_3^- concentrations in soil pore water. The underlying hypothesis was that the non-convergent planar hillslope should have different soil properties (soil type, texture, moisture, pH) and flow dynamics (particularly flow pathways) as compared to the convergent swale hillslope, thus resulting in differences in C and N concentrations in both the soil matrix and the soil pore water.

Chapter 4 presents DOC and total metal (Al, Fe, and Mn) concentrations in soil pore water and stream water in the Shale Hills CZO. The main objectives were to 1) evaluate the spatial patterns of total Al, Fe and Mn in soil pore water along two hillslopes of contrasting soils and topography, 2) investigate the temporal patterns of metals in soil pore water and stream water, and 3) quantify the impact of DOC and pH on metal

concentrations. The hypotheses driving this research were that spatiotemporal patterns of DOC and metals are strongly linked in this acidic forested ecosystem and that DOC is a major facilitator of metal transport. To our knowledge, few studies have conducted such extensive investigations into DOC and metal interactions at various soil depths at different landscape positions along different hillslope types within a catchment.

Chapter 5 was initiated to investigate the spatial and temporal patterns of soil Eh in relation to soil moisture, temperature, and water table levels along topographic gradients at the forested Shale Hills CZO. We examined soil Eh dynamics along two transects – one was along a hillslope from ridgetop to valley floor and the other along the valley floor down an elevational gradient from upstream to downstream. We used automated and continuous (10-minute interval) monitoring at a total of seven sites, with three depths at each site. In addition, we also assessed the influence of soil Eh on soil pore water chemistry with a focus on DOC, NO_3^- , Fe and Mn. Our hypothesis was that distinct soil Eh patterns exist at different topographic positions and soil depths and that soil Eh has a significant influence on soil pore water chemistry.

The final chapter elucidates the overall conclusions of this research. Synopses of each of the chapters are presented as well as future research directions.

These objectives were based on the premise that water and solute dynamics will be strongly influenced by topography, soils, and hydrology. The impact of these factors has been conceptualized for a hillslope (Figure 1-2). Compared to upslope areas, valley floor areas are highly dynamic (both hydrologically and biogeochemically) and are of great significance when it comes to controls on streamwater chemistry (Bencala, 1993; Hill, 1996; Cirimo and McDonnell, 1997; Ohrui and Mitchell, 1998). Valley floor areas

are characterized by abrupt changes in hydrologic flowpaths (Lin, 2006) and biogeochemical conditions (Burt and Pinay, 2005). Because of their streamside location, these areas have the potential to regulate the chemistry of subsurface flows moving from uplands to streams (Findlay, 1995; Brunke and Gonser, 1997; Hill, 2000; Yeakley et al., 2003; Fisher et al., 2004).

Soils also play an important role in coupling hydrologic pathways and nutrient concentrations. However, one major gap in understanding the C cycle is that the vertical distribution of organic C in the soil remains poorly understood (Jobbágy and Jackson, 2000). Soil properties (such as texture, depth and amount of organic matter) have a major influence on how, when and where this movement of water occurs. Soil texture, in particular, clay content plays an important role in stabilizing soil organic matter. Fine-textured soils are known to have higher organic C and N than coarse-textured soils.

Subsurface preferential flow pathways such as water-restricting layers and soil horizon interfaces can also impact the transport of water and nutrients through soil from upslope to the stream. Preferential flows may cause increases in the export of nutrients since the length of time water remains in the soil via these preferential pathways may be too short for interaction with the soil matrix, plants or microbes (Feyen et al., 1999). Subsurface flow processes not only control the quantity of runoff from upland but also the flushing of soluble nutrients into surface waters (e.g. Creed et al., 1996). Therefore, the ability to identify hydrologic flow pathways is an essential step in understanding solute dynamics at the hillslope scale as well as the watershed level.

Furthermore, soil moisture can strongly influence the hydrologic flow paths that contribute water to the stream and, thus, stream water chemistry (Turgeon and

Courchesne, 2008). Similar to water movement, the distribution of nutrients, the chemical speciation of elements and their availability for leaching during a precipitation event can be strongly conditioned by soil moisture conditions (Turgeon and Courchesne, 2008), since during periods of high soil moisture, hillslopes can be highly transmissive with respect to water and solutes.

In addition, rainfall events influence nutrient dynamics, as they may cause large temporal variations in solute concentrations at very short time scales. Rainfall intensity and duration have been shown to have a flushing effect on water and nutrient movement. Dissolved organic carbon concentrations have also been shown to increase during periods of high discharge in association with precipitation events or snowmelt (e.g. Ágren et al., 2007; Turgeon and Courchesne, 2008). Such observations clearly establish the role of rainfall events in mobilizing nutrients.

Finally, water table fluctuations can lead to changes in the biogeochemical environment; particularly through changes in redox conditions which have been associated with the mobilization of nutrients and metals (Inamdar et al., 2004; Harms and Grimm, 2008). Valley floor areas have been associated with high water tables (Ohri and Mitchell, 1998) and low redox values as compared to upslope areas, where saturation may only rarely occur and which are typically oxidized. For example, in valley floor areas, when the water table rises, redox potential may decrease and if DOC is available as a source of energy, microorganisms can remove NO_3^- (Hefting et al., 2004; Schilling et al., 2004), and thus, decrease the amount of NO_3^- transported into the stream system.

A novel part of this work is the combination of evaluating biogeochemical solutes of DOC, NO_3^- , and metals (Al, Fe and Mn) at different landscape positions at varying soil

depths along two hillslopes of contrasting soils, hydrology, and topography in an upland forested catchment. Few studies have done such extensive investigations. We used these data to develop a conceptual diagram illustrating hydrogeological controls on solutes at the hillslope and stream scale.

References

- Ágren, A., I. Buffam, M. Jansson, and H. Laudon. 2007. Importance of seasonality and small streams for the landscape regulation of dissolved organic carbon export. *Journal of Geophysical Research* 112, G03003, doi:10.1029/2006JG000381.
- Asano, Y., J. E. Compton, and M. R. Church. 2006. Hydrologic flowpaths influence inorganic and organic nutrient leaching in a forest soil. *Biogeochemistry*. 81: 191-204.
- Bencala, K. E. 1993. A perspective on stream-catchment connections. *Journal of North American Benthological Society* 12: 44-47.
- Brunke, M. and T. Gonser. 1997. The ecological significance of exchange processes between rivers and groundwater. *Freshwater Biology* 37: 1-33.
- Burt, T. P. and G. Pinay. 2005. Linking hydrology and biogeochemistry in complex landscapes. *Progress in Physical Geography* 29: 297-316.
- Cirno, C. P. and J. J. McDonnell. 1997. Linking the hydrologic and biogeochemical controls of nitrogen transport in near-stream zones of temperate-forested catchments: a review. *Journal of Hydrology* 199: 88-120.
- Creed, I. F., L. E. Band, N. W. Foster, I. K. Morrison, J. A. Nicholson, R. S. Semkin, and D. S. Jeffries. 1996. Regulation of nitrate-N release from temperate forests: a test

- of the N flushing hypothesis. *Water Resources Research* 32: 3337-3354.
- Feyen, H., H. Wunderli, H. Wydler, and A. Papritz. 1999. A tracer experiment to study flow paths of water in a forest soil. *Journal of Hydrology* 225: 155-167.
- Findlay, S. 1995. Importance of surface-subsurface exchange in stream ecosystems. The hyporheic zone. *Limnology and Oceanography* 40: 159-164.
- Futter, M. N. and H. A. de Wit. 2008. Testing seasonal and long-term controls on streamwater DOC using empirical and process-based models. *Science of the Total Environment* 407: 698-707.
- Harms, T. K. and N. B. Grimm. 2008. Hot spots and hot moments of carbon and nitrogen dynamics in a semiarid riparian zone. *J. Geophys. Res.* 113, G01020, doi10.1029/2007JG000588.
- Hefting, M., J. C. Clément, D. Dowrick, A. C. Cosandey, S. Bernal, C. Cimpian, A. Tatur, T. P. Burt, and G. Pinay. 2004. Water table elevations controls on soil nitrogen cycling in riparian wetlands along a European climatic gradient. *Biogeochemistry*. 67: 113-134.
- Hill, A. R. 2000. Stream chemistry and riparian zones. In Jeremy B. Jones and Patrick J. Mulholland (eds.) *Streams and Ground Waters*. Academic Press, Boston. pp 83-110.
- Hornberger, G. M., K. E. Bencala and D. M. McKnight. 1994. Hydrological controls on dissolved organic carbon during snowmelt in the Snake River near Montezuma, Colorado. *Biogeochemistry* 25: 147-165.
- Inamdar, S. P., S. F. Christopher, and M. J. Mitchell. 2004. Export mechanisms for dissolved organic carbon and nitrate during summer storm events in a glaciated

- forested catchment in New York, USA. *Hydrological Processes* 18: 2651-2661.
- Inamdar, S., J. Rupp, and M. Mitchell. 2008. Differences in dissolved organic carbon and nitrogen responses to storm-event and ground-water conditions in a forested, glaciated watershed in western New York. *Journal of American Water Resources Association* 44 (6): 1458-1473.
- Jobbágy, E. G. and R. B. Jackson. 2000. The vertical distribution of soil organic carbon and its relation to climate and vegetation. *Ecological Applications* 10 (2): 423-436.
- Kalbitz, K. and K. Kaiser. 2008. Contribution of dissolved organic matter to carbon storage in forest mineral soils. *Journal of Plant Nutrition and Soil Science* 171: 52-60.
- Lin, H. 2006. Temporal stability of soil moisture spatial pattern and subsurface preferential flow pathways in the Shale Hills Catchment. *Vadose Zone Journal* 5: 317-340.
- Lohse, K. A., P. D. Brooks, J. C. McIntosh, T. Meixner, and T. E. Huxman. 2008. Interactions between biogeochemistry and hydrologic systems. *The Annual Review of Environment and Resources* 14:13, doi: 10.1146/annurev.enviro.33.031207.111141.
- Neill, C., H. Elsenbeer, A. V. Krusche, J. Lehmann, D. Markewitz, and R. de O. Figueiredo. 2006. Hydrological and biogeochemical processes in a changing Amazon: results from small watershed studies and the large-scale biosphere-atmosphere experiment. *Hydrological processes* 20: 2467-2476.
- Ocampo, C. J., C. E. Oldham, M. Sivaplan, and J. V. Turner. 2006. Hydrological versus

biogeochemical controls on catchment nitrate export: a test of the flushing mechanism. *Hydrological Processes* 20: 4269-4286.

Ohroi, K. and M. J. Mitchell. 1998. Stream water chemistry in Japanese forested watersheds and its variability on a small regional scale. *Water Resources Research* 34 (6): 1553-1561.

Schilling, K. E., Y. K. Zhang, and P. Drobney. 2004. Water table fluctuations near an incised stream, Walnut Creek, Iowa. *Journal of Hydrology* 286: 236-248.

Turgeon, J. M. L. and F. Courchesne. 2008. Hydrochemical behaviour of dissolved nitrogen and carbon in a headwater stream of the Canadian Shield: relevance of antecedent soil moisture condition. *Hydrological processes* 22: 327-339.

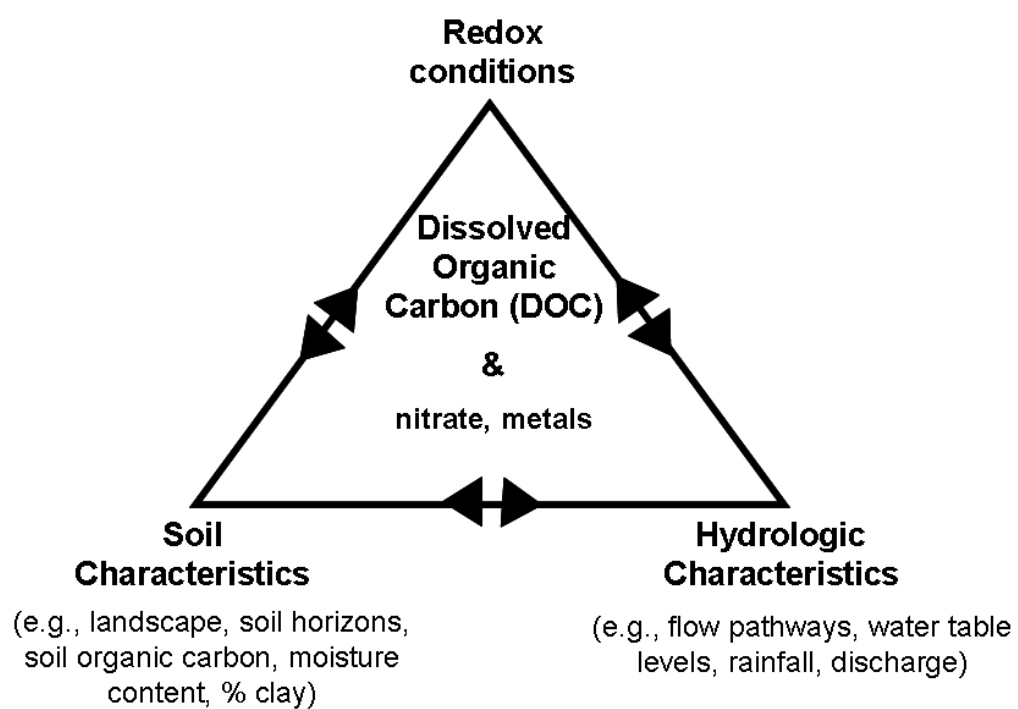


Figure 1-1: Framework for dissertation research.

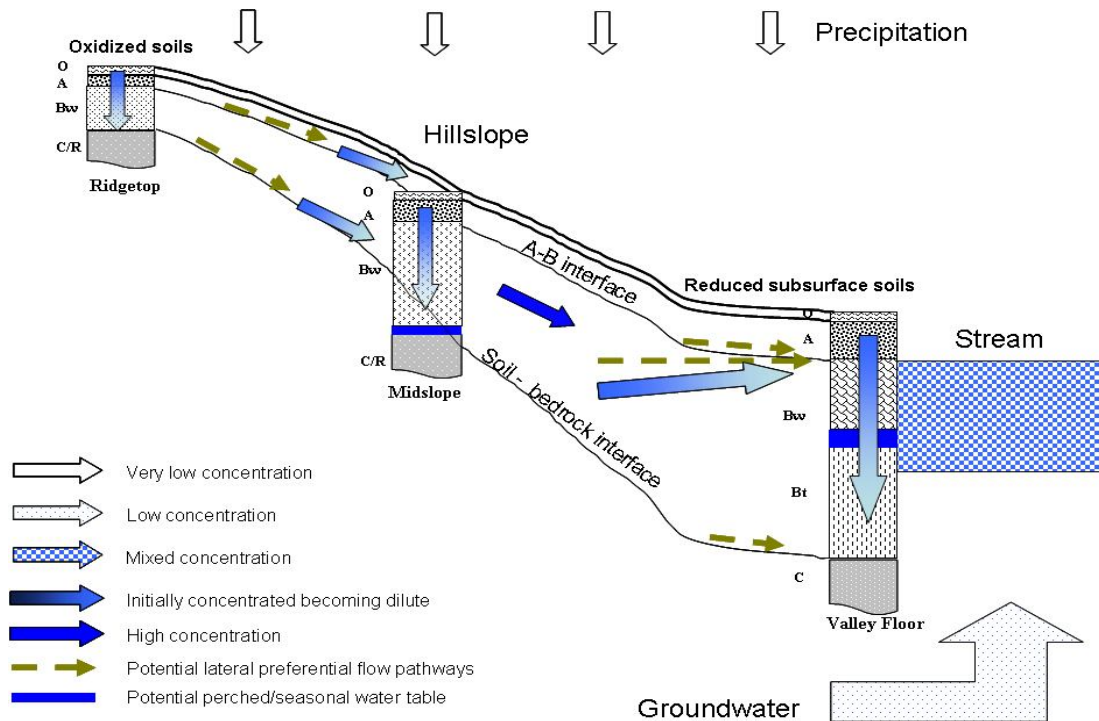


Figure 1-2: Schematic diagram of hypothesized hillslope water and solute transport in the Shale Hills CZO (Modified from Lin et al., 2006). Three typical soil profiles are shown along the hillslope and dashed arrows indicate potential lateral flow pathways while block arrows represent solute concentration and transport.

Chapter 2

Dissolved Organic Carbon Export and Soil Carbon Storage in the Shale Hills Critical Zone Observatory

Abstract

Changes in climate can impact soil carbon (C) storage, dissolved organic carbon (DOC) export from watersheds, and the overall global terrestrial C cycle. However, predictions of these impacts are uncertain because factors that control DOC export from watersheds and its relation to soil C storage remain elusive. This study examined the trends of DOC in soil water along two hillslopes of contrasting soils and topography in the Shale Hills Critical Zone Observatory (CZO). We also investigated the linkage between DOC export and soil organic C (SOC) storage as well as the impacts of rainfall, stream discharge, and stream temperature on DOC export. In the two north-facing slopes investigated in this study, average soil pore water DOC concentrations were noticeably higher along the swale as compared to the planar hillslope. Soil pore water DOC was also elevated at the soil-bedrock interface at the ridgetop and at the Bw-Bt horizon interface at the valley floor. This suggested transport-driven “hot spots” of soil pore water DOC at these restrictive interfaces. Based on SOC distribution in the entire catchment, south-facing swales of the catchment appeared to be hot spots for C storage and potentially DOC export. The SOC storage in the top 1.1-m solum was positively correlated with the amount of clay in the profile, depth to bedrock, and topographic wetness index, but

negatively correlated with slope. The stream water DOC at the catchment outlet averaged 6.2 ± 5.3 mg/L from May 2008 to October 2010, and was significantly related to stream discharge and stream water temperature in nonlinear manners, reflecting combined controls by flushing (linked to discharge) and biological activity (related to temperature). Precipitation indices showed no significant correlation to stream water DOC. In the wet year of 2009, stream water DOC export was estimated as 56 kg C/ha, while during the dry years of 2008 and 2010, DOC export was over 40% lower. Transport-driven “hot moments” of stream water DOC were observed during the periods of snowmelt and late summer to early fall wet-up, which, when combined, contributed to ~55% of DOC exported in 2009. This study showed the impacts of complex soil and topography interactions – coupled with changing weather and seasonal biological activity – on DOC export and SOC storage in the Shale Hills CZO.

Introduction

Growing concerns about future climatic conditions have evoked interest in the role of dissolved organic matter (DOM) in the global carbon (C) cycle (Kalbitz and Kaiser, 2008). Previously, the role of DOM in the global C cycle was thought to be negligible as these numbers were based on stream fluxes which are small as compared to primary productivity and heterotrophic respiration in terrestrial ecosystems (Kalbitz and Kaiser, 2008). However, more recent research has shown that soil DOM fluxes are several-fold larger than stream fluxes and DOM may be essential to C sequestration (Neff and Asner, 2001; Kalbitz and Kaiser, 2008).

Dissolved organic matter is usually measured as dissolved organic C (DOC), which comprises about 40 to 60% of its mass depending on soil type and soil horizon (Howard and Howard, 1990; Nelson and Sommers, 1996; Buckingham et al., 2008). Dissolved organic C fulfills a range of functions in forest ecosystems as it plays an important role in acid-base chemistry in acid sensitive ecosystems, impacts nutrient cycling, and affects the complexation, solubility, and mobility of metals (Qualls and Haines, 1991; Hornberger et al., 1994; Inamdar and Mitchell, 2008; Futter and de Wit, 2008).

While significant progress has been made in the last 30 years in understanding the dynamics of DOC in both terrestrial and aquatic ecosystems, much remains to be understood regarding the controls on DOC export from catchments (Meyer and Tate, 1983; Dalva and Moore, 1991; Mulholland and Hill, 1997; Neff and Asner, 2001; McHale et al., 2002; Wagner et al., 2008; Inamdar and Mitchell, 2008; Turgeon and Courchesne, 2008). Several research questions that would prove fruitful are: What are the main controls on DOC concentration in soils and streams? How would changes in the environment (especially precipitation, temperature, water flux) influence DOC production and flux in soils and streams? What is the impact of landscape features on the sources and pathways of DOC?

Stream water DOC flux has been reported to range from <10 to >200 kg/ha/yr for rivers within North America (Dalva and Moore, 1991) and is believed to be controlled by both biochemical and hydrological mechanisms (Dalva and Moore, 1991; Mulholland, 1997; Turgeon and Courchesne, 2008). Biochemical mechanisms refer to the sorption and immobilization of DOC as well as microbial mineralization, while hydrological

mechanisms include different types of hydrologic flowpaths in soils between and during storms (e.g., fast, shallow surface or subsurface flow versus slow, deep flow) (Turgeon and Courchesne, 2008).

McDowell and Wood (1984) showed that soil processes such as podzolization control the transport of DOC to surface water, while many studies have documented an elevated export of DOC from temperate watersheds during rainfall events (Hornberger et al., 1994; Boyer et al., 1997; Inamdar et al., 2004). Increased concentrations during these events have been attributed to DOC released during throughfall, enhanced litter leaching during events, enhanced flushing of organic-rich soil horizons by near-surface runoff, and release of instream and hyporheic sources of solutes with elevated streamflow (Hornberger et al., 1994; Mulholland, 1997; Boyer et al., 1997; Inamdar et al., 2004).

While a strong seasonality in DOC export has been observed, there can be a decoupling between runoff and DOC export such that lower DOC export is generally observed in winter and spring and higher export during late summer and fall (Tetzlaff and Laudon, 2010). During late summer, higher temperatures and aerobic conditions can promote high decomposition rates of litter and as the catchment begins to wet-up in early fall, accumulated organic matter can be flushed easily, leading to increased DOC export during late summer and fall (Tetzlaff and Laudon, 2010).

According to Keller et al. (2008), the role of climatic factors in determining DOC concentration and export is still not well understood. Changes in temperature and precipitation can directly impact DOC export by altering DOC production through organic matter decomposition and mineralization, both of which are sensitive to variations in moisture and temperature (Dalva and Moore, 1991).

In addition to the uncertainty of factors controlling DOC concentration and export in soils and streams, C storage estimates in terrestrial ecosystems also remain uncertain (de Wit et al., 2006). Terrestrial ecosystems are known to be major sinks for atmospheric C, storing more C in soils than in plants and atmosphere combined (Jobbágy and Jackson, 2000; Kalbitz and Kaiser, 2008). As such, the distribution of soil organic carbon (SOC) storage is critical for the understanding of climate change impacts on the terrestrial C cycle. However, the variability of SOC within forested ecosystems is influenced by different landform units such as hillslopes versus riparian or near-stream areas that have different C dynamics associated with differences in their soil and hydrological characteristics.

The ability to predict the impact of climate and hydrology on DOC export and SOC storage in watersheds depends on adequate understanding of spatial and temporal variability involved in DOC movement and SOC storage. In particular, hot spots and hot moments of SOC storage and DOC export need to be better understood. Vidon et al. (2010) made a distinction between biogeochemical hot spots and hot moments and transport-driven hot spots and hot moments. While not mutually exclusive, biogeochemical hot spots typically show disproportionately high *reaction rates* relative to the surrounding area, whereas hot moments are defined as short periods of time that exhibit disproportionately high *reaction rates* relative to longer intervening time periods (McClain et al., 2003). On the other hand, transport-driven hot spots are areas where *solute concentrations and/or fluxes* are disproportionately higher than in surrounding areas and transport-driven hot moments are short periods during which *solute*

concentrations and/or fluxes are significantly greater than that during the intervening time (Vidon et al., 2010).

Biogeochemical hot spots and hot moments of DOC are focused on C inputs and pools as well as processes such as mineralization and decomposition, while transport-driven hot spots and hot moments are focused on rainfall events and flow pathways that lead to DOC flushing. Therefore, intense precipitation events or snowmelt periods can lead to transport-driven hot moments while transport-driven hot spots may be defined by preferential flowpaths that channelize water and solutes through the soil and into groundwater or stream water (Bundt et al., 2001; Vidon et al., 2010).

The objectives of this study were to: (1) investigate the impact of combined soil and landscape features on the spatial variability of SOC storage and soil pore water DOC concentration in the Shale Hills Critical Zone Observatory (CZO) and (2) evaluate the influence of precipitation, discharge, and temperature on stream water DOC concentration and export. We evaluated the factors influencing DOC export and SOC storage along different soil-landform units (especially swales versus planar hillslopes) in this CZO.

We hypothesize that SOC distribution will be significantly different along swales versus planar hillslopes because of differences in soil thickness, soil texture, vegetation, and slope. We also hypothesize that the export of DOC in the catchment stream water is strongly correlated to climate variables (mainly rainfall, discharge, and temperature). We assess the transport-driven hot spots and hot moments of SOC storage and DOC export in this catchment. For this study, hot spots are identified as zones along hillslopes with elevated DOC concentration (> 20% increase as compared to surrounding areas), while

hot moments are identified as time periods within a year with elevated DOC export (< 20% of total time as compared to the intervening time periods).

Materials and Methods

Site description

The 7.9-ha Shale Hills CZO is a headwater forested catchment typical of the low-lying shale hills of the Ridge and Valley Physiographic Province in central Pennsylvania (Figure 2-1). Within the CZO is a first-order stream with an average channel gradient of 4.5% (Lynch, 1976). The mean annual temperature is 10°C and the mean annual precipitation is 1070 mm (NOAA, 2007). Annual precipitation for the study period (2008, 2009, and 2010 until October 1 2010) was 860 mm, 1030mm, and 700 mm respectively. This catchment is characterized by moderate to steep slopes, with an average slope of 28° for the north-facing slope and 23° for the south-facing slope. Depth to bedrock ranges from <0.25 m at the ridge tops and upper side slopes to over 2-3 m in the valley floor and swales (Lin, 2006). Elevation of the area ranges from 256 to 310 m from the outlet to the highest ridgetop (Lin et al., 2006). The moderately uniform slopes are interspersed with seven topographic depressional areas (swales) on both sides of the stream, with five on the south-facing slope and two on the north-facing slope (Figure 2-1).

The soils in this catchment were formed from shale colluvium or residuum and have a dominant texture of silt loam in the surface (with silty clay loam and clay loam in the B horizons in deeper soils). Five soil series have been identified (Figure 2-1), characterized and mapped based on landscape position, soil thickness or depth to

bedrock, and redoximorphic features (Lin et al., 2006). Since the catchment is completely forested, all soils have an organic horizon comprised of decaying leaf litter and other organic material. The south-facing slope has primarily hardwood forest (mostly maple, oak, and hickory) and thick underbrush. The north-facing slope also has hardwood forest but with little underbrush. On both sides of the stream, there are softwood trees (mostly pine and hemlock) along toward the western side and deciduous forest towards the eastern side.

Study design and data collection

To understand DOC patterns and export from the catchment, two transects were established on each of the north-facing and south-facing slopes of the catchment to investigate the characteristics of planar hillslopes (non-convergent flow) versus swales (convergent flow) (Figure 2-1). Nested porous-cup tension lysimeters (Soil water samplers, 1900 series, SoilMoisture Equipment Corp., Santa Barbara, CA, USA) were installed at three landscape positions – ridgetop, midslope, and valley floor - along each transect (Jin et al., 2010). For this paper, we focus on the soil pore water DOC concentrations from the two transects on the north-facing slope because of limited data collected so far on the south-facing slope (lysimeters were installed later). The lysimeters were installed at 10-cm or 20-cm depth interval from the soil surface down to weathered shale (or depth of hand-augering refusal), depending on soil thickness. Soil pore waters were collected between August 2007 and October 2009 from the lysimeters using PVC tubing and a syringe and placed in pre-combusted glass bottles. Soil pore water chemistry was monitored by approximately weekly sampling. The catchment is generally dry most

of the summer and frozen during the winter, so most of the soil pore water samples in this study were collected in early spring and late fall.

Intact soil cores were collected from 56 locations throughout the catchment to determine SOC concentration (Figure 2-1). These soil cores were collected when installing PVC tubes for soil moisture monitoring (Lin et al., 2006). Unless restricted by shallow bedrock, intact soil cores of 0.038-m diameter were extracted to a depth of 1.1 m (Lin et al., 2006). Soil horizon delineations of all soil cores were determined following the procedure of Soil Survey Staff (1993). Soil samples from different horizons of each soil core were air-dried and sieved (2 mm mesh size) for chemical analysis. For each of the five soil series, three small soil cores (6-cm in diameter and 6.2-cm long) for each soil horizon were also collected for bulk density measurements.

Collection of daily stream and groundwater samples using automated ISCO samplers (Teledyne ISCO Inc., Lincoln, NE) began in May 2008. Stream water samples were collected at the weir located at the outlet of the stream (Figure 2-1). No stream water samples were collected during the summers of 2008 (7/10/08 to 10/16/08) and 2010 (5/19/10 to 10/23/10) since the stream was not flowing. Also, no stream water samples were collected during the winters of 2008 (11/16/08 to 3/11/09) and 2009 (11/14/09 to 4/9/10) because of failure to retrieve samples from the ISCO samplers. Groundwater samples were collected from a 3.5 m deep well installed approximately 5 m from the weir (Figure 2-1). Precipitation samples were collected automatically using an Eigenbrodt NSA 181/S precipitation collector (Biral, Bristol, Great Britain). Stream discharge was measured at the catchment outlet using a V-notch weir with Druck continuous water level recorders (Campbell Scientific Inc., Logan, Utah). Temperatures

of stream water and air were also measured with these sensors and recorded at 10-min intervals.

Laboratory analyses

All DOC samples were filtered in the laboratory with 0.45 μm Nylon syringe filters (VWR International, West Chester, PA), acidified with two drops of 50% HCl and refrigerated at 4°C until analysis. Analysis was performed with a Shimadzu TOC-5000A analyzer (Shimadzu Scientific Instruments, Columbia, MD). To ensure data quality, standards (0 to 20 ppm calibration standards), analytical blanks (de-ionized water), replicates (every 10 samples), and spikes (25 μL of a 1000 ppm TOC standard) were used in each analysis batch.

Sieved ≤ 2 mm soil samples from the intact soil cores were analyzed for organic matter concentration using the loss on ignition (LOI) method (Soil Survey Staff, 1996) and particle size analysis (Kettler et al., 2001). Ground and air-dried soil subsamples from the north-facing swale and planar hillslope transects were also analyzed for total C using a CHNS-O Elemental Analyzer, EA 1110 (Leco, St. Joseph, MI). A system of analytical blanks, commercial standards (every 20 samples) and replicates (every 10 samples) were used for these analyses. As little or no carbonate ($< 0.01\%$ by weight) was present in these soils, total C is considered the same as organic C (Jin et al., 2010).

Calculations of SOC storage, DOC export, and precipitation indices

Soil organic carbon (SOC) storage

Storage of SOC per unit area (g C/cm^2) was calculated using the following formula for each soil horizon:

$$\text{SOC storage} = \text{SOC concentration} \times \rho_b \times \text{HT}, \quad [1]$$

where SOC concentration (% by weight) is determined from soil organic matter using a conversion factor of 2.42 (41% of SOM is SOC in this catchment) (Figure 2-2), ρ_b is soil dry bulk density (g/cm^3), and HT (cm) is soil horizon thickness. Storage of SOC for both the A and B horizon was then summed to give total profile storage for each site, i.e., top 1.1-m solum or depth to bedrock, whichever is shallower.

Maps of SOC concentration in the A and B horizons and storage in the top 1.1-m solum (or to bedrock) were interpolated using the 56 point data collected from soil cores using ArcGIS 9.1 (ESRI, Redlands, CA). Ordinary kriging was used to interpolate SOC concentration in the A and B horizons and the SOC storage in the top 1.1-m solum based on the procedures proposed by Zhu and Lin (2010).

The SOC concentrations in different horizons and the SOC storage in the top 1.1-m solum (or to bedrock) for all cells (3×3 m) in the interpolated maps were tested for their normality in SAS (SAS institute, Cary, NC). In addition, these interpolated maps were clipped for different landforms (hillslope versus swale) and south- versus north-facing slopes (Figure 2-1). The SOC storage in these different landforms and the south- and north-facing slopes were then summarized and statistically tested for differences.

Dissolved organic carbon (DOC) export

The daily stream DOC load (kg/hr) was calculated as DOC concentration (mg/L) measured at the outlet of the catchment multiplied by discharge (L/day). This was then summed over monthly time period to detect possible seasonal trends. Export of DOC from the whole catchment (kg/ha/yr) was then calculated as annual DOC load by summing monthly DOC load for a whole year and then dividing by the watershed area (7.9 ha). We calculated the DOC export for the entire year of 2009 (Table 2-1) and from May to December for 2008 and from January to October for 2010. In order to compare the export of DOC among different years, we compared DOC exported in 2009 to DOC exported in 2008 or 2010 for the same time period (May to December for 2008 and January to October for 2010).

Precipitation indices

To determine factors that control stream water DOC concentrations and export, we evaluated precipitation indices, including rainfall amount, antecedent precipitation index (API), and current precipitation index (CPI) time series with stream water DOC concentration and flux time series. The API (mm) is used to compare the antecedent moisture conditions among pre-storm events and is defined as (Christopher et al., 2007)

$$API_x = \sum_{i=1}^x \frac{P_i}{i}, \quad [2]$$

where $x = 7$ days before an event for this study and P_i (mm) is the total precipitation on the i th day before the event.

The CPI (mm) is used to convert the daily rainfall information into a continuous daily hydrograph. The CPI reflects the current catchment wetness (Smakhtin and Masse, 2000):

$$CPI_t = CPI_{t-1} K + R_t \quad , \quad [3]$$

where CPI_t is a current precipitation index (mm) for day t , R_t is the catchment precipitation for day t and K is the daily recession coefficient. The daily recession coefficient K normally varies from 0.85 to 0.98 (Smakhtin and Masse, 2000). For this study K was determined to be 0.85 based on the distribution of daily recession ratios (today's flow divided by yesterday's flow) and was calculated for all recession periods for the study period when discharge was less than long-term mean daily flow (Smakhtin and Masse, 2000). We also tested for $K = 0.9$ and 0.99 according to Graham and Lin (in review) for this CZO.

Statistical analyses

The analysis of variance (ANOVA) was used to test whether there were significant impacts on SOC storage from different soil horizons (A and B) SOC concentration, landforms units (valley floor, ridgetop, swale and planar hillslopes), aspect (south- versus north-facing slopes), and their interactions (Table 2-2). An ANOVA was also used to test significant differences in soil water DOC concentrations over different landscape positions (ridgetop, midslope, and valley floor), soil depths (10 to 30 cm as top portion, 30 to 50 cm as middle portion, and ≥ 50 cm as bottom portion), seasons (spring - March to May, summer - June to August, and fall - September to November), and their

interactions for the swale and planar hillslopes (Table 2-3). Since each landscape position has multiple soil depths, the landscape position is considered as the main plot factor and the soil depth is treated as the subplot factor that is nested within the landscape position. This is similar to split-plot in a randomized complete block design in statistics (Scheffe, 1999).

Since DOC samples were collected at different soil depths along the two hillslopes on a weekly basis during the study period, we used a repeated-measures ANOVA. The repeated-measures ANOVA tests the equality of means and is used when the dependent variable is measured under a number of different conditions (Delwiche and Slaughter, 2003). For this study, the soil pore water DOC concentration at a particular soil depth at a particular landscape position is the main observation, season changes within this observation, and its effect is estimated by the repeated-measures ANOVA. We used the *proc mixed* procedure in SAS (version 9.2, SAS Institute, Cary, NC) to conduct repeated-measures ANOVA. Additionally, *t*-tests were used to determine whether the average SOC storage values of different landform units differed significantly ($p < 0.05$).

To understand the main factors correlated with SOC storage and DOC export, regression analysis was performed. For SOC storage, the dependent variable was SOC storage in the top 1.1-m solum, while the independent variables were total clay amount, depth to bedrock, TWI, slope, and elevation. For DOC, dependent variables were DOC concentration or DOC load, while the independent variables were precipitation indices (rainfall amount, API, CPI), stream discharge, and temperature (air and stream water) that were all time series data. These analyses were carried out using Minitab 16.0 (Minitab Inc., State College, PA).

Results and Discussion

Catchment SOC storage and its influencing factors

Soil organic C and DOC are intimately linked, because DOC production is derived from SOC decomposition or DOM desorption. Thus, understanding SOC distribution in the catchment could shed light on the possible hot spots of DOC export. Soil organic C storage in this catchment was significantly correlated to a number of soil and landscape characteristics. The ANOVA results showed that landform unit and slope aspect influenced SOC storage at $p < 0.05$ level (Table 2-2).

Overall, the whole catchment's SOC concentration ranged from 2.0 to $> 5.0\%$ (by weight) and from < 1.2 to 2.0% for the A and B horizons, respectively (Figure 2-3), which were normally distributed throughout the catchment. The total SOC storage for the soil solum (A and B horizons) of the whole catchment was estimated as 130 Mg C/ha. At each site, SOC decreased exponentially with increasing soil depth, with the decrease being steeper for the swale as compared to the planar hillslope (Figure 2-4). The vertical decrease in SOC was greatest between the A and B horizons, with approximately 65% and 58% lower SOC in the B horizons as compared to the A horizons in the swale and the planar hillslope, respectively. These trends are similar to other studies that have observed a significant decrease in SOC in the B horizon as compared to the A horizon and are consistent with sorption (metal oxides and clay minerals) and precipitation (polyvalent cations) within the B horizon (e.g. Currie et al., 1996; Dosskey and Bertsch, 1997; Neff and Asner, 2001).

Soil organic carbon concentration shown in Figures 2-3 and 2-4 has slight differences because Figure 2-3 maps were interpolated from soil organic matter

converted to SOC, while SOC in Figure 2-4 was obtained directly from the elemental analyzer. Abella and Zimmer (2007) suggested that directly measuring SOC with an elemental C analyzer may be more accurate than estimating SOC from the loss on ignition method.

Storage of SOC was 27% and 33% (on average) higher along the south-facing swales and planar hillslopes, respectively, as compared to the north-facing counterparts (Figure 2-5). This is because the south-facing slope has a less steep slope (average 23°), deeper soils and a higher number of swales as compared to the north-facing slope (average 28°). Soils increase from < 30 cm at the ridgetop to >2 m at the valley floor and within the swales, with five swales on the south-facing slope and two swales on the north-facing slope. Additionally, the south-facing slope has thicker underbrush and thus higher biomass accumulation as compared to the north-facing slope. While the total catchment area occupied by the swales was only 1.8 ha ($\sim 23\%$ of the total catchment area), the swales overall had 22% higher SOC storage in the solum as compared to the planar hillslopes (Figure 2-5).

For the entire Shale Hills catchment, using multiple regression analysis, clay amount in the profile was the best single predictor of SOC storage for both the south- and north-facing slopes ($R^2 = 0.86$ and $R^2 = 0.64$, respectively). However, SOC storage in the solum was also correlated positively ($p < 0.001$) with the depth to bedrock ($R^2 = 0.36$), and TWI ($R^2 = 0.22$), but negatively with slope ($R^2 = 0.37$) (Figure 2-6). There was no statistically significant correlation with elevation ($R^2 = 0.04$) (Figure 2-6).

DOC in soil pore water and stream water and their influencing factors

Soil pore water

Concentrations of DOC in precipitation collected at the ridgetop of the catchment averaged 1.0 ± 0.2 mg/L from October 2008 to October 2009, which were comparable to other temperate watersheds in North America (Table 2-1). Soil pore water DOC concentrations in the Shale Hills catchment were also comparable to those in other temperate forested catchments in North America (Table 2-1). The ANOVA results showed that soil pore water DOC was significantly ($p < 0.05$) correlated to landscape position and soil depth (Table 2-3).

Soil pore water DOC concentrations were generally higher in the swale as compared to the planar hillslope (Figure 2-7). At the ridgetop, soil pore water DOC concentrations were, on average, 25% higher along the swale transect as compared to the planar hillslope transect. At the valley floor, average pore water DOC concentration from the swale transect was almost 45% higher within the top 0.4 m of the soil profile as compared to the same soil depth in similar location from the planar hillslope transect.

Concentrations of DOC in the soil pore water were not significantly different between the ridgetop and the valley floor along the soil profiles, but both were significantly higher than those in the midslope along both the swale and the planar hillslope (Figure 2-8a). Soil pore water DOC was highest in the surface A horizon and generally decreased exponentially with depth in all of the six soil profiles investigated (Figure 2-8a). The decline in soil pore water DOC concentrations at the ridgetop was the greatest between the A and B horizons (a 32% decrease in the swale transect and 56% in the planar hillslope transect). This decline is related to the similar declining trend of SOC

with soil depth (Figure 2-4). The decline in soil pore water DOC concentrations in the B horizon is consistent with the increase in clay content in the B horizon (Figure 2-8b), particularly along the swale. Additionally, the low organic matter concentration (~ 6 %) and acidic (pH ~ 4.5) conditions at our study site are known to favor sorption of DOC to clays (Schimel et al., 1994; Qualls et al., 2002). Furthermore, Qualls (2000) observed that DOC is removed from solution when concentrations are high (surface organic horizon as compared to mineral soil) but released or desorbed when little or no DOC is present in solution. These mechanisms may explain the vertical distribution of soil pore water DOC with the soil profile.

In contrast to the vertical trend of soil pore water DOC, no obvious seasonal variations were observed in soil pore water DOC concentrations (Table 2-3). Soil pore water DOC concentrations were variable over time particularly in the surface horizon; however, this variability was not well correlated with rainfall. This lack of seasonal trend should be interpreted cautiously because our field site is typically dry during the summer and frozen during the winter so our observations so far were limited to spring and fall in the two-year monitoring period.

Stream water

Daily stream water DOC concentrations between May 2008 and October 2010 ranged from 0.6 to 28.6 mg/L, with an average of 6.2 mg/L (Figure 2-9). Stream water DOC concentrations were higher than groundwater DOC (which was relatively invariant, with an average of 1.4 ± 0.5 mg/L). The stream water DOC concentrations at the Shale

Hills catchment were comparable to other hardwood forests in temperate climates (Table 2-1), but were lower as compared to coniferous forests (Liu and Sheu, 2003).

Stream water DOC concentrations showed peaks during the periods of snowmelt and late summer/early fall wet-up (Figure 2-9). These elevated DOC concentrations were stronger during the wet year of 2009 than in the relatively dry years of 2008 and 2010. Stream water DOC concentrations during the 2009 snowmelt period (mid-March to mid-April) reached a maximum of 28.6 mg/L (averaging 5.8 mg/L). A second peak was observed in between mid-August and September 2009 as the catchment began to wet up, reaching an average DOC of 16.0 mg/L (± 4.7), and another peak during snowmelt in April 2010 (4.3 ± 1.3 mg/L).

Export of DOC from the stream for 2009 was estimated as 56 kg/ha/yr, while that during 2008 (7 kg/ha/yr from May to December) and 2010 (14 kg/ha/yr from January to September) were much lower. This was most likely due to 2009 being much wetter as compared to 2008 and 2010. The DOC export in 2009 was above the range reported for other temperate forests listed in Table 2-1 (20-30 kg/ha/yr), which was likely due to the small size of the Shale Hills catchment. Ågren et al. (2007) found a significant inverse relationship between watershed area and DOC export, such that the smaller the area, the larger the export of DOC. Ågren et al. (2007) also suggested that small headwaters may be the largest contributor to the terrestrial DOC export per unit area.

Stream discharge and stream water temperature were significantly correlated to stream water DOC, but not rainfall, API, or CPI. This observation is consistent with precipitation indices not being a consistent predictor for water movement within the Shale Hills catchment (Graham and Lin, in review). The relationship between stream

water DOC and stream water discharge ($p < 0.01$; $R^2 = 0.30$) and stream water temperature ($p < 0.01$; $R^2 = 0.33$) was obvious but nonlinear (Figure 2-10). The percentage of variation explained by discharge and temperature improved when data were aggregated on a monthly basis, with R^2 increased to 0.47 for discharge and 0.45 for stream water temperature.

Both high (snowmelt period) and low discharge (late summer to early fall period) corresponded to high stream water DOC concentrations during the monitoring period of this study (Figure 2-10). Many studies have observed weak relationships between discharge and DOC (e.g. Clark et al., 2007; Turgeon and Courchesne, 2008; Koehler et al., 2009). While rainfall is a driver of discharge, the complex and variable discharge-DOC relationship (Figure 2-10) suggested that rainfall itself is not a good predictor of stream water DOC concentrations in this catchment.

Mulholland (1997), Mulholland and Hill (1997), and Vidon et al. (2010) also observed higher stream water DOC during summer periods and attributed it to in-stream processing. This high stream water DOC during late summer to early fall period can also be attributed to the greater decomposition of organic matter. During the late summer, higher temperatures and aerobic conditions would promote high decomposition rates of SOC. As the catchment wets up in early fall, accumulated DOC in soils could then be flushed.

In the Shale Hills catchment, it is likely that during the low flow period, most of the stream water is recharged by groundwater (Jin et al., 2010), which has relatively low DOC concentrations (Figure 2-9). Thus the high stream water DOC during the late summer/early fall likely develops from in-situ stream-processes as well as flushing of

accumulated DOC from the decomposition of SOC from shallow soils, both of which are temperature-dependent. In the high flow period (fall and spring), stream water DOC has a higher contribution from soil pore waters, which contain much higher DOC concentrations (Figures 2-8 and 2-9).

Hot spots and hot moments of DOC export and SOC storage

At the ridgetop, both the planar hillslope and swale transects displayed a noticeable vertical trend: average soil pore water DOC concentrations decreased from 10 to 20 cm and then increased at ~30 cm at the soil-bedrock interface (Figure 2-8a). The elevated soil pore water DOC at the soil-bedrock interface was 35% higher as compared to the overlying B horizon in the planar hillslope transect while those in the swale transect was 17% higher. Similarly, at the restrictive Bw-Bt horizon interface (~30 cm depth) in the valley floor, elevated soil pore water DOC concentrations were observed (Figure 2-8a), with a 37% increase as compared to the overlying Bw horizon and the underlying Bt horizon.

Elevated soil pore water DOC concentrations at these restrictive interfaces correspond to lateral preferential flow pathways commonly observed at Shale Hills (Lin, 2006; Lin and Zhou, 2008). Soil pore water deuterium concentrations were also observed to be highly variable at these restrictive soil interfaces (Jin et al., in review) which is indicative of fast flowing water. These results are consistent with soil profile characteristics, namely restrictive soil layers, providing transport-driven hot spots for soil pore water DOC (Figure 2-11), such that they indicate zones of elevated (> 20% increase) concentrations and/or fluxes as compared to the surrounding areas or soil horizons above

(e.g., B horizon above the soil-bedrock interface) and/or below (e.g., Bw horizon over and Bt horizon below the Bw-Bt horizon interface).

Preferential flow pathways have been reported to have higher solute concentrations in other watersheds since they are more exposed to wetting and drying cycles and have a better nutrient supply than the soil matrix (e.g., Mulholland, 1997; Feyen et al., 1999; Bundt et al., 2001). The ability to sustain the mass balance on water, the high flow (with high DOC concentrations) along the restrictive soil interfaces must be provided with water flowing from the shallow to deeper soils which would require the presence of vertical macropores (Jin et al., in review). However, there still exist disputes about the origin of these elevated concentrations observed along preferential flow pathways – displacement of “old water” and/or infiltration of new water (McDonnell, 1990; Feyen et al., 1999; Kirchner, 2003).

The observed higher SOC storage within the swales (particularly along the south-facing slope) in the catchment (Figure 2-3c) and the higher DOC concentrations along the swale as compared to the planar hillslope (north-facing slope) (Figure 2-7) are consistent with the swales being potential hotspots for or areas of higher C storage and DOC export as compared to the rest of the catchment. Results from a mass transport model (based upon an assumption that soils are at steady state thickness) applied to the planar hillslope could not eliminate physical accumulation as being important at the valley floor due to transport from upslope (Jin et al., 2010). This inference is consistent with high DOC and SOC concentrations at the valley floor and potentially within the swales which are topographic depressions and have soils as thick as the valley floor.

While soil pore water DOC and SOC were significantly and positively correlated (data shown in chapter 3), they were not perfectly correlated such that elevated soil pore water DOC concentrations were not associated with a corresponding increase in SOC concentrations at the restrictive soil horizon interfaces. These observations underscore the importance of both biotic and abiotic controls on the transport of DOC and SOC and potentially, the mechanisms that control DOC and SOC concentrations may not be similar or may occur at different timescales and should be further investigated.

Elevated stream water DOC concentrations occurred during the snowmelt period as well as during the late summer to early fall (Figure 2-9). These time periods may be considered as transport-driven hot moments, that is, short periods (< 20% of total time period considered) during which solute concentrations (and/or fluxes) are elevated as compared to the rest of the time period (Figure 2-11). Transport-driven hot moments have often been observed during snowmelt where pulses of DOC are flushed from soils to streams (e.g. Boyer et al., 1997; Inamdar et al., 2006).

In this study, average hillslope DOC concentrations were observed to be higher than stream DOC concentrations, while groundwater DOC concentrations were low. This indicates that hillslope DOC or in-stream processing is likely the source of elevated stream water DOC concentrations. Approximately 55% of the total DOC exported from the catchment in 2009 was attributed to snowmelt (29% contribution) and the late summer/early fall wet-up periods (26% contribution), which seemed to be crucial time periods for DOC export from this catchment. These two periods accounted for 21% (two and half months) of the whole year.

The pulses of stream water DOC during these two periods are consistent with the catchment being more hydrologically connected (hillslope - near stream area - stream channel) as compared to the rest of the year. Similar to our study, Harms and Grimm (2008) observed that hot moments of nutrient retention and removal occurred during high discharge periods, and concluded that hydrologic flowpaths may be the ultimate driver of hot spots and hot moments within valley floor – stream areas.

Summary and Conclusions

Interactions between soil and landscape characteristics are the main factors correlated to SOC storage variability and soil pore water DOC trends in the Shale Hills CZO. Results from this study showed that soil profile clay content was the best single predictor of SOC storage in the catchment. Moreover, higher clay content, lower slope, thicker soils, greater topographic wetness index, and a higher number of swales in the south-facing slope resulted in 30% more SOC storage as compared to that in the north-facing slope. Since DOC production is derived from SOC decomposition, higher SOC in the swales likely led to the observed higher soil pore water DOC concentrations in the swale as compared to the planar hillslope.

In the two north-facing hillslopes studied, average DOC concentration at the ridgetop was 25% higher along the swale transect as compared to the planar slope transect; while at the valley floor (zone of accumulation), average DOC concentration was 45% higher along the swale transect as compared to the planar slope transect within the top 0.4 m of the soil profile. Soil pore water DOC within the catchment was influenced by a combination of soil and landscape characteristics. Elevated soil pore

water DOC concentrations were observed within the soil profile at the Bw-Bt horizon interface in the valley floor and at the soil-bedrock interface at the ridgetop. This indicates that restrictive subsurface interfaces are potential transport-driven hot spots for soil pore water DOC.

Transport-driven hot spots are known to be important to the transport of labile solutes from upland to streams (Vidon and Hill, 2004; Vidon et al., 2010). Thus, it is important to measure DOC at varying depths within the soil profile as well as to assess different hydrologic flow pathways and confining subsurface layers for identifying transport-driven hot spots.

While precipitation indices showed no significant relationship with stream water DOC export at the Shale Hills CZO, stream discharge and water temperature were significantly related to stream water DOC export over the 2008-2010 monitoring period. High DOC concentrations occurred during the snowmelt period (high discharge, flushing effect) and the late summer to early fall wet-up period (low discharge, temperature effect). This indicates the complex nonlinear discharge-DOC relationship.

Increases in stream water DOC concentrations during late summer to early fall were attributed to the greater decomposition of organic matter, enhanced flushing of DOC after late summer/early fall storms from shallow soil horizons, and in-stream processing promoted by higher temperature. The late summer to early fall wet-up period and the snowmelt period are noticeable hot moments for DOC transport in this catchment. However, because 2008 and 2010 were relatively dry years, DOC export in this catchment was over 40% lower in 2008 and 2010 as compared to 2009. Such year to year variability with changes in climate suggests that longer monitoring is needed to gain

a fuller understanding of DOC movement in this catchment to decipher the transport and storage of C within the soil profile and in the stream.

References

- Abella, S. R. and B. W. Zimmer. 2007. Estimating organic carbon from loss-on ignition in Northern Arizona forest soils. *Soil Science Society of America Journal* 71 (2): 545-550.
- Ågren, A., I. Buffam, M. Jansson, and H. Laudon. 2007. Importance of seasonality and small streams for the landscape regulation of dissolved organic carbon export. *Journal of Geophysical Research* 112, G03003, doi: 10.1029/2006JG000381.
- Boyer, E. W., G. M. Hornberger, K. E. Bencala, and D. M. McKnight. 1997. Response characteristics of DOC flushing in an Alpine catchment. *Hydrological Processes* 11 (12): 1635-1647.
- Buckingham, S., E. Tipping, and J. Hamilton-Taylor. 2008. Concentrations and fluxes of dissolved organic carbon in UK topsoils. *Science of the Total Environment* 407: 460-470.
- Bundt, M., M. Jäggi, P. Blaser, R. Siegwolf, and F. Hagedorn. 2001. Carbon and nitrogen dynamics in preferential flow paths and matrix of a forest soil. *Soil Science Society of America Journal* 65:1529-1538.
- Christopher, S. F., M. J. Mitchell, M. R. McHale, E. W. Boyer, D. A. Burns, and C. Kendall. 2008. Factors controlling nitrogen release from two forested catchments with contrasting hydrochemical responses. *Hydrological Processes* 22 (1): 46-62.
- Clark, J. M., S. N. Lane, P. J. Chapman, and J. K. Adamson. 2007. Export of dissolved

- organic carbon from an upland peatland during storm events: implications for flux estimates. *Journal of Hydrology* 347: 438– 447.
- Cronan, C. S. and G. R. Aiken. 1995. Chemistry and transport of soluble humic substances in forested watersheds of the Adirondack Park, New York. *Geochimica et Cosmochimica Acta* 49: 1697-1705.
- Currie, W. S., J. D. Aber, W. H. McDowell, R. D. Boone, and A. H., Magill. 1996. Vertical transport of dissolved organic C and N under long-term N amendments in pine and hardwood forests. *Biogeochemistry* 35 (3): 471-505.
- Dalva, M. and T. R. Moore. 1991. Sources and sinks of dissolved organic carbon in a forested swamp catchment. *Biogeochemistry* 15 (1): 1-19.
- Delwiche, L. D. and S. J. Slaughter. 2003. *The Little SAS Book: A Primer*. 3rd Edition. Systems Seminar Consultants. Wisconsin, USA.
- de Wit. H. A., T. Palosuo, G. Hylen, and J. Liski. 2006. A carbon budget for forest biomass and soils in southeast Norway calculated using a widely applicable method. *Forest Ecology and Management* 225: 15-26.
- Dosskey, M. G. and P. M. Bertsch. 1997. Transport of dissolved organic matter through a sandy forest soil. *Soil Science Society of America Journal* 61: 920-927.
- Feyen, H., H. Wunderli, H. Wydler, and A. Papritz. A tracer experiment to study flow paths of water in a forest soil. *Journal of Hydrology* 225: 155-167.
- Futter, M. N. and H. A. de Wit. 2008. Testing seasonal and long-term controls on streamwater DOC using empirical and process-based models. *Science of the Total Environment* 407: 698-707.
- Graham, C. and H. Lin. Controls and frequency of preferential flow occurrence at

the Shale Hills Critical Zone Observatory: A 175 event analysis of soil moisture response to precipitation. *In review: Vadose Zone Journal*.

Harms, T. K. and N. B. Grimm. 2008. Hot spots and hot moments of carbon and nitrogen dynamics in a semiarid riparian zone. *Journal of Geophysical Research* 113, G01020, doi:10.1029/2007JG000588.

Hornberger, G. M., K. E. Bencala and D. M. McKnight. 1994. Hydrological controls on dissolved organic carbon during snowmelt in the Snake River near Montezuma, Colorado. *Biogeochemistry* 25: 147-165.

Howard, P.J.A. and D.M. Howard. 1990. Use of organic carbon and loss-on-ignition to estimate soil organic matter in different soil types and horizons. *Biology and Fertility of Soils* 9: 306-310.

Inamdar, S. P., S. F. Christopher, and M. J. Mitchell. 2004. Export mechanisms for the dissolved organic carbon and nitrate during summer storm events in a glaciated forested catchment in New York, USA. *Hydrological Processes* 18: 2651-2661.

Inamdar, S., J. Rupp, and M. Mitchell. 2008. Differences in dissolved organic carbon and nitrogen responses to storm-event and ground-water conditions in a forested, glaciated watershed in western New York. *Journal of American Water Resources Association* 44 (6): 1458-1473.

Jin, L., R. Ravella, B. Ketchum, P.R. Bierman, P. Heaney, T.S. White, and S. L. Brantley. 2010. Mineral weathering and elemental transport during hillslope evolution at the Susquehanna/Shale Hills Critical Zone Observatory. *Geochimica et Cosmochimica Acta* 74 (13): 3669-3691.

Jin, L., D. M. Andrews, G. H. Holmes, C. J. Duffy, H. Lin and S. L. Brantley.

Water chemistry reflects hydrological controls on weathering in
Susquehanna/Shale Hills Critical Zone Observatory (Pennsylvania, USA).

In review: Vadose Zone Journal.

Jobbágy, E. G. and R. B. Jackson. 2000. The vertical distribution of soil organic carbon and its relation to climate and vegetation. *Ecological Applications* 10 (2): 423-436.

Kalbitz, K. and K. Kaiser. 2008. Contribution of dissolved organic matter to carbon storage in forest mineral soils. *Journal of Plant Nutrition and Soil Science* 171: 52-60.

Keller, W. A. M. Paterson, K. M. Somers, P. J. Dillon, J. Heneberry, and A. Ford. 2008. Relationships between dissolved organic concentrations, weather, and acidification in small Boreal Shield Lakes. *Canadian Journal of Fisheries and Aquatic Sciences* 65: 786-795.

Kettler, T.A., J. W. Dorany, and T. L. Gilbertz. 2001. Simplified Method for Soil Particle-Size Determination to Accompany Soil-Quality Analyses. Publications from USDA-ARS / UNL Faculty. USDA Agricultural Research Service Lincoln, Nebraska.

Kirchner, J. W. 2003. A double paradox in catchment hydrology and geochemistry. *Hydrological Processes* 17: 871-874.

Koehler, A., K. Murphy, G. Kiely, and M. Sottocornola. 2009. Seasonal variation of DOC concentration and annual loss of DOC from an Atlantic blanket bog in South Western Ireland. *Biogeochemistry* DOI 10.1007/s10533-009-9333-9.

Lin, H. 2006. Temporal stability of soil moisture spatial pattern and subsurface

- preferential flow pathways in the Shale Hills Catchment. *Vadose Zone Journal* 5: 317-340.
- Lin, H. and X. Zhou. 2008. Evidence of subsurface preferential flow using soil hydrologic monitoring in the Shale Hills Catchment. *European Journal of Soil Science* 59: 34-49.
- Lin, H., W. Kogelmann, C. Walker, M.A. Bruns. 2006. Soil moisture patterns in a forested catchment: a Hydropedological perspective. *Geoderma* 131: 345–368.
- Liu, C. P. and B. H. Sheu. 2003. Dissolved organic carbon in precipitation, throughfall, stemflow, soil solution, and stream water at the Guandaushi subtropical forest in Taiwan. *Forest Ecology and Management* 172: 315-325.
- Lynch, J. A. 1976. Effects of antecedent soil moisture on storm hydrographs. PhD Dissertation. The Pennsylvania State University, University Park, PA.
- McClain, M. E., E. W. Boyer, C. L. Dent, S. E. Gergel, N. B. Grimm, P. M. Groffman, S. C. Hart, J. W. Harvey, C. A. Johnson, E. Mayorga, W. H. McDowell, and G. Pinay. 2003. Biogeochemical hot spots and hot moments at the interface of terrestrial and aquatic ecosystems. *Ecosystems* 6: 301-312.
- McDonnell, J. J. 1990. A rationale for old water discharge through macropores in a steep, humid catchment. *Water Resources Research* 26: 2821-2832.
- McDowell, W. H. and T. Wood. 1984. Podzolization: soil processes control organic carbon concentrations in stream water. *Soil Science* 137: 23-32.
- McDowell, W. H. and G. E. Likens. 1988. Composition and flux of dissolved organic carbon in the Hubbard Brook Valley. *Ecological Monographs* 58 (3): 177-195.
- McHale, M. R., J. J. McDonnell, M. J. Mitchell, and C. P. Cirimo. 2002. A field-based

- study of soil water and groundwater nitrate release in an Adirondack forested watershed. *Water Research Resources* 38(4), 1031, doi:10.1029/2000WR000102.
- Meyer, J. L. and C. M. Tate. 1983. The effects of watershed disturbance on dissolved organic carbon dynamics of a stream. *Ecology* 64 (1): 33-44.
- Mulholland, P. J. 1997. Dissolved organic matter concentration and flux in streams. *Journal of the North American Benthological Society* 16 (1): 131-141.
- Mulholland, P. J. and W. R. Hill. 1997. Seasonal patterns in streamwater nutrient and dissolved organic carbon concentrations: separating catchment flow path and in stream effects. *Water Resources Research* 33 (6): 1297-1306.
- National Oceanographic and Atmospheric Administration (NOAA). 2007. U.S. divisional and station climatic data and normals: Asheville, North Carolina, U.S. Department of Commerce, National Oceanic and Atmospheric Administration, National Environmental Satellite Data and Information Service, National Climatic Data Center. <http://cdo.ncdc.noaa.-gov/CDO/cdo>.
- Neff, J. C. and G. P. Asner. 2001. Dissolved organic carbon in terrestrial ecosystems: synthesis and a model. *Ecosystems* 4: 29-48.
- Nelson, D.W. and L.E. Sommers. 1996. Total carbon, organic carbon, and organic matter. In: *Methods of Soil Analysis, Part 2, 2nd Ed.*, A.L. Page et al., Ed. Agronomy 9: 961-1010. American Society of Agronomy, Inc. Madison, WI.
- Qualls, R. G. 2000. Comparison of the behavior of soluble organic and inorganic nutrients in forest soils. *Forest Ecology and Management* 138: 29-50.
- Qualls, R. G., B. L. Haines, W. T. Swank, and S. W. Tyler. 2002. Retention of soluble organic nutrients by a forested ecosystem. *Biogeochemistry* 61: 135-171.

- Qualls, R. G. and B. L. Haines. 1991. Geochemistry of dissolved organic nutrients in water percolating through a forest ecosystem. *Soil Science Society of America Journal* 55: 1112-1123.
- Scheffe, H. 1999. *The Analysis of Variance*. 1st edition. John Wiley and Sons Inc. New York, USA.
- Schimel, D. S., B. H. Braswell, E. A. Holland, R. McKeown, D. S. Ojima, T. H. Painter, W. J. Parton, and A. R. Townsend. 1994. Climatic, edaphic, and biotic controls over storage and turnover of carbon in soils. *Global Biogeochemical Cycles* 8: 279–93.
- Smakhtin, V. Yu. and B. Masse. 2000. Continuous daily hydrograph simulation using duration curves of a precipitation index. *Hydrological processes* 14: 1083-1100.
- Soil Survey Division Staff. 1993. *Soil Survey Manual*. U.S. Dept. Agri. Handbook No 18. U.S. Gov. Printing Office, Washington, DC.
- Soil Survey Division Staff. 1996. Total carbon, dry combustion, method 6A2 – Soil Survey Laboratory methods manual Soil Survey Investigations Report No 42, version 30. US Gov Print Office, Washington, DC.
- Tetzlaff, D. and H. Laudon. 2010. Dissolved organic carbon in Northern catchments and understanding hydroclimatic controls. *Eos. Northern Watershed Ecosystem Response to Climate Change (North-Watch) Workshop II: Hydrological Regulation of Stream DOC in Northern Catchments*.
- Turgeon, J. M. L. and F. Courchesne. 2008. Hydrochemical behaviour of dissolved nitrogen and carbon in a headwater stream of the Canadian Shield: relevance of antecedent soil moisture conditions. *Hydrological Processes* 22: 327-339.

- Vidon, P. and A. R. Hill. 2004. Denitrification and patterns of electron donors and acceptors in eight riparian zones with contrasting hydrogeology. *Biogeochemistry* 71: 259-283.
- Vidon, P., C. Allan, D. Burns, T. P. Duval, N. Gurwick, S. Inamdar, R. Lowrance, J. Okay, D. Scott, and S. Sebestyen. 2010. Hot spots and hot moments in riparian zones: potential for improved water quality management. *Journal of the American Water Resources Association* 46(2): 278-298.
- Wagner, L.E., P. Vidon, L. P. Tedesco, and M. Gray. 2008. Stream nitrate and DOC dynamics during three springs storms across land uses in glaciated landscapes of the Midwest. *Journal of Hydrology* 362: 177-190.
- Zhu, Q., and H.S. Lin. 2010. Comparing ordinary kriging and regression kriging for soil properties in contrasting landscapes. *Pedosphere* 20 (5): 594-606.

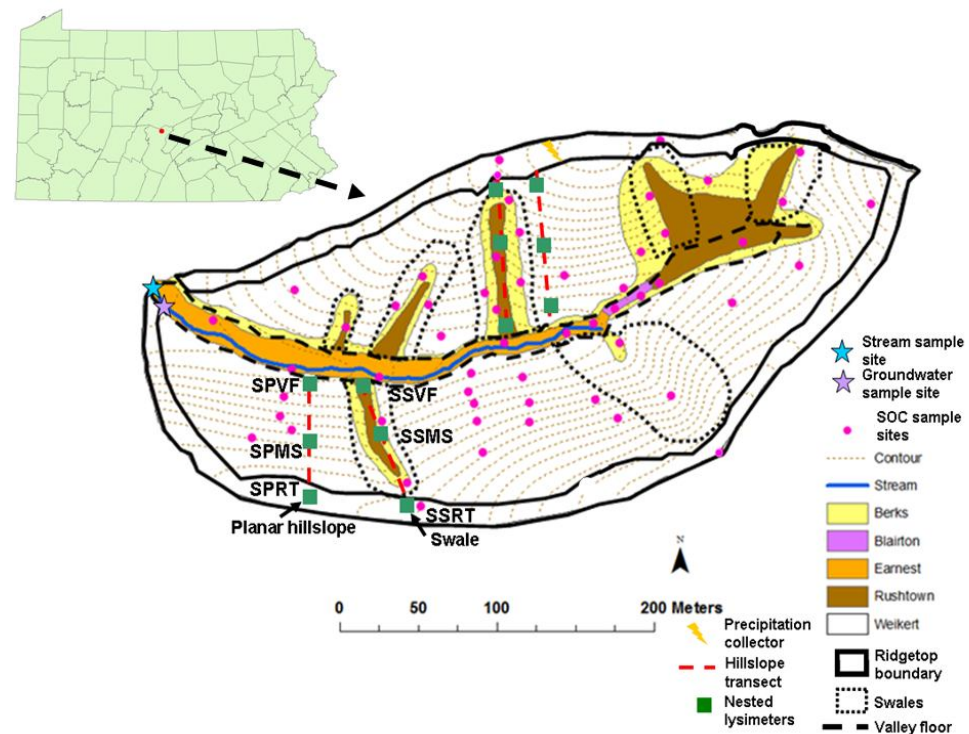


Figure 2-1: Map of the Shale Hills CZO in central Pennsylvania and the location of the hillslope transects monitored (Jin et al., 2010). Red dashed lines represent the swale and planar transects; green boxes represent the ridgetop, midslope, and valley floor positions (SPRT – planar hillslope ridgetop, SPMS – planar hillslope midslope, SPVF – planar hillslope valley floor position, SSRT – swale ridgetop, SSMS – swale midslope, and SSVF – swale valley floor).

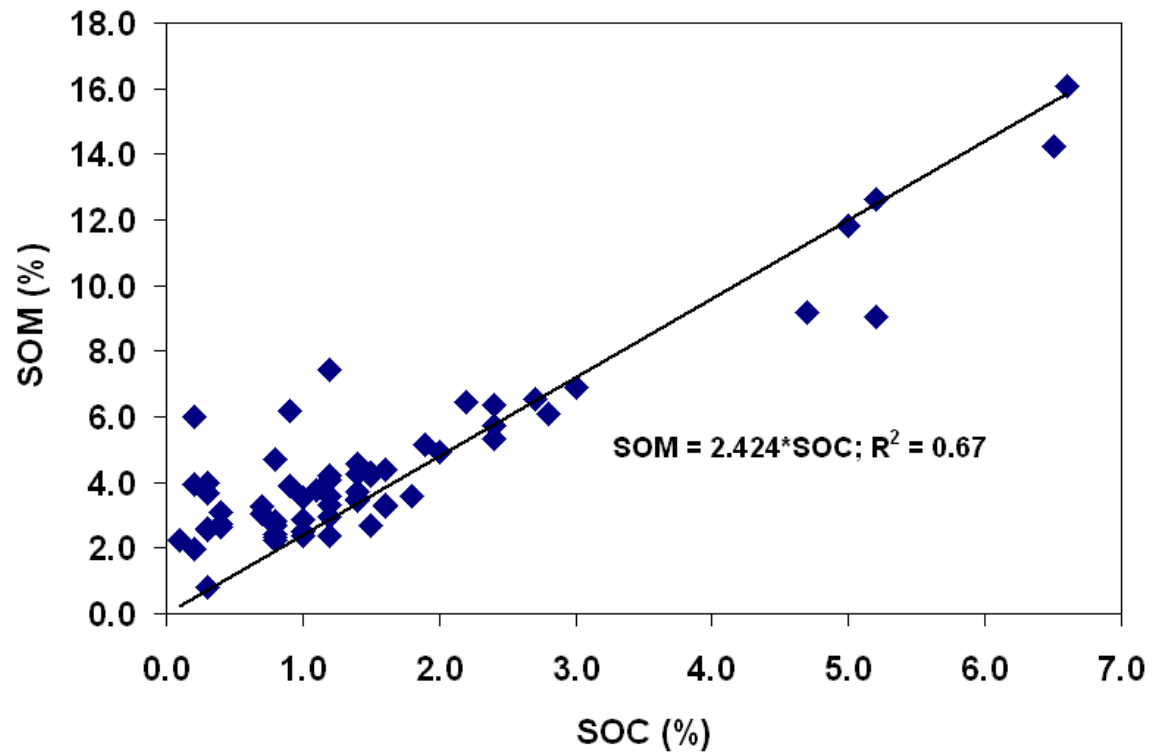


Figure 2-2: Soil organic matter (SOM) concentration (% by weight) in relation to soil organic carbon (SOC) concentration (% by weight) for 61 soil samples from the Shale Hills.

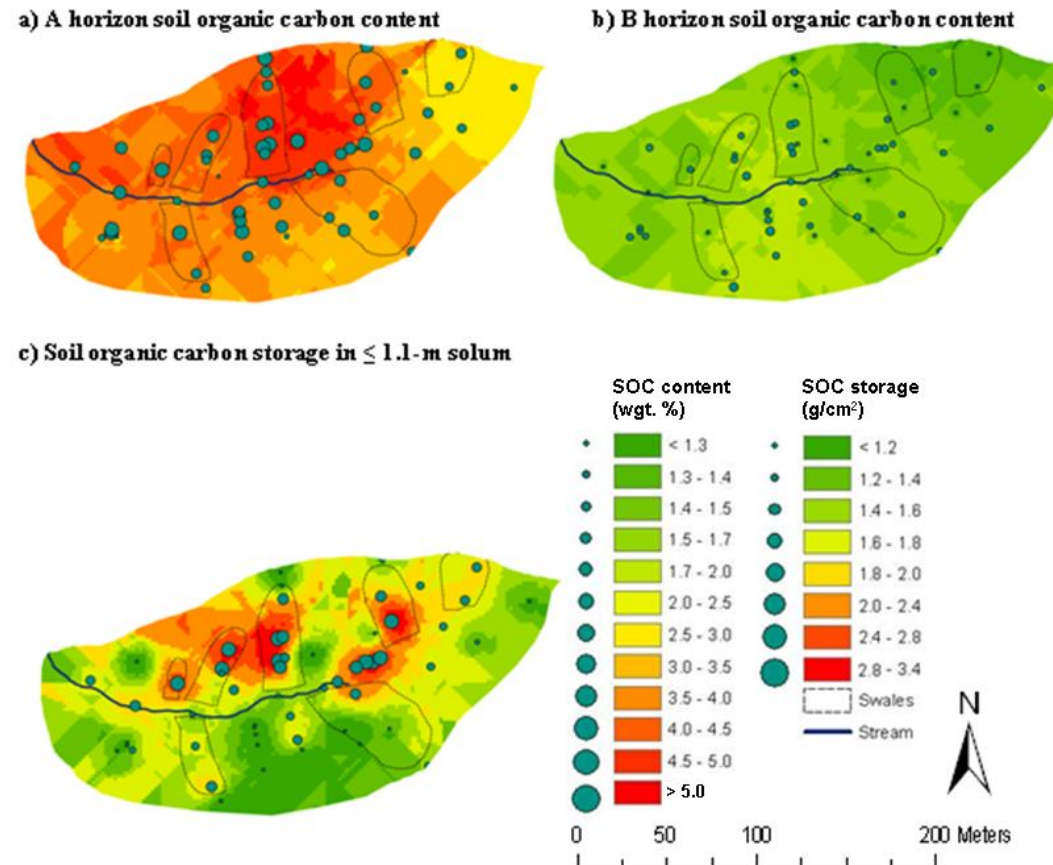


Figure 2-3: Interpolated maps of soil organic carbon (SOC) concentration (% by weight) in the A and B soil horizons, respectively, and SOC storage (g/cm²) within ≤ 1.1 -m solum based on 56 sampling sites shown on each map.

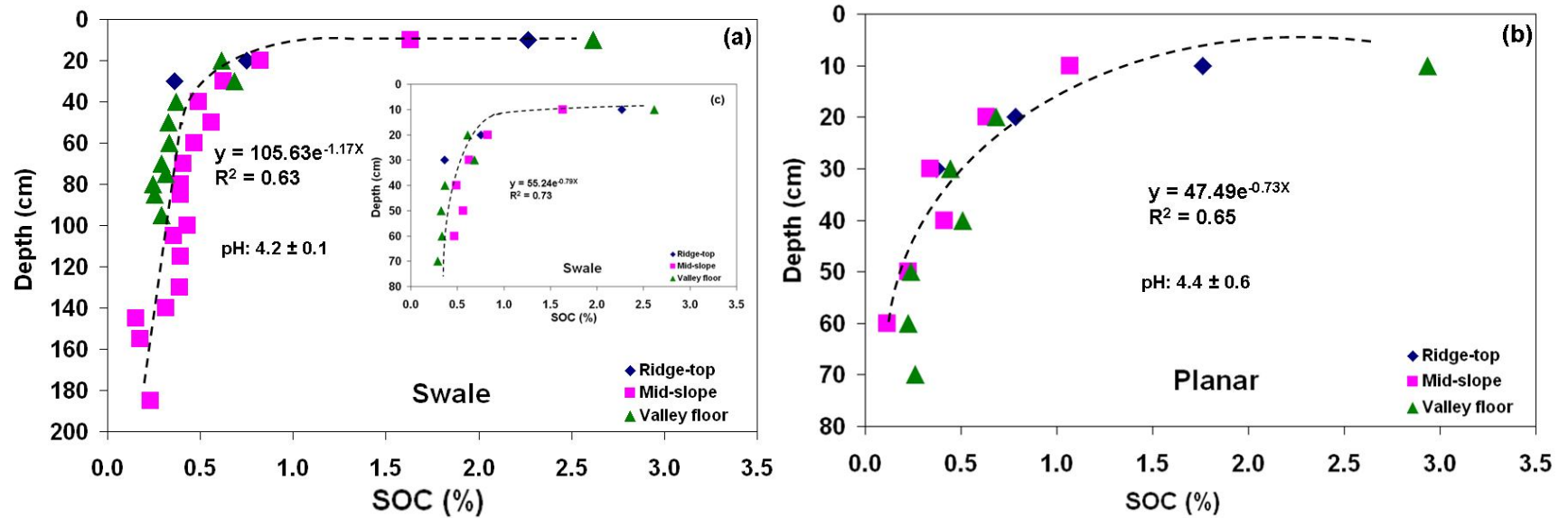


Figure 2-4: Vertical distribution of soil organic carbon (SOC) concentration (% by weight) for the ridgetop, midslope, and valley floor in the north-facing swale (a) and planar hillslope (b). Inset in (a) shows the swale data for the same soil depth as the planar hillslope.

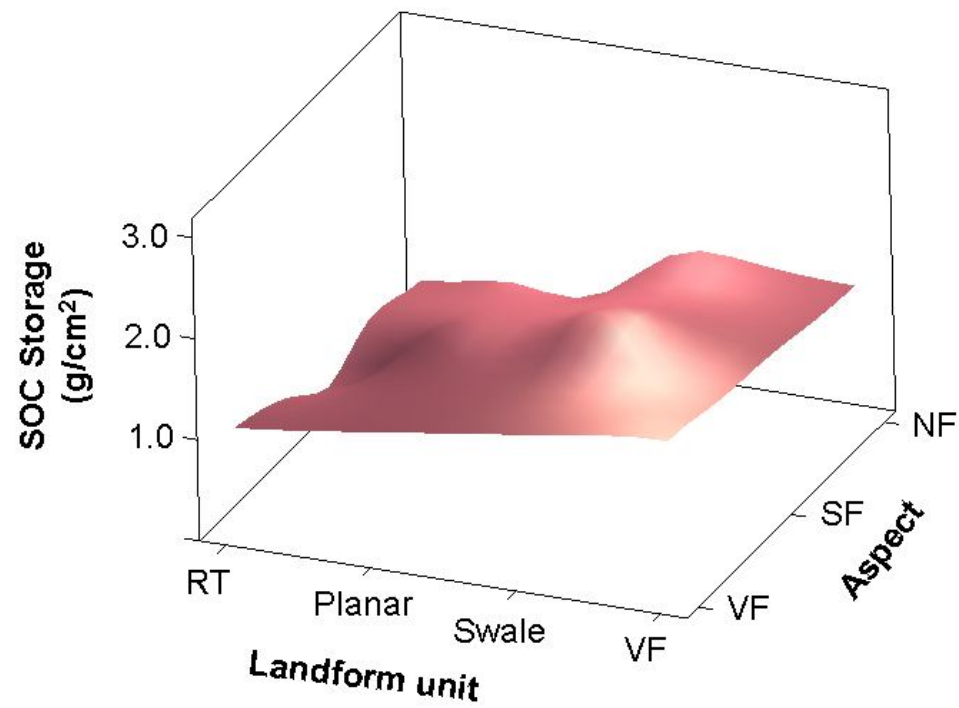


Figure 2-5: Soil organic carbon (SOC) storage within ≤ 1.1 -m solum as a function of landform unit (RT – ridgetop, planar hillslope, swale, VF – valley floor) and aspect (VF – valley floor, SF – south-facing slope, NF – north-facing slope) based on 56 sampling sites.

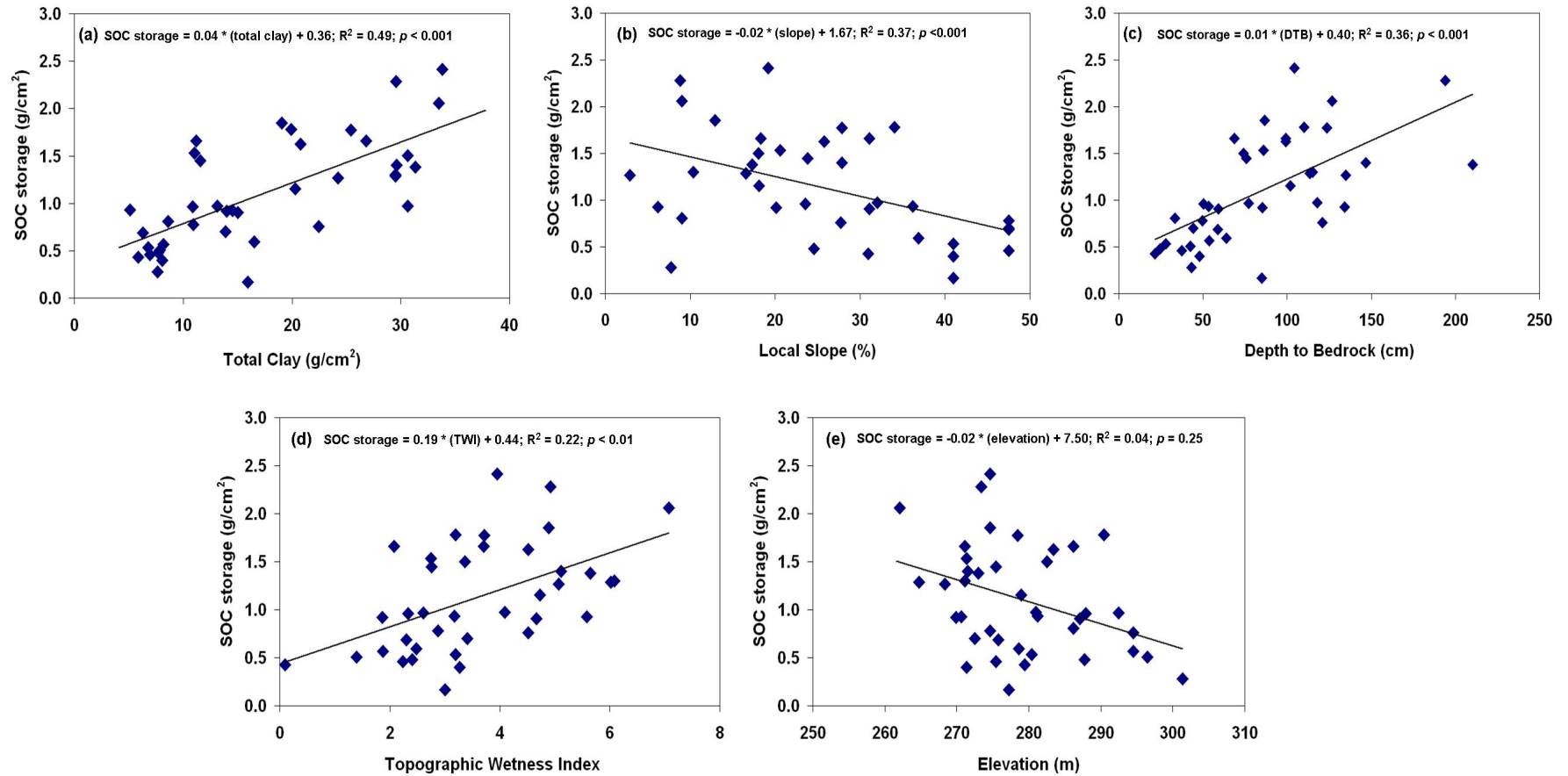


Figure 2-6: Soil organic carbon (SOC) storage for the Shale Hills catchment within ≤ 1.1 -m solum ($N = 56$) plotted as a function of (a) clay amount (within ≤ 1.1 -m solum), (b) slope, (c) depth to bedrock, (d) topographic wetness index, and (e) elevation.

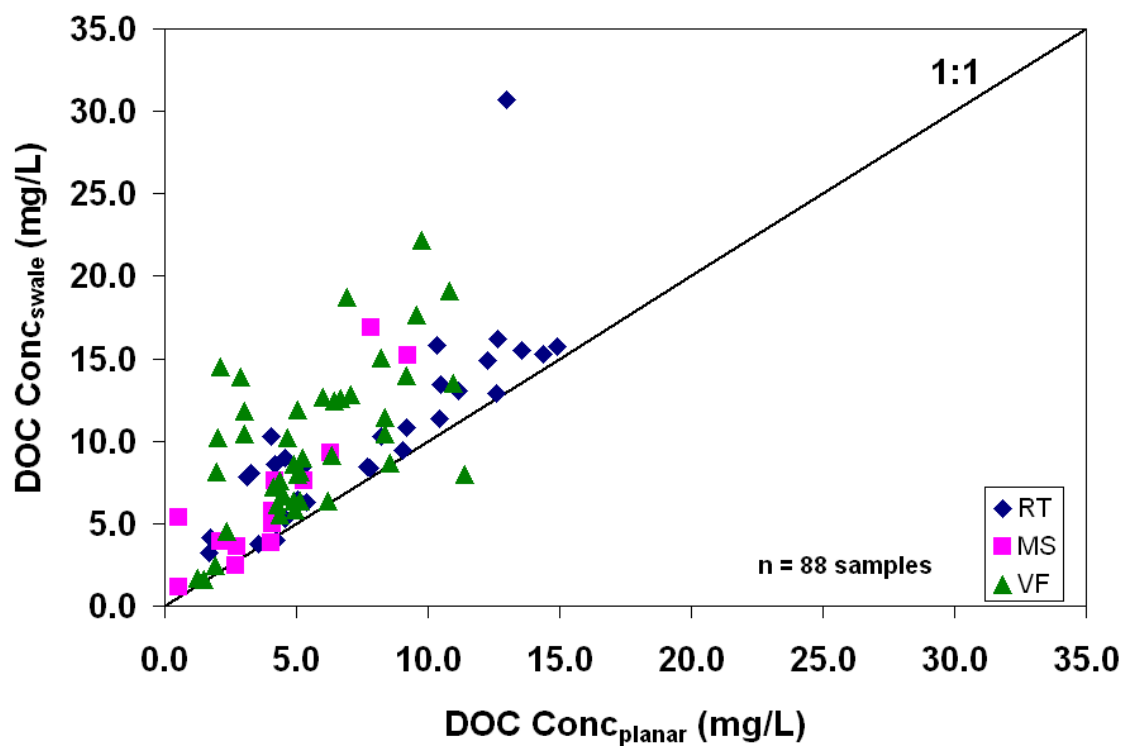


Figure 2-7: Soil pore water DOC concentration for the swale transect (y-axis) versus the planar hillslope transect (x-axis) at similar soil depths for all landscape positions investigated in this study from Aug. 2007 to Oct. 2009 (RT: ridgetop; MS: midslope; VF: valley floor).

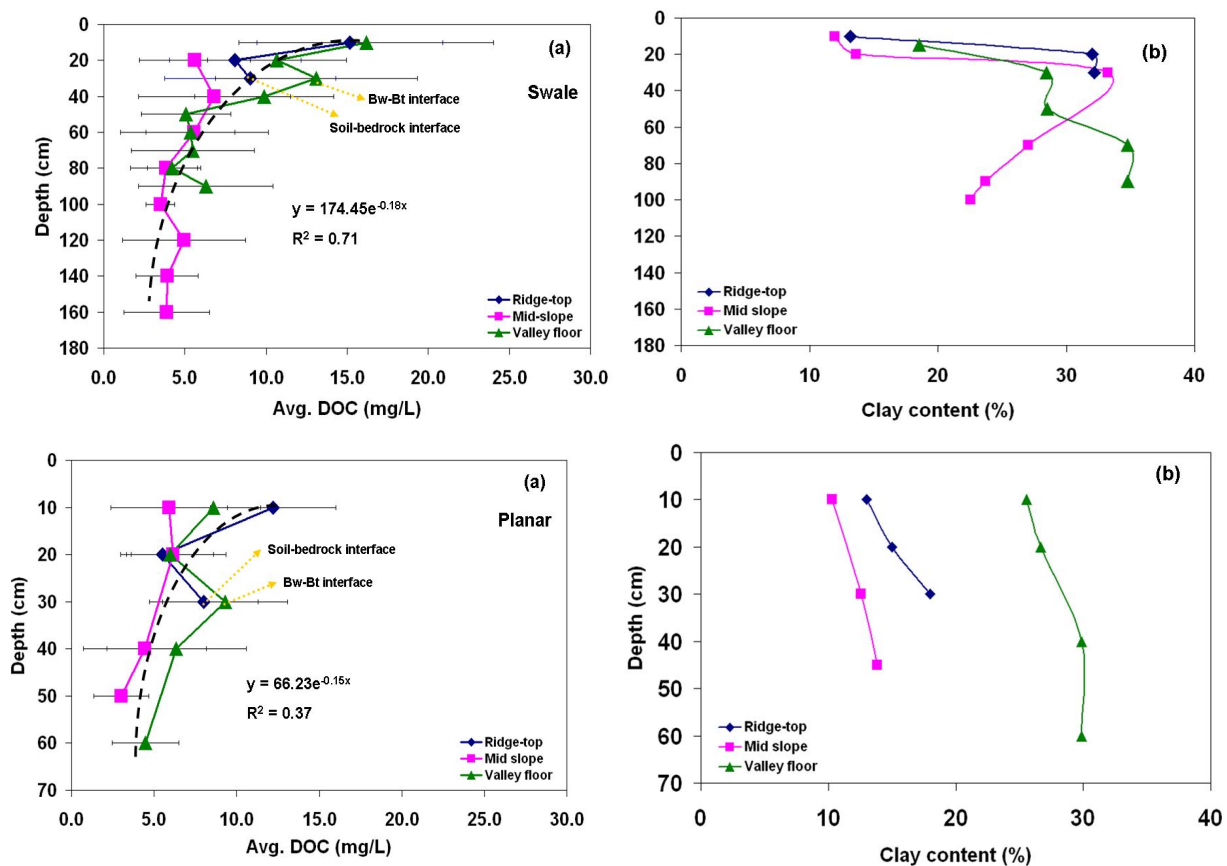


Figure 2-8: Depth function of (a) soil pore water DOC concentration (mean and standard deviation for the period from Aug. 2007 to Oct. 2009), with fitted dashed curves showing the exponential decline with depth, and (b) soil clay content (% by weight). Upper panel is for the swale transect and the lower panel for the planar hillslope transect.

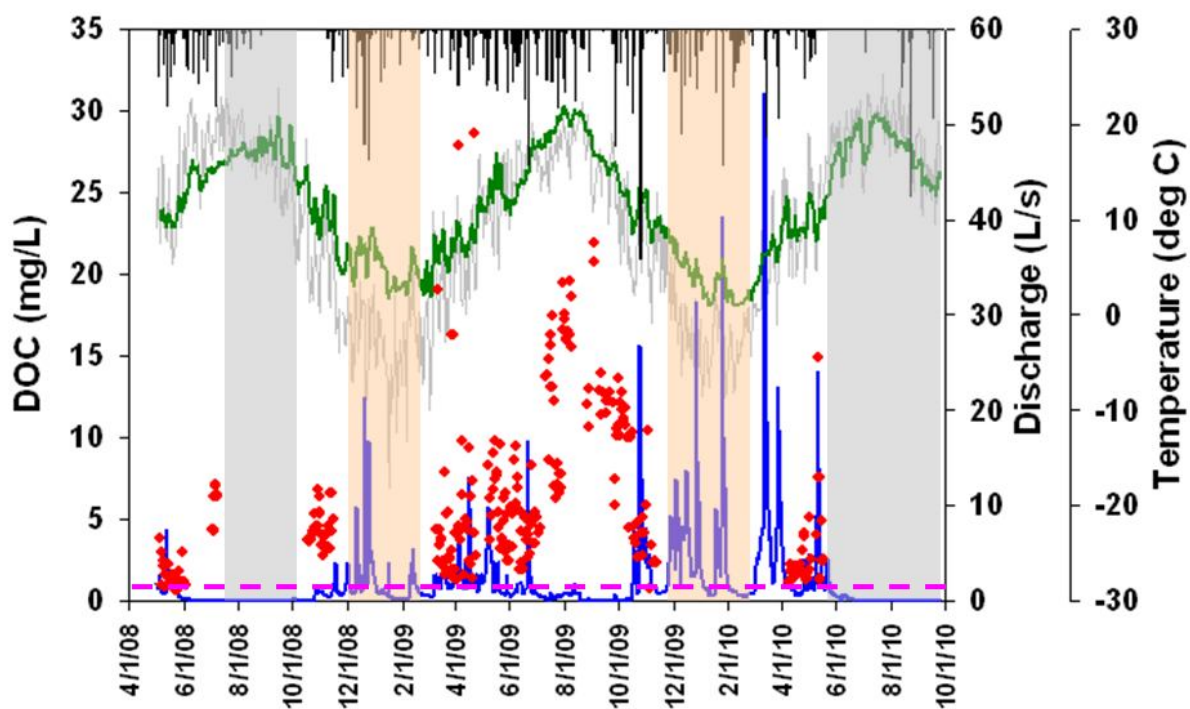


Figure 2-9: Time series data from May 2008 to Oct. 2010 for daily stream water DOC concentration (red dots), precipitation (black bar), discharge (blue line), air temperature (gray line), and stream water temperature (green line) ($n = 353$ for daily stream water DOC, with no samples collected during the summers of 2008 and 2010 due to no flow conditions and during the winters due to frozen conditions). Gray bars represent summer no flow periods and brown bars represent winter periods. The pink dashed line is groundwater DOC concentration (averaging 1.4 ± 0.5 mg/L) for this time period.

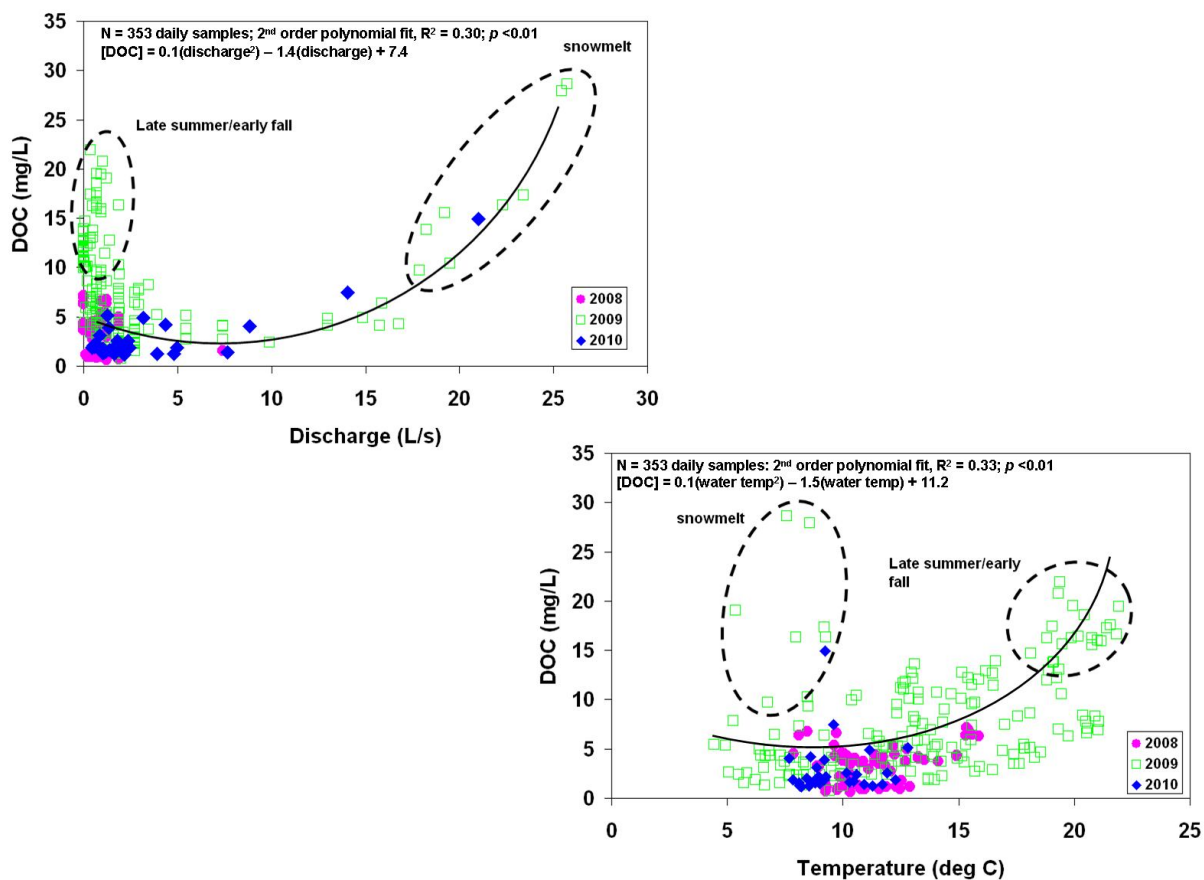


Figure 2-10: Daily stream water DOC concentration plotted as a function of (a) stream discharge and (b) stream water temperature for the period from May 2008 to May 2010 ($n = 353$, with no samples collected during the summers of 2008 and 2010 due to no flow conditions and during the winters due to frozen conditions). Only 2009 has a complete dataset for the entire year. Fitting equation is for the entire dataset from May 2008 to May 2010.

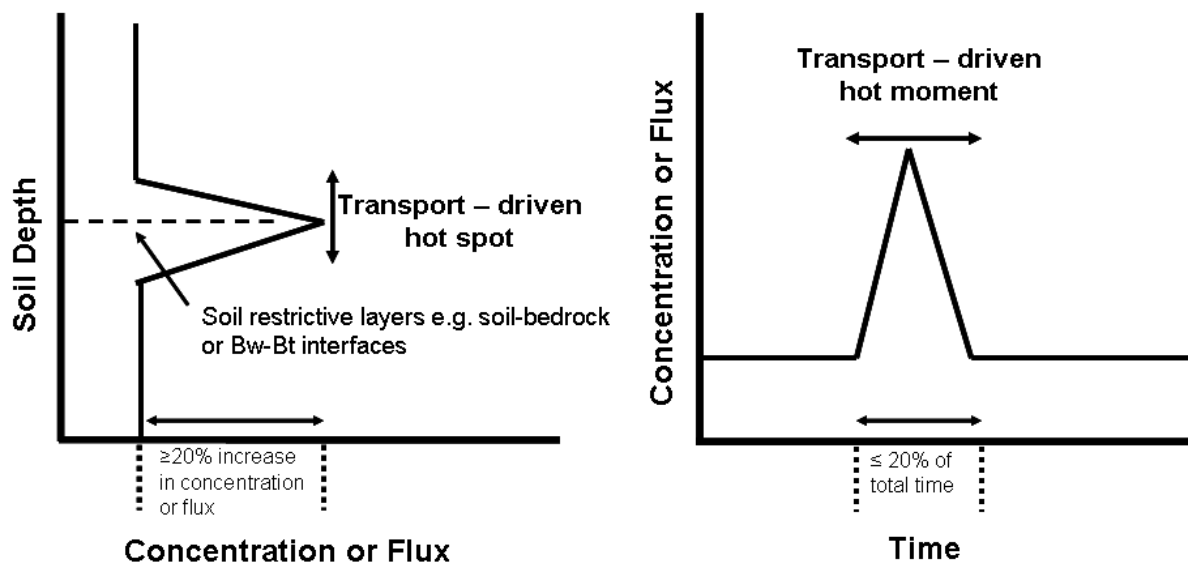


Figure 2-11: Illustration showing transport-driven hot spots and hot moments (modified from Harms and Grimm, 2008): Transport-driven hot spots are zones with elevated ($> 20\%$ increase) concentrations and/or fluxes compared to surrounding areas. Transport-driven hot moments are short periods ($< 20\%$ of total time period considered) during which solute concentrations (and/or fluxes) are elevated compared to the rest of the time period.

Table 2-1: Dissolved organic carbon (DOC) concentrations and fluxes in precipitation, throughfall, soil pore water, and stream water for various temperate forested catchments in Northeastern USA and Canada.

Site	Catchment size (ha)	Vegetation	Compartment	DOC Conc	DOC Flux	Reference
				mg/L	kg/ha/yr	
Coweeta Forest, NC, US	80 - 96	Hardwoods	Precipitation	1	-	Meyer and Tate (1983)
			Soil (0-20cm)	2 - 18	420	Soil solution collected biweekly
			2 nd order Stream	0.3 - 1.4	20	<i>Stream Flux for 1979 -1980</i>
Hubbard Brook Forest, NH, US	85	Hardwoods	Precipitation	1	16	McDowell and Likens (1988)
			Soil (15cm)	6	55	Soil solution collected weekly
			Soil (30cm)	3	23	
			3 rd order Stream	2	20	<i>Stream Flux for 1976 -1977</i>
Shale Hills CZO, PA, US	7.9	Mixed Forests	Precipitation	1	7.5	<i>This study</i>
			Ridgetop soil (10cm)	6-31, 5-16	-	<i>Range for Swale, Planar hillslope, respectively (2007 to 2009, collected weekly)</i>
			Ridgetop soil (20cm)	5-21, 3-10	-	
			Ridgetop soil (30cm)	3-28, 2-14	-	
			Valley floor (20cm)	5-22, 2-10	-	
			Valley floor (40cm)	3-19, 3-20	-	
			Valley floor (60cm)	2-10, 1-8	-	
			1 st order Stream	1 - 29	56	<i>Stream Flux for 2009</i>

Site	Catchment size (ha)	Vegetation	Compartment	DOC Conc	DOC Flux	Reference
				mg/L	kg/ha/yr	
Adirondack Park, NY, US	135	Mixed Forests	Soil (B horizon)	5 - 7	-	Inamdar et al. (2004)
			1 st order Stream	6 - 8	-	Cronan and Aiken (1985) <i>Stream Flux for 1980 – 1981</i>
Harvard Forest, MA, US	15 - 1200	Hardwoods (H) Conifer (C)	Precipitation	2	14	Currie et al. (1996)
			Soil (60cm)_H	21	123	Soil solution collected monthly
			Soil (60cm)_C	26	167	
Mount St. Hilaire, Quebec, Canada	50	Mixed Forests	Precipitation	2	-	Dalva and Moore (1991)
			Soil (A horizon)	46 - 49	-	Soil solution collected weekly
			Soil (B horizon) Streams	17 - 19 1 - 50	- -	

Table 2-2: Analysis of variance of soil organic carbon (SOC) storage for the top ≤ 1.1 m solum, showing the effects of soil horizon (A and B horizons), landform unit (ridgetop, valley floor, swale, planar hillslope), aspect (south- and north-facing slopes), and their interactions. The F value is the test statistic used to determine whether the sample means are within the sampling variability of each other, and p value is the statistical significance level.

Effects	F value	p-value
Soil horizon	1.30	0.26
Landform unit	3.24	0.07
Aspect	3.78	0.05
Soil horizon * Landform unit	1.69	0.20
Soil horizon * Aspect	0.52	0.47
Landform unit * Aspect	6.44	0.01

Table 2-3: Analysis of variance of soil pore water dissolved organic carbon (DOC) concentrations, showing the effects of landscape position, soil depth, season, and their interactions. The F value is the test statistic used to determine whether the sample means are within the sampling variability of each other, and p value is the statistical significance level.

Effects	F value	p-value
Landscape position	5.84	0.05
Soil depth	5.95	0.04
Season	1.08	0.35
Landscape position * Soil depth	5.87	0.05
Landscape position * Season	0.83	0.53
Soil depth * Season	1.01	0.42

Chapter 3

Dissolved Organic Carbon and Nitrate Patterns along Two Contrasting Hillslopes in the Shale Hills Critical Zone Observatory

Abstract

Dissolved organic carbon (DOC) and nitrate (NO_3^-) are essential to forest ecosystem functions and can provide a direct link between hillslope processes and stream water quality. Understanding hydrogeological patterns along hillslopes can reveal factors that control the spatiotemporal patterns of soil- and stream- water DOC and NO_3^- . We investigated the vertical profiles of carbon (C) and nitrogen (N) along two contrasting hillslopes (swale versus planar hillslope) and the associated headwater stream in the Shale Hills Critical Zone Observatory. Different landscape positions (ridgetop, midslope and valley floor) along both hillslopes and soil properties (depth, texture, organic carbon concentration (SOC), total nitrogen (TN), carbon to nitrogen ratio (C:N), and moisture content) were analyzed to examine their influences on C and N concentrations. Our results show that DOC and NO_3^- concentrations were higher along the swale as compared to the planar hillslope, indicating the importance of soil properties and flow dynamics (convergent versus non-convergent) on DOC and NO_3^- concentrations along the contrasting hillslopes. Along both hillslopes, the ranges in SOC (~ 0.1 to 3.0 %) and TN (0.06 to 0.20 %) exponentially decreased with increasing soil depth, with an average 60 % decrease across the A - B soil horizon interface. Soil pore water DOC (0.4 to 33.6

mg/L) also exponentially decreased with soil depth for both hillslopes, while NO_3^- (0.01 to 8.7 mg/L) did not show a significant exponential decrease within the soil profile. Soil pore water DOC were correlated with soil pore water pH, SOC, soil TN, C:N ratio, but none of these properties were significantly related to soil pore water NO_3^- . However, at the Bw-Bt and the soil-bedrock interfaces, both DOC and NO_3^- concentrations were consistently elevated as compared to other soil depths, suggesting that these horizon interfaces are the locations of lateral preferential flowpaths (short contact time) and are important to the transport of both DOC and NO_3^- along the hillslope. There were no clear seasonal trends in stream water DOC (0.6 to 28.6 mg/L) and NO_3^- (0.0 to 2.4 mg/L) concentrations, but elevated concentrations for both were observed during snowmelt and rainfall events during the early fall period suggesting flushing of shallow soil pore waters, rather than ground water (which had extremely low concentrations of DOC and NO_3^-) contributed to the elevated stream concentrations.

Introduction

Carbon (C) and nitrogen (N) cycles function and interact with each other at different spatial (e.g. laboratory, catchment, global) and temporal (e.g. event, seasonal, decades) scales; however, coupling these cycles has become one of the biggest challenges in environmental sciences because of changes in climate as well as other environmental changes such as N deposition (Lohse et al., 2008). Dissolved C and N compounds such as dissolved organic carbon (DOC), and nitrate (NO_3^-) are essential to forest ecosystem functions and can influence stream water quality (e.g. Mulholland, 1997; Bernhardt and Likens, 2002; Mitchell et al., 2003; Taylor and Townsend, 2010).

Dissolved organic C provides the link by which soil C is made available for plant and microbial uptake and affords a direct link between land and water ecosystems via the hydrologic cycle (Amundson and Sanderman, 2006). Dissolved organic C also plays a crucial role in establishing the nutrient status of a soil and actively participates in soil forming processes such as podzolization, the translocation of organo-metal (iron or aluminum complexes) downward in the soil profile (Neff and Asner, 2001; Vestin et al., 2008). However, one major gap in understanding the C cycle is that the vertical distribution of organic C in the soil remains poorly understood (Jobbágy and Jackson, 2000).

Bio-available N (particularly NO_3^-) is often a limiting nutrient for biological production. However, human activities have extensively altered the global N cycle through industrial and agricultural practices increasing the atmospheric deposition of N (Rusjan et al., 2008). The fate of this excess N in terrestrial ecosystems is not well understood but for the northeastern USA, atmospheric deposition accounts for < 40% of variation of NO_3^- (Aber et al., 2003), suggesting that other watershed properties (e.g. flow pathways) contribute to variation in NO_3^- concentrations in watersheds.

One approach to better understanding C and N patterns, at the catchment scale, is to understand the patterns along different hillslope types. Hydrologic connectivity along hillslopes is a key determinant of the movement of DOC and NO_3^- downslope (Stieglitz et al., 2003). However, while hillslopes make up the largest portion of catchments, most research has focused on riparian or valley floor areas such that DOC and NO_3^- patterns along hillslopes are poorly understood compared to riparian areas (Cirimo and McDonnell, 1997). From previous work, the Shale Hills catchment can be divided

convergent hillslopes/swales versus non-convergent hillslopes/planar hillslopes (Jin et al., 2010). As such, we expect that these different morphologies may result in differences in C and N cycling and transport due to differences in soil properties (soil type, texture, moisture, pH) and flow dynamics (particularly flow pathways).

Furthermore, while many studies have examined the interaction between DOC and NO_3^- in hyporheic zones, riparian zones and surface waters (e.g., Findlay et al., 1993; Mulholland, 1997; Hedin et al., 1998; Bernhardt and Likens, 2002; Mitchell et al., 2003; Nakagawa et al., 2008), research examining the relationship between DOC and NO_3^- dynamics along different hillslope types, at different landscape positions has been limited. The hyporheic and riparian zones are strongly associated with fluctuating water tables, when the water table rises, if DOC is available, microorganisms can remove NO_3^- (via denitrification) and thus decrease the amount of NO_3^- transported into surface waters. These zones are likely reduced enough to function as a net sink for NO_3^- and a net source for DOC (Nakagawa et al., 2008). Moreover, DOC is a critical link between energy and nutrient dynamics and often controls microbial biomass and can therefore determine microbial N demand (Bernhardt and Likens, 2002).

However, different landscape positions can influence C and N processing and transport depending on soil properties (e.g. soil depth and moisture). Soil horizon interfaces have been associated with lateral preferential flow in catchments which is important to subsurface solute transport and is important to the transport of DOC and NO_3^- to deeper soil depths (e.g. Asano et al., 2006; Bundt et al., 2001). Bundt et al. (2001) suggested that these flow paths along the hillslopes can have increased DOC and NO_3^- concentrations due to higher turnover rates (higher microbial biomass) and younger,

less recalcitrant organic matter, while Asano et al. (2006) suggested that higher DOC concentrations along preferential flow pathways were due to reduced interaction of DOM with the soil matrix .

The aim of this paper was to characterize the spatial and temporal patterns of C (in particular DOC) and N (in particular NO_3^-) in the Shale Hills catchment. Our objective was to investigate how soil and landscape features combined influence C and N concentrations along two contrasting hillslopes (swale versus planar hillslopes). Different landscape positions (ridgetop, midslope, and valley floor) along both hillslopes, together with various soil properties (depth, texture, organic carbon content, total nitrogen, carbon to nitrogen ratio, pH, and moisture content), were analyzed to examine how they influence DOC and NO_3^- concentrations in soil pore water. Our underlying hypothesis was that non-convergent planar hillslope should have different soil properties (soil type, texture, moisture, pH) and flow dynamics (particularly flow pathways) as compared to convergent swale hillslope, thus resulting in differences in C and N concentrations in both soil matrix and soil pore water.

Materials and Methods

Site description and soils

The Shale Hills catchment is a 7.9 ha V-shaped forested watershed typical of the Ridge and Valley Physiographic Province in Central Pennsylvania (Figure 3-1). The mean annual temperature is 10°C and the mean annual precipitation is 1070 mm (NOAA, 2007). This catchment is characterized by moderate slopes (up to 25-48%) and has four basic landforms: 1) south-facing slopes with deciduous forest (mostly maple, oak, and

hickory) and underbrush, 2) north-facing slopes with deciduous forest and thicker underbrush, 3) valley floor or near-stream area with evergreen trees along the western side and deciduous forest on the eastern side, and 4) topographic depressional areas (swales) with deciduous forest cover and deeper soils (Lin and Zhou, 2008). The catchment is defined by a first-order headwater stream that flows east to west into Shavers Creek, a tributary within the Susquehanna watershed.

The soils in this catchment were formed from shale colluvium or residuum, with five different soil series identified, characterized, and mapped from previous studies (Lin, 2006). The Weikert series (*loamy-skeletal, mixed, active, mesic Lithic Dystrudepts*) covers about 78% of the catchment and is a thin soil found on the hilltops or on planar hillslopes. The Rushtown series (*loamy-skeletal over fragmental, mixed, mesic Typic Dystrochrepts*) is mostly located in the center of swales and a large area at the back of the catchment and the Berks series (*loamy-skeletal, mixed, active, mesic Typic Dystrudepts*) is largely distributed along the slope transitional areas between the shallow Weikert and the deep Rushtown. The two other soil series are found in the near-stream area of the catchment, which are deep with more clay accumulations: 1) the Ernest series (*fine-loamy, mixed, superactive, mesic, Aquic Fragiudults*) which has many redox features (iron depletion areas) and a restrictive horizon (Bt) at 0.3-0.5 m depth; and 2) the Blairton series (*fine-loamy, mixed, superactive, mesic, Aquic Fragiudults*) has an argillic (Bt) horizon and few redox features starting at 1.1 m depth. Since the catchment is completely forested, all soils have about a 0.05-m thick organic layer comprised of decaying leaf litters and other organic materials. Soil thickness ranges from 0.3m at the ridgetop to >1m at the valley floor (see Lin, 2006 for details). Soils show evidence of bioturbation and

tree throw (Lin et al, 2006). Additionally, in recent history (~ 70 yrs ago), the catchment was perturbed due to clearing of forests during colonial occupation (Jin et al., 2010).

Soil and water sampling

Two hillslope transects of soil pore water sampling sites were established on the south slope of the catchment – planar hillslope (non-convergent hillslope) and swale (convergent hillslope) by Jin et al. (2010) (Figure 3-1). Along the two hillslope transects, nested porous cup tension lysimeters (Soil water samplers, 1900 series, SoilMoisture Equipment Corp., Santa Barbara, CA, USA) were installed at three landscape positions – ridgetop, midslope and valley floor - in 2006 and 2007. The lysimeters along these transects were emplaced at 10 cm to 20 cm intervals depending on the soil thickness. Soil pore waters were collected between August 2007 and November 2009 from the lysimeters using PVC tubing and a syringe. Samples for DOC analysis were placed in pre-combusted glass bottles, while samples for NO_3^- were placed in high density polyethylene plastic bottles. A portable vacuum pump was used to place a vacuum (-500 mbar) on the lysimeters approximately one week before sampling.

Soil pore waters were collected approximately weekly along both transects at the ridgetop, midslope and valley floor. However, the catchment is generally dry most of the summer and frozen during the winter, so most of soil pore water samples were collected in early spring and late fall. Also, stream and ground water samples were collected near the outlet of the catchment (Figure 3-1) using ISCO samplers (Teledyne ISCO Inc., Lincoln, NE, USA) which were programmed to collect samples daily. Precipitation

samples were automatically collected using an Eigenbrodt NSA 181/S precipitation collector (Biral, Bristol, Great Britain).

Upon collection of water samples, a portable pH meter was used to measure pH on all soil pore water samples and intermittently on stream water samples. The SymPHony SP70P pH electrode (VWR, West Chester, PA, USA) was calibrated with two pH buffers (4 and 7) on every sampling date. As well, soil moisture content (SMC) was measured approximately weekly, although sparse data was collected in winter months due to weather constraints. Soil moisture content was measured using time domain reflectometry (TDR) with a TRIME- FM3 mobile moisture meter (IMKO, Ettlingen, Germany). Details on SMC measurements were reported in Lin (2006) and Lin et al. (2006). Soil samples collected during installation of the PVC tubes for SMC monitoring were air-dried and sieved (2mm mesh size) for analysis (texture, organic matter content and pH).

Additionally, soil samples were collected at the time of lysimeter installation at 10 cm intervals by hand-augering as described previously (Jin et al., 2010). The zero depth is defined here as the bottom of the organic matter layer, i.e. the top of the mineral soil. For the planar hillslope, the ridgetop site soils were collected until auger refusal to 30cm; for the midslope to 50cm, and for the valley floor, to 60cm. For the swale, the ridgetop soils were also collected to 30cm; for the midslope to 180cm and for the valley floor 90cm. These samples were air-dried, sieved (2mm mesh size) and grounded to a fine powder for total C and N analysis.

Laboratory analyses

All DOC samples were filtered with 0.45 μm filters, acidified with two drops of 50% HCl, and refrigerated at 4°C until analysis. DOC concentrations were measured with a Shimadzu TOC-5000A analyzer (Shimadzu Scientific Instruments, Columbia, MD, USA). Nitrate analysis was performed on a Dionex Ion Chromatograph (Dionex, Bannockburn, IL, USA). To ensure data quality, a system of standards, analytical blanks (de-ionized water), replicates (every 10 samples) and spikes (25 μL of a 1000 ppm TOC standard) were used for each DOC analysis batch, while a system of standards, (de-ionized water), and replicates (every 20 samples) were used for NO_3^- analyses.

Sieved soil subsamples were used to perform particle size analysis (Kettler et al., 2001) and analyzed for organic matter content using the loss on ignition (LOI) method (Soil Survey Staff, 1996). Additionally, soil pH was measured on sieved soil subsamples with a portable SymPHony SP70P pH meter (VWR, West Chester, PA, USA) using a 1:1 (soil:water) mixture. Grounded soil subsamples were analyzed for total C and N using a CHNS-O Elemental Analyzer, EA 1110 (Leco, St. Joseph, MI, USA). A system of analytical blanks, commercial standards (every 20 samples) and replicates (every 10 samples) were used for these analyses. As little or no carbonate (< 0.01% by weight) was present in these soils, total C is considered the same as organic C (Jin et al., 2010).

Data analysis

Spatial and temporal variability were calculated for the study period using methodology described by Asano et al. (2006) and Kohlpaintner et al. (2009). Spatial variability was calculated as the coefficient of variation (CV) among lysimeters at a

certain depth for each sample date. These CVs characterize spatial variation averaged across the study period (2007 to 2009). Temporal variability was calculated as the CV for each lysimeter over all sample dates for the study period. The CV for each lysimeter represents temporal variation which was then averaged across all lysimeters.

The analysis of variance (ANOVA) was used to test significant differences in soil pore water DOC and NO_3^- concentrations over different landscape positions (ridgetop, midslope, and valley floor), soil depths (10 to 30 cm as top portion, 30 to 50 cm as middle portion, and ≥ 50 cm as bottom portion), seasons (spring - March to May, summer - June to August, and fall - September to November), and their interactions for the swale and planar hillslopes. Since DOC and NO_3^- samples were collected at different soil depths along the two hillslopes on a weekly basis during the study period, we used repeated-measures ANOVA. For this study, the soil pore water DOC and NO_3^- concentrations at a particular soil depth at a particular landscape position is the main observation, season changes within this observation and as such its effect is estimated by the repeated-measures ANOVA. We used the *proc mixed* procedure in SAS (version 9.2, SAS Institute, Cary, NC) to conduct repeated-measures ANOVA.

Results and Discussion

Spatial and temporal variability of C and N

In this study, we investigated the spatial and temporal variability of C and N concentrations along two contrasting hillslope transects - a swale and planar hillslope - at different landscape positions and soil depths. We used the coefficient of variance (CV) to compare spatial and temporal variability of DOC and NO_3^- concentrations in soil pore

waters collected from the lysimeters over 20 sample dates. Soil pore water chemistry was consistently more variable over space (CV = ~ 60%) than over time (CV = ~ 45%), since mean CV by depth (along both hillslopes) was greater than the mean CV calculated over time. Both Asano et al. (2006) and Kohlpaintner et al. (2009) observed that soil solution chemistry was more variable over space than over time. These results underscore the importance of spatial heterogeneity on soil solution chemistry as compared to seasonal patterns.

Spatial variability of DOC and NO₃⁻ in soil waters along contrasting hillslopes

For both transects, the average soil pore water DOC concentration was higher at the ridgetop and the valley floor than at the midslope and exponentially decreased with increasing depth; however, the depth distribution of soil pore water DOC concentrations differed between the swale and the planar hillslope ($p < 0.05$) (Figure 3-2). The highest DOC concentrations were measured in the A horizon for both transects at the ridgetop and at the valley floor, resulting in the largest decrease in DOC concentrations occurring across the B horizon ($p < 0.05$) (Figure 3-2). For the midslope slope position, the surface concentrations were similar to subsurface concentrations for both hillslope transects. The greatest variability in DOC concentrations was in the surface or A horizon but this variability was damped with increasing soil depth. These results are consistent with high input from throughfall and litter leachate as well as high decomposition of organic matter in the A horizon. Soil pore water DOC concentrations were higher along the swale than along the planar hillslope (Figure 3-4).

As expected, a significantly strong relationship was found between DOC concentration and soil depth (R^2 : swale ridgetop – 0.46, midslope – 0.49 and valley floor – 0.70; planar ridgetop – 0.31, midslope – 0.94 and valley floor 0.61). With respect to soil profile distribution of DOC, our findings were in agreement with previous studies of DOC in soils (Dosskey and Bertsch, 1997; Michalzik et al., 2001; Qualls et al., 2002; Jones et al., 2008; and Sanderman et al., 2008), such that, the deeper the soil depth, the lower the concentration of DOC. This is consistent with the relatively low pH and organic matter content at this site which suggest sorption by metal oxides or clays in the mineral soils. Additionally, the difference between the two hillslopes is attributed to the differences in hydrologic flow pathways since flow dynamics are such that planar hillslopes are non-convergent hillslopes and swales are convergent hillslopes where solutes may be expected to accumulate and more flow is also expected due to thicker soils.

In contrast to DOC, soil pore water NO_3^- concentrations showed a decrease with increasing depth at the ridgetop of the planar hillslope and at the midslope and the valley floor of the swale (Figure 3-3). Dittman et al. (2007) also observed NO_3^- concentrations decreasing with increasing soil depth and attributed this decline to retention within the soil profile. However, other studies have found NO_3^- concentrations to increase with increasing soil depth, which is characteristic of greater contributions from subsurface pathways with high NO_3^- concentrations (e.g. Inamdar et al. 2004; Jones et al., 2008).

The greatest variability in NO_3^- concentrations was observed at the valley floor site (30 cm for the swale, Bw-Bt horizon interface and 40 cm for the planar hillslope, Bt horizon). Soil pore water NO_3^- concentrations were also higher along the swale than the

planar hillslope (Figure 3-4). High average NO_3^- concentration at the valley floor compared to other landscape positions suggest that the near-stream area is accumulating NO_3^- and is the source of streamwater NO_3^- . Soil pore water NO_3^- though on average was < 1 mg/L, was much higher than those in N limited ecosystems (Jones et al., 2008). Additionally, lack of microbial N limitation is also supported by the presence of subsoil NO_3^- and the soil's low C:N ratio (discussed later on) (Jones et al., 2008). A significant correlation (nonlinear, power fit) was observed between soil pore water DOC and NO_3^- concentrations (like Taylor and Townsend, 2010), but DOC explained less than 8 % of the variability observed in soil pore water NO_3^- concentrations (Figure 3-5).

Like soil pore water DOC (Chapter 2), a consistent peak in NO_3^- concentration was observed at the Bw-Bt soil horizon interface for the swale at the valley floor site (Figure 3-3). Elevated soil pore water NO_3^- concentrations were also observed at the Bt horizon for the planar hillslope. These observed soil pore water NO_3^- concentrations were on average higher than the NO_3^- concentration observed at the A horizon. Moreover, the additional peaks in soil pore water NO_3^- concentrations along the planar hillslope and the swale at the midslope correspond to other soil horizon interfaces (CR-R and BC-C respectively).

While some studies within other small headwater catchments have found soil water above the Bt horizon to have consistently low DOC concentrations (e.g. Dosskey and Bertsch, 1997), this was not observed in our study. The trends observed along the soil horizon interfaces at this study site may be attributed to fast moving unabated soil water via potential lateral preferential flowpaths, that is water flowing rapidly via preferential flowpaths will have little interaction with the soil matrix and this would result in too short

of a residence time for easy uptake of C and N by plants and microbes. There are some studies of C and N dynamics that have found high concentrations of C and N along preferential flowpaths as compared to the soil matrix (e.g. Kaplan and Newbold, 1993; Feyen et al., 1999; and Bundt et al., 2001). The findings in this study are consistent with the conclusion that preferential flow pathways along these two hillslope transects are dominant controls for the transport DOC and NO_3^- . Preferential flow is common in this catchment, particularly at restrictive soil horizon interfaces or at the soil-bedrock interface (Lin, 2006; Lin and Zhou, 2008; Graham and Lin, in review).

Temporal variability of DOC and NO_3^- in soil-, stream- and ground waters

Temporal variability for soil pore water DOC for May 2008 to November 2009 is shown in Figure 3-6. There were no clear temporal trends observed during the study period, with no significant difference ($p > 0.68$) in DOC concentrations between spring and fall. Over this time period, soil pore water DOC ranged from about 15 – 30 mg/L in surface horizons and was generally less than 10 mg/L for all subsurface depths along both transects. Since soil pore waters were collected weekly, the time lag between a rainfall event and sample collection ranged anywhere between one to seven days. No significant dilution of soil pore water DOC concentrations by larger rainfall events was observed. This is consistent with the inference that DOC generation may be fast enough to sustain constant flushing in this catchment.

Unlike DOC, soil pore water NO_3^- was significantly higher ($p = 0.02$) during the spring as compared to the fall along the swale for all depths at all landscape positions but not along the planar hillslope ($p = 0.37$), where clear seasonal trends were not observed

(Figure 3-7). High soil pore water NO_3^- in the spring likely reflects a combination of low biotic activity and fast hydrologic flow pathways (Dittman et al., 2007). Some peaks in soil pore water NO_3^- concentrations occurred during certain rainfall events. These were primarily large rainfall events ($> 2\text{mm}$) but they were not consistent with the rainfall events that resulted in peak DOC concentrations.

In general, hillslope DOC concentrations were observed to be higher than stream and groundwater DOC concentrations, indicating that hillslope DOC is the source of stream water DOC. Stream water DOC concentrations were high during the snowmelt period (March - April) and peaked again as the catchment wetted up between late August and September, (Figure 3-8). During rainfall and snowmelt events, higher proportions of shallow soil pore waters (high DOC) contribute more to the stream, relative to groundwater (low DOC) (like Hornberger et al., 1994).

Over the entire sampling period, stream water DOC varied from 0.6 and 28.6 mg/L, while groundwater DOC was relatively invariant, averaging 1.4 mg/L (± 0.5). Export of DOC from the stream for 2009 was estimated as 56 kg/ha. Average stream water DOC concentration at Shale Hills was higher than other studied Hardwood study sites in tropical and temperate climates (~ 6.3 mg/L compared to 2.0 to 5.0 mg/L) but were lower compared to conifer study sites (Liu and Sheu, 2003) (see Table 2-1 for details). This difference in average stream water concentration is likely linked to catchment characteristics such as watershed size and slope, since this CZO is much smaller in size and steeper compared to the study sites compared in Liu and Sheu (2003).

In contrast to DOC, hillslope NO_3^- concentrations were not always higher than stream water concentrations. On average, stream water NO_3^- concentrations were lowest

from March to May (snowmelt period) and highest between July and October, with some peaks during snowmelt, which is consistent with rapid leaching of NO_3^- from the soils to the stream along shallow flow pathways during snowmelt (Dittman et al., 2003) (Figure 3-8). Over the entire sampling period, stream water NO_3^- varied from 0.0 and 2.4 mg/L, averaging 0.41 mg/L (± 2.0) while groundwater NO_3^- was very low averaging 0.1 mg/L (± 0.3). Export of NO_3^- from the stream for 2009 was 3.4 kg/ha. The average stream water NO_3^- concentration of this watershed is higher than the average stream water NO_3^- concentrations (0.31 mg/L) of over 300 small forested streams across the USA, but lower than the average stream water NO_3^- concentrations (0.50 mg/L) of the small forested streams in the northeast USA (Binkley et al., 2004).

In the northeastern US, some of the highest rates of anthropogenic N input occur, and inorganic N dominates both deposition and stream chemistry (Hedin et al. 1995). Nitrogen deposition in Pennsylvania is relatively high (10-12 kg N/ha/yr) (Aber et al., 2003). Precipitation at Shale Hills is currently acidic (average pH 4.4) and enriched in NO_3^- (NADP). High rates of atmospheric N-deposition suggest the lack of N limitation, which have also been observed in other studies where NO_3^- concentration exceeds that of DON in surface waters (Jones et al., 2008) and DON was below detection limit in our stream water (unpublished data). Our results do suggest that hydrological flow pathways along the two contrasting hillslopes rather than specific rainfall events are likely to have significant implications on DOC and NO_3^- transport from this catchment and catchments with similar characteristics.

Influence of soil properties on DOC and NO₃⁻

We evaluated the relationship of DOC and NO₃⁻ concentrations with site variables including soil pH, SMC, soil texture, soil organic carbon (SOC), total soil N and the C:N ratio along gradients of hillslope type, landscape position and soil depth. Soil physiochemical data were amalgamated for both transects for the different landscape positions (Table 3-1, Figures 3-9 to 3-12). Data for all soil variables showed significant correlations with soil depth ($p < 0.05$). Soil pore water pH, texture (clay percent), SMC, SOC, TN and the C:N ratio were correlated with DOC concentrations, but only soil pore water pH, SOC, TN, and the C:N ratio were found to be significantly correlated with DOC. Unlike DOC, soil pore water pH, SOC, TN, and the C:N ratio were not observed to influence NO₃⁻ concentrations.

pH. In general, the soils were acidic with an average soil pH of 4.4 ± 0.5 with no significant difference between the swale (average pH of 4.2 ± 0.2) and the planar hillslope (average pH of 4.4 ± 0.6). Average soil pore water pH was found to be 4.6 ± 0.4 , with average pH for the swale soil pore waters equal to 4.5 ± 0.4 and 4.8 ± 0.4 for the planar hillslope. Soil pore water pH was relatively acidic but increased with soil depth, as expected for soils largely formed in place from underlying bedrock or from downslope transport from higher on the hillslope as described by Jin et al. (2010). In this study, soil pore water pH and DOC had a significantly strong relationship ($p < 0.05$), but not NO₃⁻ ($p = 0.07$).

Texture. Clay content increased in the following order for both hillslope transects: valley floor > ridgetop > midslope. Although our data showed no significant association between clay content and DOC, NO₃⁻, SOC, total N or the C/N ratio; the

higher clay content in the B horizon corresponded with the decrease in DOC, total C, total N, and C/N ratio from the surface soil layer to the underlying soil layer. This observation is consistent with greater SOC/DOC adsorption to clays or metal oxides in the B horizon. Many studies have observed a significant association between soil texture (particularly clay and silt) and C and N in both temperate and tropical regions but most of these studies were conducted under agricultural or arable land-uses (including Hassink, 1997; Plante et al., 2006), so this significant relationship may not be applicable to forested ecosystems.

Soil moisture content (SMC). The two-year average of SMC increased from the ridgetop to the midslope to the valley floor for the swale at all depths; however, for the planar hillslope the two-year average SMC was highest at the valley floor but similar between the ridgetop and midslope at all depths (Figure 3-9). Soil moisture content shows evidence of influencing both DOC and NO_3^- concentrations. Consistently elevated DOC and NO_3^- concentrations at restrictive soil horizon interfaces corresponded well with higher SMC at those soil depths (discussed previously). For DOC, this relationship was not as obvious for the swale where water flow is expected to be convergent, but was clearly seen for NO_3^- . Nitrate is soluble in water and moves with soil moisture. High SMC at the restrictive soil horizon interfaces do suggest the presence of lateral preferential flow pathways, which is consistent with high concentrations of C and N along preferential flowpaths compared to the soil matrix (e.g. Feyen et al., 1999; Bundt et al., 2001).

C and N content and C:N ratio. As little or no carbonate (< 0.01 wt. %) is present in these soils (< 20m soil depth), total C is considered the same as organic C (Jin

et al., 2010). Total SOC and N content declined with soil depth for both hillslopes at all landscape positions (Figure 3-10). Consequently, the C:N ratio also declined with soil depth for all landscape positions for both hillslope types from about 15 to < 8 (Figure 3-10).

Based on all landscape positions, SOC was found to be approximately 65% lower in the B horizon compared to the A horizon for the swale and 58% for the planar hillslope. Total soil N showed the same trend except that the decline was less, averaging 38% for both hillslope transects. These trends may be due to the retention of C and N by clay minerals or metal oxides within the soil profile, especially in the B horizon or microbial decomposition of the organic matter which is expected to be higher in surface horizons as compared to the subsurface.

Unlike the synthesis for temperate forests for DOC (and DON) compiled by Michalzik et al. (2001), SOC was significantly correlated to soil pore water DOC concentration in this catchment. This is not surprising since this compilation of 42 sites (38 temperate) was not a good representation of the Shale Hills catchment since it only included one mixed forest site and only 10 of the sites had ultisols or inceptisols as the dominant soil type, which would lead to differences in SOC content and storage and therefore influence DOC concentrations and fluxes.

Across all landscape positions for both hillslope transects, the concentration of DOC in the soil profile correlated positively and significantly with SOC (non-linear regression (exponential fit), $R^2 = 0.60$, $p < 0.001$) and TN (non-linear regression (exponential fit), $R^2 = 0.59$, $p < 0.001$) (Figure 3-10). Soil organic carbon and TN was not significantly different between the swale and planar hillslopes but was higher along the

swale than the planar hillslope. Comparing both hillslope transects, SOC and TN explained 55% and 58 % of the variability in DOC concentrations along the swale respectively and 44% and 40% of the variability in DOC concentrations along the planar hillslope respectively. This finding indicates that there must be some physical control over DOC generation (Neff and Asner, 2001) and that this differs for hillslope types. Dissolved organic C concentrations were also significantly correlated to the C:N ratio (non-linear regression (exponential fit), $R^2 = 0.47$, $p < 0.05$) (Figure 3-11) (Like Aitkenhead and McDowell, 2000).

No significant relationships with SOC, total N or C:N ratio were observed for NO_3^- suggesting that the factors that control the spatial and temporal patterns of DOC and NO_3^- are not the same (Figure 3-12). In contrast, Lovett et al. (2002) found a significantly strong inverse relationship between NO_3^- export from forested watersheds in North America and soil C:N ratio. The C:N ratios synthesized in Lovett et al.'s study ranged from ~ 15 to 21 and was the best single predictor of NO_3^- . The C:N ratios of this catchment were on the lower end of this range for the surface soils. Carbon to nitrogen ratios measured for the subsurface soils for this site were less than 8 for both transects (Figure 3-10). Low C:N ratios can allow for the release of mineral N from the soil resulting in losses of inorganic N (especially NO_3^-) from the system (Schipper et al., 2004; Schilling et al., 2007). Schipper et al., (2004) suggested that C:N ratios below 10 have substantial risk of N leaching. However, persistent but small losses of NO_3^- from the system can lead to reduced accumulation of N stores and thus limit productivity (Neff et al., 2003). Low C:N ratios do also suggest a lack of N limitation (e.g. Jones et al., 2008).

Furthermore, while the soils of this watershed have a relatively low residence time (15KY), it may not be N limited but may be phosphorus limited (Jin et al., 2010). Forests such as Shale Hills with ultisols are typically phosphorus (P) limited and data collected by Jin et al., (2010) showed that there is very little P in the bedrock of Shale Hills. Wardle et al., (2004) suggested that most ecosystems that have not been subjected to catastrophic disturbances start of N limited but evolve towards P limitation. Another explanation for the observed low C:N ratios is the vegetation and acidic conditions within this watershed. Sugar maples (present within this site) are consistent with low soil C:N ratio. However, red oaks are more dominant than sugar maples at this site and soils under red oaks are known to have high C:N ratio (Lovett et al., 2002). The acidic conditions at this site may contribute to the contradictory relationship observed between vegetation and C:N ratio. Additionally, the parent material within this catchment has a very low C:N ratio (0.5 to 1.2) and may influence the C:N ratio of the soil.

Summary and Conclusions

This study elucidated C and N patterns along a convergent and a non-convergent hillslope in the forested the Shale Hills CZO. Soil profile trends of SOC, TN, and pore water chemistry showed that the main controls of DOC and NO_3^- concentrations in soil pore water are not similar. Additionally, while soil pore water DOC and NO_3^- concentrations were significantly correlated, soil pore water DOC concentrations explained very little of the variability in soil pore water NO_3^- concentrations. This is consistent with the inference that the main controls of DOC and NO_3^- concentrations in soil pore water are not similar.

Soil pore water DOC (but not NO_3^-) was significantly correlated to pH, SOC, TN, and C:N ratio. However, both DOC and NO_3^- concentrations in soil pore water were elevated at restrictive soil horizon interfaces (particularly the Bw-Bt and the soil-bedrock interfaces). Because of lateral preferential flow, elevated concentrations of DOC and NO_3^- consistently occurred at these soil interfaces compared to the surrounding soil matrix during the 2007-2009 monitoring period.

While no clear seasonal trends were observed in stream water, elevated concentrations of DOC and NO_3^- during snowmelt and rainfall events during the late summer/early fall, are consistent with higher proportions of shallow soil pore waters (high concentrations) contributing to the stream concentrations, relative to groundwater (low concentrations).

Preferential flow is common in this catchment, especially in late summer/early fall as the catchment wets-up (Graham and Lin, in review), and consistently higher DOC and NO_3^- concentrations at the restrictive soil interfaces, where preferential flow occurs, supports the proposal that higher proportions of shallow soil pore waters contribute to the higher stream concentrations of DOC and NO_3^- during late summer/early fall rainfall events in this watershed.

The extremely low C:N ratio (<10) suggest that in forested ecosystems such as this watershed, the C:N ratios may be strongly influenced by N deposition, vegetation, and parent material. Furthermore, while the soils of this watershed have a relatively low residence time (15KY) (Jin et al., 2010), it does not appear to be N limited but may be phosphorus limited, most likely due to the low phosphorus in the parent material (Jin et al., 2010). Additional studies at this CZO will address other controls (water table and

redox levels) on DOC and NO_3^- dynamics as well as the characterization of DOC and the interaction of DOC with metal oxides.

References

- Aber, J. D., C. L. Goodale, S. V. Ollinger, M. Smith, A. H. Magill, M. E. Martin, R. A. Hallett, and J. L. Stoddard. 2003. Is nitrogen deposition altering the nitrogen status of northeastern forests? *BioScience* 53(4): 375-389.
- Aitkenhead, J. A. and W. H. McDowell. 2000. Soil C:N ratio as a predictor of annual riverine DOC flux at local and global scales. *Global Biogeochemical Cycles* 14 (1): 127-138.
- Amundson, R. and J. Sanderman. 2006. Dissolved organic matter controls on terrestrial carbon sequestration and export in contrasting California ecosystems. *Kearney Foundation of Soil Science: Soil Carbon and California's Terrestrial Ecosystems Final Report: 2004215.*
- Asano, Y., J. E. Compton, and M. R. Church. 2006. Hydrologic flowpaths influence inorganic and organic nutrient leaching in a forest soil. *Biogeochemistry* 81: 191-204.
- Bernhardt, E. S. and G. E. Likens. 2002. Dissolved organic carbon enrichment alter nitrogen dynamics in a forest stream. *Ecology* 83: 1689-1700.
- Binkley, D., G. G. Ice, J. Kaye, and C. A. Williams. 2004. Nitrogen and phosphorus concentrations in forest streams of the United States. *Journal of the American Water Resources Association* 40 (5): 1277-1291.
- Bundt, M., M. Jäggi, P. Blaser, R. Siegwolf, and F. Hagedorn. 2001. Carbon and nitrogen

- dynamics in preferential flow paths and matrix of a forest soil. *Soil Science Society of America Journal* 65: 1529-1538.
- Cirno, C. P. and J. J. McDonnell. 1997. Linking the hydrologic and biogeochemical controls of nitrogen transport in near-stream zones of temperate-forested catchments: a review. *Journal of Hydrology* 199: 88-120.
- Dittman, J. A., C. T. Driscoll, P. M. Groffman, and T. J. Hahey. 2007. Dynamics of nitrogen and dissolved organic carbon at the Hubbard Brook Experimental Forest. *Ecology* 85 (5): 1153-1166.
- Dosskey, M. G. and P. M. Bertsch. 1997. Transport of dissolved organic matter through a sandy forest soil. *Soil Science Society of America Journal* 61: 920-927.
- Feyen, H., H. Wunderli, H. Wydler, and A. Papritz. A tracer experiment to study flow paths of water in a forest soil. *Journal of Hydrology* 225: 155-167.
- Findlay, S., D. Strayer, C. Goumbala, and K. Gould. 1993. Metabolism of streamwater dissolved organic carbon in the shallow hyporheic zone. *Limnology and Oceanography* 38: 1493-1499.
- Graham, C. and H. Lin. Controls and frequency of preferential flow occurrence at the Shale Hills Critical Zone Observatory: A 175 event analysis of soil moisture response to precipitation. *In review: Vadose Zone Journal*.
- Hassink, J. 1997. The capacity of soils to preserve organic C and N by their association with clay and silt particles. *Plant and Soil* 191: 77-87.
- Hedin, L.O., J. J. Armesto, and A. H. Johnson. 1995. Patterns of nutrient loss from unpolluted, old-growth temperate forests- evaluation of biogeochemical theory. *Ecology* 76: 493-509.

- Hedin, L. O., J. C. von Fischer, N. E. Ostrom, B. P. Kennedy, M. G. Brown, and G. P. Robertson. 1998. Thermodynamic constraints on nitrogen transformation and other biogeochemical processes at soil-stream interfaces. *Ecology* 79: 684-703.
- Hornberger, G. M., K. E. Bencala and D. M. McKnight. 1994. Hydrological controls on dissolved organic carbon during snowmelt in the Snake River near Montezuma, Colorado. *Biogeochemistry* 25: 147-165.
- Inamdar, S. P., S. F. Christopher, and M. J. Mitchell. 2004. Export mechanisms for dissolved organic carbon and nitrate during summer storm events in a glaciated forested catchment in New York, USA. *Hydrological Processes* 18: 2651-2661.
- Jobbágy, E. G. and R. B. Jackson. 2000. The vertical distribution of soil organic carbon and its relation to climate and vegetation. *Ecological Applications* 10(2): 423-436.
- Jin, L., R. Ravella, B. Ketchum, P.R. Bierman, P. Heaney, T.S. White, and S. L. Brantley. 2010. Mineral weathering and elemental transport during hillslope evolution at the Susquehanna/Shale Hills Critical Zone Observatory. *Geochimica et Cosmochimica Acta* 74 (13): 3669-3691.
- Jones, D. L., L. T. Hughes, D. V. Murphy, and J. R. Healey. 2008. Dissolved organic carbon and nitrogen dynamics in temperate coniferous forest plantations. *European Journal of Soil Science* 59: 1038-1048.
- Kaplan, L. A. And J. D. Newbold. 2000. Surface and subsurface dissolved organic carbon. *Streams and Groundwaters*. Edited by Jones and Mulholland. Academic Press. California, USA.
- Kettler, T.A., J. W. Dorany, and T. L. Gilbertz. 2001. Simplified Method for Soil Particle-Size Determination to Accompany Soil-Quality Analyses. *Publications*

from USDA-ARS / UNL Faculty. USDA Agricultural Research Service Lincoln, Nebraska.

- Kohlpaintner, M., C. Huber, W. Weis, and A. Göttlein. 2009. Spatial and temporal variability of nitrate concentration in seepage water under a mature Norway spruce [*Picea abies* (L.) Karst] stand before and after clear cut. *Plant Soil* 314: 285-301.
- Lin, H. 2006. Temporal stability of soil moisture spatial pattern and subsurface preferential flow pathways in the Shale Hills Catchment. *Vadose Zone Journal* 5: 317-340.
- Lin, H., W. Kogelmann, C. Walker, M.A. Bruns. 2006. Soil moisture patterns in a forested catchment: a Hydropedological perspective. *Geoderma* 131: 345–368.
- Lin, H. and X. Zhou. 2008. Evidence of subsurface preferential flow using soil hydrologic monitoring in the Shale Hills Catchment. *European Journal of Soil Science* 59: 34-49.
- Liu, C. P. and B. H. Sheu. 2003. Dissolved organic carbon in precipitation, throughfall, stemflow, soil solution, and stream water at the Guandaushi subtropical forest in Taiwan. *Forest Ecology and Management* 172: 315-325.
- Lohse, K. A., P. D. Brooks, J. C. McIntosh, T. Meixner, and T. E. Huxman. 2008. Interactions between biogeochemistry and hydrologic systems. *The Annual Review of Environment and Resources* 14:13, doi: 10.1146/annurev.enviro.33.031207.111141.
- Lovett, G. M., K. C. Weathers, M. A. Arthur. 2002. Control of nitrogen loss from forested watersheds by soil carbon:nitrogen ratio and tress species composition.

Ecosystems 5 (7): 712-718.

Michalzik, B., K. Kalbitz, J. H. Park, S. Solinger, and E. Matzner. 2001. Fluxes and concentrations of dissolved organic carbon and nitrogen: a synthesis for temperate forests. *Biogeochemistry* 52 (2): 173-205.

Mitchell, M. J., C. T. Driscoll, S. Inamdar, G. G. McGee, M. O. Mbila, and D. J. Raynal. 2003. Nitrogen biogeochemistry in the Adirondack Mountains of New York: hardwood ecosystems and associated surface waters. *Environmental Pollution* 123: 355-364.

Mulholland, P. J. 1997. Dissolved organic matter concentration and flux in stream. *Journal of the North American Benthological Society* 16 (1): 131-141.

Nakagawa, Y., H. Shibata, F. Satoh, and K. Sasa. 2008. Riparian control on NO_3^- , DOC, and dissolved Fe concentrations in mountainous streams, northern Japan. *Limnology* 9 : 195-206.

National Atmospheric Deposition Program. <http://nadp.sws.uiuc.edu/>>

National Oceanographic and Atmospheric Administration (NOAA). 2007. U.S. divisional and station climatic data and normals: Asheville, North Carolina, U.S. Department of Commerce, National Oceanic and Atmospheric Administration, National Environmental Satellite Data and Information Service, National Climatic Data Center. <http://cdo.ncdc.noaa.-gov/CDO/cdo>.

Neff, J. C. and G. P. Asner. 2001. Dissolved organic carbon in terrestrial ecosystems: synthesis and a model. *Ecosystems* 4: 29-48.

Neff, J. C., F. S. Chapin III, P. M. Vitousek. 2003. Breaks in the cycle: dissolved organic nitrogen in terrestrial ecosystems. *Frontiers in Ecology and the Environment* 1

(4): 205-211.

- Qualls, R. G., B. L. Haines, W. T. Swank, and S. W. Tyler. 2002 . Retention of soluble organic nutrients by a forested ecosystem. *Biogeochemistry* 61: 135-171.
- Plante, A. F., R. T. Conant, C. E. Stewart, K. Paustian, and J. Six. 2006. Impact of soil texture on the distribution of soil organic matter in physical and chemical fractions. *Soil Science Society of America Journal* 70: 287–296.
- Rusjan, S., M. Brilly, and M. Mikoš. 2008. Flushing of nitrate from a forested watershed : an insight into hydrological nitrate mobilization mechanisms through seasonal high-frequency stream nitrate dynamics. *Journal of Hydrology* 354: 187-202.
- Sanderman, J., J. A. Baldock, and R. Amundson. 2008. Dissolved organic carbon chemistry and dynamics in contrasting forest and grassland soils. *Biogeochemistry* 89: 181-198.
- Schilling, K. E., M. D. Tomer, Y.-K. Zhang, T. Weisbrod, P. Jacobson, and C. A. Cambardella. 2007. Hydrogeologic controls on nitrate transport in a small agricultural catchment, Iowa. *Journal of Geophysical Research* 11: G03007, doi:10.1029/2007JG000405.
- Schipper, L. A., H. J. Percival, and G. P. Sparling. 2004. An approach for estimating when soils will reach maximum nitrogen storage. *Soil Use and Management* 20: 281– 286.
- Soil Survey Division Staff. 1996. Total carbon, dry combustion, method 6A2 – Soil Survey Laboratory methods manual Soil Survey Investigations Report No 42, version 30. US Gov Print Office, Washington, DC.

- Stieglitz, M., J. Shaman, J. McNamara, V. Engel, J. Shanley, and G. W. Kling. 2003. An approach to understanding hydrologic connectivity on the hillslope and the implication for nutrient transport. *Global Biogeochemical Cycles* 17 (4), 1105, doi:10.1029/2003GB002041.
- Taylor, P. T. and A.R. Townsend. 2010. Stoichiometric controls over carbon-nitrate relationships from soils to the sea. *Nature* 464: 1178-1181.
- Vestin, J. L. K., S. H. Norström, D. Bylund, and U. S. Lundström. 2008. Soil solution and stream water chemistry in a forested catchment II: influence of organic matter. *Geoderma* 144 (1-2): 271-278.
- Wardle, D. A., L. R. Walker, and R. D. Bardgett. 2004. Ecosystem properties and forest decline in contrasting long-term chronosequences. *Science* 305: 509-513.

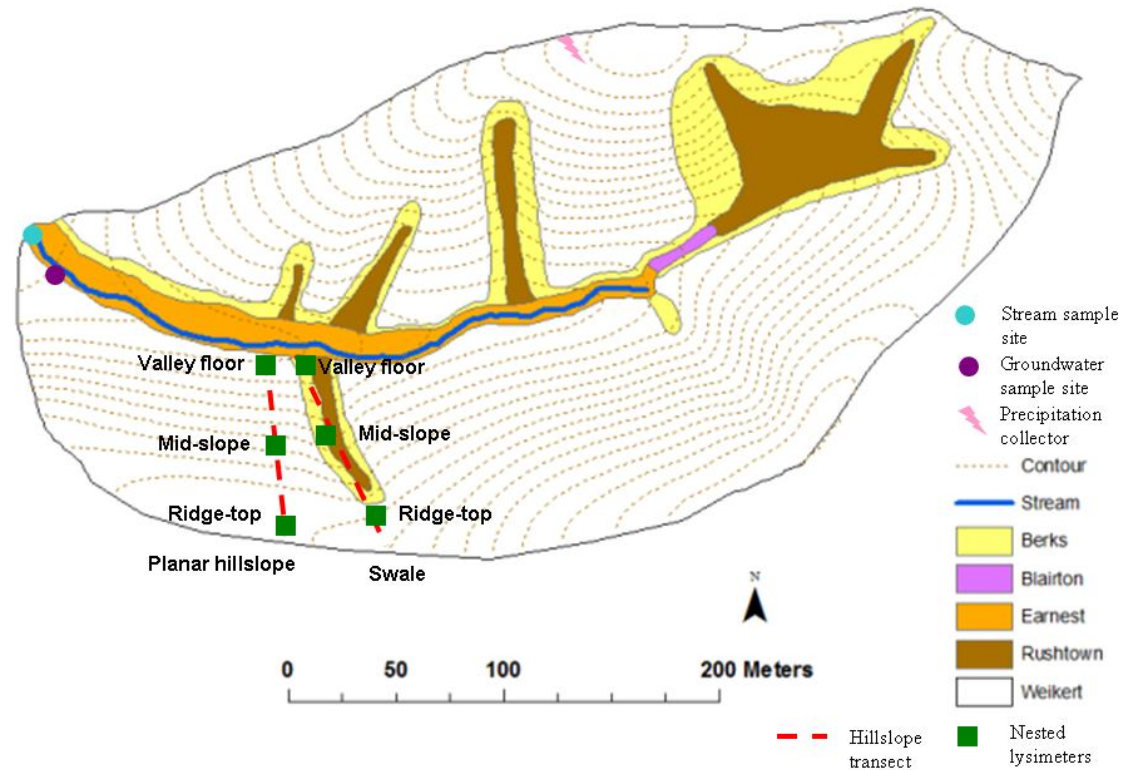


Figure 3-1: Map of the Shale Hills Critical Zone Observatory. Red dashed lines represent the swale and planar transects, green boxes represent the ridgetop, midslope, and valley floor positions, blue and purple dots at the west end of catchment represents the stream and groundwater collection points, respectively.

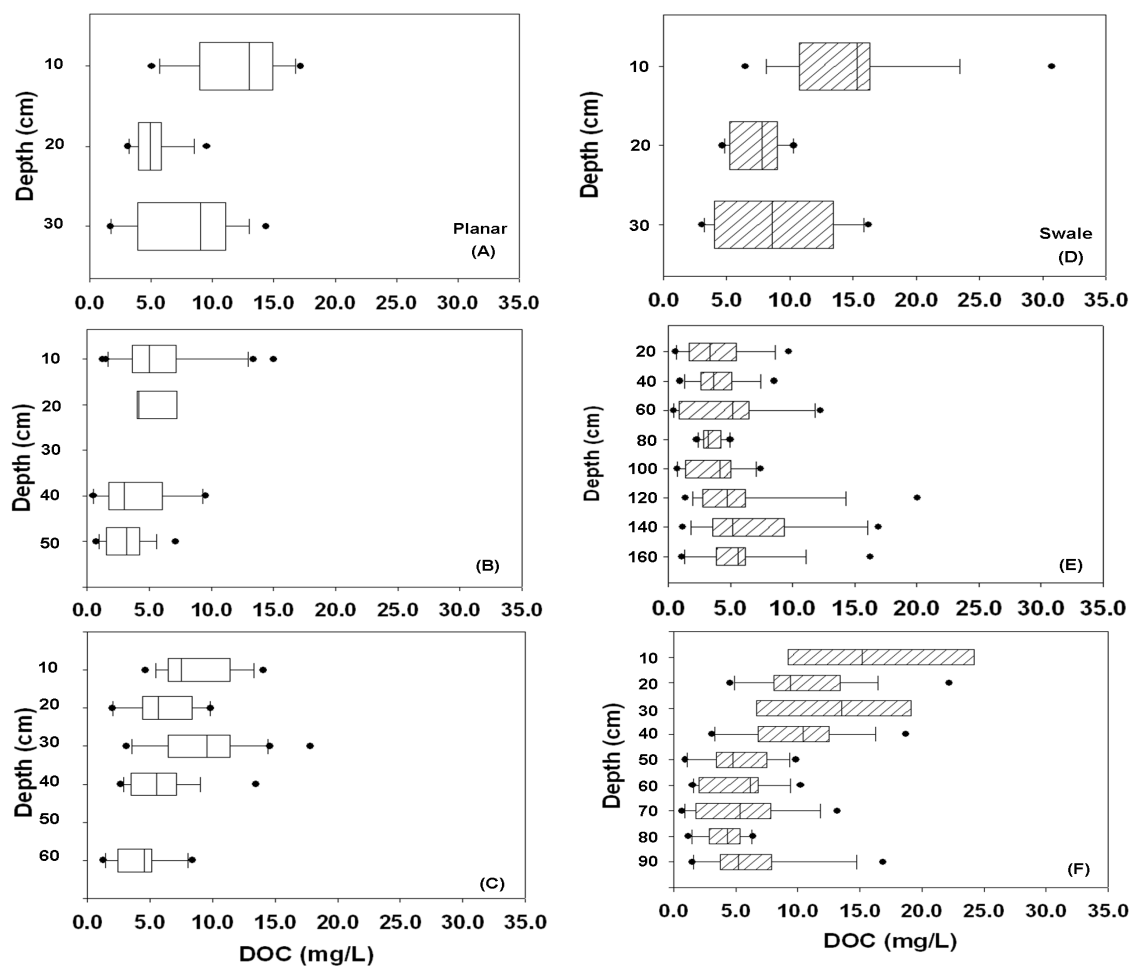


Figure 3-2 Vertical soil profile distribution of dissolved organic carbon (DOC) concentrations in soil pore water for the planar (left panel) and swale (right panel) hillslopes at the ridgetop (A, D), midslope (B, E) and the valley floor (C, F) (n = 29 sampling dates from 2007 to 2009).

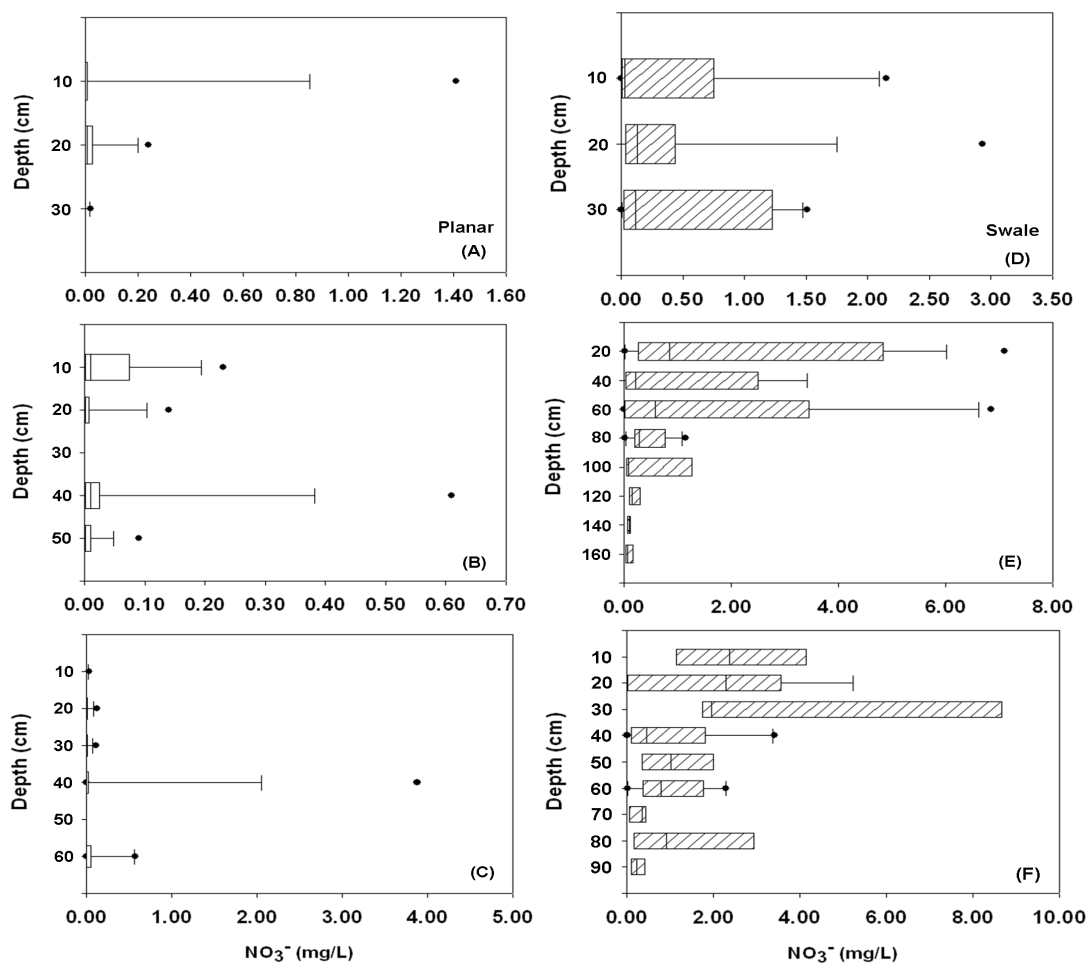
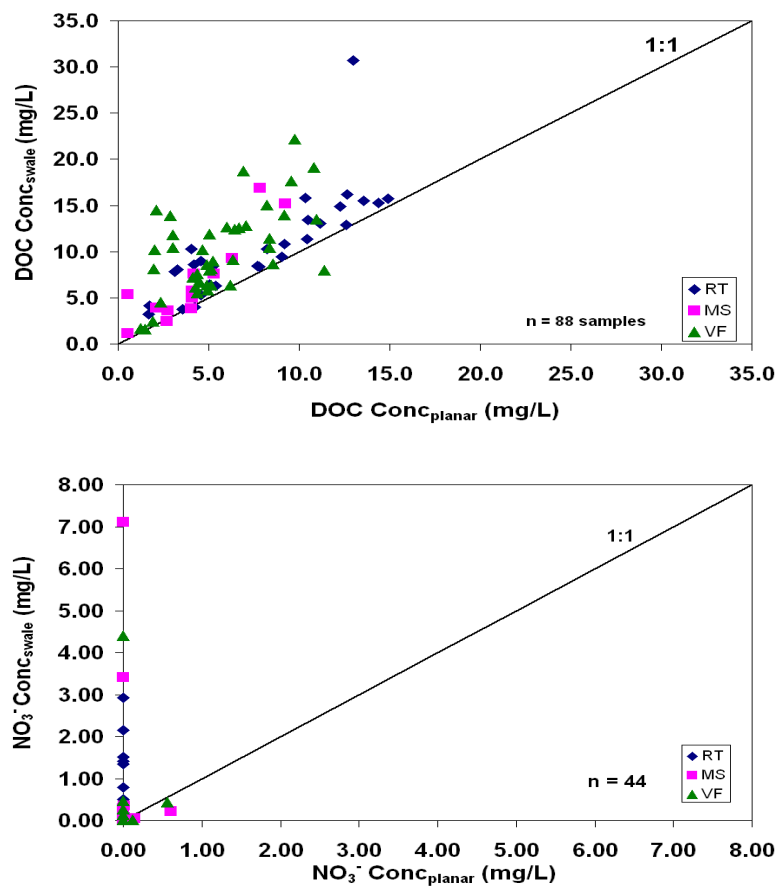


Figure 3.3: Vertical soil profile distribution of nitrate (NO_3^-) concentrations in soil pore water for planar (left panel) and swale (right panel) hillslopes at the ridgetop (A, D), midslope (B, E) and the valley floor (C, F) ($n = 29$ sampling dates from 2007 to 2009).



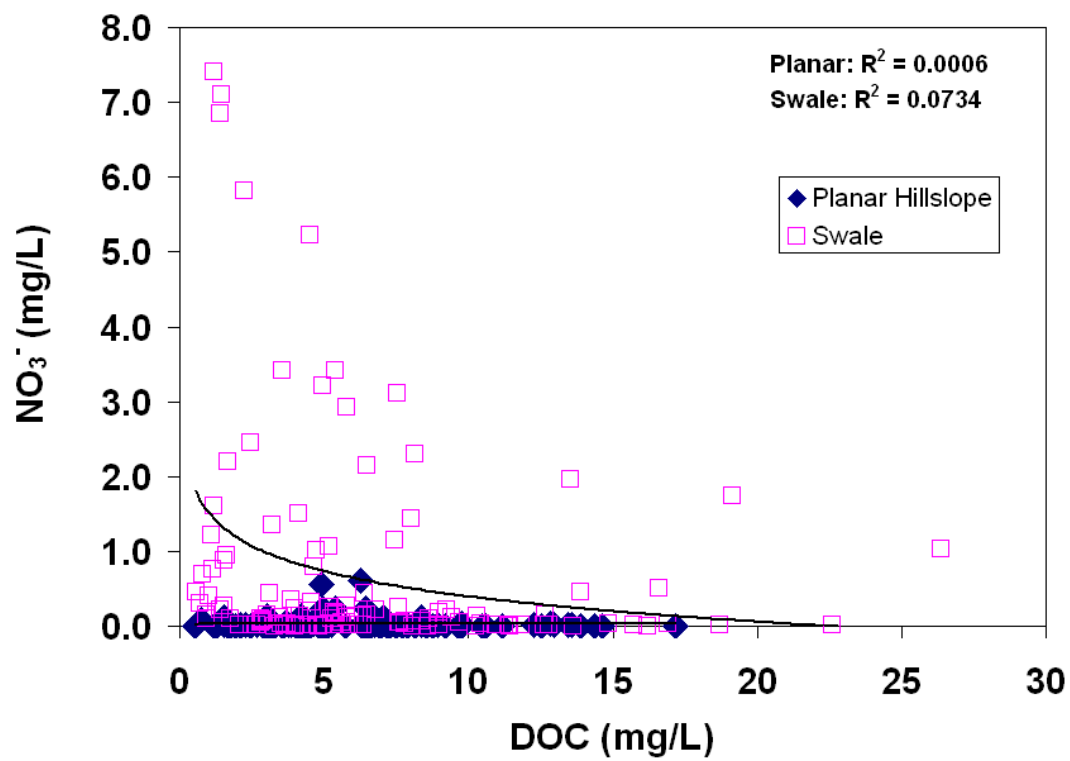


Figure 3-5: Relationship between dissolved organic carbon (DOC) and nitrate (NO₃⁻) concentrations for all soil pore water samples from 2007 to 2009 for the planar and swale hillslopes.

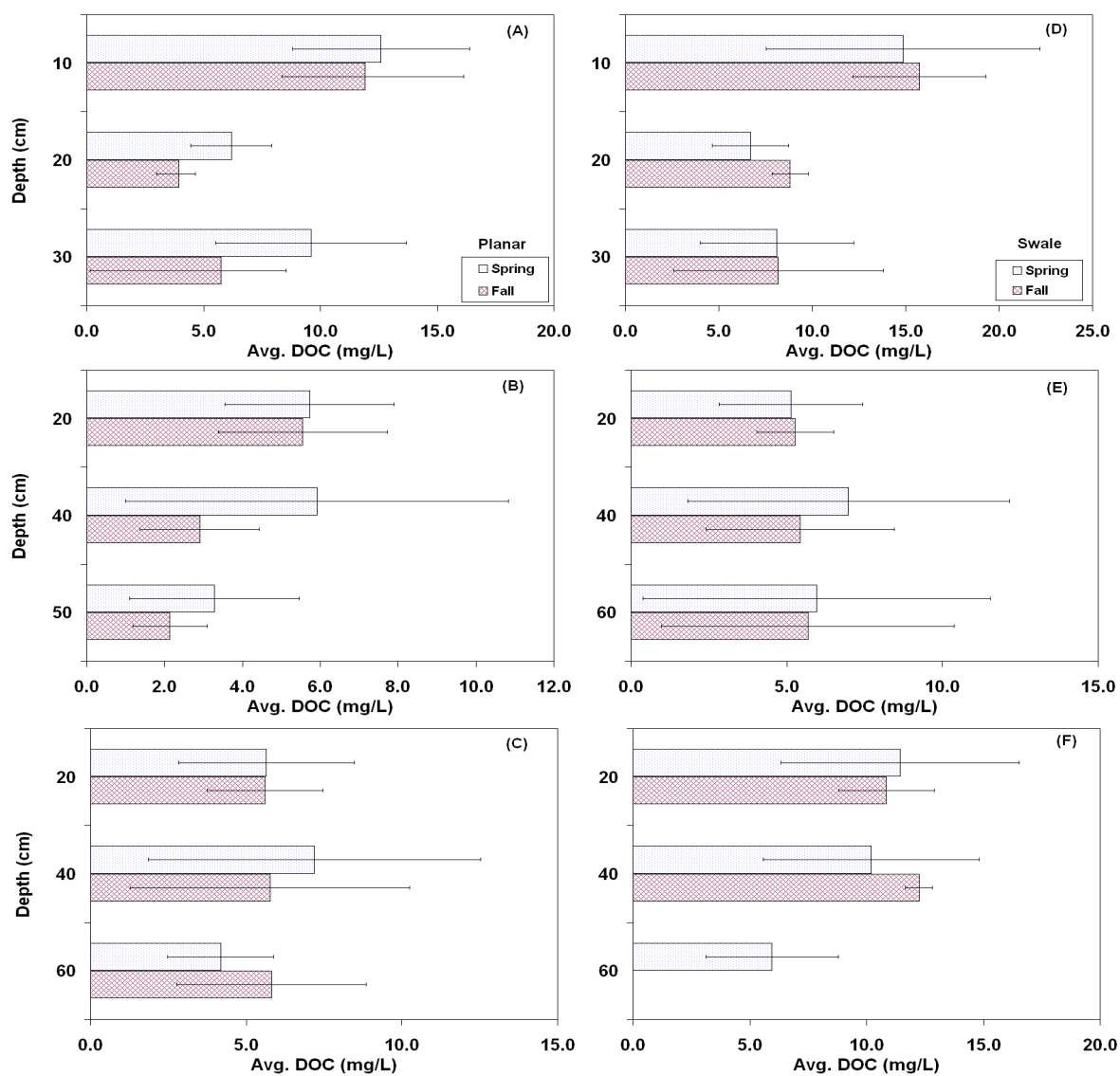


Figure 3-6: Average of weekly soil pore water dissolved organic carbon (DOC) concentrations for spring and fall for different depths at the ridgetop (A, D), midslope (B, E), and valley floor (C, F) sites for the planar (left panel) and swale (right panel) hillslopes from 2008 to 2009.

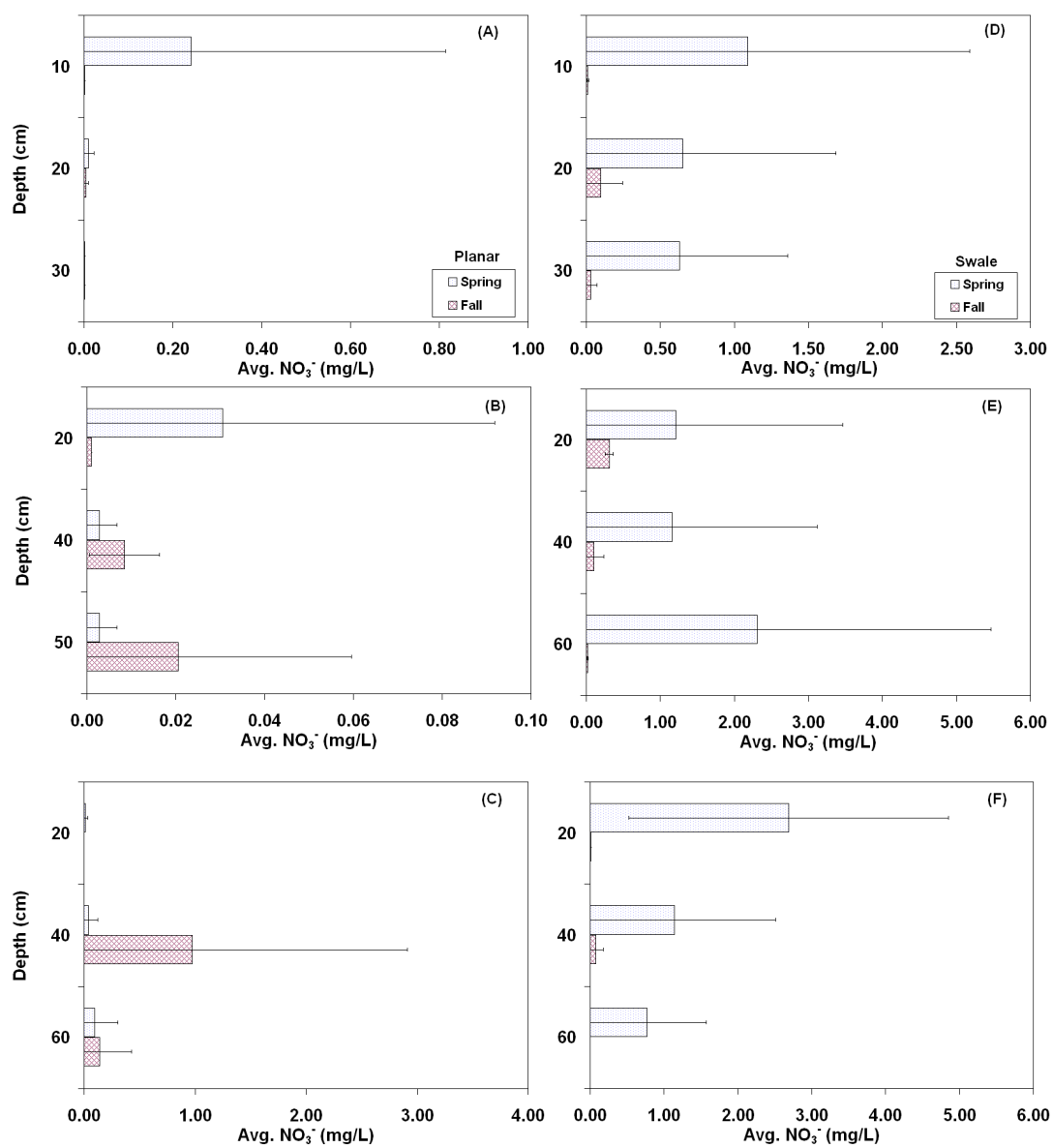


Figure 3-7: Average of weekly soil pore water nitrate (NO_3^-) concentrations for the spring and fall for different depths at the ridgetop (A, D), midslope (B, E), and valley floor (C, F) for the planar (left panel) and swale (right panel) hillslopes from 2008 to 2009.

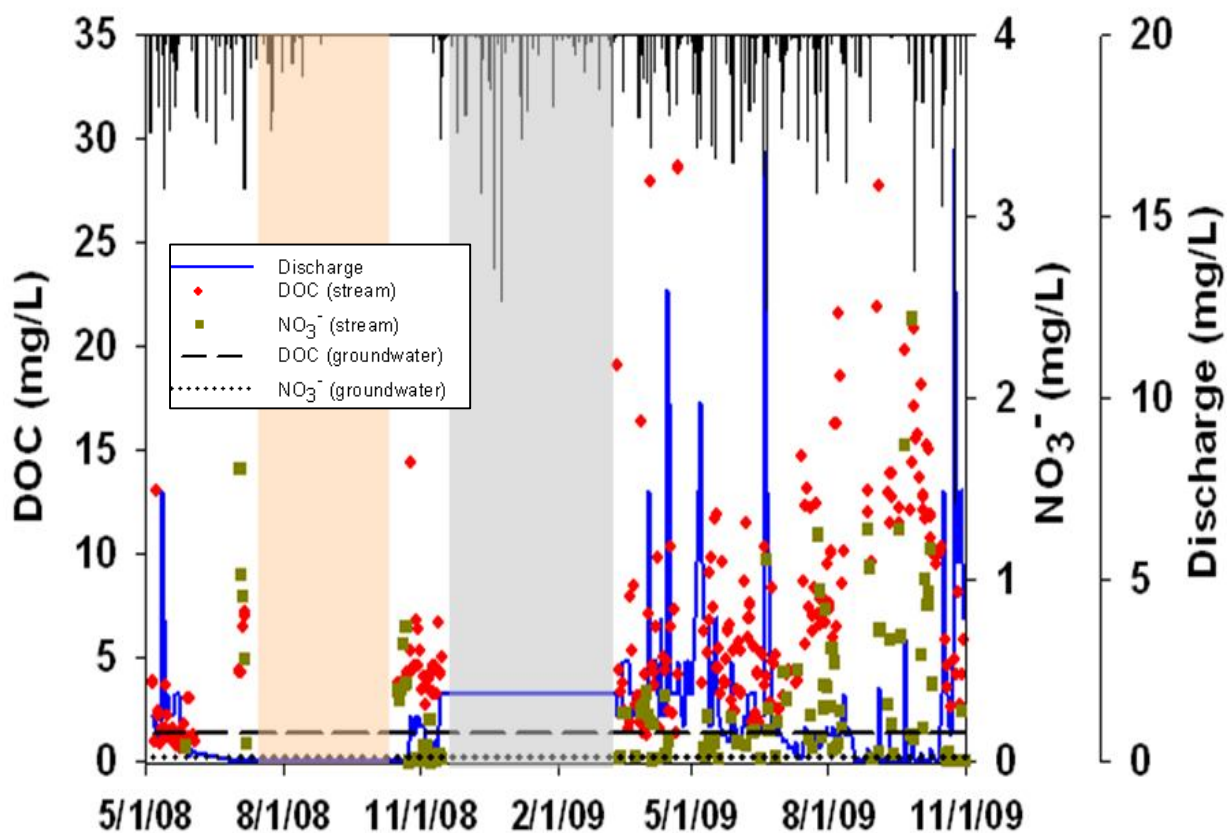


Figure 3-8: Temporal trends of dissolved organic carbon (DOC) and nitrate (NO_3^-) concentrations in the headwater stream from 2008 to 2009. Dashed line represents the average groundwater DOC concentration during this period (1.4 ± 0.5 mg/L), and dotted line represents the average groundwater NO_3^- concentration during this period (0.02 ± 0.02 mg/L). Black bars represent rainfall. Brown and gray bars represent the dry summer and frozen winter periods respectively during which no samples were collected.

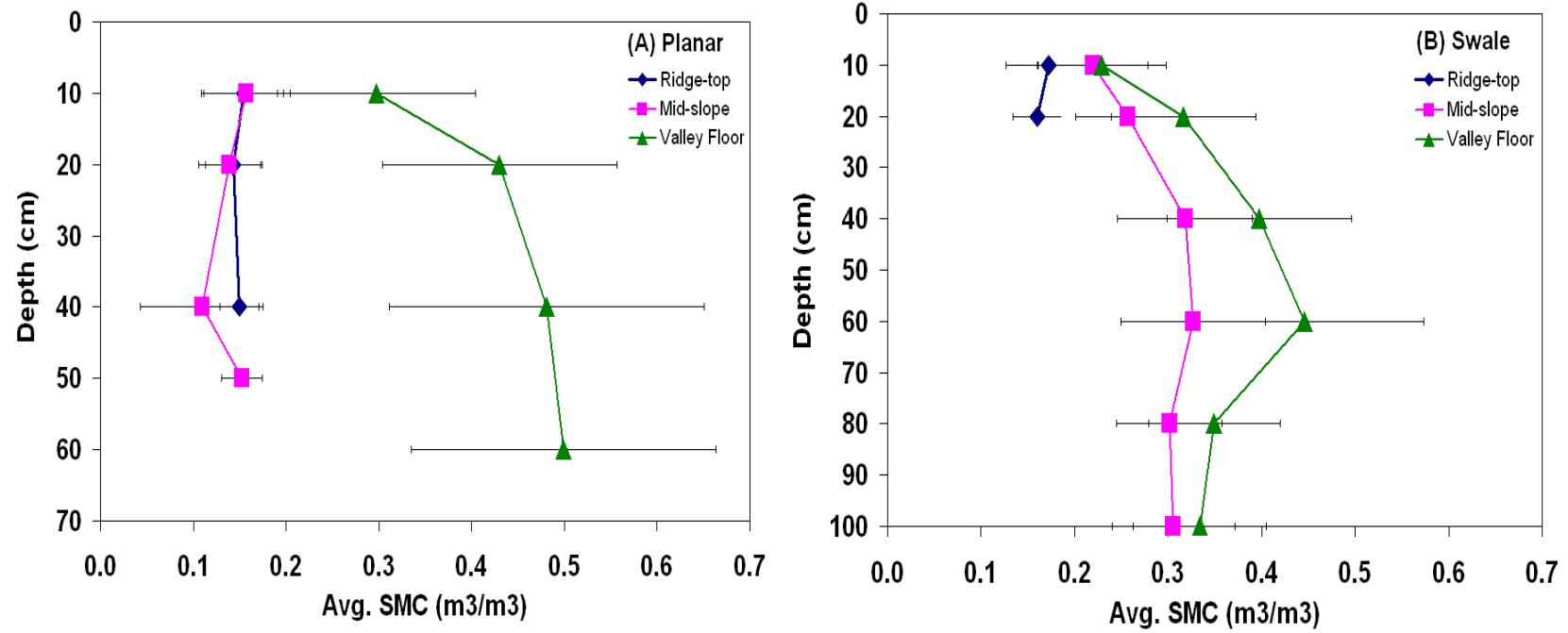


Figure 3-9: Vertical soil profile moisture content for (a) the planar and (b) swale hillslopes in different landscape positions (mean \pm SD, n = 30 sampling dates from 2007 to 2009).

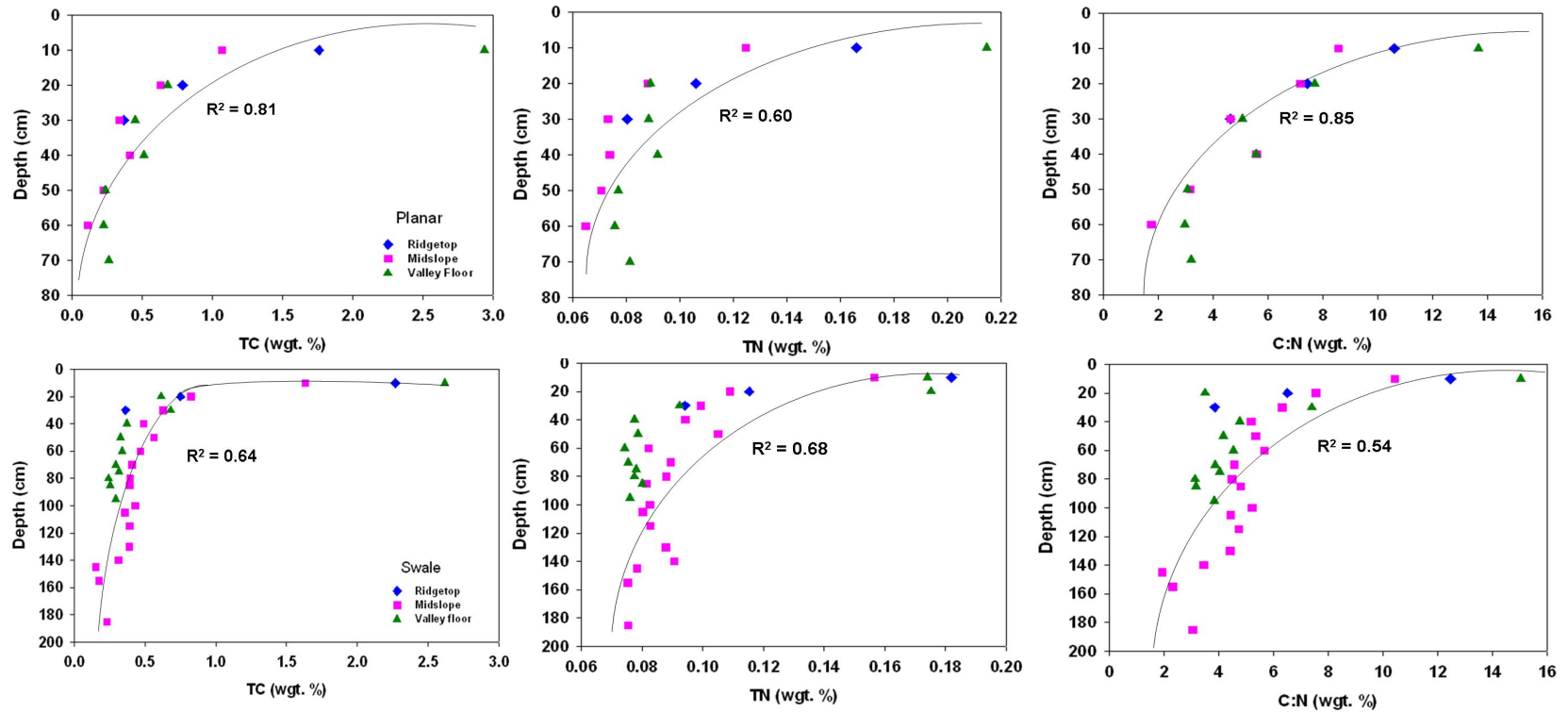


Figure 3-10: Vertical soil profile distribution of total carbon (TC), total nitrogen (TN), and C:N for the planar (upper panel) and swale (lower panel) hillslopes at different landscape positions in the Shale Hills Critical Zone Observatory.

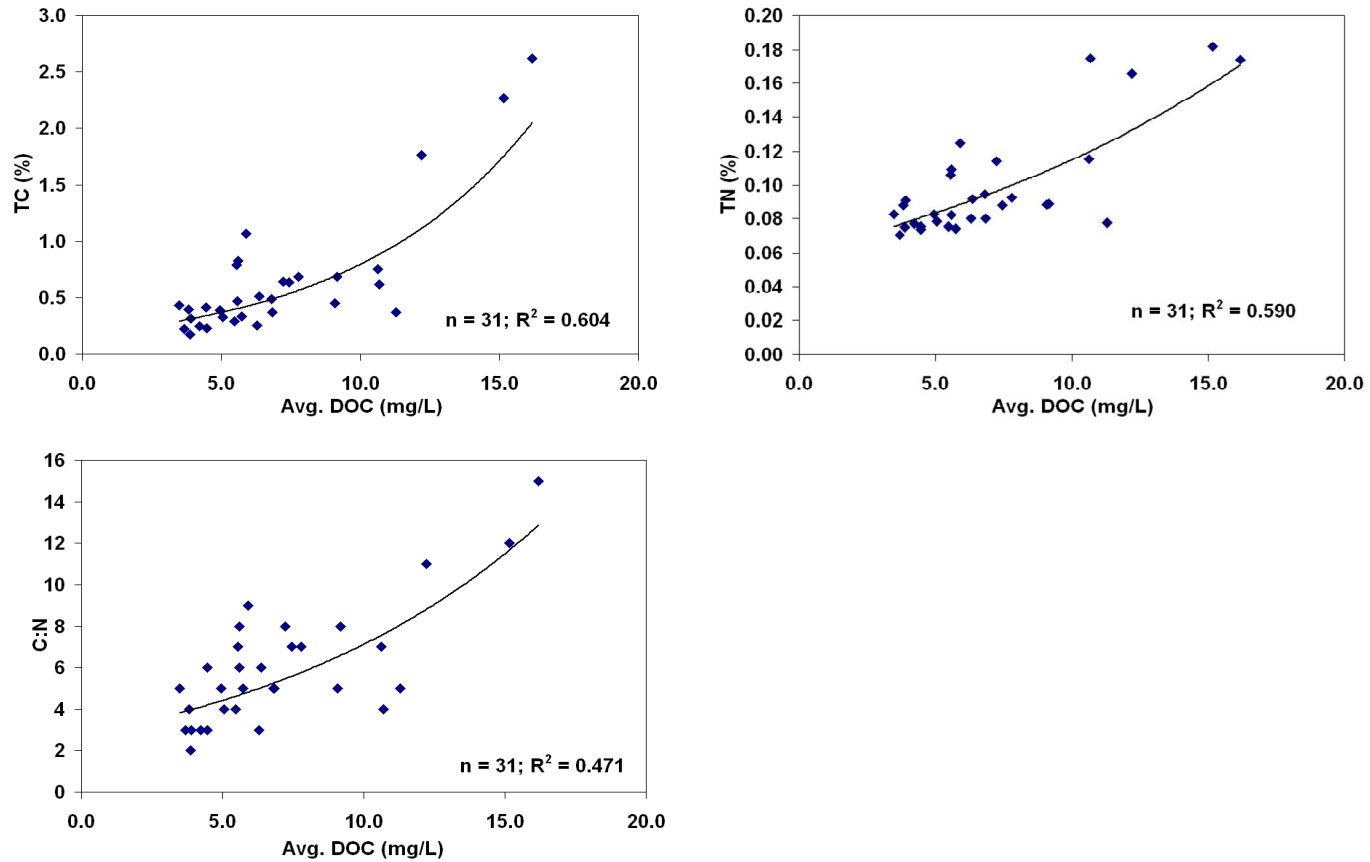


Figure 3-11: Relationship between average soil pore water dissolved organic carbon (DOC) concentration (concentrations for each lysimeter are averaged over time from April 2008 to November 2009) and (a) soil organic carbon (TC) ($p < 0.001$; $R^2 = 0.60$), (b) soil total nitrogen (TN) ($p < 0.001$; $R^2 = 0.59$), and (c) soil C:N ratio ($p < 0.05$; $R^2 = 0.47$).

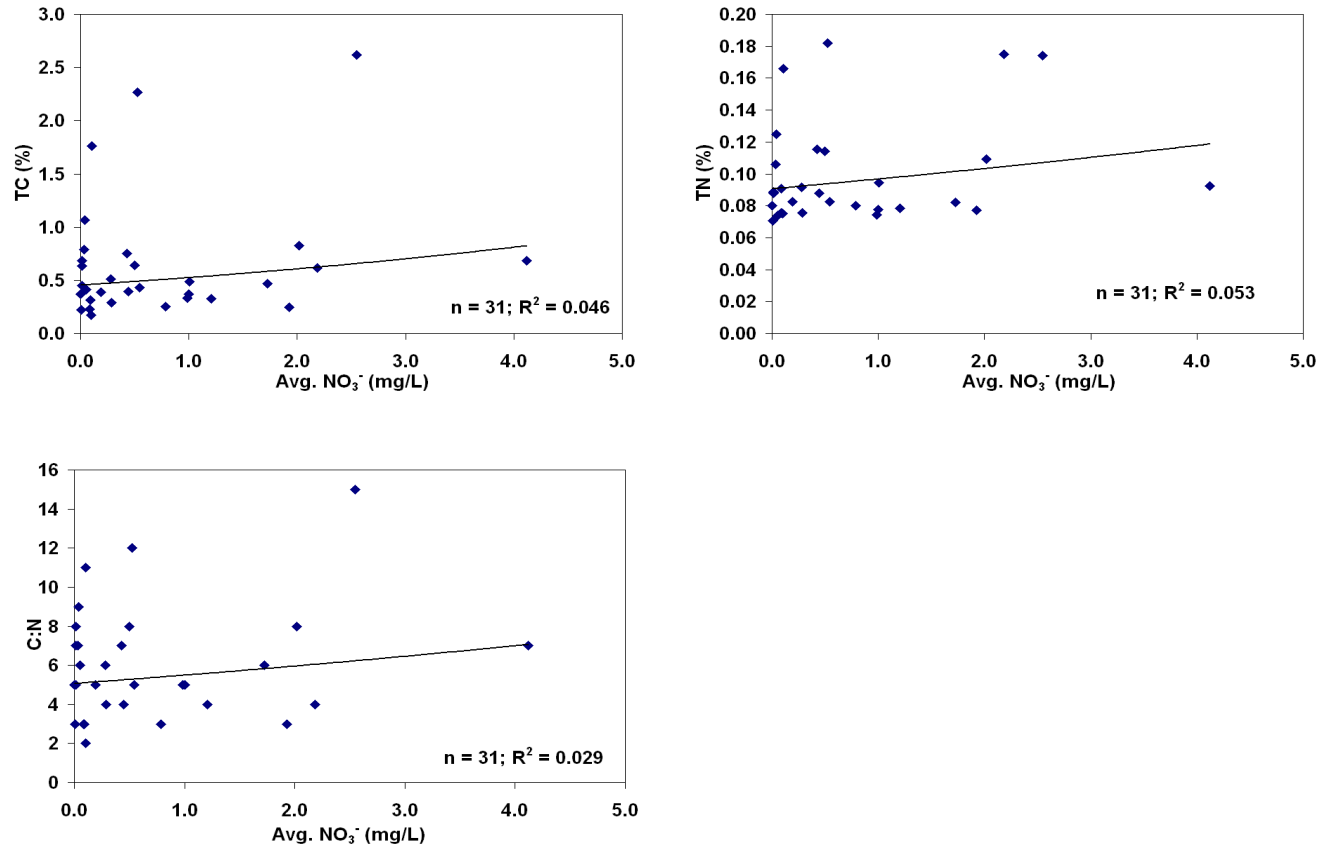


Figure 3-12: Relationship between average soil pore water nitrate (NO₃⁻) concentration (concentrations for each lysimeter are averaged over time from April 2008 to November 2009) and (a) soil organic carbon (TC) ($p > 0.05$; $R^2 = 0.05$) (b) soil total nitrogen (TN) ($p > 0.05$; $R^2 = 0.05$), and (c) soil C:N ratio ($p > 0.05$; $R^2 = 0.03$).

Table 3-1: General soil properties for the swale and planar hillslopes in the Shale Hills Critical Zone Observatory.

<i>Hillslope/Landscape Position, Soil Series Name</i>	<i>Soil horizon (Soil depth interval (cm))</i>	<i>Soil pH (1:1, Soil:Water)</i>	<i>Clay (wt. %)</i>	<i>Organic Matter Content (wt. %)</i>
<i>Swale</i>				
Ridgetop (SSRT), Weikert soil	A (5-12)	4.41	13.2	6.5
	Bw1 (12-31)	4.34	32.2	6.3
Midslope (SSMS), Rushtown soil	A (5-11)	NES	12.0	14.2
	Bw1 (11-16)	4.54	13.6	6.1
	Bw2 (16-32)	4.32	33.2	3.4
	Bw3 (32-68)	4.30	27.0	2.4
	BC (68-86)	4.40	23.7	2.2
Valley floor (SSVF), Ernest soil	AE (5-15)	3.80	18.5	4.9
	Bt1 (15-50)	4.07	28.5	3.1
	Bt2 (50-87)	4.36	34.8	3.1
<i>Planar</i>				
Ridgetop (SPRT), Weikert soil	A (5-10)	4.00	18.0	6.9
	Bw (10-28)	3.86	13.8	3.5
	C (28+)	3.95	26.3	-
Midslope (SPMS), Weikert soil	A (5-10)	4.22	10.3	16.1
	Bw (10-30)	4.11	12.6	3.6
	C (30-45)	4.09	13.8	-
	R (45-75)	4.19	12.6	-
Valley floor (SPVF), Ernest soil	AE (5-10)	4.04	25.6	11.8
	Bw (10-23)	4.65	26.7	5.1
	Bt1 (42-92)	4.86	29.9	4.1
	Bt2 (92-127)	5.45	38.0	2.7
	BC (127+)	NES	12.9	-

NES: not enough sample for analysis.

Chapter 4

Control of DOC and pH on Spatio-temporal Concentrations of Al, Fe, and Mn in Soil Pore Water and Stream Water in the Shale Hills Critical Zone Observatory

Abstract

This study investigated the relationship between metal concentrations (aluminum, iron, and manganese) and dissolved organic carbon (DOC) content and pH in soil pore water along two hillslopes of contrasting soils and topography and the associated headwater stream in the Shale Hills Critical Zone Observatory. Soil pore water DOC and metals concentrations were noticeably higher and pH was lower along the swale as compared to the planar hillslope, which is consistent with the presence of more organics in the swale as well as more percolation of acid rain through the thicker soils of the swale. Average soil pore water DOC concentrations of 264 and 191 soil pore water samples for the swale and planar hillslopes respectively were 7.1 ± 5.2 and 6.4 ± 3.8 mg/L respectively, while average soil pore water pH for the swale and planar hillslopes were 4.5 ± 0.4 and 4.8 ± 0.4 , respectively. Soil pore water concentrations of DOC and total Al, Fe, and Mn generally decreased with increasing soil depth, but pH generally increased slightly with depth. This depth function was especially evident in the swale where soils were much thicker and thus an exponential decline trend was observed. In both the swale and the planar hillslope, soil pore water concentrations of DOC and total

Al, Fe, and Mn were the highest at the ridgetop. High soil pore water DOC was likely due to higher inputs from litter leachate or organic matter decomposition, while high metal concentrations were likely due to higher inputs of acidic precipitation because of less dense canopy cover. The observed high soil pore water DOC to metal ratios (> 50) in this study area is consistent with increased solubility and mobility of organically-complexed metals. Regardless of landscape position and soil depth, the variability in soil pore water metal concentrations was best predicted by the combination of DOC and pH ($R^2 = 0.76$). In contrast to soil pore water, the relationship between DOC and dissolved metals in stream water was more complicated. Changes in stream water DOC and metal concentrations were synchronized in this catchment during the late summer/early fall wet up period such that elevated stream water concentrations of both DOC and metals (especially Fe and Mn) were observed. Average Fe and Mn stream water concentrations during the late summer/early fall wet up were approximately two times greater than the average concentrations for the entire study period (May 2008 to November 2009). Overall, the results from the study are consistent with DOC and metals being strongly correlated in this acidic forested ecosystem, such that DOC is a major facilitator of metal transport.

Introduction

Metals occur naturally in both terrestrial and aquatic ecosystems. However, with increases in acid deposition, metal contamination has become of great environmental concern. In temperate northern latitude regions, such as the northeast USA, where acid deposition is severe (Lorieri and Elsenbeer, 1997; Landre et al., 2010), there has been an

observed increase in the mobilization of metals in soils and consequential increase in surface water metal concentrations (e.g., Lorieri and Elsenbeer, 1997; Landre et al., 2010). Increases in metal concentrations may be toxic to trees, microorganisms, and aquatic life.

Many factors affect metal mobility, including chemical properties of metals, physiochemical properties of the environment, hydrologic flowpaths, and changes in climate (Landre et al., 2010). Acidity may have a major influence on metal mobility due to its control over metal solubility and speciation. Low pH increases the solubility of metal and reduces the capacity of metals to remain adsorbed to solids due to competition for negatively charged binding sites (Muscutt et al., 1993; Lorieri and Elsenbeer, 1997; van Hees et al., 2001; Lange et al., 2006; Landre et al., 2010).

Another factor that significantly influences metal mobility is dissolved organic carbon (DOC). Retention and degradation of DOC in soils is known to be closely related to the mobility and transformation of metals especially in acid forest systems, where DOC and soluble metals can be strongly interdependent (Nierop et al., 2002; Schwesig et al., 2003; Lange et al., 2006; Ogendi et al., 2007). High DOC concentrations can enhance metal complexation and increase metal solubility (Landre, et al., 2010). The organic acids in DOC are a source of acidity (dissolved protons), and by increasing acidity (the proton concentration), DOC generally increases metal solubility (Nierop et al., 2002; Schwesig et al., 2003; Cory et al., 2006; Ogendi et al., 2007).

However, DOC-metal complexes can render the metals less bio-available and less toxic to aquatic life, especially in less acidic environments (Schwesig et al., 2003; Ogendi et al., 2007). Evidenced by the observed DOC-metal correlations, the role of DOC in

metal complexation has been proposed as a primary mechanism for metal transport (Ogendi et al., 2007). However, while strong correlations between metals and C concentrations have been observed in field soils (Wagai and Mayer, 2007), DOC and its relation to dissolved metal concentrations in soil pore waters and streams is still poorly understood (Ogendi et al., 2007).

While many studies have researched aluminum (Al) due to its potentially toxic nature (e.g., Lawrence et al., 1988; Musutt et al., 1993; van Hees et al., 2000; Pellerin et al., 2001; Dijkstra and Fitzhugh, 2003; Cory et al., 2006), the interaction between DOC and metals such as iron (Fe) and manganese (Mn) in acidic ecosystems have received noticeably less attention, except as part of water quality investigations (Lorieri and Elsenbeer, 1997; Jansen et al., 2003).

Iron in its reduced form (Fe II) is more mobile than the more oxidized form (Fe III) which is the more abundant form in soils. However, in wet soils, Fe III is often reduced to Fe II and this is reflected in an increase in Fe solubility and mobility (Jansen et al., 2003; Molot and Dillon, 2003; Xue et al., 2006; Bjorkvald et al., 2008). The complexation of Fe with DOC is known to be influenced by pH such that dissolved Fe is generally precipitated rapidly with increasing pH (Jansen et al., 2003). However, the controls on dissolved Fe concentrations in stream water are complex and not clearly understood because of the abundance of different complexing agents (e.g. DOC and anions such as chloride and sulfate) in stream water and the aerobic conditions of the stream environment (Jansen et al., 2003).

Manganese, like iron, occurs in different oxidation states in the environment, with the two most common states being Mn (II) (soluble) and Mn (IV) (insoluble). Previous

studies have shown that both complexation with organic matter (Reid et al., 1981) as well as acidic and wet conditions (Gilkes and McKenzie, 1988) promote Mn transport.

Streamwater concentrations of Mn have been observed to be positively correlated with flow; however, while no clear seasonal patterns have been observed, maximum Mn export has been observed in fall during a 16-month monitoring program of two upland, headwater catchments in the Pennines, UK (Heal et al., 2002).

This study presents DOC and total metal (Al, Fe, and Mn) concentrations in soil pore water and stream water in the forested Shale Hills Critical Zone Observatory (CZO). The main objectives were to 1) evaluate the spatial patterns of total Al, Fe and Mn in soil pore water along two hillslopes of contrasting soils and topography, 2) investigate the temporal patterns of metals in soil pore water and stream water, and 3) quantify the impact of DOC and pH on metal concentrations. The hypotheses driving this research were that spatiotemporal patterns of DOC and metals are strongly linked in this acidic forested ecosystem and that DOC facilitates the transport of metals. To our knowledge, few studies have conducted extensive investigations into DOC and metal interactions at various soil depths in different landscape positions along contrasting hillslopes within the same catchment.

Materials and Methods

Site description

The Shale Hills CZO is a headwater forested catchment typical of the low-lying shale hills of the Ridge and Valley Physiographic Province in central Pennsylvania (Figure 4-1). Within the CZO is a first-order stream with 4.5% average channel gradient

(Lynch, 1976). The mean annual temperature is 10°C and the mean annual precipitation is 1070 mm (NOAA, 2007). This catchment has moderate to steep slopes (25-48%). Depth to bedrock ranges from <0.25 m at the ridge tops to over 2-3 m in the valley floor and swales (Lin, 2006). Elevation of the area ranges from 256 to 310 m from the outlet to the highest ridgetop (Lin et al., 2006).

The soils in this catchment were formed from shale colluvium or residuum and have a dominant texture of silt loam in the surface (with silty clay loam and clay loam in the B horizons in deeper soils). Five soil series have been identified (Figure 4-1), characterized and mapped based on landscape position, depth to bedrock, and redoximorphic features (Lin et al., 2006). Since the catchment is completely forested, all soils have an organic horizon comprised of decaying leaf litter and other organic material. Both the south- and north-facing slopes have primarily hardwood forest (mostly maple, oak, and hickory). On both sides of the stream, there are softwood trees (mostly pine and hemlock) along toward the western side and deciduous forest towards the eastern side.

Study design and data collections

Two transects were established on each of the north-facing and south-facing slopes of the catchment to investigate the characteristics of planar hillslopes versus swales (Figure 4-1). Nested porous-cup tension lysimeters (Soil water samplers, 1900 series, SoilMoisture Equipment Corp., Santa Barbara, CA, USA) were installed at varying depths at three landscape positions – ridgetop, midslope, and valley floor - along each transect (Jin et al., 2010). For this paper, we focus on the soil pore water DOC and metal concentrations from the two transects on the north-facing slope. Soil waters were

collected between August 2007 and October 2009 from the lysimeters using PVC tubing and a syringe. Samples for DOC analysis were stored in pre-combusted glass bottles and samples for total metal concentrations in Nalgene[®] High-Density Polyethylene plastic bottles (VWR International, West Chester, PA). Soil pore water chemistry was monitored by approximately weekly sampling. The catchment is generally dry most of the summer and frozen during the winter, so most of soil pore water samples collected in this study were in early spring and late fall.

In May 2008, collection of daily stream and groundwater samples using automated ISCO samplers (Teledyne ISCO Inc., Lincoln, NE) commenced. Stream water samples were collected at the weir located at the outlet of the stream (Figure 4-1). No stream water samples were collected during the summer of 2008 since the stream was not flowing and during the winter of 2008 and 2009 because of failure to retrieve samples from the ISCO samplers. Groundwater samples were collected from a 3.5 m deep well installed approximately 5 m from the weir (Figure 4-1). Precipitation was measured automatically using an Eigenbrodt NSA 181/S precipitation collector (Biral, Bristol, Great Britain), while stream discharge was measured at the catchment outlet using a V-notch weir with Druck continuous water level recorders (Campbell Scientific Inc., Logan, UT).

Upon collection of water samples, a portable pH meter was used to measure pH on all soil pore water samples and intermittently on stream water samples. The SymPHony SP70P pH electrode (VWR International, West Chester, PA) was calibrated with two pH buffers (4 and 7) on every sampling date. Additionally, soil samples were

collected along the two hillslope transects at varying depths (Lin et al., 2006). These samples were air-dried and sieved (2-mm mesh size) for pH analysis.

Laboratory analyses

All DOC samples were filtered in the laboratory with 0.45 μm Nylon syringe filters (VWR International, West Chester, PA), acidified with two drops of 50% HCl and refrigerated at 4°C until analysis. Analysis was performed with a Shimadzu TOC-5000A analyzer (Shimadzu Scientific Instruments, Columbia, MD). To ensure data quality, standards (0 to 20 ppm calibration standards), analytical blanks (de-ionized water), replicates (every 10 samples), and spikes (25 μL of a 1000 ppm TOC standard) were used in each analysis batch.

All samples for analysis of total Al, Fe and Mn concentrations were acidified with two drops of high purity HNO_3 . Metal concentrations were measured with an ICP- AES (Inductively coupled plasma atomic emission spectroscopy) (PerkinElmer Inc., Waltham, MA). To ensure data quality, a system of standards, analytical blanks, and replicates were used in each batch of metal analysis. Additionally, soil pH analysis was conducted on the air-dried and sieved soil samples (1:1; soil: deionized water) using the SymPHony SP70P pH electrode (VWR International, West Chester, PA).

Statistical analyses

To evaluate the spatial patterns and seasonal trends of Al, Fe, and Mn in soil pore water along the swale and planar hillslopes, we used the analysis of variance (ANOVA) to test significant differences in soil pore water metal concentrations over different

landscape positions (ridgetop, midslope, and valley floor), soil depths (10 to 30 cm as top portion, 30 to 50 cm as middle portion, and ≥ 50 cm as bottom portion), and seasons (spring - March to May, summer - June to August, and fall - September to November), as well as their interactions. Since soil pore water samples were collected at different depths along two hillslopes on a weekly basis, we used a repeated-measures ANOVA. The repeated-measures ANOVA tests the equality of means and is used when the dependent variable is measured under a number of different conditions (Delwiche and Slaughter, 2003). For this study, the soil pore water metal concentrations at a particular soil depth at a particular landscape position is the main observation, season changes within this observation, and its effect is estimated by the repeated-measures ANOVA. We used the *proc mixed* procedure in SAS (version 9.2, SAS Institute, Cary, NC) to conduct the repeated-measures ANOVA.

To understand the main factors that are significantly correlated to metal concentrations in soil pore water and stream water, multiple regression analysis was performed. For soil pore water, the dependent variable was metal concentrations, while the independent variables were DOC concentrations, and pH. For stream water, the dependent variable was metal concentrations, while the independent variables were precipitation amount, discharge, DOC concentrations, and pH. These analyses were conducted using Minitab 16.0 (Minitab Inc., State College, PA).

Results and Discussion

Spatial patterns of Al, Fe and Mn in soil pore water

Soil pore water total metal concentrations were generally higher along the swale compared to the planar hillslope (Figure 4-2a): Al ranged from 0.01 to 5.68 mg/L for the swale as compared to 0.01 to 0.72 mg/L in the planar hillslope; Fe ranged from 0.01 to 3.86 mg/L for the swale and from 0.01 to 0.28 mg/L for the planar hillslope; Mn ranged from 0.01 to 10.49 mg/L for the swale and 0.01 to 0.86 mg/L for the planar hillslope. This is likely due to the potential of higher percolation of rainfall (average pH of rainwater is 4.4) through the thicker soil profiles along the swale as compared to the planar hillslope.

The ANOVA results showed that soil pore water metal concentrations were significantly ($p < 0.05$) correlated with both landscape position and soil depth, but not season (Table 4-1). With respect to landscape position, average soil pore water Al, Fe and Mn concentrations showed the following general trend: ridgetop > valley floor > midslope for the swale (Figures 4-2a and 4-3). In the planar hillslope, the trend was similar except for Mn where the trend was: ridgetop > midslope > valley floor (Figures 4-2a and 4-3). With respect to depth, soil pore water metal concentrations in both the swale and the planar hillslopes generally decreased with increasing soil depth (Figure 4-2a).

The depth distribution of soil pore water total metal concentrations is consistent with soil pore water DOC distribution along soil depth as well as soil pore water pH. The general decrease of soil pore water DOC concentrations and the increase of soil pore water pH with increasing soil depth (Figure 4-2b) are consistent with decreasing metal concentrations with increasing soil depth as seen in this study (Figure 4-2a). High total

metal concentrations at the ridgetop and in surface soils are likely due to higher atmospheric inputs from acid deposition. Also, Jin et al. (2010) noted that low pH in surface soils of the Shale Hills catchment is consistent with divalent cations (magnesium and calcium) being replaced by Al (high Al composition of cation exchange capacity).

Elevated soil pore water Al concentrations were generally observed at 30 cm at the valley floor position (which corresponds to Bw-Bt interface) and at 20 cm at the midslope (corresponding to Bw-C horizon) in the planar hillslope (Figure 4-2a). Elevated soil pore water Fe and Mn concentrations were also observed at 30 cm at both the ridgetop (corresponding to soil-bedrock interface) and the valley floor (corresponding to Bw-Bt soil interface), as well as at 20 cm at the midslope (corresponding to Bw-C horizon) in the planar transect (Figure 4-2a). These observations were not as obvious along the swale transect. Elevated, highly variable concentrations at the restrictive soil interfaces are indicative of flushing by fast flowing waters such as preferential flow pathways, especially for Mn which is often used as an indicator of subsurface water movement (Heal et al., 2002).

Detailed soil characterization in the Shale Hills CZO has shown that Mn is elevated in the soil matrix especially at the ridgetop and in surface soils compared to the shale parent material while Fe is consistently lower in the soil compared to the parent material, which can be explained by the loss of Fe due to weathering but the gain of Mn owing to atmospheric inputs. It has been suggested that the high Mn at the ridgetop and in surface soils are from industrial sources since natural mineral dust and/or vegetative cycling could not explain the extent of Mn enrichment in surface soils (Herndon et al., 2010). Additionally, Al and Fe concentrations in the soil matrix has shown little variation

with depth for the ridge top soils, but at the middle slope and valley floor sites, concentrations of Al and Fe oxides in the soil matrix increase with increasing soil depth (Jin et al., 2010). In contrast, such trends were not observed in the soil pore water for Al and Fe (and Mn) as they decreased with increasing soil depth which suggests the influence of lower DOC concentrations and higher pH with increasing soil depth (Figure 4-2a).

Seasonal patterns of metals in soil pore water and stream water

Soil pore water metals concentrations were not significantly correlated to season based on the data collected in this study (Table 4-1). This lack of seasonal trend needs to be interpreted with caution because our field site is typically dry during the summer and frozen during the winter so our data were limited to spring and fall. A few field studies have observed seasonal trends in soil pore water metal concentrations, particularly Al. Dijkstra and Fitzhugh (2003) and Lange et al. (2006) observed high temporal variability and seasonal behavior of soil pore water Al during storms and the spring, where higher Al concentrations were observed and was attributed to DOC complexation, in mixed hardwood and coniferous forests respectively, while Tolpesha and Sokolova (2009) observed high Al concentrations in soil pore water within a coniferous forest during the spring season which they attributed to high soil water content and low pH during that season.

Average Al and Mn concentrations were found to be lower in the stream water compared to that of the soil pore water; whereas average Fe concentrations were higher in the stream compared to the soil pore water. Since groundwater concentrations of Fe are

low (Fe: 0.02 ± 0.01 mg/L) and groundwater concentrations of Al and Mn are below detection limit, it is likely that stream water concentrations are a combination of inputs from groundwater and soil water. Stream water in this watershed has been observed to be a mixture of groundwater and shallow soil water (based on isotopic investigations) where the relative proportions change seasonally (Jin et al., in review).

From May 2008 to October 2009, daily stream water total Al, Fe and Mn concentrations ranged from 0.01 to 0.15 mg/L, 0.01 to 5.99 mg/L, and 0.01 to 3.79 mg/L respectively (Figure 4-4). Seasonality was significantly correlated with stream water concentrations of Al, Fe and Mn. Stream water metal concentrations were lowest in spring and highest during the late summer/early fall (Figure 4-4). Elevated stream water concentrations (especially Fe and Mn) observed during late summer/early fall wet up period were approximately 2 times greater than the overall average of the entire study period, such that during the late summer/early fall average stream water concentrations of Fe and Mn were 0.39 ± 0.22 and 0.22 ± 0.31 respectively, while the overall average of Fe and Mn was 0.17 ± 0.42 and 0.08 ± 0.32 respectively.

The higher stream concentrations during the late summer/early fall are consistent with the flushing of organo-metal compounds from shallow soils with high DOC and metal concentrations which may have accumulated during the relatively dry summer period and then flushed when the catchment wetted up during the fall. During the low flow period of the summer, most of the stream water is recharged by groundwater, which has very low DOC and metal concentrations suggesting that stream water concentrations likely develops from flushing of accumulated DOC-metal complexes as DOC and metals are strongly linked in this watershed (discussed further below). This trend of higher metal

concentrations (and DOC:metal complexes) during the late summer/early fall has been observed in other studies and have been attributed to flushing from surface soils of other forested catchments (e.g. Heal et al., 2002; Cory et al., 2006; Lange et al., 2006).

Relationships of pH and DOC with metal concentrations in soil pore water and stream water

Based on multiple regression analysis, DOC and pH were found to be significant predictors of the variability in soil pore water metal concentrations ($R^2 = 0.76$) (Figures 4-5a and b). The R^2 was slightly improved by adding landscape position and soil depth ($R^2 = 0.78$) to the multiple regression model. This is likely due to co-linearity of variables. In comparison, daily stream water metal concentrations were significantly correlated with season ($p < 0.001$), less so by DOC ($p = 0.1$), and not by stream water pH, discharge, or rainfall amount ($p > 0.05$).

In Figure 4-5b, there are some variations from the overall smooth surface. For (a) and (d) which are the ridgetop (< 30cm) and top soil (< 30cm) respectively, the observed drop in the surface is probably due to a decrease in DOC concentrations and rise in pH in the B horizon which led to a drop in total metal concentrations. Additionally, high variability in the surface plot for the midslope (b) is likely due to the lack of variation in soil pore water pH, DOC and metal concentrations within the soil profile of the midslope for both the swale and planar hillslopes. In other words, there was a weak relationship between soil pore water pH, DOC and metal concentrations at the midslope. As for the bottom soil (f), which represented soil depths > 50cm, a less distinct relationship was observed due to the limited number of samples that were collected at depth > 50cm, most

of which were from the swale midslope which had a weak relationship between soil pore water pH, DOC and metal concentrations.

- pH and metal interactions in soil pore water and stream water

The soils in the Shale Hills catchment are acidic with an average pH of 4.4 ± 0.5 , with no significant difference between the swale (average pH of 4.2 ± 0.2) and the planar hillslope (average pH of 4.4 ± 0.6). Average soil pore water pH was found to be 4.6 ± 0.4 , with 4.5 ± 0.4 for the swale and 4.8 ± 0.4 for the planar hillslope (Figure 4-2b).

Regardless of hillslope, landscape position, or soil depth; soil pore water pH showed a negative exponential relationship with soil pore water total metal concentrations (Figure 4-6), accounting for ~50% of the variability in soil pore water total metal concentrations ($p < 0.001$). Low pH is commonly associated with a higher solubility of metal-containing phases and a lower potential for metals to remain sorbed to soil surfaces. The lower soil pore water pH observed at the shallow soil depths resulted in the higher metal concentrations observed at these depths as compared to deeper soils. Lower soil pore water pH at the shallow soil depths is likely due to input of acid rain. The metal concentration in soil solution is known to depend mainly on the soil pH but the influence of soil pH on metal behavior can be strongly modified by complexation with DOC (Alleoni et al., 2010).

Average stream water pH (5.8 ± 0.8) was significantly higher than soil pore water pH (4.6 ± 0.4). Stream water pH is likely higher than soil pore water pH because soil pore water is influenced by a combination of acid deposition and the replacement of divalent cations by Al (Jin et al., 2010), while stream water pH is likely due to increased alkalinity

of groundwater because of carbonate dissolution as well as the presence of ankerite (Jin et al., in review). Stream water metal concentrations were not significantly correlated with stream water pH but rather with seasonality (see discussion above). However, the higher pH of the stream water as compared to the soil pore water may account for the lower Al concentrations observed in the stream water because Al is not as mobile at pH greater than 5 (Dijkstra and Fitzhugh, 2003; Lange et al., 2006; Alleoni et al., 2010).

- DOC and metal interactions in soil pore water and stream water

In acid forest soils, metals can form relatively stable complexes with DOC and may be mobilized and transported through the soil profile (Marschner and Kalbitz, 2003). Like the soil pore water metal concentrations, soil pore water DOC concentrations decreased with increasing depth (Figure 4-2b). Dissolved OC concentrations were found to be significantly ($p < 0.001$) correlated with metal concentrations, thus supporting the hypothesis that DOC and metals are strongly linked (Figure 4-7). Soil pore water DOC concentrations explained ~70 % of the variability in soil pore water metal concentrations (Figure 4-7). This result is consistent with the findings of Jin et al. (2010), who suggested that Al and Fe in the Shale Hills catchment is likely transported by micron-sized particles.

Average soil pore water DOC concentrations had a positive linear relationship with soil pore water concentrations of Al ($R^2 = 0.86$), Fe ($R^2 = 0.74$), and Mn ($R^2 = 0.54$) when aggregated over all landscape positions (Figure 4-6). However, a second order polynomial fit improved the R^2 values: 0.93 for Al, 0.91 for Fe, 0.71 for Mn. The influence of DOC on metal concentration is two-fold: DOC is a source of acidity and it

forms complexes with metals (Nierop et al., 2002; Schwesig et al., 2003; Cory et al., 2006; Ogendi et al., 2007). Therefore, high DOC would decrease pH and increase the potential for forming DOC-metal complexes.

Under highly acidic pH conditions ($\text{pH} < 5$) as observed in this study, metals are known to be highly complexed with dissolved organic matter (Alleoni et al., 2010). Compared to Al and Fe, the slightly weaker correlation between Mn and DOC in soil pore waters observed in this study (Figure 4-6) has also been observed in previous studies (e.g. Heal et al., 2002). This observation may be due to the fact that Mn does not form stable complexes with organic matter to the same extent as Al and Fe (Bjorkvald et al., 2008).

The ratios of carbon to metal in soils can provide insight into the nature of organo-metal associations. High carbon to metal ratios and low pH suggest that soluble organo-metal complexes are present (Nierop et al., 2002; Jansen et al., 2003; Wagai and Mayer, 2007). Furthermore, Jansen et al. (2003) observed in their laboratory experiments that at small metal to DOC ratios (< 0.03), soluble DOM-metal complexes are dominant. In this study, metal to DOC ratios were generally below 0.03 (data not shown) suggesting that soluble DOC-metal complexes are predominant.

Average mass ratios of DOC to metal did not show a consistent trend with increasing soil depth for soil pore waters (Table 4-2). However, high soil pore water DOC to metal (particularly Al and Fe) ratios (> 50) as observed in this study is consistent with increased solubility and mobility of soluble organically-complexed metals, while low ratios (< 50) typically suggest precipitation of metals (e.g. Jansen et al., 2003; Tolpeshta and Sokolova, 2009). High soil pore water DOC to metal ratios at the

restrictive soil interfaces compared to surrounding soil depths confirm high mobility of DOC-metal complexes likely due to flushing along these restrictive soil interfaces.

Stream water metal concentrations were synchronized with stream water DOC concentrations during late summer/early fall wet up such that elevated stream water concentrations of both DOC and metals (especially Fe and Mn) were observed (Figure 4-4). This observation supports the hypothesis that DOC facilitates metal transport. Flushing of Fe and Mn when the soil re-wets after prolonged drying has been observed in other studies and can be attributed to high concentrations of soluble organically-complexed metals in shallow surface soils that can be easily flushed into the stream when the catchment wets up after high accumulation during the dry summer period (Heal et al., 2002; Bjorkvald et al., 2008). Stream water DOC to metal ratios were fairly stable for the entire study period (~ 85); however, high ratios (> 500) were observed during spring when stream water DOC concentrations were elevated compared to metal concentrations and stream flow was high.

Summary and Conclusions

We evaluated the spatial and temporal patterns of soil pore water and stream water metal concentrations and assessed the impact of DOC and pH on these concentrations in the Shale Hills CZO. The combination of soil pore water DOC and pH was found to be significantly correlated to soil pore water metal trends. Higher soil pore water DOC and lower pH explained 76% of the variability in soil pore water metal concentrations all year round. Along the two hillslopes studied, average metal concentrations were higher along the swale as compared to the planar hillslope and

generally decreased with increasing soil depth. The elevated soil pore water DOC and metal concentrations at restrictive soil interfaces (particularly the Bw-Bt horizon interface and the soil-bedrock interface) and the generally high DOC to metal ratios (> 50) indicate high mobility of organically-complexed metals along lateral preferential flow pathways.

While discharge was not significantly correlated to stream water metal concentrations during the study period, seasonality and stream water DOC were found to be significantly related to stream water metal concentrations in this CZO over the 2008-2009 monitoring period. Stream water metal concentrations were low during spring and elevated during the late summer/early fall wet up period. These stream water metal concentrations (especially Fe and Mn) showed similar trends with stream water DOC concentrations during late summer/early fall wet up. Increases in stream water DOC and metal concentrations during late summer to early fall were attributed to enhanced flushing of DOC-metal complexes after late summer/early fall storms from shallow soil horizons, as groundwater concentrations were too low to account for these elevated concentrations.

Results from this field scale study are consistent with laboratory observations (e.g. van Hees et al., 2001; Nierop et al., 2002; Dijkstra and Fitzhugh et al., 2003; Jansen et al., 2003; Molot and Dillon, 2003) that show the importance of complexation of metals with organic carbon in controlling the mobility of metals in acidic forest soils. Dissolved organic carbon appears to be a major facilitator of metal transport in this CZO.

References

- Alleoni, L. R. F., M. A. Cambri, E. F. Caires, and F. J. Garbuió. 2010. Acidity and aluminum speciation as affected by surface liming in Tropical no-till soils. *Soil Science Society of America Journal* 74 (3): 1010–1017.
- Bjorkvald, L., I. Buffman, H. Laudon, and C. Mörth. 2008. Hydrogeochemistry of Fe and Mn in small boreal streams: the role of seasonality, landscape type and scale. *Geochimica et Cosmochimica Acta* 72: 2789-2804.
- Cory, N., I. Buffam, H. Laudon, S. Köhler, and K. Bishop. 2006. Landscape control of stream water aluminum in a boreal catchment during spring flood. *Environmental Science and Technology* 40: 3494-3500.
- Delwiche, L. D. and S. J. Slaughter. 2003. *The Little SAS Book: A Primer*. 3rd Edition. Systems Seminar Consultants. Wisconsin, USA.
- Dijkstra, F. A. and R. D. Fitzhugh. 2003. Aluminum solubility and mobility in relation to organic carbon in surface soils affected by six tree species of the northeastern United States. *Geoderma* 114: 33-47.
- Gilkes, R. J. and R. M. McKenzie. 1988. Geochemistry of manganese in soils. In: *Manganese in Soils and Plants* (Eds. R. D. Graham, R. J. Hannam and N. C. Uren), 23-35. Kluwer, Dordrecht, The Netherlands.
- Heal, K. V., P. E. Kneale, and A. T. McDonald. 2002. Manganese in runoff from upland catchments: temporal patterns and controls on mobilization. *Hydrological Sciences Journal* 47 (5): 769-780.
- Herndon, E., L. Jin, and S. Brantley. 2010. Soils reveal widespread manganese enrichment from industrial inputs. *Accepted to Environmental Science and*

Technology.

- Jansen, B., K. G. J. Nierop, J. M. Verstraten. 2003. Mobility of Fe(II), Fe(III) and Al in acidic forest soils mediated by dissolved organic matter: influence of solution pH and metal/organic carbon ratios. *Geoderma* 113: 323-340.
- Jin, L., R. Ravella, B. Ketchum, P.R. Bierman, P. Heaney, T.S. White, and S. L. Brantley. 2010. Mineral weathering and elemental transport during hillslope evolution at the Susquehanna/Shale Hills Critical Zone Observatory. *Geochimica et Cosmochimica Acta* 74 (13): 3669-3691.
- Jin, L., D. M. Andrews, G. H. Holmes, C. J. Duffy, H. Lin and S. L. Brantley. Water chemistry reflects hydrological controls on weathering in Susquehanna/Shale Hills Critical Zone Observatory (Pennsylvania, USA). *In review: Vadose Zone Journal.*
- Landre, A. L., S. A. Watmough, and P. J. Dillon. 2010. Metal pools, fluxes, and budgets in an acidified forested catchment on the Precambrian Shield, Central Ontario, Canada. *Water, Air, and Soil Pollution* 209: 209–228. DOI 10.1007/s11270-0090193-7.
- Lange, H., S. Solberg, N. Clarke. 2006. Aluminum dynamics in forest soil waters in Norway. *Science of the Total Environment* 367: 942–957.
- Lawrence, G. B., C. T. Driscoll, R.D. Fuller. 1988. Hydrologic control of aluminum chemistry in an acidic headwater stream. *Water Resources Research* 24 (5): 659-669.
- Lin, H. 2006. Temporal stability of soil moisture spatial pattern and subsurface preferential flow pathways in the Shale Hills Catchment. *Vadose Zone Journal*

5: 317-340.

- Lin, H., W. Kogelmann, C. Walker, M.A. Bruns. 2006. Soil moisture patterns in a forested catchment: a Hydropedological perspective. *Geoderma* 131: 345–368.
- Lorieri, D. and H. Elsenbeer, 1997. Aluminum, iron and manganese in near-surface waters of tropical rainforest ecosystem. *The Science of the Total Environment* 205: 13-23.
- Lynch, J. A. 1976. Effects of antecedent soil moisture on storm hydrographs. PhD Dissertation. The Pennsylvania State University, University Park, PA.
- Marschner, B. and K. Kalbitz. 2003. Controls of bioavailability and biodegradability of dissolved organic matter in soils. *Geoderma* 113: 211-235.
- Molot, L. A. and P. J. Dillon. 2003. Variation in iron, aluminum and dissolved organic carbon mass transfer coefficients in lakes. *Water Research* 37:1759–1768.
- Musutt, A. D., B. Reynolds, and H. S. Wheater. 1993. Sources and controls of aluminum in storm runoff from headwater catchment in Mid-Wales. *Journal of Hydrology* 142: 409-425.
- National Oceanographic and Atmospheric Administration (NOAA). 2007. U.S. divisional and station climatic data and normals: Asheville, North Carolina, U.S. Department of Commerce, National Oceanic and Atmospheric Administration, National Environmental Satellite Data and Information Service, National Climatic Data Center. <http://cdo.ncdc.noaa.-gov/CDO/cdo>.
- Nierop, K.G. J., B. Jansen, J. M. Verstraten. 2002. Dissolved organic matter, aluminum and iron interactions: precipitation induced by metal/carbon ratio, pH and competition. *The Science of the Total Environment* 300: 201-211.

- Ogendi, G. M. R. E. Hannigan, and J. L. Farris. 2007. Association of dissolved organic carbon with stream discharge and dissolved metals concentrations in black shale draining streams. *Developments in Environmental Science* 5: 247-272.
- Pellerin, B. A., I. J. Fernandez, S. A. Norton, and J. S. Kahl. 2002. Soil aluminum distribution in the near-stream zone at the Bear Brook watershed in Maine. *Water, Air, and Soil Pollution* 134: 189–204.
- Reid, J. M., D. A. MacLeod, and M. S. Cresser. 1981. Factors affecting the chemistry of precipitation and river water in an upland catchment. *Journal of Hydrology* 50: 129-145.
- Schwesig, D. K. Kalbitz, and E. Matzner. 2003. Effects of aluminum on the mineralization of dissolved organic carbon derived from forest floors. *European Journal of Soil Science* 54: 311-322.
- Tolpeshta, I. I. and T. A. Sokolova. 2009. Aluminum Compounds in Soil Solutions and their migration in Podzolic soils on two-layered deposits. *Eurasian Soil Science* 42 (1): 24-35.
- van Hees, P., U. S. Lundström, M. Starr, and R. Giesler. 2000. Factors influencing aluminum concentrations in soil solution from podzols. *Geoderma* 94: 289-310.
- Wagai, R. and L. M. Mayer. 2007. Sorptive stabilization of organic matter in soils by Hydrous iron oxides. *Geochimica et Cosmochimica Acta* 71: 25-35.
- Xue, N., H. Seip, J. Guo, B. Liao, and Q. Zeng. 2006. Distribution of Al-, Fe- and Mn-pools and their correlation in soils from two acid deposition small catchments in Hunan, China. *Chemosphere* 65: 2468–2476.

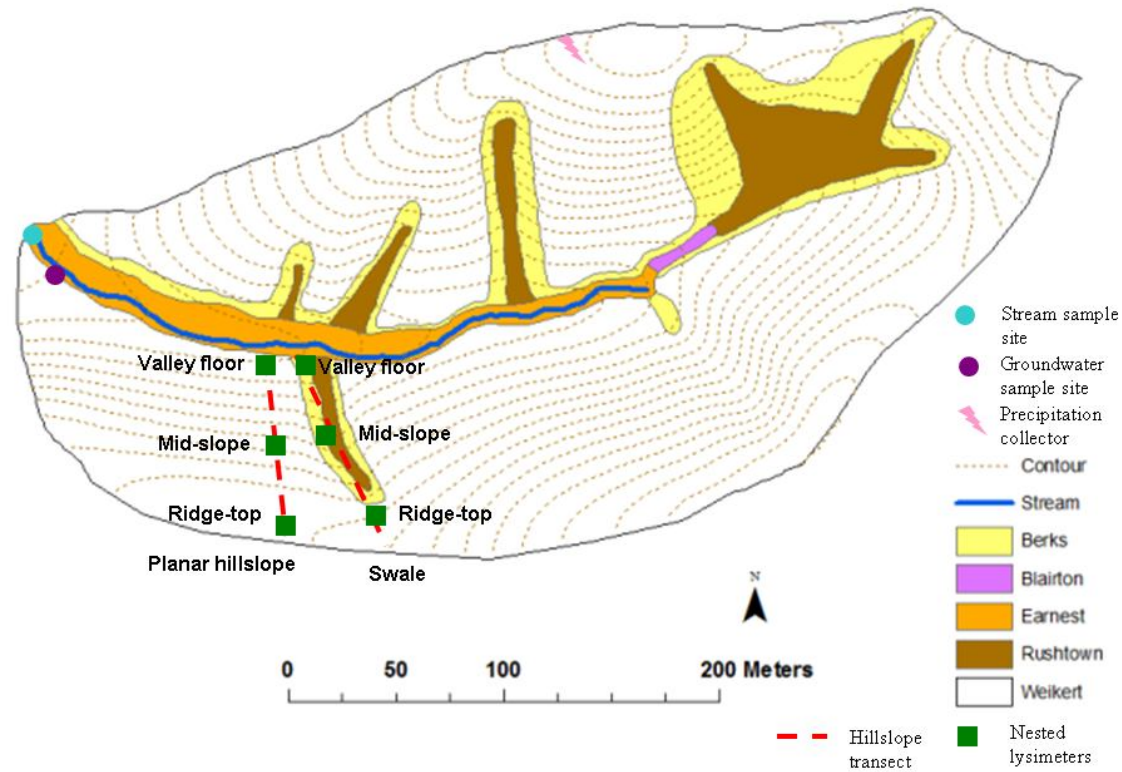


Figure 4-1: Map of the Shale Hills CZO in central Pennsylvania and the location of the hillslope transects monitored (Jin et al., 2010). Red dashed lines represent the swale and planar transects; green boxes represent the ridgetop, midslope, and valley floor positions (SPRT – planar hillslope ridgetop, SPMS – planar hillslope midslope, SPVF – planar hillslope valley floor position, SSRT – swale ridgetop, SSMS – swale midslope, and SSVF – swale valley floor).

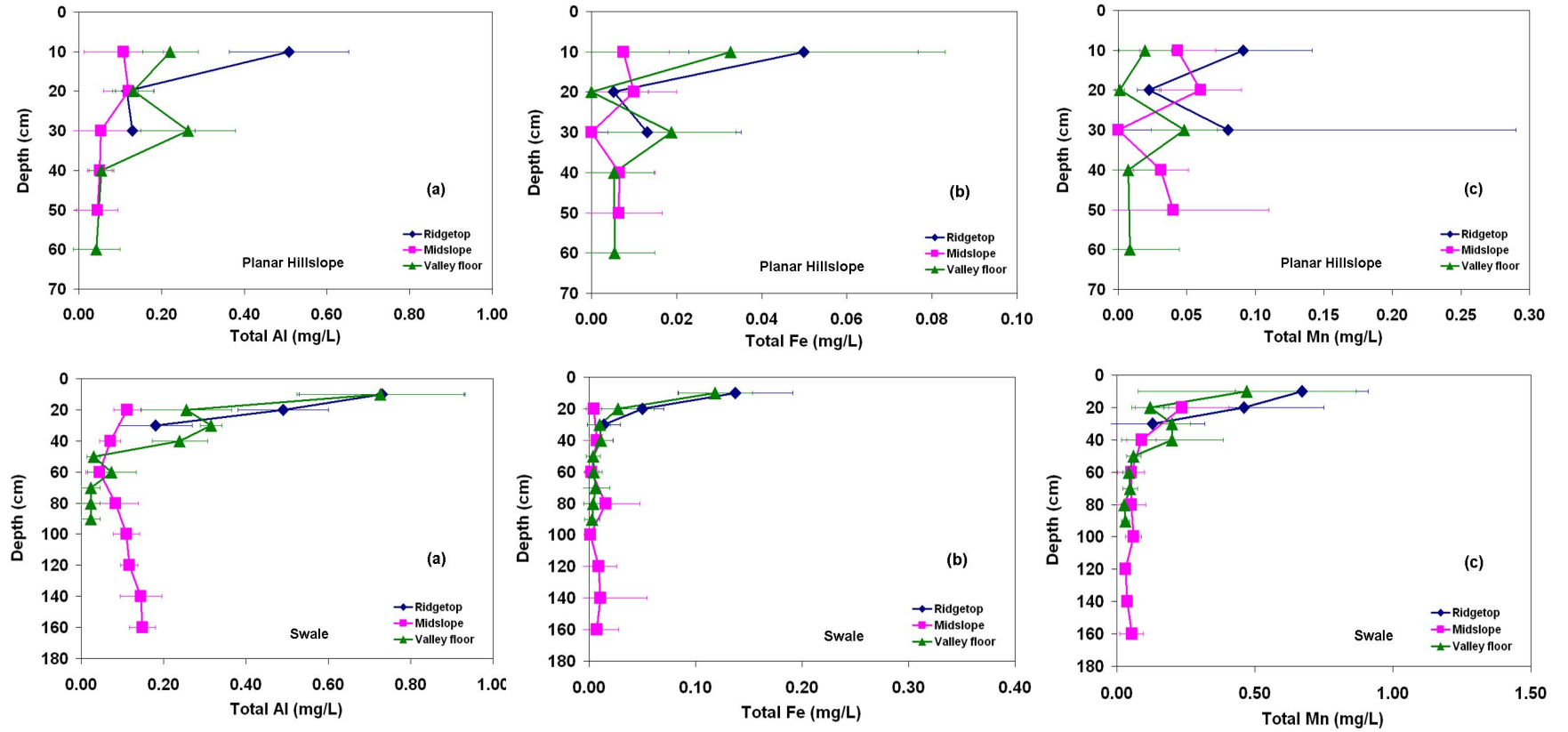


Figure 4-2a: Depth profiles of soil pore water concentrations of total Al (a), Fe (b), and Mn (c) (mean and standard deviation from Aug. 2007 to Oct. 2009, n = ~ 20 sample dates). Upper panel is for the planar hillslope transect and the lower panel for the swale transect.

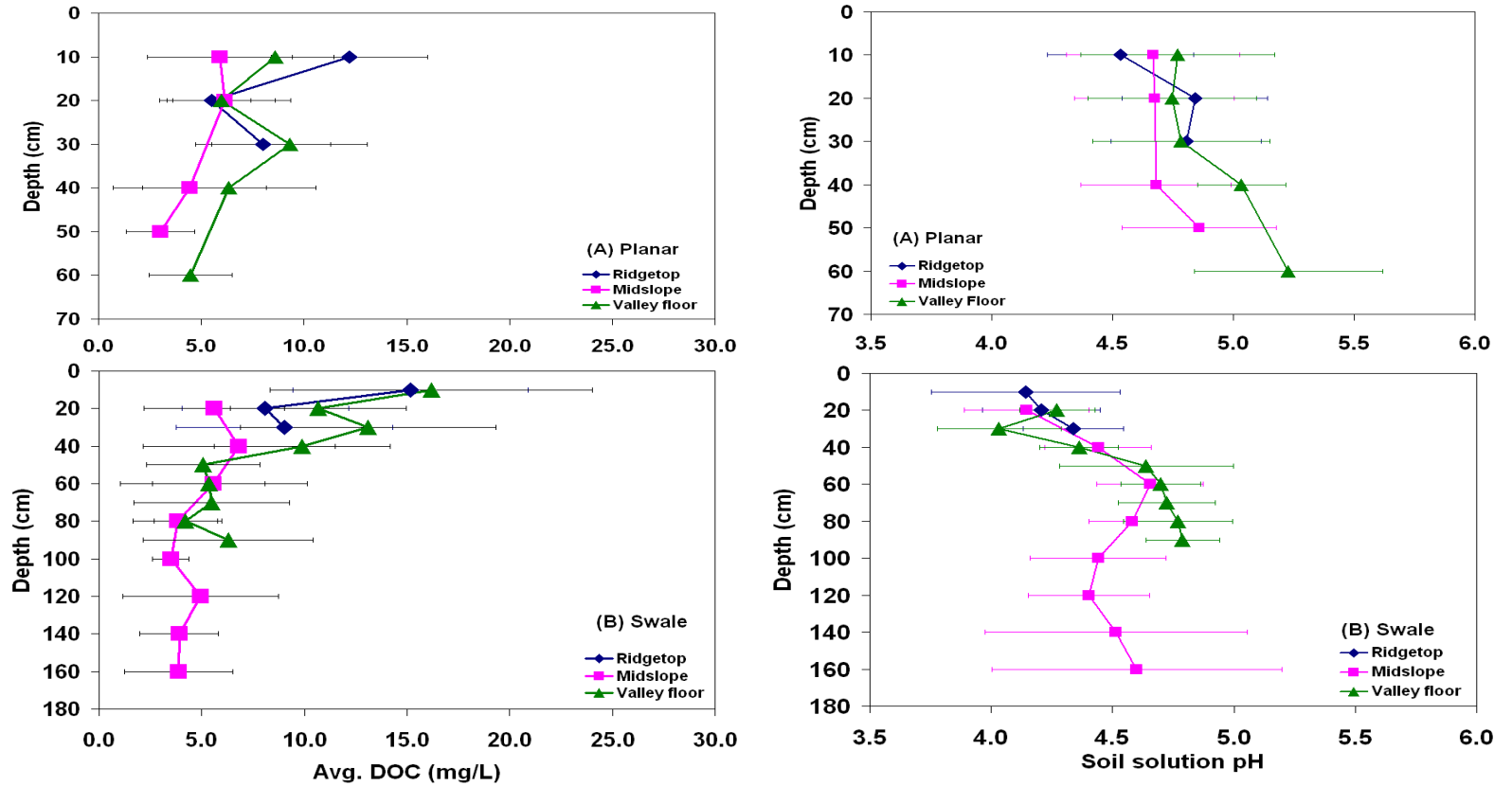


Figure 4-2b: Depth profiles of soil pore water concentrations of DOC (left panel) and pH (right panel) (mean and standard deviation from Aug. 2007 to Oct. 2009, n = ~ 20 sample dates). Upper panel is for the planar hillslope transect and the lower panel for the swale transect.

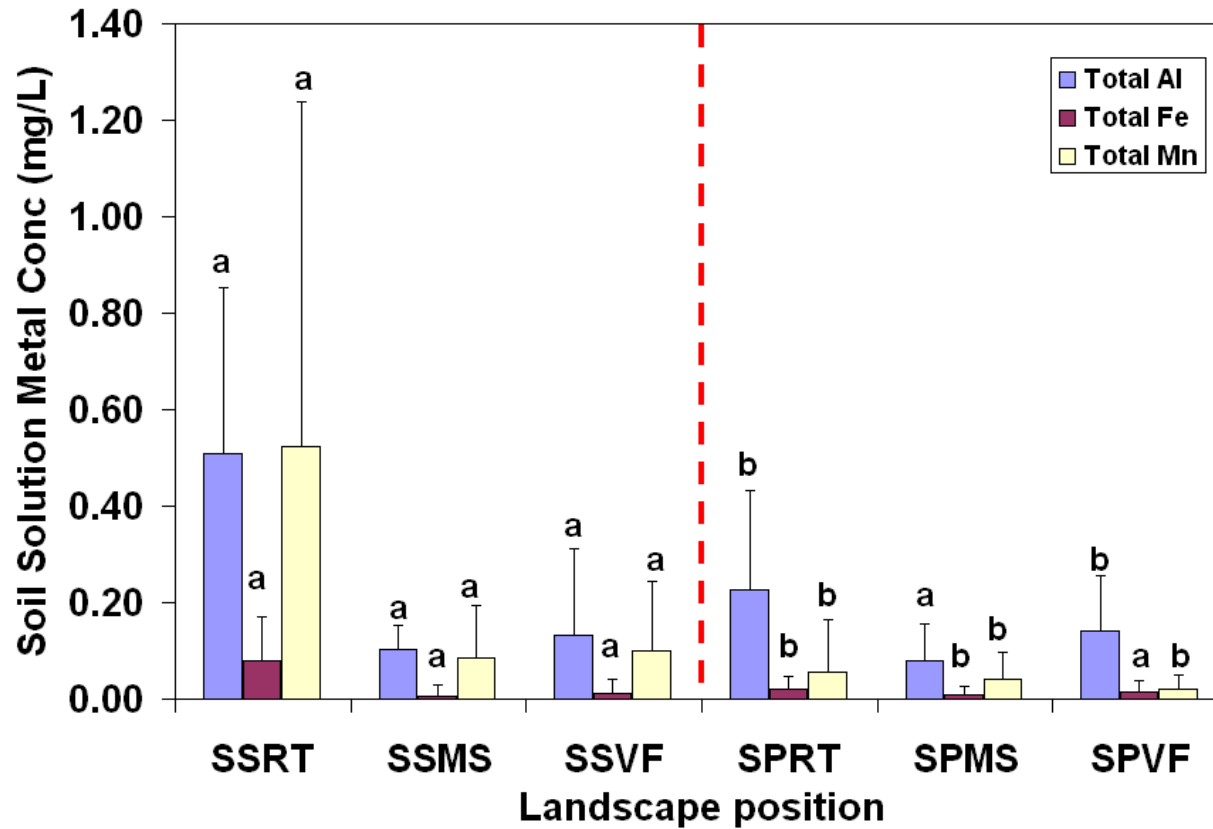


Figure 4-3: Soil pore water concentrations of total Al, Fe, and Mn (mean and standard deviation from Aug. 2007 to Oct. 2009, n = 294 and 191 lysimeter samples for the swale and planar hillslopes respectively) as a function of landscape position. Different letters indicate significant difference between each landscape position for swale versus planar hillslope for total Al, Fe, and Mn concentrations. SSRT represents swale ridgetop, SSMS - swale midslope, SSVF - swale valley floor, SPRT - planar ridgetop, SPMS - planar midslope, and SPVF - planar valley floor.

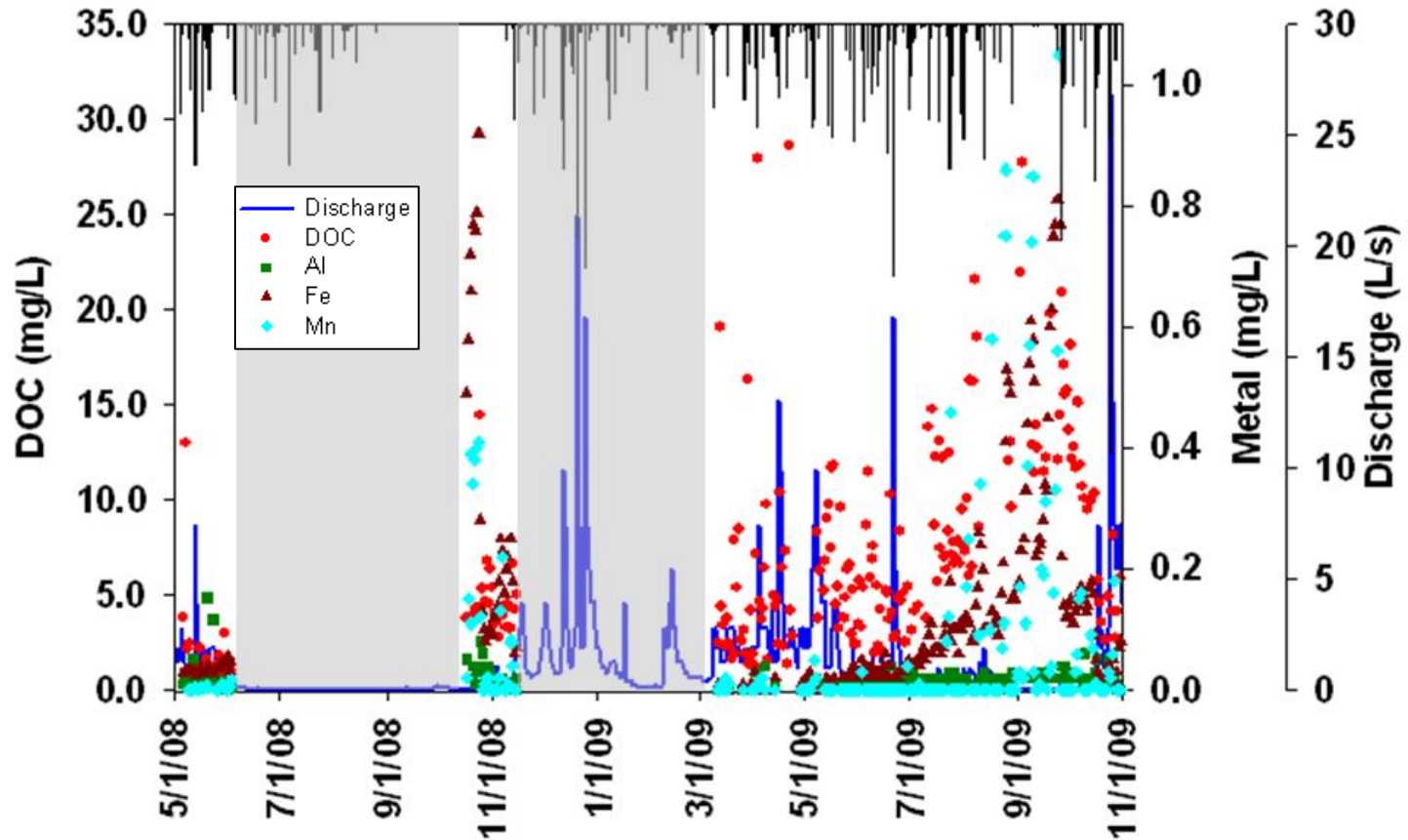


Figure 4-4: Time series data from May 2008 to Oct. 2009 for daily stream water concentrations of DOC, total Al, total Fe, and total Mn along with precipitation (black bar) and stream discharge (n = 300 for daily stream water DOC and total metal, with no samples collected during the summer of 2008 due to no flow condition and during the winters due to frozen condition). Gray bars represent summer or winter periods during which no samples were collected.

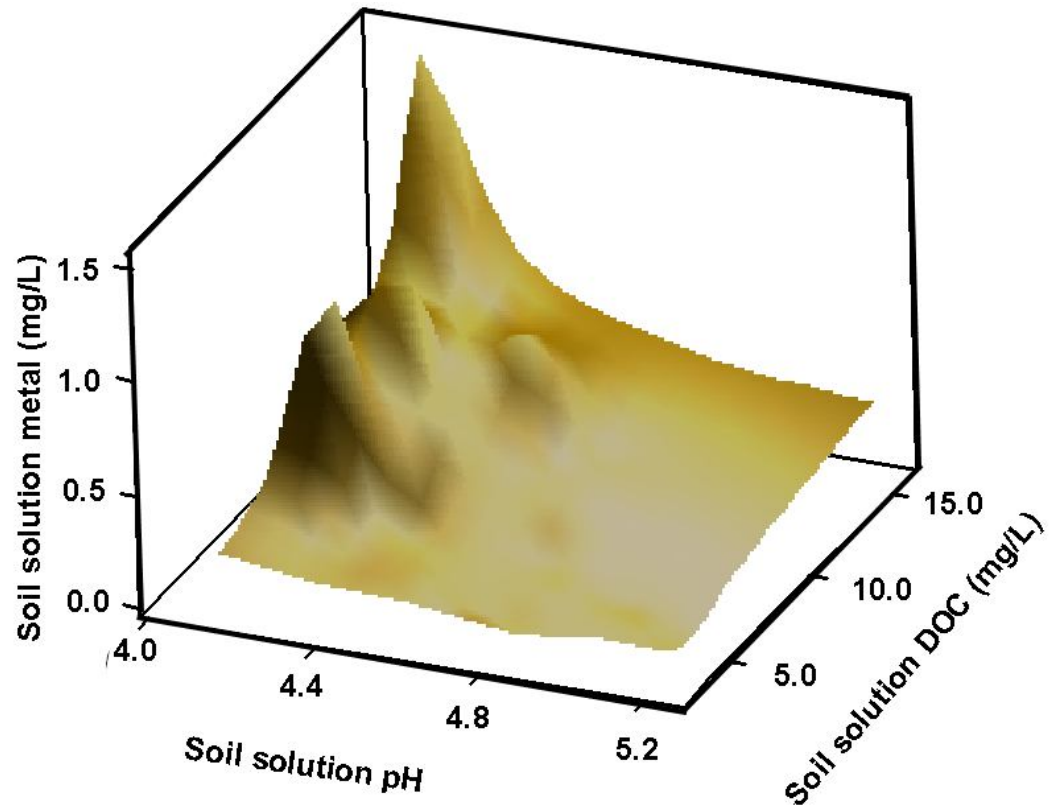


Figure 4-5a: Soil pore water total metal concentration (Al + Fe + Mn) as a function of soil pore water pH and DOC based on a total of 725 soil pore water samples (from all three landscape positions and all soil depths) collected during the time period of Aug. 2007 to Oct. 2009.

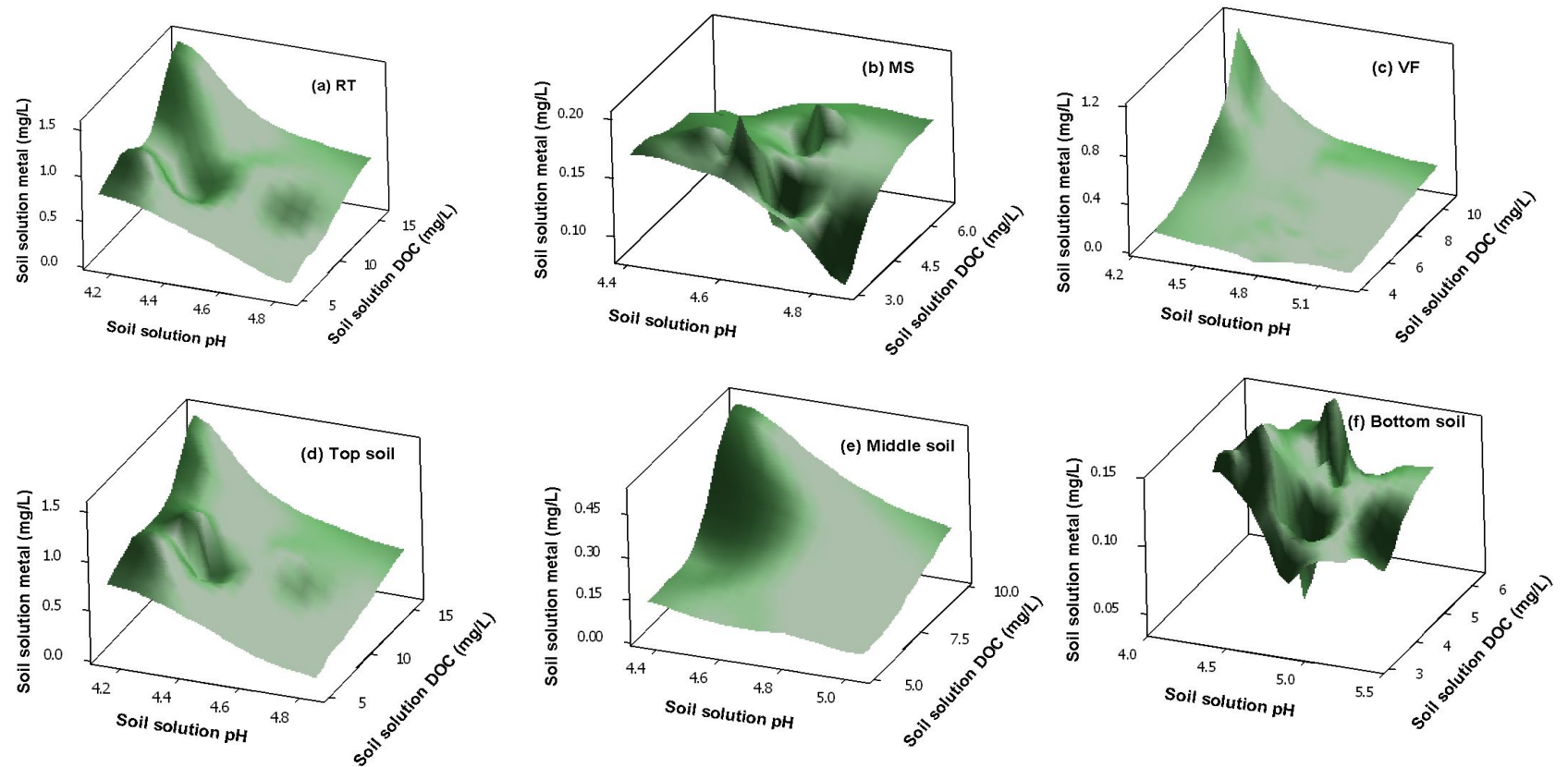


Figure 4-5b: Soil pore water total metal concentration (Al + Fe + Mn) as a function of soil pore water pH and DOC for the three landscape positions: (a) ridgetop (RT), (b) midslope (MS), and (c) valley floor (VF) and for the three soil depths: (d) topsoil (< 30cm), (e) middle (30-50cm), and (f) bottom (>50cm). The data were combined for both the swale and planar hillslopes for the time period from Aug. 2007 to Oct. 2009.

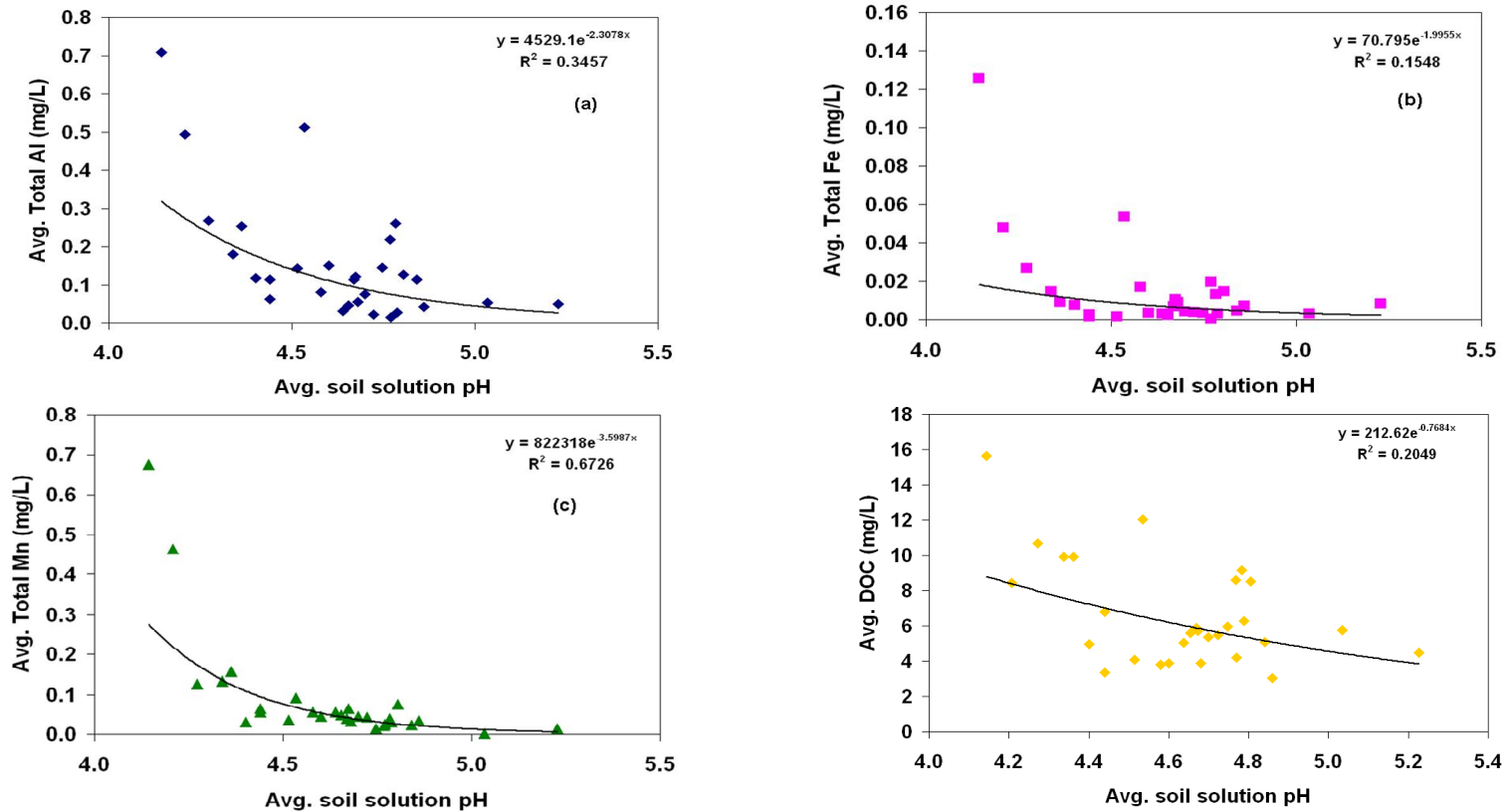


Figure 4-6: Average soil pore water total Al (a), Fe (b), Mn (c), and DOC (d) concentrations plotted as a function of average soil pore water pH. Average values ($n = 33$) were calculated for each soil depth at all six landscape positions for both the swale and planar hillslopes over the time period from Aug. 2007 to Oct. 2009.

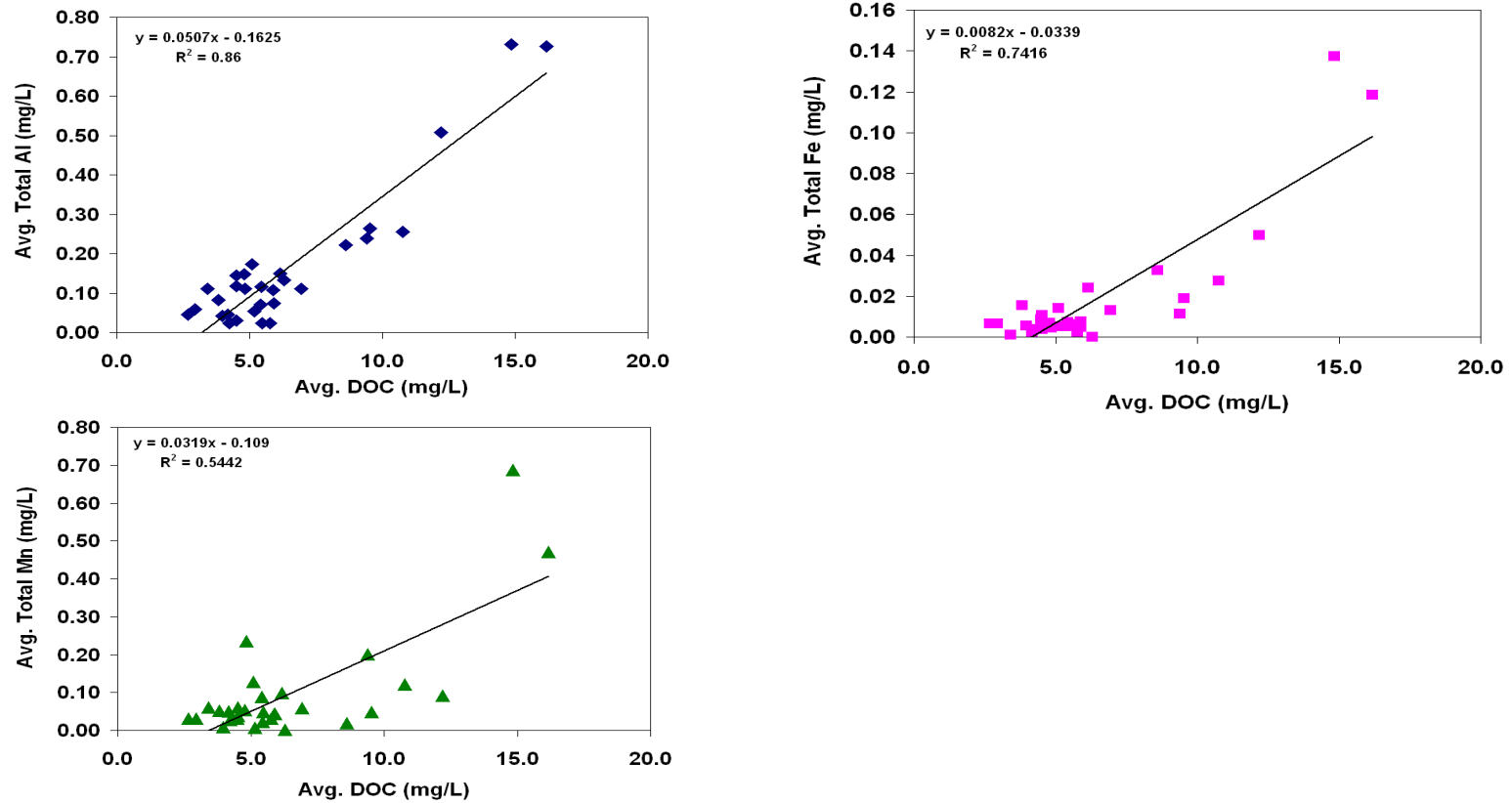


Figure 4-7: Average soil pore water total Al (a), Fe (b), and Mn (c) concentration plotted as a function of average soil pore water DOC. Average values ($n = 33$) were calculated for each soil depth at all six landscape positions for both the swale and planar hillslopes over the time period from Aug. 2007 to Oct. 2009.

Table 4-1: Analysis of variance of soil pore water concentrations of total metal (Al + Fe + Mn), showing the effects of landscape position, soil depth, season, and their interactions. The *F* value is the test statistic used to determine whether the sample means are within the sampling variability of each other, and *p* value is the statistical significance level.

Effects	<i>F</i> value	<i>p</i>-value
Landscape position	62.25	0.001
Soil depth	12.81	0.001
Season	0.06	0.810
Landscape position * Soil depth	45.87	0.001
Landscape position * Season	1.34	0.257
Soil depth * Season	1.07	0.300

Table 4-2: Average \pm standard deviation and range (in parenthesis) of DOC:metal ratios for the soil pore water in the swale and planar hillslopes investigated in this study from 2007 to 2009.

Hillslope, Landscape Position, Soil Series	Soil horizon (depth (cm))	DOC/Al (mass ratio)	DOC/Fe (mass ratio)	DOC/Mn (mass ratio)
<i>Swale</i>				
Ridgetop (SSRT), Weikert soil	A (10)	30 \pm 41 (9-192)	117 \pm 34 (44-175)	63 \pm 176 (13-769)
	Bw (20)	20 \pm 17 (10-74)	182 \pm 159 (80-723)	24 \pm 20 (6-94)
	Bw-CR (30)	59 \pm 42 (20-199)	929 \pm 1861 (112-6991)	145 \pm 142 (11-496)
<i>Average</i>		39 \pm 40	377 \pm 1052	83 \pm 142
Midslope (SSMS), Rushtown soil	Bw2 (20)	60 \pm 55 (12-190)	409 \pm 437 (55-1036)	59 \pm 94 (4-381)
	Bw3 (40)	140 \pm 185 (18-758)	949 \pm 917 (145-1791)	131 \pm 103 (9-339)
	Bw3 (60)	164 \pm 180 (13-680)	980 \pm 1169 (81-2585)	178 \pm 221 (11-1005)
	BC (80)	50 \pm 29 (14-113)	116 \pm 117 (43-348)	100 \pm 72 (15-226)
	C (100)	32 \pm 12 (18-63)	1341 \pm 1125 (190-2438)	66 \pm 23 (34-110)
	C (120)	40 \pm 31 (5-102)	87 \pm 87 (35-217)	189 \pm 167 (13-500)
	C (140)	29 \pm 13 (8-53)	1683 \pm 2299 (57-3309)	126 \pm 80 (35-283)
	C (160)	25 \pm 16 (4-57)	304 \pm 254 (51-570)	105 \pm 92 (14-323)
<i>Average</i>		73 \pm 112	613 \pm 881	120 \pm 130
Valley floor (SSVF), Ernest soil	AE (10)	N/A	N/A	N/A
	Bt1 (20)	41 \pm 15 (20-85)	615 \pm 329 (91-1143)	108 \pm 63 (25-278)
	Bt1 (30)	N/A	N/A	N/A
	Bt1 (40)	40 \pm 19 (17-85)	426 \pm 354 (112-1045)	120 \pm 80 (6-267)
	Bt2 (50)	189 \pm 137 (34-452)	473 \pm 678 (54-1255)	107 \pm 70 (16-246)
	Bt2 (60)	80 \pm 31 (20-128)	542 \pm 596 (85-1533)	150 \pm 91 (20-256)
	Bt2 (70)	307 \pm 235 (18-781)	140 \pm 136 (60-344)	168 \pm 136 (14-466)
	Bt2 (80)	260 \pm 133 (40-475)	-	186 \pm 144 (36-533)
	Bt2 (90)	243 \pm 217 (52-843)	180 \pm 174 (58-303)	296 \pm 274 (40-844)
<i>Average</i>		149 \pm 166	492 \pm 448	153 \pm 140

Hillslope, Landscape Position, Soil Series	Soil horizon (depth (cm))	DOC/Al (mass ratio)	DOC/Fe (mass ratio)	DOC/Mn (mass ratio)
<i>Planar</i>				
Ridgetop (SPRT), Weikert soil	A (10)	29 ± 24 (7-93)	221 ± 103 (101-421)	245 ± 368 (60-1298)
	Bw (20)	48 ± 25 (18-106)	130 ± 31 (90-174)	207 ± 82 (92-385)
	Bw-CR (30)	89 ± 49 (16-179)	267 ± 142 (163-477)	501 ± 468 (13-1438)
<i>Average</i>		58 ± 42	206 ± 107	315 ± 347
Midslope (SPMS), Weikert soil	A (10)	64 ± 41 (10-191)	171 ± 24 (143-188)	184 ± 140 (130-668)
	Bw (20)	47 ± 15 (30-73)	-	115 ± 83 (39-242)
	C (30)	N/A	N/A	N/A
	C (40)	63 ± 36 (8-131)	-	169 ± 226 (16-922)
	R (50)	86 ± 42 (15-178)	-	175 ± 170 (11-714)
<i>Average</i>		67 ± 38	N/A	169 ± 168
Valley floor (SPVF), Ernest soil	AE (10)	45 ± 32 (23-156)	485 ± 155 (333-642)	565 ± 433 (99-1630)
	Bw (20)	44 ± 19 (8-70)	-	364 ± 322 (42-979)
	Bt1 (30)	119 ± 319 (11-1460)	479 ± 129 (252-626)	257 ± 165 (39-594)
	Bt2 (40)	125 ± 70 (39-336)	-	549 ± 271 (302-839)
	CB (60)	191 ± 142 (16-512)	213 ± 112 (96-331)	394 ± 326 (19-806)
	<i>Average</i>		108 ± 177	400 ± 180

N/A – no values because of too few sample dates ; ‘-‘ – Fe concentrations below detection limit

Chapter 5

Spatiotemporal Patterns of Soil Redox Potential in relation to Soil Moisture, Temperature, and Water Table in the Shale Hills Critical Zone Observatory

Abstract

Soil redox potential (Eh) is of biogeochemical significance not only in anaerobic soils but also in upland aerobic soils. This study investigated the spatiotemporal patterns of soil Eh along a hillslope and a valley floor transect in the forested Shale Hills Critical Zone Observatory. We examined the impacts of soil moisture, soil temperature, and water table on soil Eh dynamics using real-time (10-minute) monitoring. The 6-month monitoring showed that soil Eh ranged from -240 to +750 mV from April to October 2010 across the catchment and a combination of landscape position, soil depth, and season explained 72% of the soil Eh variability within the catchment. Soil Eh varied with topographic position as the ridgetop site was consistently oxidized (> 400 mV), while the valley floor was generally moderately to strongly reduced (< 200 mV), with the midslope falling within this range. Soil Eh did not show a consistent decrease with increasing soil depth. Variability in the trends between soil Eh and soil depth is likely due to differences in microsites with respect to soil temperature, type of moisture conditions, rock fragments and other soil properties. At each landscape position, soil Eh reflected variability due to differences in soil moisture, soil temperature, and water table levels, which when

combined, explained 20 to 90 % of soil Eh variation. In general, soil Eh significantly decreased with increasing soil temperature across sites. Soil Eh along the hillslope, increased with increasing soil moisture, which is consistent with oxyaquic moisture conditions (wet but not reduced); whereas at the valley floor, a 2 – 4% increase in volumetric soil moisture during rainfall events (≥ 20 mm) resulted in a decrease in soil Eh. Soil Eh significantly ($p < 0.05$) decreased from spring to summer and during rainfall events and a negative nonlinear relationship with water table height at the valley floor was observed. This study also examined the influence of soil Eh on soil pore water chemistry. High dissolved organic carbon and low nitrate at the valley floor are consistent with denitrification occurring under the anaerobic (< 300 mV) conditions of the valley floor. The disappearance of nitrate coincided with the appearance of iron and manganese below 140 mV. This study demonstrates that spatiotemporal variation in soil Eh in upland forested ecosystems is best interpreted in conjunction with landscape position, soil depth, and seasonal differences in soil temperature, soil moisture, and water table level, rather than water table levels alone as in wet/anaerobic environments.

Introduction

Soil redox potential (Eh) is critical to ecosystem functioning and biogeochemical cycling (Mansfeldt, 2003). Redox potential characterizes the oxidation-reduction status of an environment and is a measure of electron availability in the system (DeLaune and Reddy, 2005). Redox potential generally ranges from -300 to +800 mV, such that Eh values can vary from oxidizing (+400 mV) to weakly reducing (+200 to +400 mV) to moderately reducing (-100 to +200 mV), or strongly reducing (< -100 mV) (Table 5-1)

(Mansfeldt, 2003; Thomas et al., 2009). However, the controls on soil Eh particularly in forested environments are poorly understood due to the limited number of *in-situ* studies conducted in upland forested ecosystems (Fiedler et al., 2007; Sajedi et al., 2010).

In a literature search in Web of Science for soil Eh research, ~ 2400 peer-reviewed articles were found of which only 45 studies were conducted in forested environments. Almost all studies were conducted in anaerobic environments such as in wetlands (e.g. Mitsch and Gosselink, 1993; Dušek et al., 2008; Thomas et al. 2009), marshes (e.g. Mansfeldt, 2003, 2004), and marine sediments (e.g. de Mars and Wassen, 1999; Aldridge and Ganf, 2003). Furthermore, many of these studies were conducted under laboratory-controlled conditions (e.g. Stepniewski et al., 1991; Pezeshki et al., 1997; and Ashworth and Shaw, 2006).

While pioneering work in soil Eh began almost 80 years ago, *in-situ* measurements of soil Eh using temporary or permanently installed electrodes only routinely began in the 1960s (Fiedler et al., 2007). However, the interpretation of soil Eh can be difficult due to both spatial and temporal variability, and can be missed by manual data collection as manual measurements do not capture daily variation in Eh and single redox measurements at one depth can be insufficient in describing Eh conditions in soil systems (Vorenhout et al. 2004; Fiedler et al., 2007; Rabenhorst et al., 2009). As a result, more recent studies have been measuring Eh both at multiple depths within the soil profile, but very limited number of studies have been measuring *in-situ* soil Eh automatically and continuously at the field scale.

In 2003, Mansfeldt studied *in-situ* long-term soil Eh in a dyked marsh soil using a portable pH meter and observed that soil Eh decreased with soil depth and was

negatively correlated with the period of water saturation. Additionally, the soil depth associated with the water table showed more distinct seasonal variation in soil Eh than the other depths where redox probes were installed. However, Gleason et al. (2003) found that differences in soil Eh (measurements made with a pH/Eh meter) reflected differences among mangrove tree species and appeared not to be associated with hydrology. Conversely, Thomas et al., (2009), who used a voltmeter for data collection, found in their study conducted in Florida Everglades wetlands that soil Eh was controlled by water levels and not by the vegetation community.

In 2004, Vorenhout et al. made automated and continuous measurements of Eh in sandy soils in mesocosms and in a salt marsh soil and observed substantial changes in Eh, from -400 to +100 mV within four days and daily cycles of 200 mV. They also observed that both the absolute redox potential values and their diurnal variations were depth-dependent. Yu et al. (2006) using a portable redox meter, showed a distinctly different pattern in soil Eh from ridgetop to valley floor (swamp) corresponding to the hydrological gradient and moisture conditions which varied with season. In the dry season, the ridge and transition soils were both strongly oxidized, while in the wet season, the soil Eh in the transition soils were as low as in the swamp soil. The soil Eh at the swamp remained low due to continuously inundated conditions.

Summarizing these studies, soil Eh can vary significantly within and between soil horizons which can lead to distinct patterns across the landscape, and soil Eh trends are subject to diurnal, event, and/or seasonal changes because of fluctuations in abiotic factors such as water table levels and soil moisture content (SMC). Valley floor areas have been associated with high water tables, high SMC and low Eh values as compared

to upland areas, where saturation may only rarely occur and are typically oxidized (Ohrui and Mitchell, 1998). Additionally, soil temperature can also influence soil Eh (Fiedler et al., 2007). Increases in soil temperature can decrease soil Eh through the acceleration of microbial processes as oxygen is consumed by microbes (Dušek et al., 2008; Thomas et al., 2009). However, other studies have found increasing temperature to increase soil Eh, as temperature has a direct effect on the solubility of oxygen. As temperature increases, evaporation and transpiration increases, causing SMC to decrease and oxygen content to increase (Dušek, et al., 2008; Thomas et al., 2009). This results in an increase in soil Eh.

Furthermore, water table fluctuations can lead to changes in the biogeochemical environment. A fluctuating WT and SMC can result in vertical changes in soil Eh conditions (decreasing Eh), which have been associated with the mobilization of nutrients and metals (e.g. Inamdar et al., 2004; Creed et al., 1996; and Harms and Grimm, 2008). Within the valley floor area, when the WT rises, if dissolved organic carbon (DOC) is available, microorganisms can remove nitrate (NO_3^-) (Hefting et al., 2004; Schilling et al., 2004), and thus decrease the amount of NO_3^- transported into surface waters.

Redox reactions can strongly control the speciation, toxicity, solubility and bioavailability of both organic and inorganic substances (Mansfeldt, 2004). The biogeochemical cycles of many major and trace elements are driven by redox processes such as C, nitrogen (N), iron (Fe), and manganese (Mn) (Borch et al., 2010). Often Fe and Mn concentrations are used as indicators of reducing conditions because as an environment becomes increasingly reduced, anaerobic bacteria are capable of using alternative electron acceptors such as Mn^{4+} and Fe^{3+} . As the environment becomes more reduced (low Eh values), concentrations of Fe^{2+} and Mn^{2+} generally increases. Typically,

the soil Eh of 300mV has been used as break between aerobic and anaerobic conditions since at this Eh oxygen becomes limited and microorganisms begin to use NO_3^- as an electron acceptor (Table 5-1) (Reddy et al., 2000, Fiedler et al., 2007).

This study was initiated to investigate the spatial and temporal patterns of soil Eh in relation to soil moisture, temperature, and water table along topographic gradients at the forested Shale Hills Critical Zone Observatory (CZO). We examined soil Eh dynamics along two transects – one along a hillslope from ridgetop to valley floor and the other along the valley floor down an elevational gradient from upstream to downstream. We used automated and continuous (10-minute interval) monitoring systems for a total of seven sites, with three depths at each site. In addition, we also assessed the influence of soil Eh on soil pore water chemistry with a focus on DOC, NO_3^- , Fe and Mn. Our hypothesis was that distinct soil Eh patterns exist at different topographic positions and soil depths because of seasonal differences in soil temperature, soil moisture content, and water table levels. Additionally, soil Eh would show distinct influence on soil pore water chemistry in this upland forested ecosystem.

Materials and Methods

Site description

This study was conducted at the 7.9-ha Shale Hills CZO, a forested headwater catchment typical of the low-lying shale hills of the Ridge and Valley Physiographic Province in central Pennsylvania (Figure 5-1). The CZO has a first-order stream with an average channel gradient of 4.5% (Lynch, 1976). The mean annual temperature is 10°C and the mean annual precipitation is 1070 mm (NOAA, 2007). This catchment is

characterized by moderate to steep slopes (up to 25-48%). The moderately uniform slopes are interspersed with seven topographic depressional areas (swales) on both sides of the stream (Figure 5-1). Depth to bedrock ranges from <0.25 m at the ridgetop and upper side slopes to over 2-3 m in the valley floor and swales (Lin, 2006).

The soils in this catchment were formed from shale colluvium or residuum and have a dominant texture of silt loam in the surface (with silty clay loam and clay loam in the B horizons in deeper soils). Five soil series have been identified, characterized and mapped based on landscape position, depth to bedrock, and redoximorphic features (Table 5-2) (Lin et al., 2006). The WT fluctuates seasonally. Soils along the valley floor are saturated or nearly saturated during the spring but can dry out during the summer (Lin et al., 2006). Since the catchment is completely forested, all soils have an organic horizon comprised of decaying leaf litter and other organic material. The south-facing slope has primarily hardwood forest (mostly maple, oak, and hickory) and thick underbrush. The north-facing slope also has hardwood forest but with little underbrush. On both sides of the stream, there are softwood trees (mostly pine and hemlock) along toward the western side and deciduous forest towards the eastern side.

Study design and data collection

To understand soil Eh patterns, two transects were established: one along a swale on the south-facing slope and one along the valley floor (Figure 5-1). Soil moisture content, soil temperature, WT level and Eh values were automatically measured at seven locations: three along the selected swale and four along the valley floor (Figure 5-1). At each of the seven sites, measurements were made at three depths which correspond to the

A, B, and C horizons. Redox probes were installed at the depths where the other probes (SMC and temperature) were previously installed. Table 5-3 shows the actual depths at which the various probes were installed at the seven sites.

Valley floor site 1, located furthest upstream (Figure 5-1) is located in the Blairton soil series, which is on the eastern end of the valley floor. The site is <25 m above the origin of streamflow. The soil is moderately well-drained and redox features are visible from 1.1 m below the surface. Percent rock fragments range from 2% in the A horizon to 10% in the B horizon to 80% in the C horizon, while soil pH range from 4.3 in the A horizon to 4.4 in the B horizon to 4.6 in the C horizon.

Valley floor sites 2, 3, and 4 are all located in the Ernest soil series (Figure 5-1). This soil series is somewhat poorly drained and located in the floodplain on the western end of the valley floor, with redox features visible from 0.4 m from the surface. Percent rock fragments range from 0% in the A and B horizons to 80% in the C horizon, while soil pH range from 5.1, 3.8, 4.0 in the A horizon for valley floor sites 2, 3, and 4 respectively to 4.9, 4.1, 4.7 in the B horizon and 5.1, 4.4, 4.9 in the C horizon. Valley floor site 2 is located on the right side of the stream when facing downstream but has been observed to exist within the stream system during snowmelt and early spring. Valley floor sites 3 and 4 are on the left side of the stream when facing downstream.

Soil moisture was measured using EC-5 capacitance-type volumetric water content probes (Decagon Devices Inc., Pullman, WA) and soil temperature data was collected using 229-L sensors (Campbell Scientific Inc., Logan, UT) for five of the seven sites. For valley floor site 4, SMC and soil temperature was measured using the 5-TE sensor (Decagon Devices Inc., Pullman, WA). No SMC and soil temperature probes are

presently located at valley floor site 3. Further details on the soil moisture probe installation can be found in Lin and Zhou (2008). To measure transient WT levels, PVC wells were installed to <0.3 m to > 4 m depth depending on the sites (Table 5-3). Water table levels were measured using Odyssey capacitance water level probes (Dataflow Systems PTY Ltd., New Zealand), which were lowered into the PVC wells.

Soil redox potential was measured with probes constructed by soldering platinum tips to brass brazing rods and 18-gauge copper wire following the method of Veprakas (2002). Once constructed, the electrodes were tested in the laboratory for accuracy using a Ferrous-Ferric solution of known and stable redox potential (Light, 1972) as well as tap water (see Appendix D). Redox probes were constructed and tested in Spring 2009 and installed in Summer 2009. Probes were installed in triplicates at each targeted depth (Table 5-3). An Accumet calomel reference electrode in a KCl-salt bridge was used to complete the circuit at each site. Due to technical issues, Eh data were not available until April 2010. Therefore, data analysis was based on data collected from April to October 2010 except at the shoulder slope (6/17 - 6/25/2010 and 9/20 - 10/12/2010) and valley floor sites 3 and 4 (5/7 - 6/24/2010) where data was lost due to equipment malfunction. The salt bridge at each monitoring site was checked weekly and replaced when necessary to ensure the continuous and proper functioning of the redox probes. All sensors were connected to Campbell Scientific dataloggers (CR10X and 1000, Campbell Scientific Inc., Logan, UT). The frequency of data collection was set to 10-min.

Soil water sample collection and lab analyses

Nested porous cup tension lysimeters (Soil water samplers, 1900 series, SoilMoisture Equipment Corp., Santa Barbara, CA, USA) were used to collect soil pore waters at two sites along the valley floor (valley floor sites 3 and 4) at soil depths of 10, 30 and 60cm (Jin et al., 2010) (Figure 5-1). A portable vacuum pump was used to place vacuum (-500 mbar) on the lysimeters one week before sampling. Soil pore water samples were collected approximately weekly between August 2007 and October 2009. Samples for DOC analysis were placed in pre-combusted glass bottles and samples for NO_3^- , and total Fe and Mn concentrations were placed in Nalgene[®] High-Density Polyethylene plastic bottles (VWR International, West Chester, PA). Measurement of pH was made on all lysimeter samples on every sampling date with the SymPHony SP70P pH electrode (VWR International, West Chester, PA) which was calibrated with two pH buffers (4 and 7). The catchment is generally dry most of the summer and frozen during the winter, so most of soil pore water samples in this study were collected in early spring and late fall. Additionally, soil samples were collected along the transects at varying depths. These samples were air-dried and sieved (2-mm mesh size) for pH analysis.

All DOC samples were filtered in the laboratory with 0.45 μm Nylon syringe filters (VWR International, West Chester, PA), acidified with two drops of 50% HCl and refrigerated at 4°C until analysis. Analysis was performed with a Shimadzu TOC-5000A analyzer (Shimadzu Scientific Instruments, Columbia, MD). For analysis of Fe and Mn concentrations, samples were acidified with two drops of high purity HNO_3 and measured with an ICP- AES (Inductively coupled plasma atomic emission spectroscopy) (PerkinElmer Inc., Waltham, MA), while NO_3^- analysis was performed on a Dionex IC

(Ion Chromatograph) (Dionex, Bannockburn, IL). To ensure data quality, a system of standards, analytical blanks, and replicates were used in each analysis batch. Soil pH analysis was conducted on the air-dried and sieved soil samples (1:1; soil: deionized water) using the SymPHony SP70P pH electrode (VWR International, West Chester, PA).

Soil Eh data corrections and analyses

Soil Eh data corrections

The soil Eh field data were corrected in order to be relative to the potential of a standard hydrogen electrode by using a +250 mV correction factor as calomel reference electrodes were used (Vepraskas, 2002):

$$\text{Eh (mV)} = \text{field voltage (mV)} + 250 \text{ mV} \quad [1]$$

Additionally, since Eh readings are influenced by pH, soil Eh data were also corrected to pH 7 by adding 59 mV per pH unit for accurate interpretation of data and comparison to other studies (Qualls et al., 2001):

$$\text{pH-corrected Eh (mV)} = \text{Eh (mV)} - [(\text{pH } 7 - \text{soil pH}) * 59] \quad [2]$$

Statistical analyses

After correction of soil Eh data, the mean Eh ($n = 3$, redox probes installed in triplicate) was calculated for each landscape position, depth, and date of sampling.

Resulting means were used in all subsequent analyses. Examples of variability between the replicated probes for a hillslope site and a valley floor site are shown in Figure 5-2 (these data for other sites are in Appendix D).

To test for significant difference in soil Eh between soil depths, Student's paired t-tests for the same topographic position for the same time period in all seven sites were used. To determine spatial patterns for the different transects, the analysis of variance (ANOVA) was used to test whether there were significant impacts on soil Eh from different soil horizons (A, B, C), topographic position (ridgetop, shoulder slope, midslope and valley floor), season (spring – April to June, summer – June to September, fall – September to October), and their interactions.

To understand temporal trends, differences in seasonal soil Eh values were evaluated. To determine the main factors that influence soil Eh, multiple regression analysis was performed on time series data of soil temperature, SMC, and WT levels and Eh values. With respect to soil pore water solute concentrations, DOC, NO_3^- and total Mn and Fe patterns were compared to soil Eh values. Soil Eh response was considered statistically significant at $p < 0.05$ and ecologically significant if redox values changed among oxidizing (+400 mV), weakly reducing (+200 to +400 mV), moderately reducing (-100 to +200 mV), or strongly reducing (<-100 mV) (Table 5-1) (Mansfeldt, 2003; Thomas et al., 2009). Analyses were performed using Minitab 16.0 (Minitab Inc., State College, PA) and Sigmaplot 10.0 (Systat Software Inc., San Jose, CA, USA).

Results and Discussion

Variability between replicates

In 1997, Fiedler noted that Eh of individual electrodes should be regarded as single-point measurements as Eh can vary up to 800 mV between two electrodes installed at a horizontal distance of 1 cm. In this study, variability between replicated redox electrodes ranged from 12 mV to 520 mV and Figure 5-2 shows data for the ridgetop and valley floor site 2 (data for other sites can be found in Appendix D). At the ridgetop, variability at both the A and B horizons were similar (~ 40 mV). At the shoulder slope and valley floor sites 1, 2, and 4, variability between replicates increased from the A to B horizons and then decreased in the C horizon, whilst at the midslope, variability between replicated decreased from the A to C horizons (356 mV to 60 mV) and increased from the A to C horizons for valley floor site 3 (150 mV to 520 mV). Variability between replicates was higher at the valley compared to the hillslope. This is likely because of the presence of a fluctuating water table at the valley floor. This has been observed in other studies summarized by Fiedler et al. (1997). Soil Eh may vary within small distances due to the presence of microsites or rock fragments. While no clear agreement has been reached for the required number of replicates, many studies have used duplicates and much fewer studies have used five to 10 replicates (Fiedler et al., 2007). Based on the variability observed between our replicates, no less than three replicates should probably be used. Moreover, more than five replicates would most likely be best if soils are as heterogeneous as in this catchment.

Spatial patterns of soil Eh

Soil Eh varied widely in the Shale Hills CZO, ranging from -240 to +750 mV during the monitoring period from April to October 2010 (Figure 5-3). This range of soil Eh covers reduced to oxidized conditions that impact many environmentally important biogeochemical processes (Table 5-1). The lowest Eh values (reducing conditions) were observed around the interface between Bw-Bt horizons in the downstream of the valley floor, where a transient water table occurs most frequently (Figures 5-3 and 5-4a). This observation is also supported by the soil profile description where soil redoximorphic features were observed at this interface for valley floor soils because of fragipan-like soil layer occurred at around 30 cm depth (Table 5-2). The ANOVA results showed that topographic position, soil depth, and season significantly influenced soil Eh at $p < 0.05$ level (Table 5-4).

Soil profile patterns of soil Eh

Soil Eh is known to vary with soil depth (Aldridge and Ganf, 2003). In general, soil Eh tends to decrease with increasing soil depth because of increasing soil moisture and fluctuating water table (Fielder et al., 2007). However, in this study, four general vertical trends of soil Eh were observed based on the overall aggregated data that depended on soil type and landscape position (Figures 5-3 and 5-4a): (1) soil Eh decreased with increasing soil depth from A to B horizons at the ridgetop; (2) soil Eh decreased from A to B horizons sharply and then slightly increased from B to C horizons (valley floor sites 3 and 4); (3) soil Eh increased with increasing soil depth from A to C

horizons (shoulder slope and valley floor sites 1 and 2); and (4) soil Eh increased from A to B but decreased from B to C horizons (midslope site).

At the ridgetop, it is likely that root and microbial processes are occurring within the top 10 cm (A horizon) of this shallow soil (< 30 cm). Lower root and microbial processes in the B horizon compared to A horizon can result in lower oxygen content in subsurface soils and thus lower soil Eh. This was also observed by Bohrerova et al. (2004) who observed lower soil Eh in the subsoils compared to the surface soils in aerobic soils. Additionally, plants are able to oxidize their rhizospheres by translocating oxygen absorbed above the ground to roots, where it then diffuses to the surrounding soil (e.g. Kalpage, 1965; Stepniewski et al., 1991; Gleason et al., 2003 and authors therein). This increase in oxygen in the rhizosphere can account to high soil Eh in the surface soils and low soil Eh at deeper soil depths.

On the other hand, low soil Eh in surface soils compared to the subsurface as observed at the shoulder slope, and valley floor sites 1 and 2, can be due to increased oxygen consumption by microbial activity within the surface soils and therefore lower oxygen content within the A horizon as compared to the B and C horizons. At these sites, rock fragment percentage increase to > 50 % in the B and C horizons and oxygen content may be higher at these horizons resulting in higher soil Eh. Valley floor sites 3 and 4 likely differed from the other valley floor sites as the Eh probes for the B horizon was installed at the Bw-Bt horizon of valley floor sites 3 and 4 and a transient water table is located at this restrictive horizon which can potentially result in lower soil Eh in the B horizon as compared to the A and C horizons.

Unlike other studies, our soil Eh data did not show a general decrease with increasing soil depth at all landscape positions. Variability in the trends between soil Eh and soil depth as to whether soil Eh decreases or increases with increasing soil depth may be due to differences in the actual soil region or microsites where the probes were installed within the different horizons with respect to differences in soil temperature, type of moisture conditions, rock fragments and other soil properties.

Hillslope and catchment patterns of soil Eh

The spatial patterns of soil Eh were examined along the hillslope and the valley floor transects. In general, averaged soil Eh was the highest at the ridgetop and decreased downslope, with the largest decrease being between the ridgetop and shoulder slope. Along the valley floor, soil Eh generally decreased down gradient with the largest significant decrease being between valley floor sites 2 and 3, with the exception of valley floor site 4, which was less reduced than valley floor site 3.

The ridgetop site was strongly oxidized (> 400 mV) over the entire study period, while valley floor sites 3 and 4 were moderately reducing (-100 to 200 mV) during the spring, summer and fall for the A and C horizons, and moderately reducing to strongly reducing (< -100 mV) during the summer and fall at the B horizon (due to the transient water table) (Table 5-5). All other sites fell within the range of weakly reducing to oxidized (200 to 400 mV). The strongly oxidized conditions at the ridgetop reflect the lack of saturation that occurs in upland soils, while the reducing conditions at the valley floor reveal the seasonally fluctuating water table and high soil moisture that has been observed in this catchment (Lin et al., 2006).

Temporal patterns of soil Eh

Temporal changes in soil Eh over the study period are showed in Figures 5-5 and 5-6. Soil Eh was observed to be significantly impacted by seasonality (Table 5-4) ($p < 0.05$). Soil Eh decreased from spring to summer; however, from summer to fall, the majority of sites had an overall increase in soil Eh but a couple sites (midslope and valley floor site 2) exhibited a decrease in soil Eh. This variation may be in part due to limited available fall data at this time. Regardless, during the fall, the catchment begins to wet up, the temperature begins to fall and there is a reduction in oxygen consumption which would result in increased soil Eh.

The decrease from spring to summer was most dramatic at the ridgetop site, although soil Eh at the ridgetop was oxidized during the three seasons. These results suggest high oxygen consumption due to increased microbial activity and vegetation growth in the summer time. Also in the summer time, the high temperatures can result in the reduced solubility of oxygen in the water present in the soil, thus decreasing soil Eh. At the shoulder slope, no data was available for the fall due to equipment malfunction, but during the spring and summer, soil Eh was oxidized to moderately reducing (> -100 mV), with the B and C horizons becoming more oxidized in the summer compared to the spring (Figure 5-6). At the midslope, soil Eh also varied between oxidized to moderately reducing for the three seasons but the frequency of oxidizing conditions decreased from spring to fall. At the valley floor, from upstream to downstream, soil Eh became more anaerobic (< 300 mV) such that at valley floor sites 3 and 4 ranged only between moderately to strongly reducing (< 200 mV).

According to Fiedler et al. (2007), Eh varies temporally due to precipitation, temperature, water table levels, oxygen diffusion, and evapotranspiration. Almost all of our sites showed a soil Eh response to rainfall particularly for rainfall events greater than 20 mm, where soil Eh was observed to drop particularly in the A and B horizons (Figure 5-7). Heavy rainfall events would increase soil moisture content and water table levels, and decrease oxygen content resulting in the observed fall in soil Eh. The extent of the response to rainfall was dependent on topographic position (Figure 5-7). The observed trends were more obvious at the ridgetop as compared to the valley floor sites. These trends are consistent with the denser canopy at the valley floor as well as a longer travel time of water from the ridgetop to the valley floor.

At the ridgetop, the decrease in soil Eh during rainfall events was not as great during the fall as compared to the spring and summer rainfall events. At the valley floor, soil Eh showed more of a response to water table levels regardless of the size of the rainfall event especially during the spring (Figure 5-7). Valley floor 2 showed this response the clearest as it is located within the stream and is therefore subjected to greater fluctuations in WT levels.

Factors controlling soil Eh

Several factors are known to influence soil Eh. Results showed that in this forested catchment, soil Eh values were significantly ($p < 0.05$) linked to soil temperature, SMC and WT levels (Table 5-5). The combination of soil temperature and SMC explained between 20 to 90 % of the variability in soil Eh depending on the topographic position. Less variation was explained at the valley floor compared to the

hillslope using just soil temperature and SMC. Along the valley floor, WT levels improved the amount of variability in average soil Eh that can be explained from 30 to 50%.

Regardless of landscape position, soil Eh was significantly correlated with soil temperature for the A and B horizons and decreased with increasing soil temperature except at Valley Floor 1 and the B horizon of the shoulder slope (Table 5-5; Figure 5-8a). This decrease in soil Eh with increasing soil temperature was most obvious during the spring as compared to the summer and fall. Additionally, these patterns were more obvious along the hillslope as compared to the valley floor area. Increases in temperature can decrease soil Eh through the acceleration of microbial processes (e.g. Dušek et al., 2008). However, other studies have found increasing temperature to increase soil Eh (e.g. Thomas et al., 2009). As temperature increases, evapotranspiration increases, causing the soil to lose water and for oxygen content to increase which results in an increase in soil Eh.

Soil moisture content was significantly correlated to soil Eh regardless of topographic position or soil depth except at the B horizons for a couple of the sites (Table 5-5). In general, soil Eh increased with increasing SMC (Figure 5-8b). While this observation is not intuitive, it may be due to the oxyaquic moisture conditions (wet but not reduced conditions and thus no redox features) especially along the hillslope. This may be related to the flashy soil water movement in the catchment, since the soil is very permeable, particularly along the hillslope. Under these conditions, the soil may become saturated but not reduced or may only be saturated for very short time periods. These observations are consistent with water moving fast (short residence time) through the soil

with an oxygen content that is higher than that of the soil itself. However, at the valley floor during rainfall events (≥ 20 mm), a 2 – 4 % increase in SMC resulted in a decrease in soil Eh, which then remained fairly constant, suggesting that there is a threshold or degree of saturation needed for an increase in SMC to result in a drop in soil Eh (most obvious at the shoulder slope and at Valley Floor 2) (Figure 5-9).

During the study period, a WT was detected only at the midslope and the valley floor sites. Water table levels were found to be strongly correlated with soil Eh particularly at the valley floor sites. An increase in WT height corresponded with a decrease in soil Eh (as seen in Figure 5-7). The Bw-Bt soil interface (30cm) of valley floor sites 3 and 4, where a transient water table may exist, experienced mostly reducing conditions compared to the A and C horizons, with soil Eh ranging between -240 to 38 mV. While WT levels have been found to be the main variable explaining soil Eh particularly in wetlands (Thomas et al., 2009), this study showed that WT levels are an important influence on soil Eh only for sites at the valley floor. This finding is likely due to the valley floor being saturated for an extended period as well as the valley floor may be influenced by groundwater contributions which generally have a lower Eh than soil water. Furthermore, soil temperature and SMC are important along the hillslope where a WT may not exist.

Soil Eh impacts on soil pore water chemistry

The soils of this catchment are acidic with an average soil pH of 4.4 ± 0.5 , while average soil pore water pH was 4.6 ± 0.4 . The concentrations of DOC, NO_3^- , total Fe and Mn in soil pore waters at the valley floor showed a distinct vertical pattern (Figure 5-10).

Soil pore water concentrations were generally higher at valley floor site 3 than at valley floor site 4. Valley floor sites 3 and 4 are both located on the left side of the stream when facing downstream and are both located in the Ernest soil series. However, the soil at valley floor site 3 (bottom of swale) is thicker than at valley floor site 4 (bottom of planar hillslope).

Soil pore water DOC concentrations were generally highest in the surface and decreased with increasing soil depth for the valley floor site 3, but for valley floor site 4, there was a peak in DOC concentration at 30 cm (Bw-Bt soil interface). The soil profile trend observed for DOC at valley floor site 3 was similar for NO_3^- and total Fe and Mn. At valley floor site 4, NO_3^- concentrations slightly increased at 60 cm and total Mn concentrations peaked at 30 cm (similar to DOC). Nitrate was rarely detected at the valley floor sites. This suggests that denitrification may be taking place under the reducing condition observed at the valley floor.

While Eh is not always been the best indicator of what species are present in soil solution, below soil Eh of +140 mV, Fe and Mn were detected. Reduction of Mn generally occurs between +220 and 450 mV and the reduction of Fe starts below +150 to 180 mV (Mansfeldt, 2004). However, as soil Eh decreased, Fe and Mn did not necessarily increase in soil pore waters suggesting that other processes may be at play in this system, such as adsorption to the soil matrix. The presence of clay in these soils may allow for adsorption, thereby lowering the Mn and Fe concentrations (Table 5-2). High total Fe and Mn in the A horizon may be due to high DOC in the A horizon as DOC was found to be significantly correlated to Fe and Mn in this catchment.

Reducing conditions observed at the valley floor sites (3 and 4) can decrease the sorption of DOC making it more mobile and thus increasing the mobility of Fe and Mn, especially at the Bw-Bt soil interface. Increase C supply can increase consumption of oxygen by microbes (and the use of alternative electron donors like NO_3^- , Fe and Mn) and this results in decreased soil Eh (Aldridge and Ganf, 2003) such as that observed at the Bw-Bt soil interface. In subsurface soils, SMC is higher and oxygen content is lower, thus low soil Eh can develop which would lead to lower NO_3^- concentrations because of decreased nitrification and/or increased denitrification (Bohrerova et al., 2004).

The behavior of NO_3^- , Fe and Mn as electron acceptors can be inferred from the complete disappearance of NO_3^- and the appearance of Fe and Mn. According to Mansfeldt (2004) numerous studies have been done using soil suspensions that show that the behavior of different electron acceptors is a sequential process (oxygen, nitrate, manganese, iron, sulfate and carbon) but from other studies it is obvious that these processes overlap. This would explain the presence on NO_3^- , Mn and Fe at the same time or the absence of NO_3^- and presence of Mn and Fe in this study.

Due to the unavailability of soil pore water chemistry along the hillslope at this time and the difference in monitoring period between the collection of Eh data (April to October 2010) and soil pore water chemistry data (August 2007 to October 2009) along the valley floor, longer monitoring of soil Eh and soil pore water chemistry (Fe and Mn species in particular) is needed. These data will provide a better interpretation of the influence of soil Eh on solution chemistry within this forested catchment. This would be beneficial to identifying the main redox processes and predicting the mobility and bioavailability of redox-sensitive components along the hillslope and valley floor.

The low redox conditions at the valley floor suggest that this area may be a biogeochemical hotspot (area of high reaction rates) as compared to the hillslope or upland area. The low redox conditions observed at the valley floor can result in denitrification or removal of NO_3^- thus, decreasing the amount of NO_3^- transported into the stream. These conditions can also result in the use of Mn^{4+} and Fe^{3+} as electron acceptors, as low redox values can strongly control the speciation, toxicity, solubility, and bioavailability of these elements (Mansfeldt, 2004).

Summary and Conclusions

Landscape position, soil depth and seasonality combined explained more than 70% of soil Eh variability in the Shale Hills CZO from April to October 2010. At each landscape position a combination of soil moisture, temperature, and water table was significantly correlated with soil Eh. Results from this study showed that regardless of topographic position, increasing soil temperatures decreased soil Eh, while increased water table height significantly decreased soil Eh at the valley floor. However, depending on topographic position the influence of soil moisture content varied: soil Eh increased with increasing soil moisture along the hillslope but at the valley floor and during rainfall events, a 2 to 4 % increase in soil moisture resulted in a decrease in soil Eh. These results are consistent with oxaquic moisture conditions along the hillslope, because of flashy soil water movement and permeable soils in this catchment, such that water with a high oxygen content (oxygen content of rainfall is likely higher than oxygen content within the soil) flows through the soil rapidly (short residence time). However, at the valley floor

reduced conditions occur only after reaching a certain degree of saturation or due to the influence of the fluctuating water table.

Soil Eh varied spatially and temporally, ranging from -240 to +750 mV, a range which can support the majority of environmental biogeochemical activities. In general, average soil Eh status was highest at the ridgetop, which had oxidizing conditions (> 400 mV) throughout the entire study period and decreased downslope, with the shoulder slope and midslope varying between oxidizing and moderately reducing conditions (> -100 mV). Average soil Eh at valley floor sites 1 and 2 ranged between oxidizing and moderately reducing conditions and valley floor site 3 was moderately to strongly reducing (< 200 mV); however, valley floor site 4 was mostly moderately reducing (-100 mV to 200mV) throughout the entire study period.

Soil Eh decreased from spring to summer. This decrease was most dramatic at the ridgetop, suggestive of high oxygen consumption due to increased microbial activity and vegetation growth from spring to summer. The extent of soil Eh response to rainfall was dependent on topographic position. The observed trends were more obvious at the ridgetop as compared to the valley floor. At the ridgetop, soil Eh showed a decrease during rainfall events greater than 20-mm; while at the valley floor, soil Eh showed a clear response to water table level (especially during the spring).

Soil Eh status did appear to be correlated with soil solution chemistry at the valley floor, where soil solution chemistry was monitored. Reduced conditions, high DOC and low NO_3^- at the valley floor imply that denitrification may proceed under the anaerobic (< 300 mV) conditions of the valley floor. The behavior of NO_3^- , Fe^{3+} , and Mn^{4+} as electron acceptors can be assumed from the loss of NO_3^- and the increase in concentration of total

Fe and Mn. The behavior of different electron acceptors is a sequential process and these processes overlap, since we observed the presence of NO_3^- , and Mn and Fe at the same time or the absence of NO_3^- but presence of Mn and Fe in the soil solution.

References

- Aldridge, K.T., and G.G. Ganf. 2003. Modification of sediment redox potential by three contrasting macrophytes: Implications for phosphorus adsorption/desorption. *Marine and Freshwater Research* 54: 87–94.
- Ashworth, D. J. and G. Shaw. 2006. Effects of moisture content and redox potential on in situ K_d values for radioiodine in soil. *Science of the Total Environment* 359: 244-254.
- Bohrerova, Z., R. Stralkova, J. Podesvova, G. Bohrer, and E. Pokorny. 2004. The relationship between redox potential and nitrification under different sequences of crop rotations. *Soil and Tillage Research* 77: 25-33.
- Borch, T., R. Kretzschmar, A. Kappler, P. Van Cappellen, M. Ginder-Vogel, A. Voegelin, and K. Campbell. 2010. Biogeochemical redox processes and their impact on contaminant dynamics. *Environmental Science and Technology* 44: 15-23.
- Creed, I. F., L. E. Band, N. W. Foster, I. K. Morrison, J. A. Nicholson, R. S. Semkin, and D. S. Jeffries. 1996. Regulation of nitrate-N release from temperate forests: a test of the N flushing hypothesis. *Water Resources Research* 32: 3337-3354.
- DeLaune, R. D. And K. R. Reddy. 2005. Redox potential. 366 – 371.
<http://wetlands.ifas.ufl.edu/publications>

- de Mars, H. and M. J. Wassen. 1999. Redox potentials in relation to water levels in different mire types in the Netherlands and Poland. *Plant Ecology* 140: 41–51.
- Dušek, J., T. Pícek, and H. Čížková. 2008. Redox potential dynamics in a horizontal subsurface flow constructed wetland for wastewater treatment: diel, seasonal and spatial fluctuations. *Ecological Engineering* 34: 223-232.
- Fiedler, S., M. J. Vepraskas, and J. L. Richardson. 2007. Soil redox potential: importance, field measurements, and observations. *Advances in Agronomy* 94: 1–54.
- Gleason, S.M., K.C. Ewel, and N. Hue. 2003. Soil redox conditions and plant–soil relationships in a micronesian mangrove forest. *Estuarine, Coastal and Shelf Science* 56: 1065–1074.
- Hagedorn, F., K. Kaiser, H. Feyen, and P. Schleppei. 2000. Effects of redox conditions and flow processes on the mobility of dissolved organic carbon and nitrogen in a forest soil. *Journal of Environmental Quality* 29: 288-297.
- Harms, T. K. and N. B. Grimm. 2008. Hot spots and hot moments of carbon and nitrogen dynamics in a semiarid riparian zone. *Journal of Geophysical Research* 113, G01020, doi: 10.1029/2007JG000588.
- Hefting, M., J. C. Clément, D. Dowrick, A. C. Cosandey, S. Bernal, C. Cimpian, A. Tatur, T. P. Burt, and G. Pinay. 2004. Water table elevations controls on soil nitrogen cycling in riparian wetlands along a European climatic gradient. *Biogeochemistry* 67: 113-134.
- Inamdar, S. P., S. F. Christopher, and M. J. Mitchell. 2004. Export mechanisms for dissolved organic carbon and nitrate during summer storm events in a glaciated forested catchment in New York, USA. *Hydrological Processes* 18: 2651-2661

- Jin, L., R. Ravella, B. Ketchum, P.R. Bierman, P. Heaney, T.S. White, and S. L. Brantley. 2010. Mineral weathering and elemental transport during hillslope evolution at the Susquehanna/Shale Hills Critical Zone Observatory. *Geochimica et Cosmochimica Acta* 74 (13): 3669-3691.
- Kalpagé, F. S. C. P. 1965. Redox potential trends in a submerged rice soil. *Plant and Soil* 23 (1): 129-136.
- Light, T. S. 1972. Standard solution for redox potential measurements. *Analytical Chemistry* 44: 1038-1039.
- Lin, H. 2006. Temporal stability of soil moisture spatial pattern and subsurface preferential flow pathways in the Shale Hills Catchment. *Vadose Zone Journal* 5: 317-340
- Lin, H. and X. Zhou. 2008. Evidence of subsurface preferential flow using soil hydrologic monitoring in the Shale Hills Catchment. *European Journal of Soil Science* 59: 34-49
- Lynch, J. A. 1976. Effects of antecedent soil moisture on storm hydrographs. PhD Dissertation. The Pennsylvania State University, University Park, PA.
- Mansfeldt, T. 2003. In situ long-term redox potential measurements in a dyked marsh soil. *Journal of Plant Nutrition and Soil Sciences* 166: 210–219.
- Mansfeldt, T. 2004. Redox potential of bulk soil and soil solution concentration of nitrate, manganese, iron and sulfate in two Gleysols. *Journal of Plant Nutrition and Soil Sciences* 167: 7-16.
- Mitsch, W.J., and J.G. Gosselink (ed.) 1993. *Wetlands*. 2nd ed. Van Nostrand Reinhold, New York.

- National Oceanographic and Atmospheric Administration (NOAA). 2007. U.S. divisional and station climatic data and normals: Asheville, North Carolina, U.S. Department of Commerce, National Oceanic and Atmospheric Administration, National Environmental Satellite Data and Information Service, National Climatic Data Center. <http://cdo.ncdc.noaa.-gov/CDO/cdo>.
- Ohruai, K. and M. J. Mitchell. 1998. Stream water chemistry in Japanese forested watersheds and its variability on a small regional scale. *Water Resources Research* 34 (6): 1553-1561.
- Pezeshki, S. R., R. D. DeLaune, and J. F. Meeder. 1997. Carbon assimilation and biomass partitioning in *Avicennia germinans* and *Rhizophora mangle* seedlings in response to soil redox conditions. *Environmental and Experimental Botany* 37: 161-171.
- Qualls, R. G., C. J. Richardson, and L. J. Sherwood. 2001. Soil reduction-oxidation potential along a nutrient-enrichment gradient in the everglades. *Wetlands* 21 (3): 403-411.
- Rabenhorst, M. C., W. D. Hively, and B. R. James. 2009. Measurements of soil redox potential. *Soil Science Society of America Journal* 73 (2): 668-674.
- Reddy, K. R., D'Angelo, E. M., and Harris, W. G. 2000. Biogeochemistry of wetlands. *In* Handbook of Soil Science. M. E. Sumner, Ed. Pp G89-G119. CRC Press, Boca Raton, FL.
- Sajedi, T., C. Prescott, and L. Lavkulich. 2010. Redox potential: An indicator of site productivity in forest management. *Geophysical Research Abstracts*, Vol. 12, 14636-2. EGU General Assembly.

- Stepniewski, W., S. R. Pezeshki, R. D. DeLaune, and W. H. Patrick Jr. 1991. Root Studies under Variable Redox Potential in Soil or Soil Suspensions Using Laboratory Rhizotrons. *Vegetatio* 94 (1): 47-55.
- Schilling, K. E., Y. K. Zhang, and P. Drobney. 2004. Water table fluctuations near an incised stream, Walnut Creek, Iowa. *Journal of Hydrology* 286: 236-248.
- Thomas, C. R., S. Miao, and E. Sindhøj. 2009. Environmental factors affecting temporal and spatial patterns of soil redox potential in Florida everglades wetlands. *Wetlands* 29 (4): 1133-1145.
- Veprakas, M. J. 2002. Redox potential measurements (online). Available at <http://www.soil.ncsu.edu/wetlands/wetlandsoils/RedoxWriteup.pdf>.
- Vorenhout, M., H. G. van der Geest, D. van Marum, K. Wattel, and H. J. P. Eijsackers. 2004. Automated and continuous redox potential measurements in soil. *Journal of Environmental Quality* 33: 1562-1567.
- Yu, K., S. P. Faulkner, and W. H. Patrick Jr. 2006. Redox potential characterization and soil greenhouse gas concentration across a hydrological gradient in a Gulf coast forest. *Chemosphere* 62: 905-914.

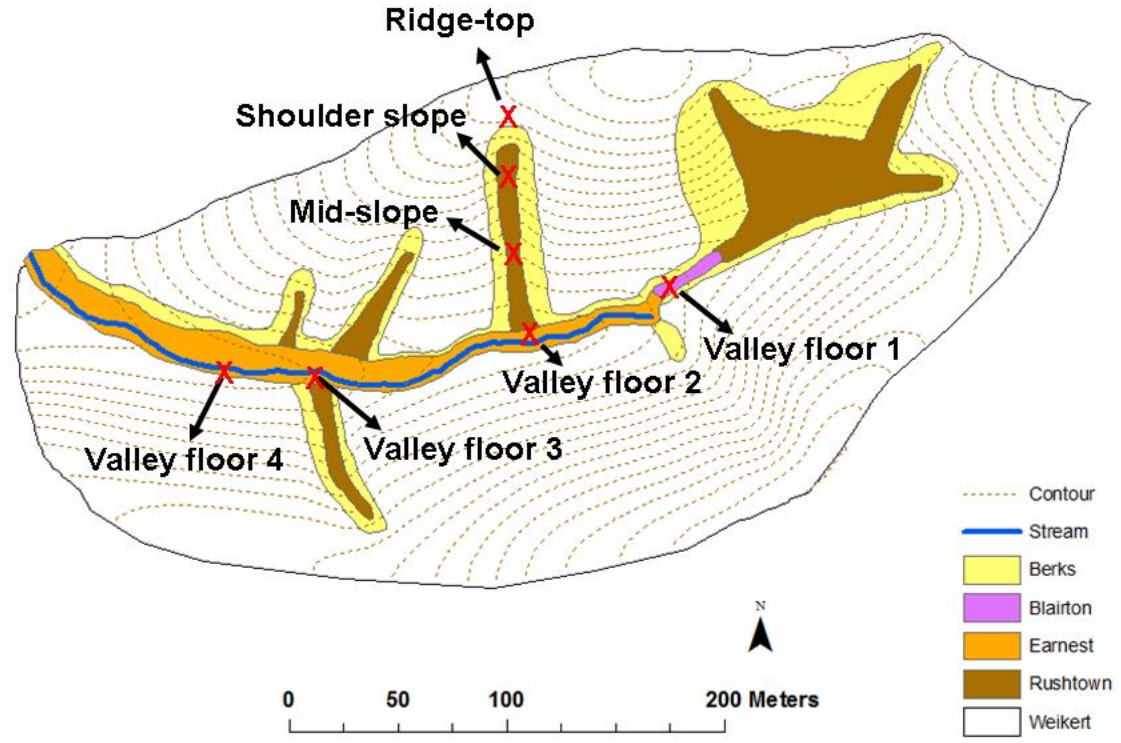


Figure 5-1: Map of the Shale Hills CZO in central Pennsylvania and the location of the monitoring sites along the hillslope and valley floor transects.

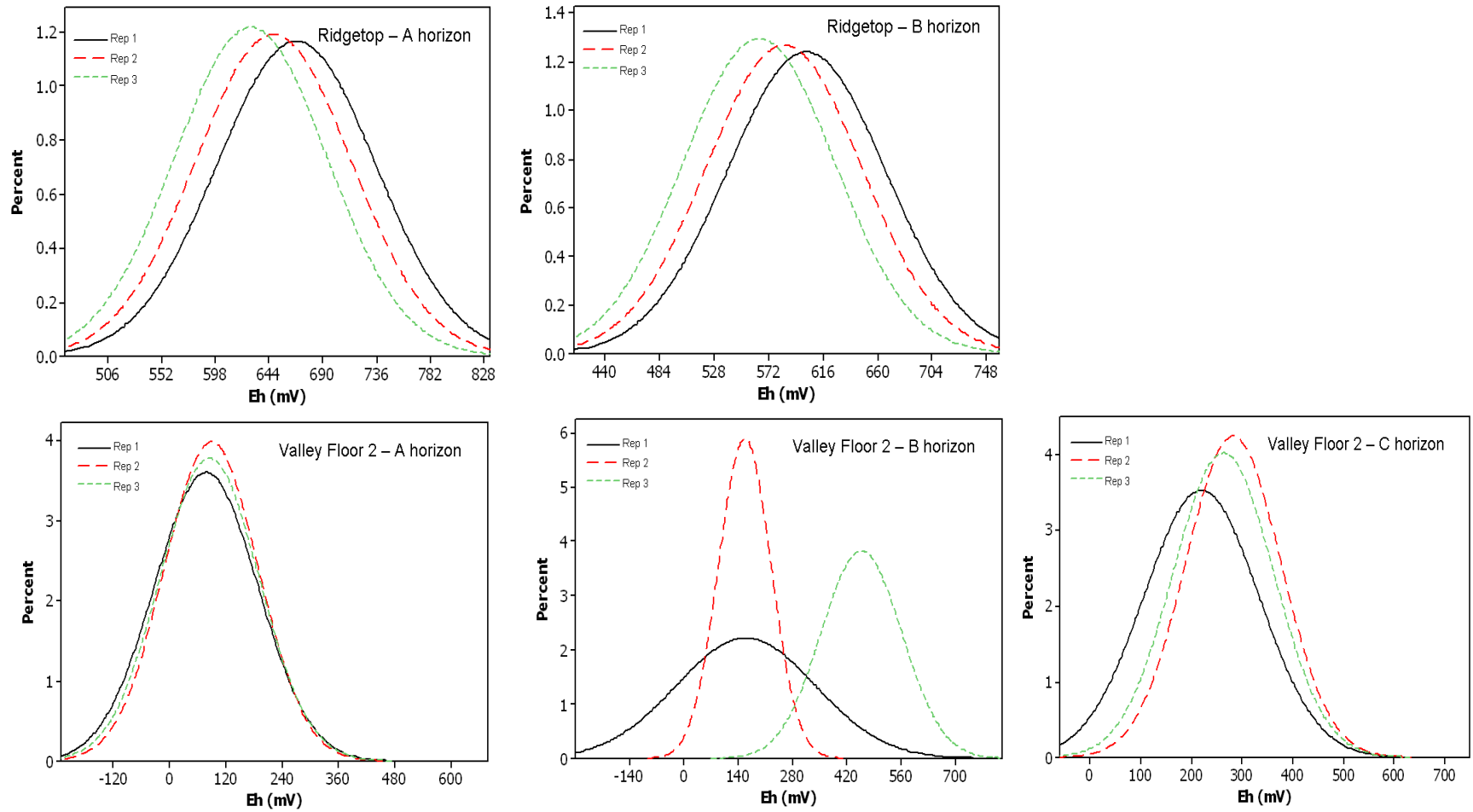


Figure 5-2: Example of variability between the replicated redox probes (n = 3) at the A, B and C soil horizons (ridgetop (upper panel) and valley floor 2 (lower panel)).

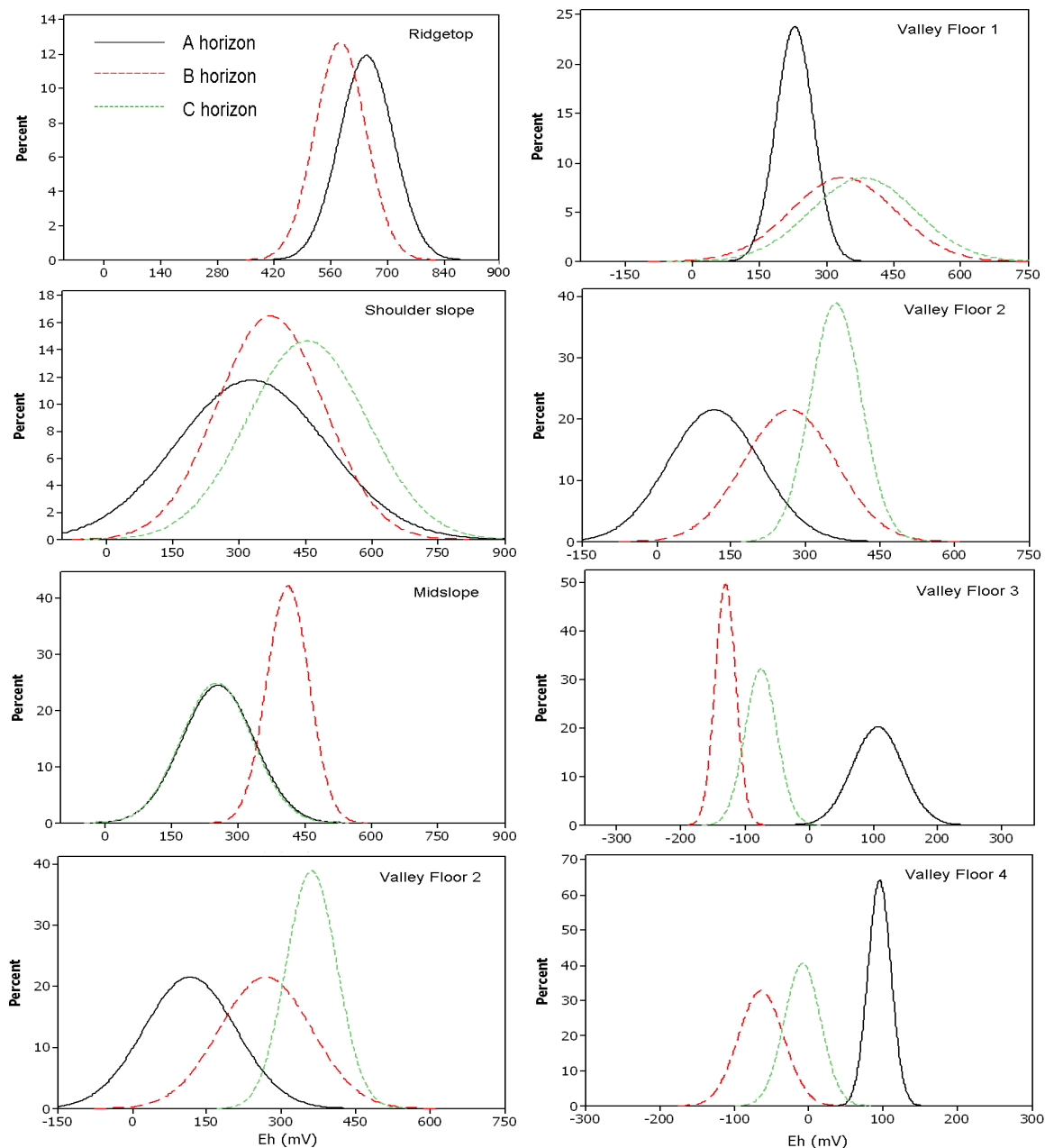


Figure 5-3: Distribution of soil redox potential (Eh) values collected between Apr. and Oct. 2010 (no data for valley floor sites 3 and 4 from 5/7/10 to 6/24/10 and the shoulder slope from 6/17/10 to 6/25/10 and 9/20/10 to 10/12/10 due to equipment malfunction) for the seven monitoring sites (hillslope transect – left panel; valley floor transect – right panel). Valley floor site 2 is duplicated as it is located along both transects.

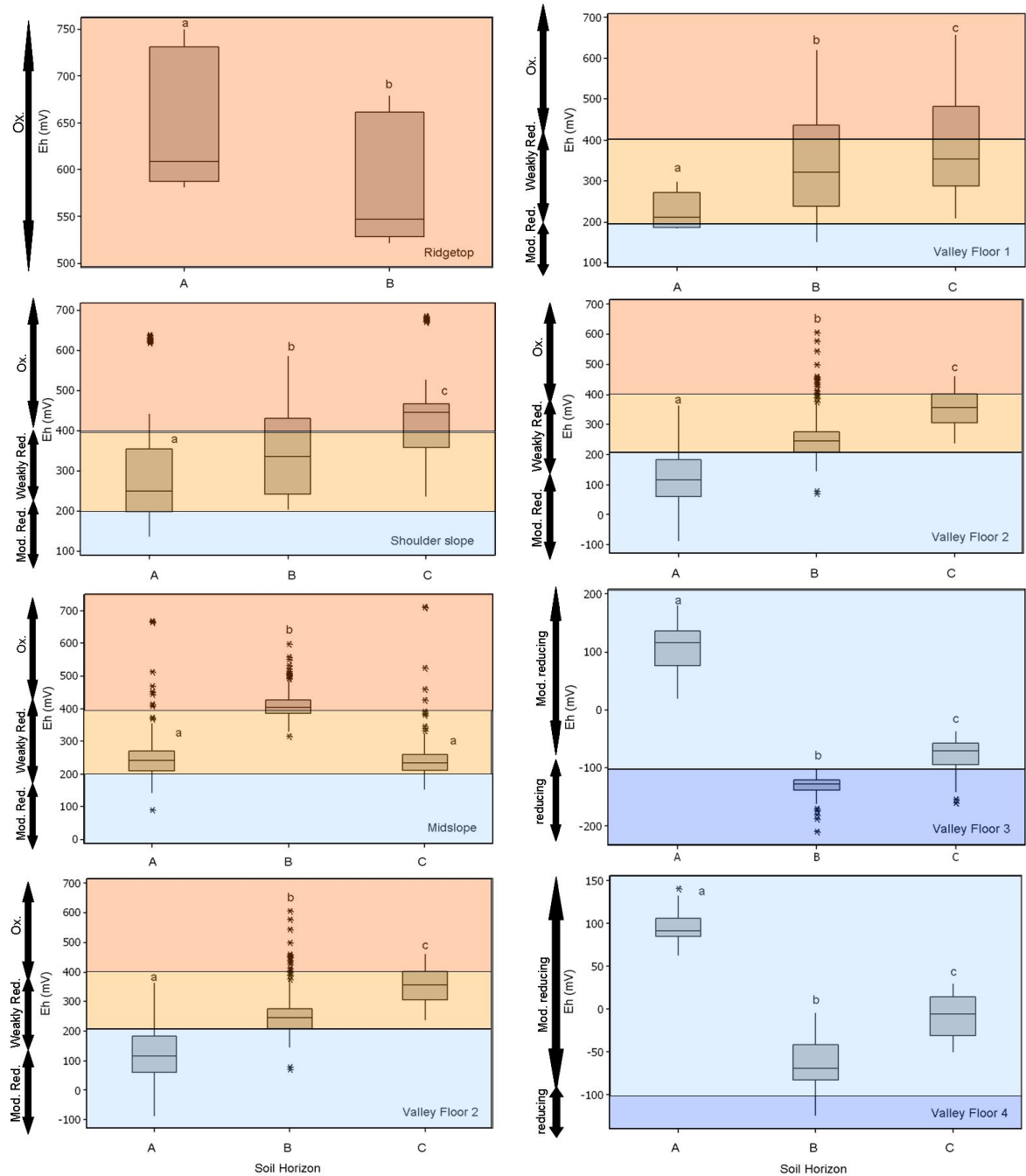


Figure 5-4a: Soil redox potential (Eh) for the A, B and C horizons in the seven monitoring sites (hillslope transect – left panel; valley floor transect – right panel) from Apr. to Oct. 2010 (no data for valley floor sites 3 and 4 from 5/7/10 to 6/24/10 and the shoulder slope from 6/17/10 to 6/25/10 and 9/20/10 to 10/12/10 due to equipment malfunction). Valley floor site 2 is duplicated as it is located along both transects. Different letters indicate significant difference between soil horizons Eh. Soil Eh values are grouped into oxidizing (>400 mV), weakly reducing (+200 to +400 mV), moderately reducing (-100 to +200 mV), or strongly reducing (<-100 mV).

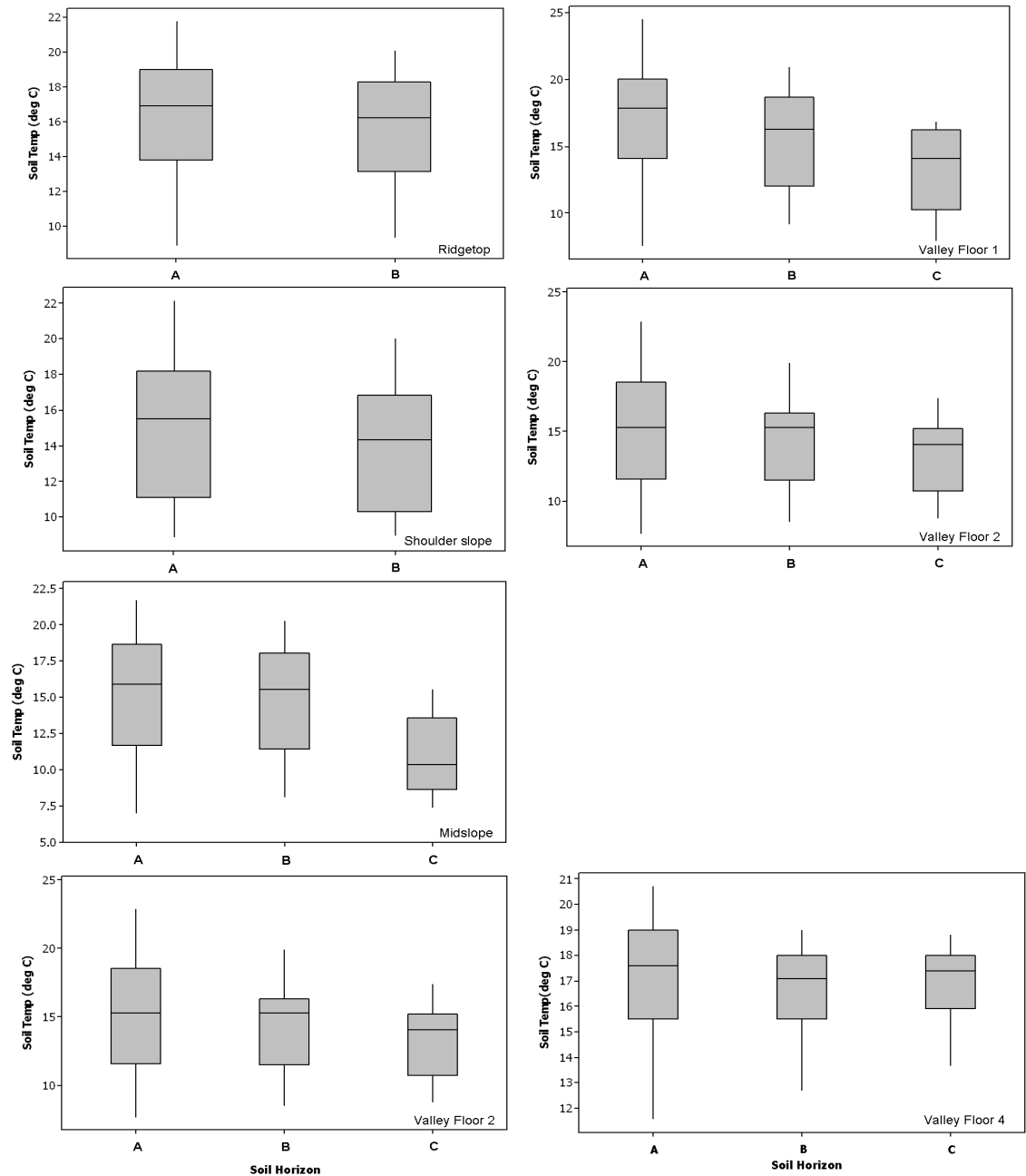


Figure 5-4b: Soil temperature for the A, B and C horizons of the seven monitoring sites (hillslope transect – left panel; valley floor transect – right panel) from Apr. to Oct. 2010. Valley floor site 2 is duplicated as it is located along both transects. (Data for Valley Floor 4 are from Jul. 2010 to Oct. 2010 and no data for Valley Floor 3).

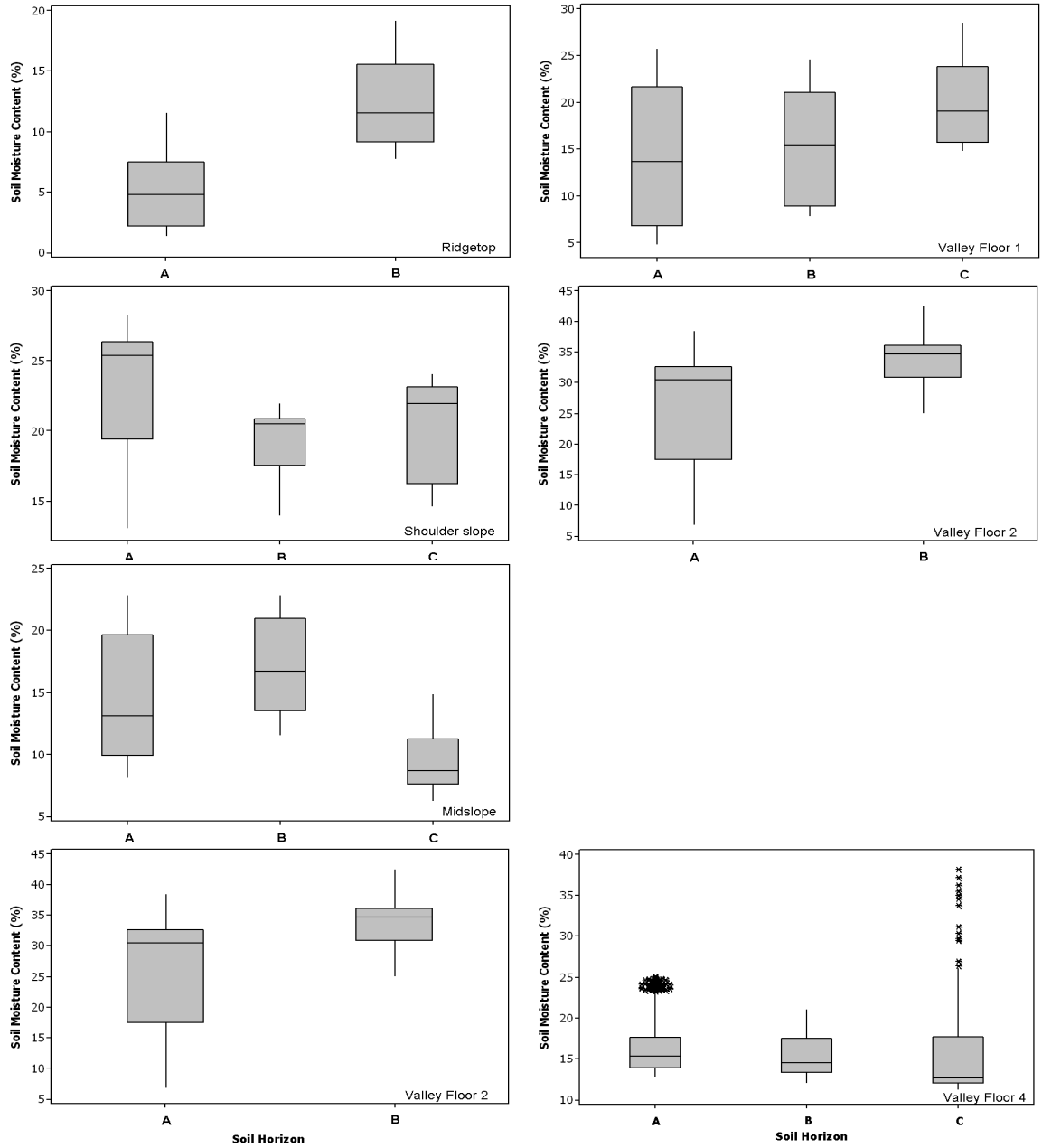


Figure 5-4c: Soil moisture content for the A, B and C horizons of the seven monitoring sites (hillslope transect – left panel; valley floor transect – right panel) from Apr. to Oct. 2010. Valley floor site 2 is duplicated as it is located along both transects. (Data for Valley Floor 4 are from Jul. 2010 to Oct. 2010 and no data for Valley Floor 3).

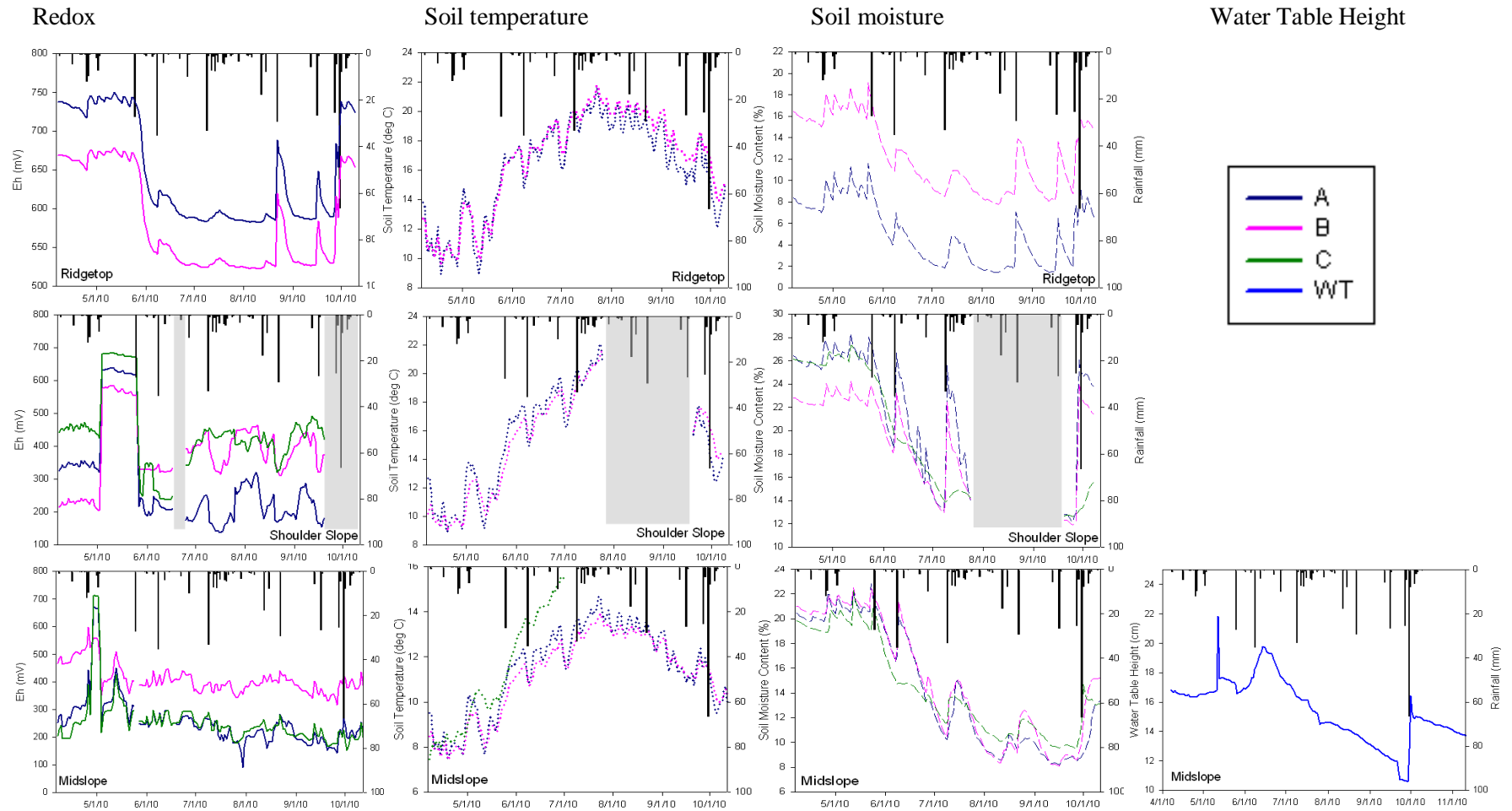


Figure 5-5: Time series of soil redox potential (Eh) measurements, along with soil temperature, volumetric soil moisture content and water table height from Apr. to Oct. 2010 in the seven monitoring sites. Blue line represents A horizon, pink line represents B horizon, green line represents C horizon, and black bars represent rainfall. Gray bars represent the period when Eh data were not collected due to equipment malfunction. *Note: no soil temperature and moisture content data for the valley floor 3, and data for the valley floor 4 were from Jul. 2010 to Oct. 2010.*

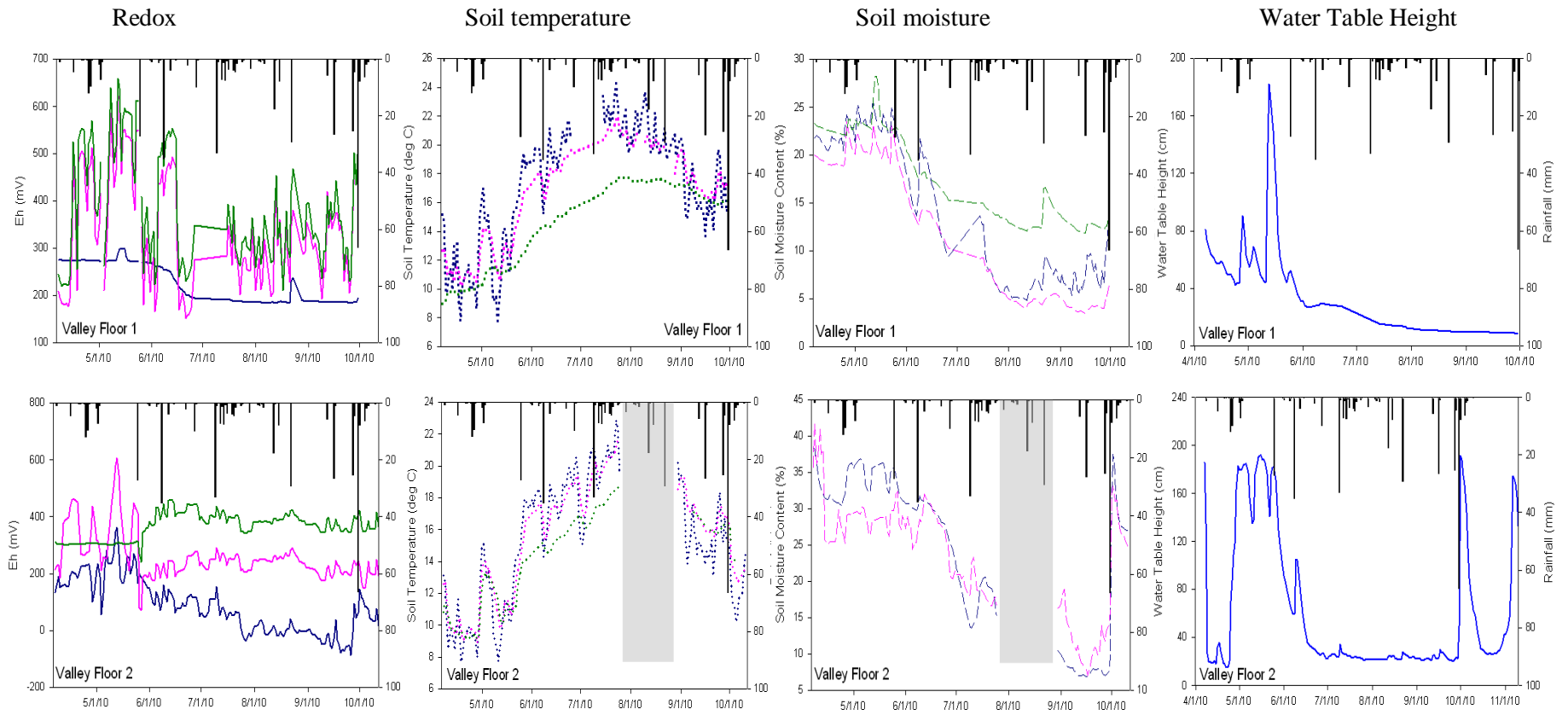
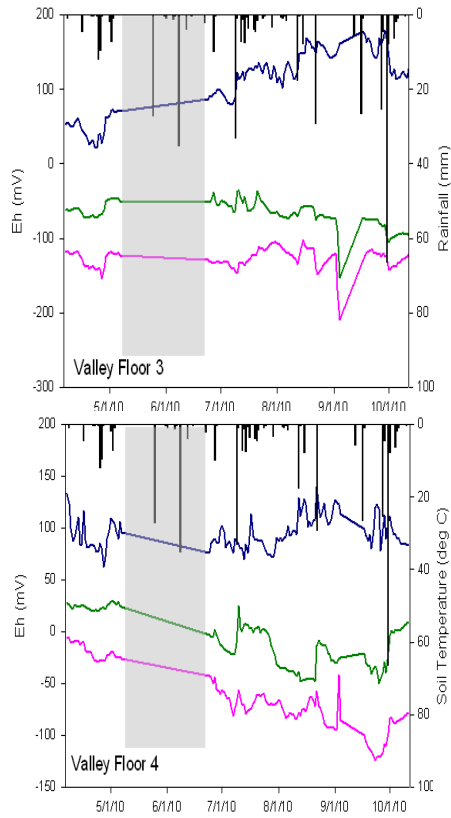
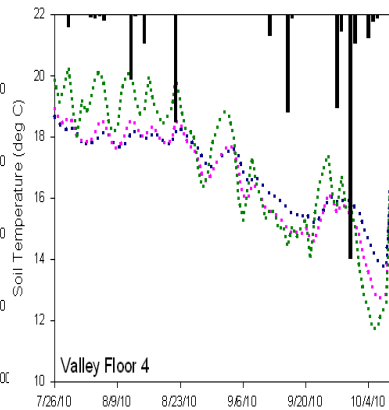


Figure 5-5 cont'd: Time series of soil redox potential (Eh) measurements, along with soil temperature, volumetric soil moisture content and water table height from Apr. to Oct. 2010 in the seven monitoring sites. Blue line represents A horizon, pink line represents B horizon, green line represents C horizon, and black bars represent rainfall. Gray bars represent the period when Eh data were not collected due to equipment malfunction. *Note: no soil temperature and moisture content data for the valley floor 3, and data for the valley floor 4 were from Jul. 2010 to Oct. 2010.*

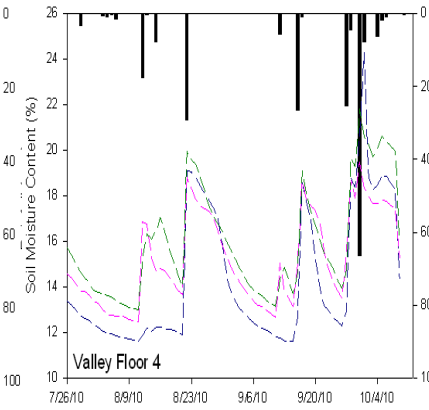
Redox



Soil temperature



Soil moisture



Water Table Height

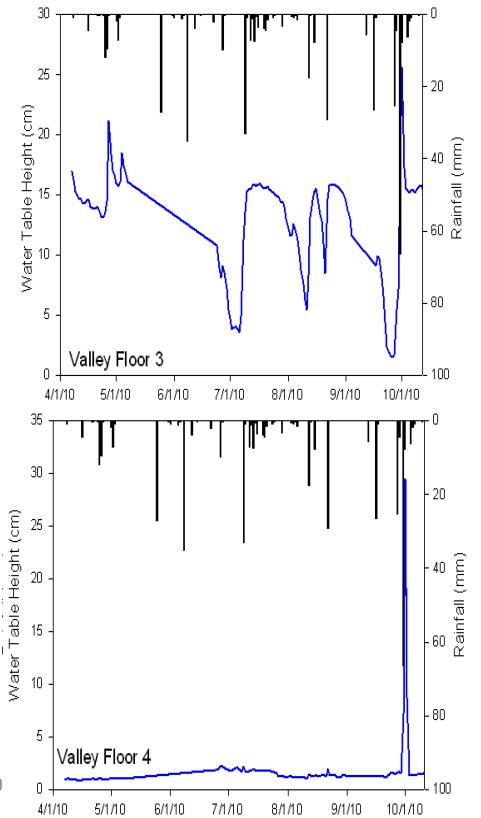


Figure 5-5 cont'd: Time series of soil redox potential (Eh) measurements, along with soil temperature, volumetric soil moisture content and water table height from Apr. to Oct. 2010 in the seven monitoring sites. Blue line represents A horizon, pink line represents B horizon, green line represents C horizon, and black bars represent rainfall. Gray bars represent the period when Eh data were not collected due to equipment malfunction. Note: no soil temperature and moisture content data for the valley floor 3, and data for the valley floor 4 were from Jul. 2010 to Oct. 2010.

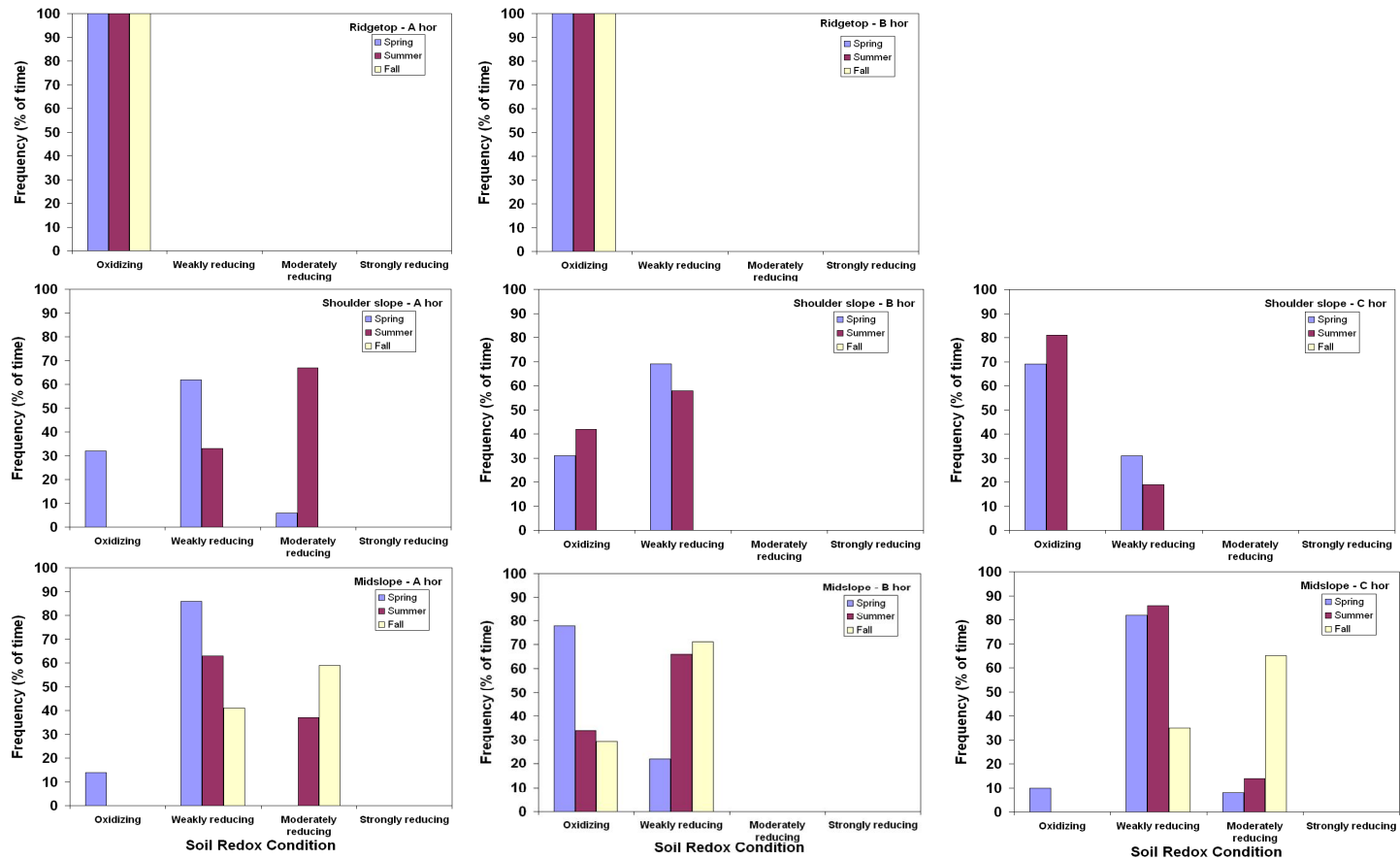


Figure 5-6: Frequency (% of time) of oxidation and reduction at different landscape positions for the A, B, and C horizons during spring, summer, and fall (April to October 2010). Soil redox (Eh) condition is grouped into oxidizing (>400 mV), weakly reducing (+200 to +400 mV), moderately reducing (-100 to +200 mV), or strongly reducing (<-100 mV).

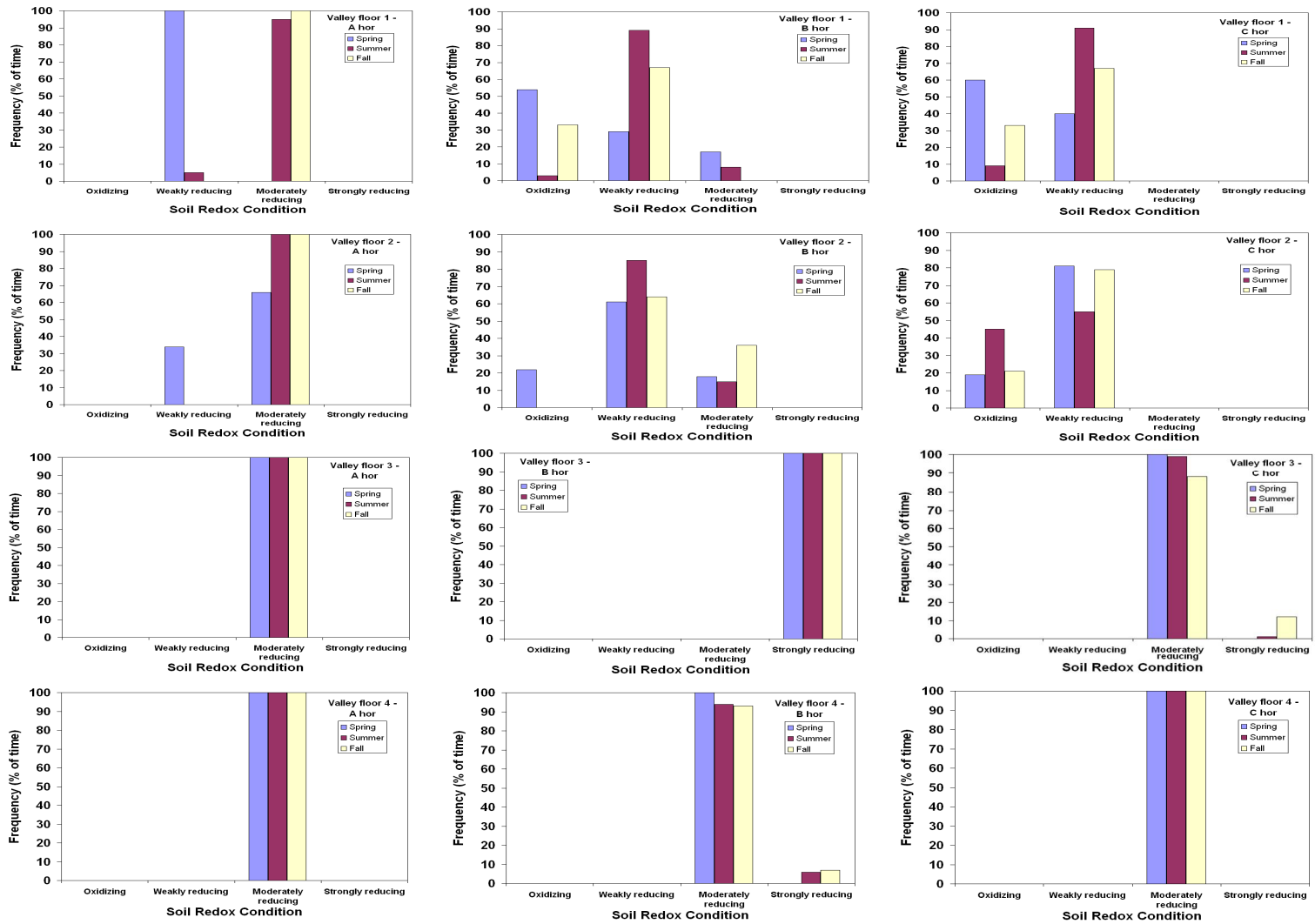


Figure 5-6 cont'd: Frequency (% of time) of oxidation and reduction at different landscape positions for the A, B, and C horizons during spring, summer, and fall (April to October 2010). Soil redox (Eh) condition is grouped into oxidizing (>400 mV), weakly reducing (+200 to +400 mV), moderately reducing (-100 to +200 mV), or strongly reducing (<-100 mV).

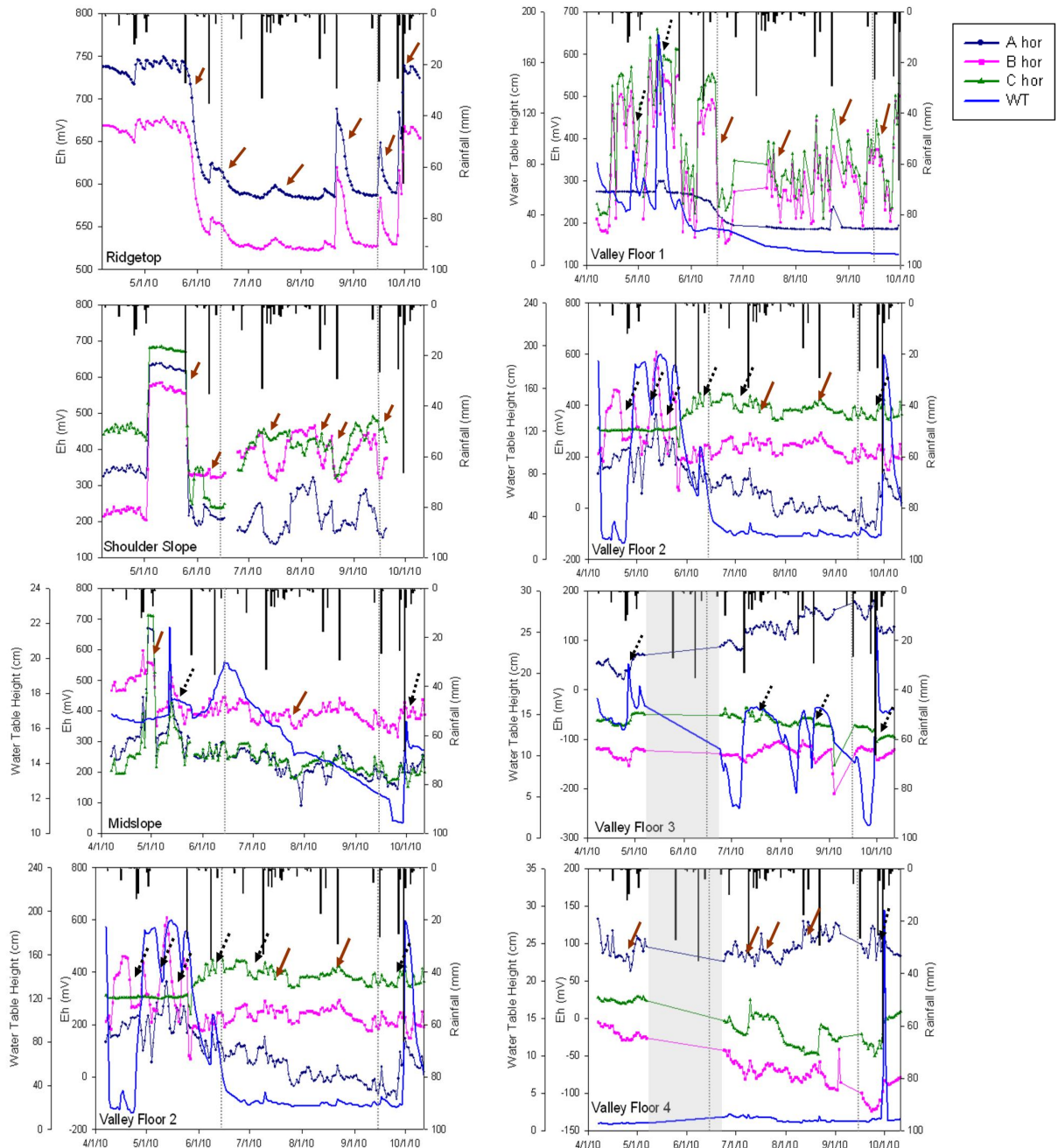


Figure 5-7: Response of soil redox potential (Eh) to rainfall events at the seven monitoring sites (hillslope transect – left panel; valley floor transect – right panel) from Apr. to Oct. 2010. Brown arrows indicate obvious drop in soil Eh due to rainfall events, black dashed arrows indicate a drop in soil Eh as water table level rises regardless of the size of the rainfall event, gray dotted line indicates division into the different seasons (spring, summer, fall), and the gray bar represents the period when Eh data were not collected due to equipment malfunction.

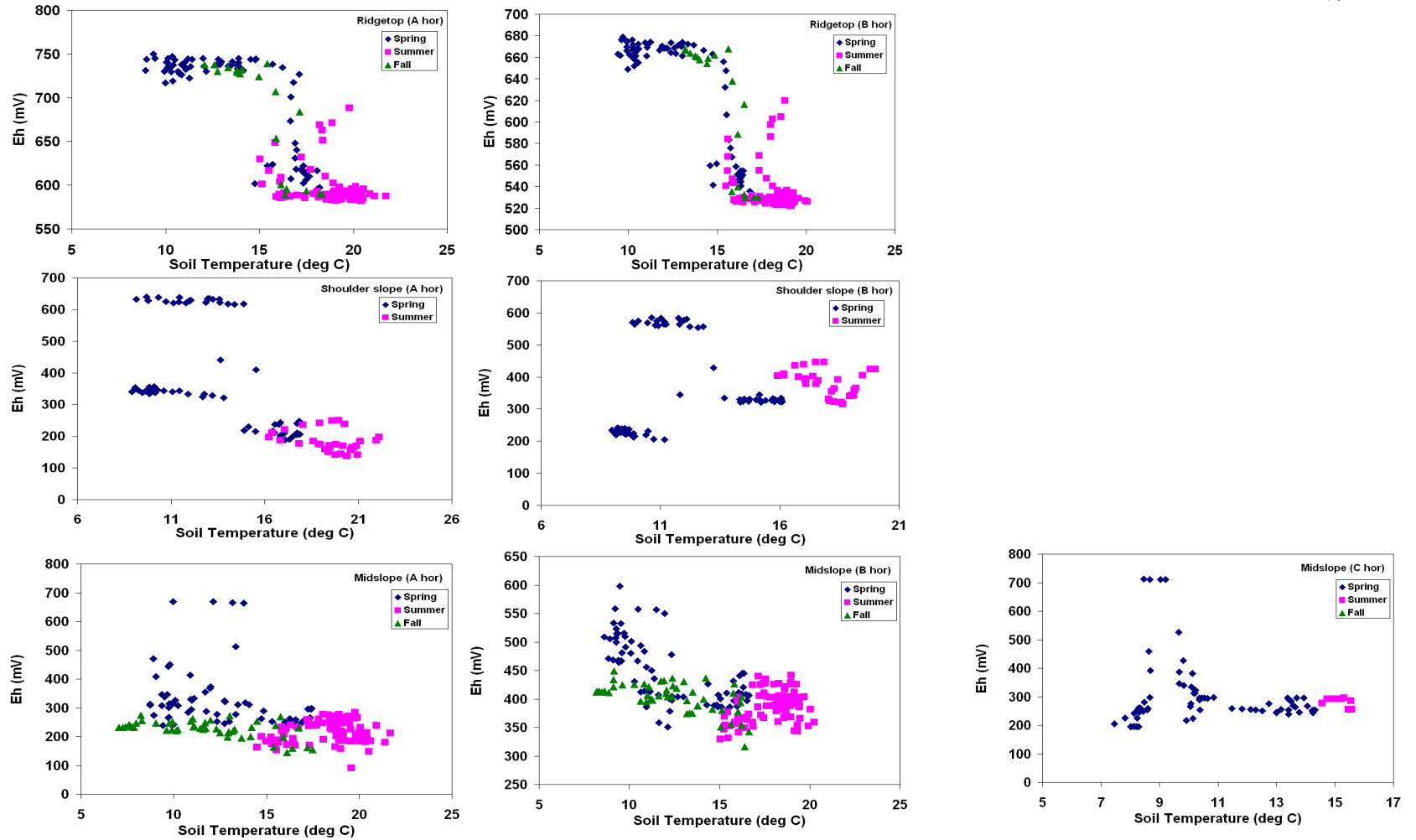


Figure 5-8a: Average daily soil redox potential (Eh) plotted as a function of soil temperature for the soil horizons of A (left panel), B (middle panel), and C (right panel) during the spring, summer, and fall periods (Apr. to Oct. 2010). No data for Valley Floor 3 and no spring data for Valley Floor 4.

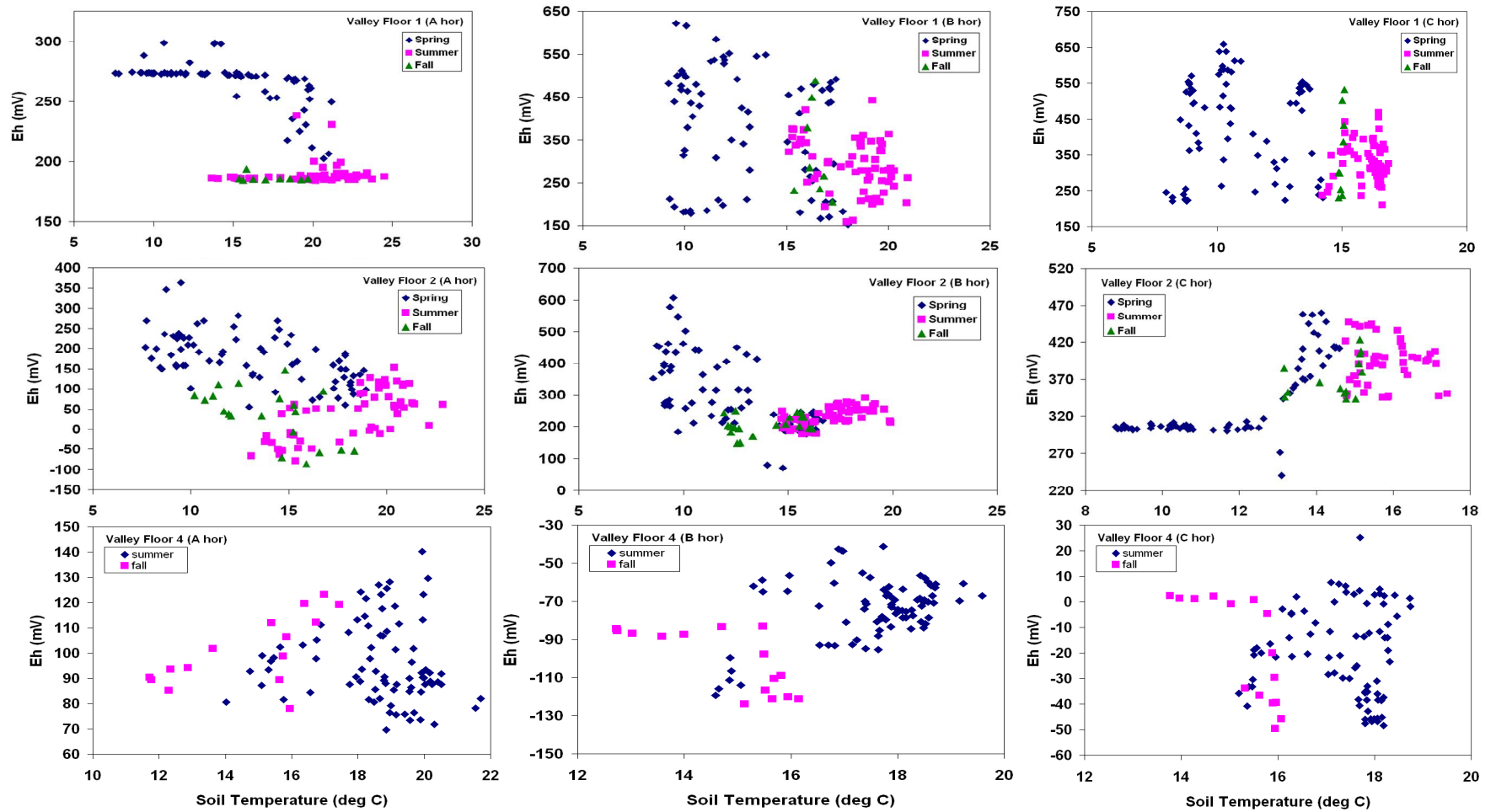


Figure 5-8a cont'd: Average daily soil redox potential (Eh) plotted as a function of soil temperature for the soil horizons of A (left panel), B (middle panel), and C (right panel) during the spring, summer, and fall periods (Apr. to Oct. 2010). No data for Valley Floor 3 and no spring data for Valley Floor 4.

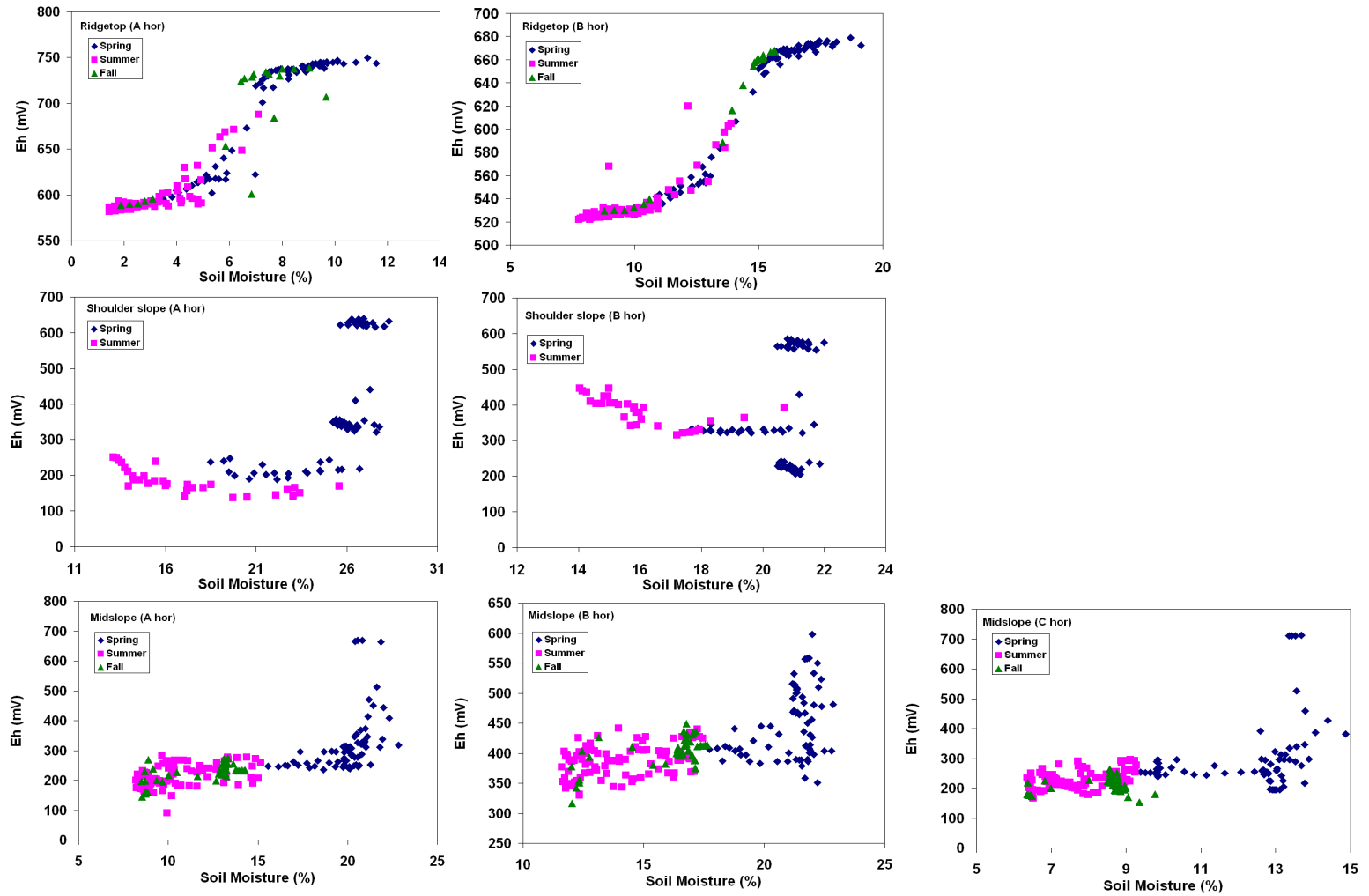


Figure 5-8b: Average daily soil redox potential (Eh) plotted as a function of soil moisture for the soil horizons of A (left panel), B (middle panel), and C (right panel) during the spring, summer and fall periods (Apr. to Oct. 2010). No data for Valley Floor 3 and no spring data for Valley Floor 4.

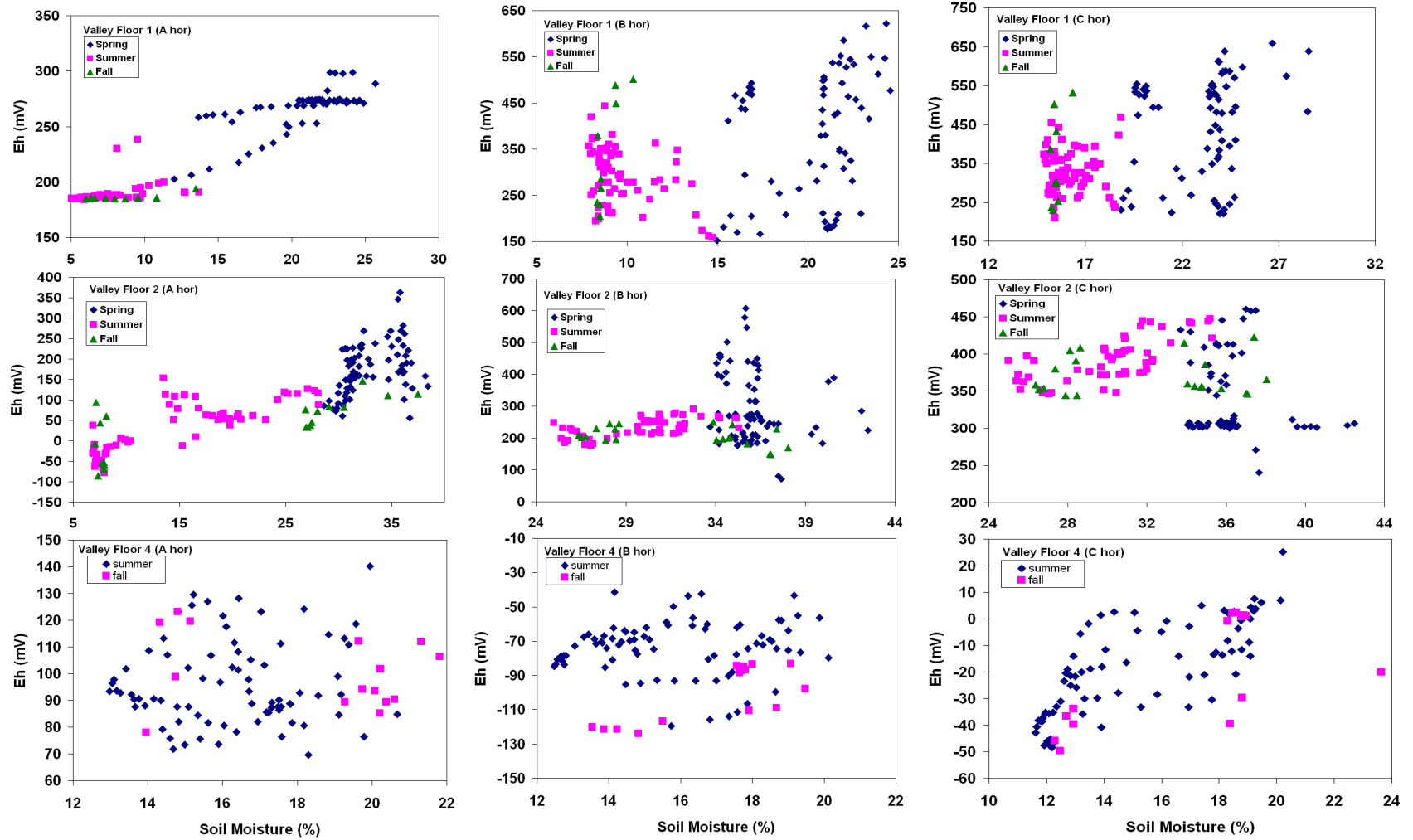


Figure 5-8b cont'd: Average daily soil redox potential (Eh) plotted as a function of soil moisture for the soil horizons of A (left panel), B (middle panel), and C (right panel) during the spring, summer and fall periods (Apr. to Oct. 2010). No data for Valley Floor 3 and no spring data for Valley Floor 4.

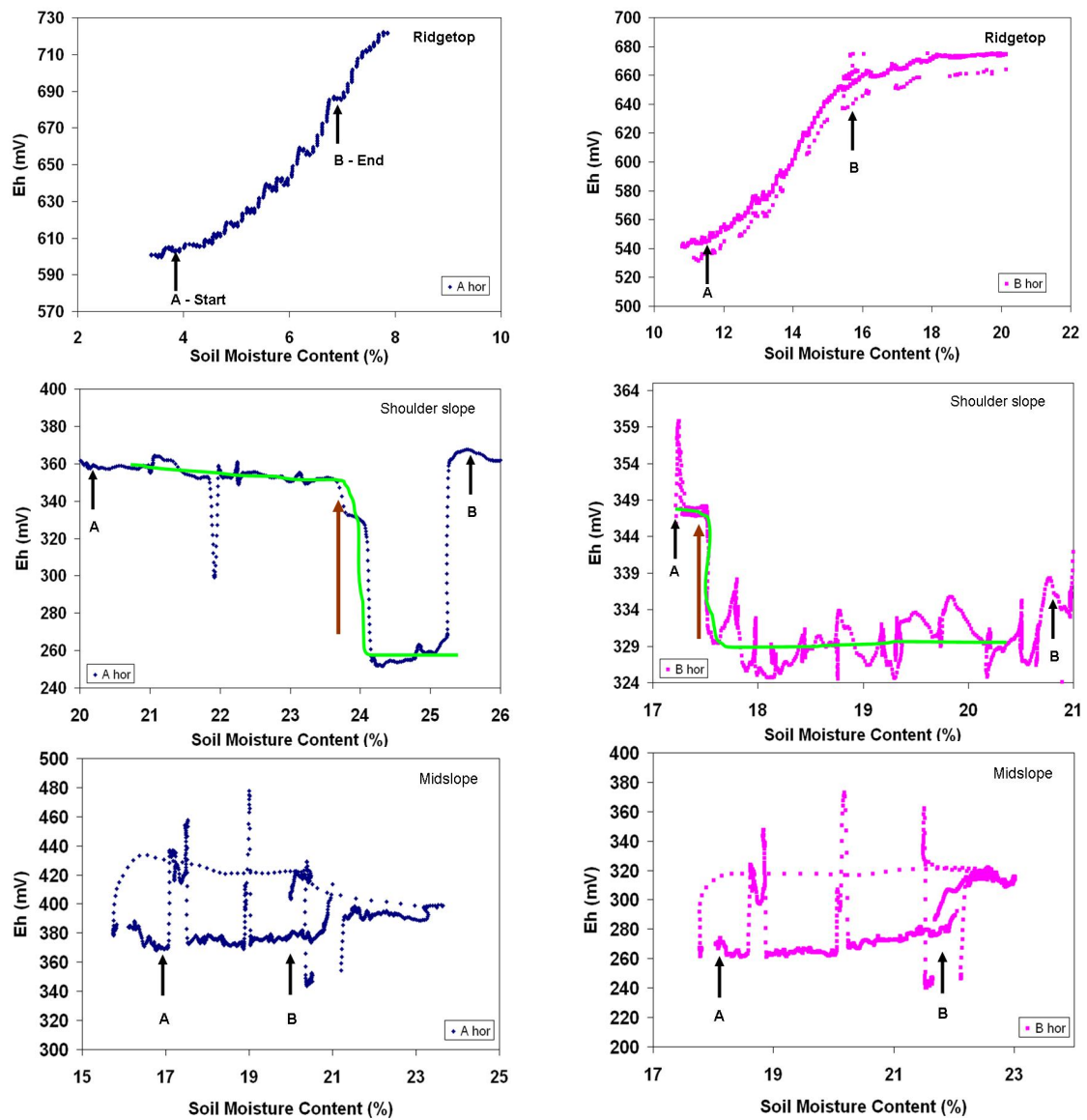


Figure 5-9: An example of soil redox potential (Eh) as a function of soil moisture content for the A (left panel) and B (right panel) soil horizons during a storm event (35 mm) that occurred on June 8th 2010 (7am to 10pm). Black arrows indicate when the rainfall event started (A) and ended (B). Solid green line represents general soil Eh pattern and brown arrow depicts soil moisture content at which soil Eh drops. No data for Valley Floor 3 and 4.

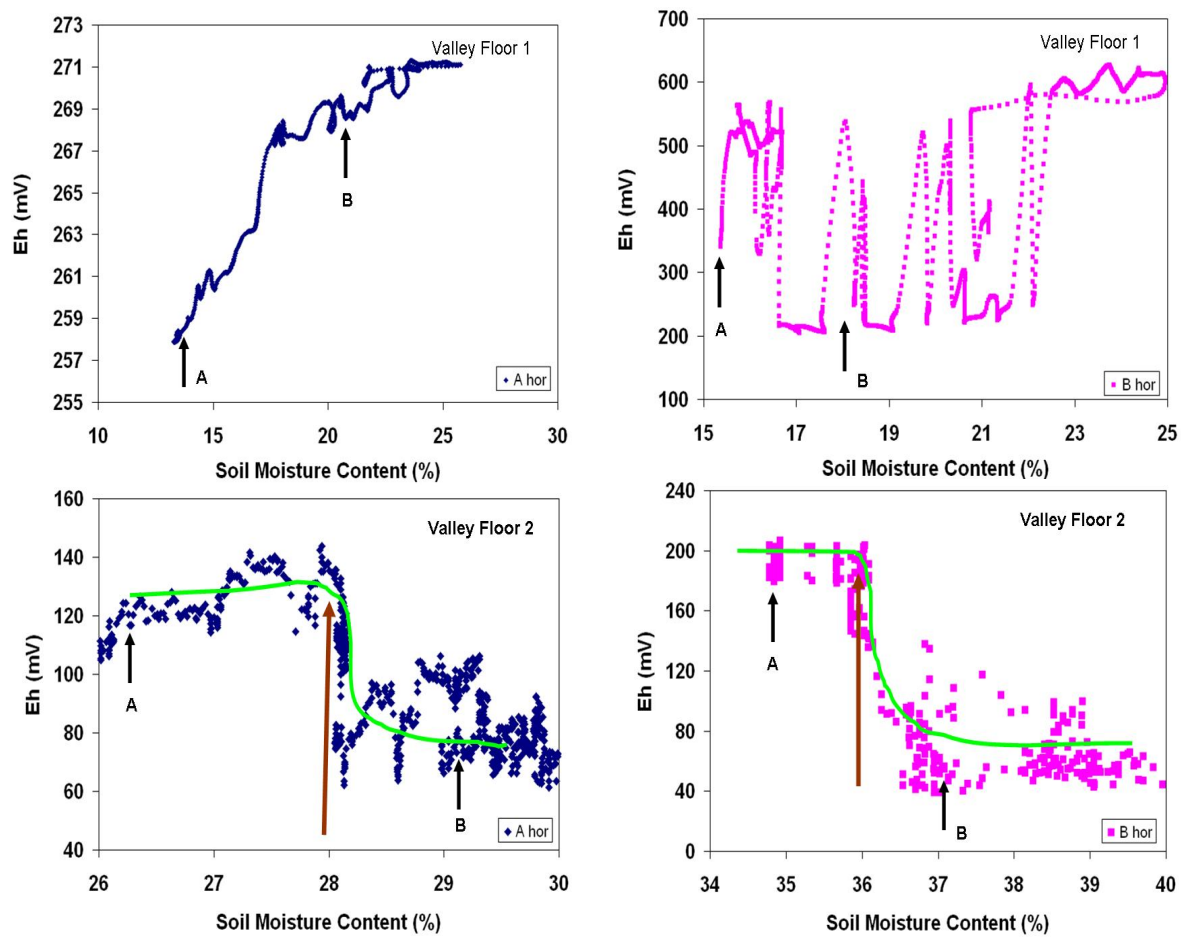


Figure 5-9 cont'd: An example of soil redox potential (Eh) as a function of soil moisture content for the A (left panel) and B (right panel) soil horizons during a storm event (35 mm) that occurred on June 8th 2010 (7am to 10pm). Black arrows indicate when the rainfall event started (A) and ended (B). Solid green line represents general soil Eh pattern and brown arrow depicts soil moisture content at which soil Eh drops. No data for Valley Floor 3 and 4.

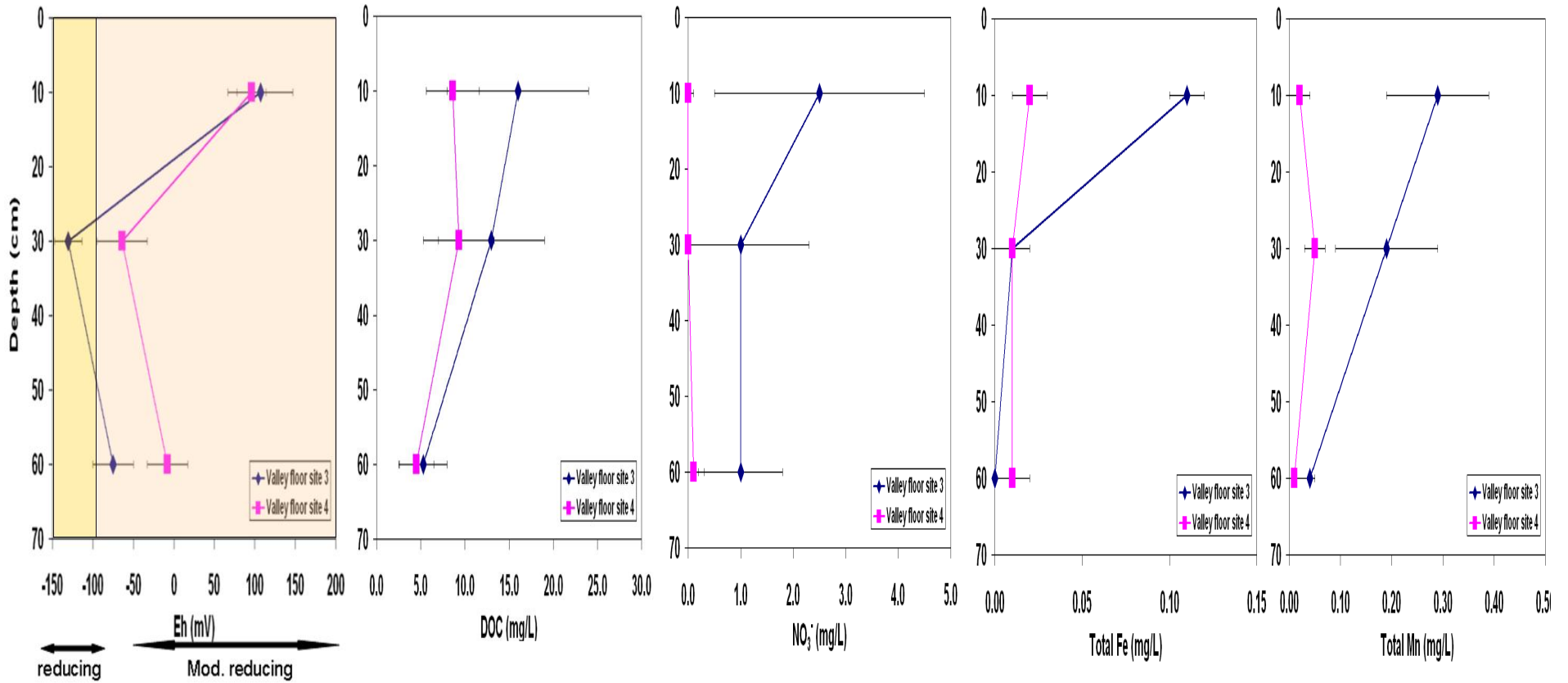


Figure 5-10: Depth function of soil redox potential (Eh) (mean and standard deviation for the period from Apr. to Oct. 2010) and soil pore water dissolved organic carbon (DOC), nitrate (NO₃⁻), total iron (Fe) and total manganese (Mn) concentrations (mean and standard deviation for the period from Aug. 2007 to Oct. 2009) at valley floor sites 3 and 4.

Table 5-1: Redox potential (Eh) range in soils showing microbial metabolism process and electron acceptor (after DeLaune and Reddy, 2005).

Anaerobic					Aerobic			Soil condition			
Highly reduced	Reduced		Moderately reduced		Oxidized			Redox condition			
CO ₂	SO ₄ ²⁻	Fe ³⁺	Mn ⁴⁺	NO ₃ ⁻	O ₂			Electron acceptor			
Anaerobic		Facultative			Aerobic			Microbial metabolism			
-300	-200	-100	0	+100	+200	+300	+400	+500	+600	+700	mV

Table 5-2: Basic soil characteristics for the seven sites monitored at the Shale Hills CZO.

Landscape Position	Soil Series	Soil Horizon	Soil Depth (cm)	Clay Content (wgt. %)	Redoximorphic Features [§]
Ridgetop	Weikert	A	10	17	none
		Bw	20	16	none
Shoulder slope	Rushtown	A	10	20	none
		BC	40	16	none
		C	97	14	none
Midslope	Rushtown	A	8	17	none
		Bw	30	22	none
		C	70	15	none
Valley floor 1	Blairton	A	13	18	none
		Bt	35	21	none
		CB	95	14	2% Fe depletions
Valley floor 2	Ernest	A	13	16	none
		Bt	40	18	20% Fe depletions
		C	70	15	none
Valley floor 3	Ernest	A	10	19	none
		Bw-Bt	30	29	20% Fe depletions
		C	60	12	none
Valley floor 4	Ernest	A	10	26	none
		Bw-Bt	30	30	20% Fe depletions
		C	60	12	none

[§] Data taken from Lin et al. (2006)

Table 5-3: Depth of sensor installation for the seven monitoring sites at the Shale Hills CZO.

Site ID	Redox probe (3 replicates per depth)	Water table sensor	Soil temperature sensor	Soil moisture content sensor
	------(cm)-----			
Ridgetop	10, 20	26	9, 23	10, 17
Shoulder slope	10, 40, 97	200	10, 40, 97	10, 40, 97
Midslope	8, 30, 70	423	8, 25, 71	8, 25, 71
Valley floor 1	13, 35, 95	202	10, 36, 97	13, 35, 95
Valley floor 2	13, 40, 70	232	12, 36, 74	13, 41, 73
Valley floor 3	10, 30, 60	153	-	-
Valley floor 4	10, 30, 60	300	10, 30, 60	10, 30, 60

Table 5-4: Analysis of variance of soil redox potential (Eh) showing the effects of soil horizon (A, B, and C horizons), landscape position (ridgetop, shoulder slope, midslope, valley floor), season, and their interactions. The *F* value is the test statistic used to determine whether the sample means are within the sampling variability of each other, and *p* value is the statistical significance level.

Effects	<i>F</i> value	<i>p</i>-value
Soil horizon	4.23	0.04
Landscape position	539.36	0.00
Season	5.77	0.02
Soil horizon * Landscape position	0.07	0.80
Soil horizon * Season	17.74	0.00
Landscape position * Season	3.34	0.07

Table 5-5: Multiple regression table showing influence of soil moisture, temperature, and water table height on soil redox potential (Eh) for the A, B and C horizons at the seven monitoring sites. The R^2 value is the proportion of variability in a data set that is accounted for by the statistical model, and p value is the statistical significance level.

Landscape Position	Soil Horizon	Soil Temperature (deg C)	Soil Moisture Content (%)	Water Table Height (cm)	Regression coefficient (R^2) for Model of the three factors combined
Ridgetop	A	$p < 0.05$	$p < 0.05$	*	0.92
	B	$p < 0.05$	$p < 0.05$	*	0.93
Shoulder slope	A	$p < 0.05$	$p < 0.05$	*	0.49
	B	$p = 0.10$	$p = 0.22$	*	0.03
	C	*	$p < 0.05$	*	0.22
Midslope	A	$p < 0.05$	$p < 0.05$	$p = 0.93$	0.44
	B	$p < 0.05$	$p < 0.05$	$p = 0.44$	0.44
	C	$p = 0.12$	$p < 0.05$	$p = 0.96$	0.11
Valley floor 1	A	$p = 0.55$	$p < 0.05$	$p = 0.23$	0.23
	B	$p = 0.36$	$p = 0.23$	$p < 0.05$	0.20
	C	$p = 0.40$	$p < 0.05$	$p < 0.05$	0.93
Valley floor 2	A	$p < 0.05$	$p < 0.05$	$p = 0.43$	0.69
	B	$p < 0.05$	$p = 0.43$	$p = 0.69$	0.31
	C	$p < 0.05$	*	$p < 0.05$	0.60
Valley floor 3	A	*	*	$p < 0.05$	0.51
	B	*	*	$p < 0.05$	0.25
	C	*	*	$p < 0.05$	0.40
Valley floor 4	A	$p < 0.05$	$p = 0.09$	$p = 0.28$	0.08
	B	$p < 0.05$	$p = 0.45$	$p < 0.05$	0.35
	C	$p = 0.36$	$p < 0.05$	$p = 0.85$	0.47

* - No data

Chapter 6

Summary and Future Needs

The main objective of this research was to use dissolved organic carbon (DOC) to couple hydrogeology and biogeochemistry at different spatial and temporal scales within the Shale Hills Critical Zone Observatory (CZO). To accomplish this, a field scale research project was initiated that examined DOC along two hillslopes of contrasting soils and topography as well as within the associated headwater stream. The concept of hydrogeology was incorporated in this research project by using soil and hydrology characteristics to examine the dynamics of DOC *in situ* at the field scale. Soil factors such as landscape position, soil- depth, moisture, temperature, and redox potential and hydrological factors such as water table levels, rainfall amount, discharge, and flow pathways were examined. Additionally, the interactions between nitrate (NO_3^-), metals (Al, Fe and Mn), and DOC were also evaluated.

Chapter 2 highlighted that clay content was the single best predictor of SOC (soil organic carbon) storage, explaining more than 70% of catchment wide variability in SOC storage. Higher clay content, lower slope, thicker soils, greater topographic wetness index, and a higher number of swales in the south-facing slope resulted in 30% more SOC storage in the soil solum (A and B horizons) as compared to the north-facing slope. Elevated soil pore water DOC concentrations (> 20 % higher compared to surrounding soil depths) were observed within the soil profile at the Bw-Bt horizon interface in the

valley floor and at the soil-bedrock interface at the ridgetop. This finding is consistent with the inference that restrictive subsurface interfaces are potential transport-driven “hot spots” for soil pore water DOC (and other solutes, since DOC is known to facilitate the transport of both organic and inorganic substances).

Stream water DOC export was significantly correlated to stream discharge and water temperature. High DOC concentrations during the snowmelt period (high discharge, flushing effect) and the late summer to early fall wet-up period (low discharge, temperature effect) were noticeable “hot moments” for DOC (short time periods, < 20 % of total time, with elevated DOC export). However, year to year variability with changes in climate suggests that longer monitoring is needed to gain a fuller understanding of DOC movement in this catchment.

Results from Chapter 3 underscored that soil pore water DOC (and not NO_3^-) concentrations were significantly correlated to pH, SOC, TN, and C:N ratio. Elevated soil pore water concentrations of both DOC and NO_3^- concentrations were observed at restrictive soil horizon interfaces (particularly the Bw-Bt and the soil-bedrock interfaces). Unexpectedly, extremely low C:N ratios were observed in this study (< 10). These low ratios are likely due to a combination of high N deposition, vegetation, and parent material.

Elevated concentrations at restrictive soil interfaces are consistent with the conclusion that flushing occurs along these restrictive soil interfaces due to preferential flow pathways. Preferential flow is common in the Shale Hills catchment, particularly along soil horizon interfaces (A-B and B-C horizon interfaces) (Lin, 2006; Lin and Zhou, 2008), and especially in late summer/early fall as the catchment wets-up (Graham and

Lin, in review). Additionally, Jin et al (in review), observed highly variable δD (deuterium) concentrations at the Bw-Bt soil interface at the valley floor of the catchment. Asano et al. (2006) proposed that the variability in δD can be used as an index of flowpath length and contact time, such that high variability is indicative of short flowpath length and contact time which results in higher solute concentrations (Asano et al., 2006). Therefore, consistently higher soil pore water solute concentrations at the restrictive soil interfaces, where preferential flow occurs, supports the proposal that higher proportions of shallow soil pore waters contribute to the higher stream concentrations during late summer/early fall rainfall events in this catchment.

Chapter 4 highlighted that DOC is a major facilitator of metal transport in acidic forest soils. High soil pore water DOC and low pH combined explained 76% of the variability in soil pore water metal (total Al, Fe and Mn) concentrations. Elevated soil pore water DOC and metal concentrations at restrictive soil interfaces and the generally high DOC to metal ratios (> 50) are consistent with high mobility of organically-complexed metals along preferential flow pathways. Seasonality and stream water DOC were significantly correlated to stream water metal concentrations over the 2008-2009 monitoring period, with elevated concentrations especially during the late summer/early fall.

Finally, in Chapter 5, results showed that soil Eh was highest at the ridgetop, which was oxidized (> 400 mV) throughout the entire study period, while the shoulder slope and midslope varied between oxidizing and moderately reducing conditions (> -100 mV). Average soil Eh generally decreased downstream; however, valley floor site 4 was in general moderately reducing like valley floor sites 1 and 2, while valley floor site 3

was strongly reducing (< -100 mV). Landscape position, soil depth, and seasonality combined explained $> 70\%$ of daily soil Eh variability in the catchment. At each landscape position a combination of soil moisture, temperature, and water table was significantly correlated to soil Eh. At all topographic position, increasing soil temperatures decreased soil Eh, while increased water table height significantly decreased soil Eh at the valley floor. However, soil Eh increased with increasing soil moisture along the hillslope but at the valley floor during rainfall events (> 20 mm), a 2 to 4 % increase in soil moisture resulted in a decrease in soil Eh. These results suggested oxaquic moisture conditions along the hillslope, because of rapid flow of water through permeable soils.

Soil Eh status did appear to influence soil solution chemistry at the valley floor. The behavior of NO_3^- , Fe^{3+} , and Mn^{4+} as electron acceptors can be assumed from the loss of NO_3^- and the increase in concentration of total Fe and Mn. The behavior of different electron acceptors is a sequential process and these processes overlap, since we observed the presence of NO_3^- , and Mn and Fe at the same time or the absence of NO_3^- but presence of Mn and Fe in the soil solution.

The overall findings of this dissertation demonstrate that explicit consideration of both soil physiochemical properties and hydrological characteristics will elucidate the main factors controlling the transport of soluble solutes. Soil profile trends are important to understanding solute transport and potential areas and timing of elevated concentrations. Furthermore, preferential flow pathways especially along restrictive soil horizon interfaces can impact the transport of solutes from upland to the stream.

These findings have resulted in a conceptual diagram of water and solute transport along the hillslope (Figure 6-1). The diagram is for the swale transect and is similar to that of the planar transect. The main difference between the swale and the planar hillslopes was that soil pore water solute concentrations (DOC, NO_3^- , total Al, Fe and Mn) were lower along the planar hillslope as compared to the swale. This is likely due to shallower soils along the planar hillslope as compared to the swale transect. Additionally, flow along the planar hillslope is non-convergent, while flow along the swale is convergent. The main difference in Figure 6-1 from what was hypothesized in Chapter 1, is that the findings of this study actually showed that while solute concentrations decreased with increasing soil depth, solute concentrations were consistently elevated at restrictive soil horizon interfaces (as discussed previously).

While this dissertation represents the first record of C for the Shale Hills CZO, it is in direct response to the need for understanding the factors that control the spatiotemporal patterns of C at the field scale. Although this research underscores the importance of both soil properties and hydrologic characteristics on DOC patterns, it has raised many others. Such as, “Why are there elevated concentrations at the restrictive soil horizon interfaces?” and “Is there a constant source of DOC and from what is it derived?”

As a result, there are many directions for future research. One hypothesis is high microbial activity at the restrictive soil interfaces because of optimal water and nutrient supply. Preliminary data have shown high microbial biomass at these interfaces (Yesavage, et al., xxxx). Further investigations into microbial biomass, diversity and activity can provide direct evidence that will test this hypothesis. Additionally, laboratory soil column studies can be used to understand DOC release from soil and complexation

with the aforementioned metals. Characterization of DOC using techniques such as fluorescence, specific ultraviolet absorbance (SUVA) and fractionation analyses may elucidate DOC composition, sources and pathways, and the incorporation of C isotopic studies will assist in the differentiation of 'old' versus 'new' organic matter as well as the determination of DOC and carbon dioxide sources. Further field studies focused on litterfall rates, carbon dioxide efflux, microbial biomass, and turnover times will help to improve the approximation of the C budget presented in Appendix C. Finally, measurement of Mn and Fe species will better elucidate the influence of soil Eh on soil pore water chemistry. Overall, long-term *in-situ* monitoring is necessary to understand year to year variability especially due to potential changes in climate.

References

- Asano, Y., J. E. Compton, and M. R. Church. 2006. Hydrologic flowpaths influence inorganic and organic nutrient leaching in a forest soil. *Biogeochemistry* 81: 191-204.
- Graham, C. and H. Lin. Controls and frequency of preferential flow occurrence at the Shale Hills Critical Zone Observatory: A 175 event analysis of soil moisture response to precipitation. *In review: Vadose Zone Journal*.
- Jin, L., D. M. Andrews, G. H. Holmes, C. J. Duffy, H. Lin and S. L. Brantley. Water chemistry reflects hydrological controls on weathering in Susquehanna/Shale Hills Critical Zone Observatory (Pennsylvania, USA). *In review: Vadose Zone Journal*.
- Lin, H. 2006. Temporal stability of soil moisture spatial pattern and subsurface

preferential flow pathways in the Shale Hills Catchment. *Vadose Zone Journal* 5: 317-340.

Lin, H. and X. Zhou. 2008. Evidence of subsurface preferential flow using soil hydrologic monitoring in the Shale Hills Catchment. *European Journal of Soil Science* 59: 34-49.

Yesavage, T., L. J. Liermann, M. S. Fantle, L. Jin, J. Vervoort, R. Mathur, and S. L. Brantley. xxxx. Fe cycling in the Shale Hills Critical Zone Observatory, Pennsylvania: An analysis of microbiology, chemical weathering, and Fe isotope fractionation. (*in preparation*).

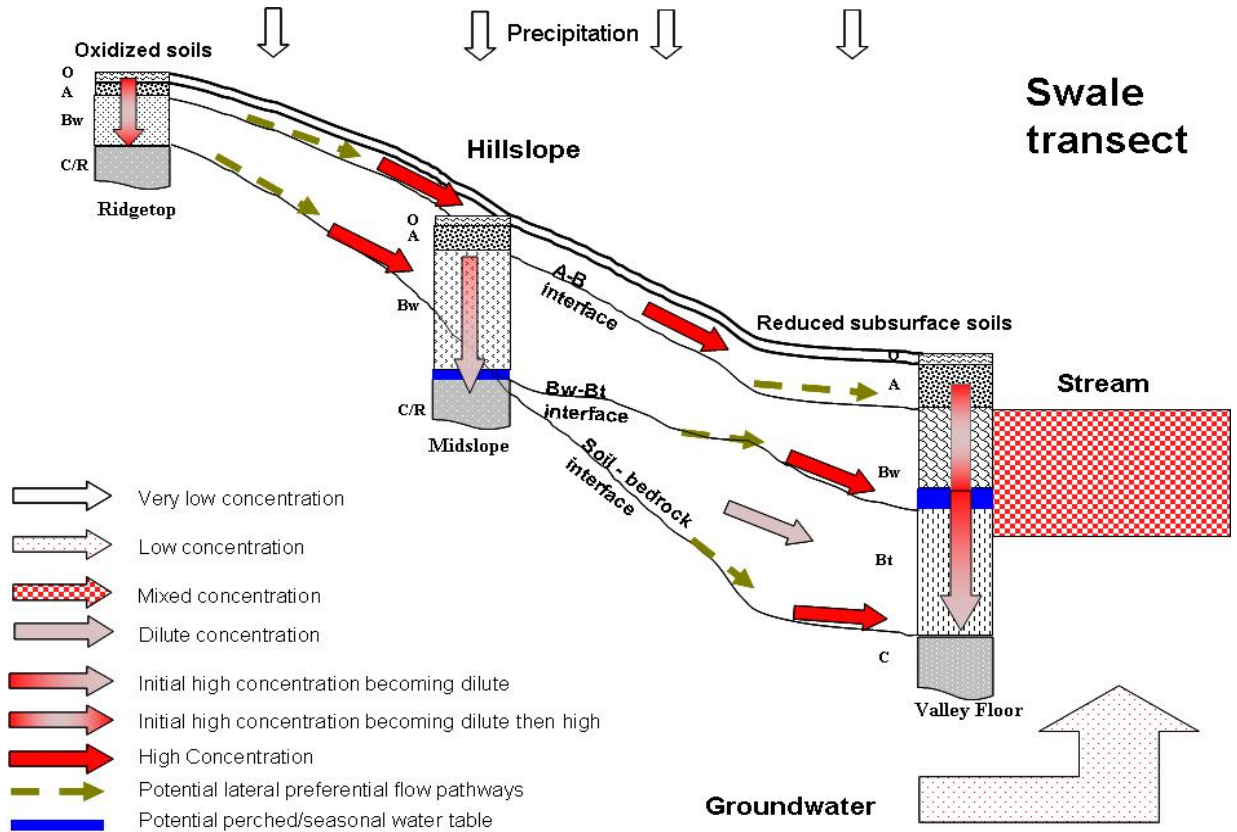


Figure 6-1: Conceptual diagram of overall dissertation findings. Solute transport along the swale is shown. Solute transport along the planar hillslope was similar to the swale except that concentrations were lower. Dashed arrows indicate potential lateral flow pathways while block arrows represent solute concentration and transport.

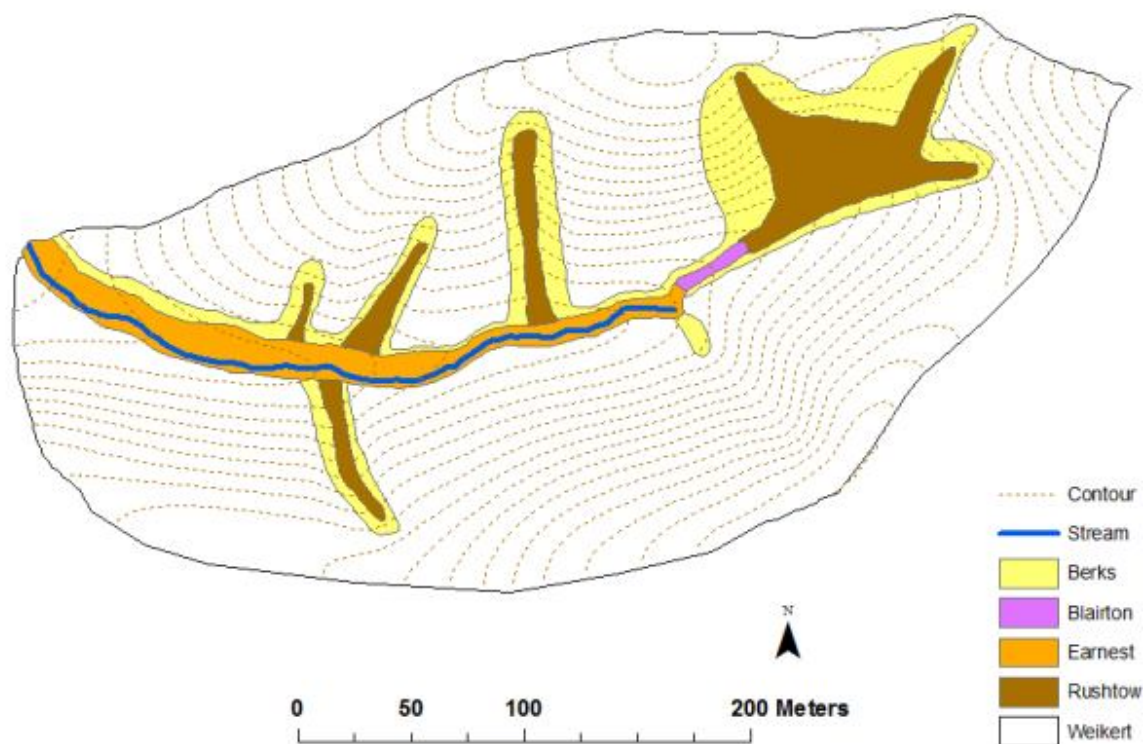
Appendix A

Soil Profile Properties

Table with basic characteristics of the five soil series indentified in the Shale Hills Critical Zone Observatory* and the associated map shows the location of the five soil series

Sample Sites & Soil Series (Description)	Horizon	Depth (cm)	Typical location of Soil Series	Area (%)	Depth to Bedrock (cm)
Weikert (Loamy-skeletal, mixed active, mesic Lithic Dystrudepts)	Oe	0 - 5	backslopes, shoulders, summits	78.69	< 50
	A	5 - 12			
	Bw	12 - 24			
	CR	24 - 37			
	R	37+			
Berks (Loamy-skeletal, mixed active, mesic Typic Dystrudepts)	Oe	0 - 5	sides of swales, edges of valley floor	9.81	50-100
	A	5 - 8			
	Bw1	8 - 14			
	Bw2	14 - 53			
	Bw3	53 - 69			
	C	69 - 145			
	R	145+			
Rushtown (Loamy-skeletal over fragmental, mixed, mesic Typic Dystruchrepts)	Oe	0 - 5	bottom of swales	6.34	>100
	A	5 - 11			
	Bw1	11 - 17			
	Bw2	17 - 26			
	Bw3	26 - 38			
	BC	38 - 60			
	C	60 - 178+			
Blairton (Fine-loamy, mixed, active, mesic Aquic Hapludults)	Oe	0 - 5	eastern end of valley floor (narrow strip)	0.22	>100
	A	5 - 11			
	BA	11 - 18			
	Bt1	18 - 29			
	Bt2	29 - 80			
	CB1	80 - 110			
Ernest (Fine-loamy, mixed, superactive, mesic Aquic Fragiudults)	Oe	0 - 5	near-stream zone western end of valley floor	4.94	>100
	A	5 - 15			
	AE	15 - 20			
	Bw	20 - 30			
	Bt	30 - 53			
	2C	53 - 89			
	3C _g	89 - 97			
	4C _g	97 - 137			
	5C _g	137 - 143			
	6C _g	143 - 147+			

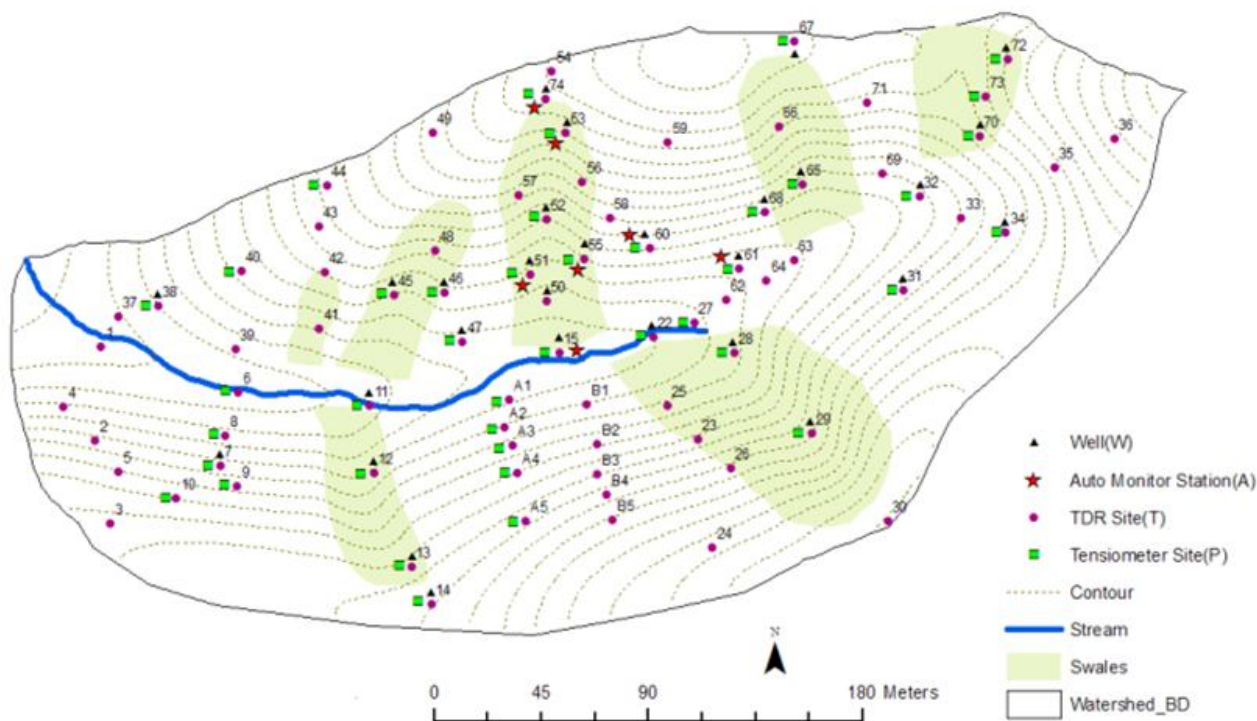
* Data adapted from Lin et al., 2006



Map of the Shale Hills CZO in central Pennsylvania and the location of the five soil series identified by Lin et al. (2006)

Appendix B

Original soil organic matter (OM), and soil pore water and stream water dissolved organic carbon (DOC) data for the Shale Hills Critical Zone Observatory



Map of the Shale Hills CZO in central Pennsylvania and the location of the sites where soil samples were collected for organic matter analysis. Site numbers correspond to the Site ID shown in the table below.

Site	Horizon	Depth Int. (cm)	OM (%)
6	Ae	(5-10)	11.8
	Bw	(10-23)	5.1
	Bt	(42-92)	4.1
	Bt2	(92-127)	2.7
7	CB	(127+)	2.2
	A	(5-10)	16.1
	Bw	(10-30)	3.6
	C	(30-45)	4.2
8	R	(45-75)	
	A	(5-11)	12.6
	Bw1	(11-31)	4.6
9	C	(31-50)	3.3
	R	(50-105)	2.3
	Bw	(5-26)	3.8
10	C	(26-121)	2.5
	Bw1	(5-10)	6.9
11	Bw2	(10-28)	3.5
	C	(28-65)	2.8
	R	(65-85)	
12	Ae	(5-15)	4.9
	Bt	15-50	3.1
	Bt2	50-87	3.1
13	A	(5-11)	14.2
	Bw1	(11-16)	6.1
	Bw2	(16-32)	3.4
	Bw3	(32-68)	2.4
14	BC	(68-86)	2.2
	C	(86+)	3.7
	A	(5-12)	8.4
	Bw1	(12-24)	5.7
	Bw2	(24-43)	3.3
15	Bw3	(43-63)	2.7
	BC	(63-102)	2.4
	C	(102+)	0.8
22	A	(5-12)	6.5
	Bw	(12-31)	6.3
	A	(5-15)	9.2
	Ae	(15-22)	50.8
	Bw	(22-46)	4.4
	Bt	(46-55)	4.0
	2C	(55-75)	3.3
	3Cg	(75-83)	3.7
	4C	(83-97)	3.6
	5Cg	(97-103)	4.3
23	6C	(103+)	4.2
	Ae	(5-15)	5.9
	Bw	(15-25)	2.5
	Bt	(25-50)	2.3
	Bt2	(50-71)	2.8
24	C	(71+)	3.0
	A	(5-10)	7.5
	Bw	(10-29)	4.4
	R	(29-78)	4.4
26	A	(0-9)	28.6
	Bw	(9-49)	6.1
27	R	(49-59)	7.1
	A	(5-13)	10.2
	Bw	(13-45)	3.3
28	C/R	(45-68)	1.6
	Ae	(5-12)	13.9
	Bw	(12-23)	2.4
	Bt	(23-60)	4.4
	C	(60-74)	2.5
29	C2	(74-96)	3.5
	2C	(96-103)	3.0
	2C2	(103+)	2.6
	A	(5-16)	8.8
30	Bw1	(16-32)	3.2
	Bw2	(32-70)	2.8
	Bw3	(70-91)	2.3
31	C	(91-114)	2.6
	A	(5-13)	6.2
	Bw	(13-50)	3.7
	C	(50-64)	3.2
32	A	(5-12)	8.1
	Bw	(12-26)	4.5
	C	(26-66)	4.2
34	Bw1	(5-20)	9.7
	C	(20-77)	3.7
	R	(77-95)	3.5
36	A	(5-11)	7.8
	Bw1	(11-17)	3.9
	Bw2	(17-40)	3.0
	Bw3	(40-70)	2.3
37	C	(70-100)	2.9
	A	(5-12)	6.3
	Bw1	(12-53)	3.7
38	CR	(53-72)	3.1
	Bw	(5-18)	4.1
	C	(18-60)	3.9
	A	(5-10)	8.1
39	Bw	(10-25)	4.7
	Bt	(25-57)	3.7
	Bt2	(57-112)	1.9
	bottom	(112-121)	3.9
	A	(5-12)	6.8
40	Bw1	(12-36)	3.6
	Bw2	(36-111)	4.4
	C	(111-121)	4.5

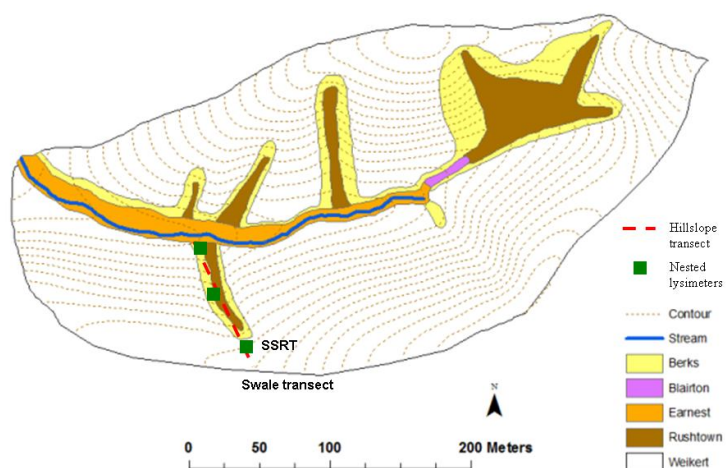
Site	Horizon	Depth Int. (cm)	OM (%)
6	Ae	(5-10)	11.8
	Bw	(10-23)	5.1
	Bt	(42-92)	4.1
	Bt2	(92-127)	2.7
7	CB	(127+)	2.2
	A	(5-10)	16.1
	Bw	(10-30)	3.6
	C	(30-45)	4.2
8	R	(45-75)	
	A	(5-11)	12.6
	Bw1	(11-31)	4.6
9	C	(31-50)	3.3
	R	(50-105)	2.3
	Bw	(5-26)	3.8
10	C	(26-121)	2.5
	Bw1	(5-10)	6.9
11	Bw2	(10-28)	3.5
	C	(28-65)	2.8
	R	(65-85)	
12	Ae	(5-15)	4.9
	Bt	15-50	3.1
	Bt2	50-87	3.1
13	A	(5-11)	14.2
	Bw1	(11-16)	6.1
	Bw2	(16-32)	3.4
	Bw3	(32-68)	2.4
14	BC	(68-86)	2.2
	C	(86+)	3.7
	A	(5-12)	8.4
	Bw1	(12-24)	5.7
	Bw2	(24-43)	3.3
15	Bw3	(43-63)	2.7
	BC	(63-102)	2.4
	C	(102+)	0.8
22	A	(5-12)	6.5
	Bw	(12-31)	6.3
	A	(5-15)	9.2
	Ae	(15-22)	50.8
	Bw	(22-46)	4.4
	Bt	(46-55)	4.0
	2C	(55-75)	3.3
	3Cg	(75-83)	3.7
	4C	(83-97)	3.6
	5Cg	(97-103)	4.3
23	6C	(103+)	4.2
	Ae	(5-15)	5.9
	Bw	(15-25)	2.5
	Bt	(25-50)	2.3
	Bt2	(50-71)	2.8
24	C	(71+)	3.0
	A	(5-10)	7.5
	Bw	(10-29)	4.4
	R	(29-78)	4.4
26	A	(0-9)	28.6
	Bw	(9-49)	6.1
27	R	(49-59)	7.1
	A	(5-13)	10.2
	Bw	(13-45)	3.3
28	C/R	(45-68)	1.6
	Ae	(5-12)	13.9
	Bw	(12-23)	2.4
	Bt	(23-60)	4.4
	C	(60-74)	2.5
29	C2	(74-96)	3.5
	2C	(96-103)	3.0
	2C2	(103+)	2.6
	A	(5-16)	8.8
30	Bw1	(16-32)	3.2
	Bw2	(32-70)	2.8
	Bw3	(70-91)	2.3
31	C	(91-114)	2.6
	A	(5-13)	6.2
	Bw	(13-50)	3.7
	C	(50-64)	3.2
32	A	(5-12)	8.1
	Bw	(12-26)	4.5
	C	(26-66)	4.2
34	Bw1	(5-20)	9.7
	C	(20-77)	3.7
	R	(77-95)	3.5
36	A	(5-11)	7.8
	Bw1	(11-17)	3.9
	Bw2	(17-40)	3.0
	Bw3	(40-70)	2.3
37	C	(70-100)	2.9
	A	(5-12)	6.3
	Bw1	(12-53)	3.7
38	CR	(53-72)	3.1
	Bw	(5-18)	4.1
	C	(18-60)	3.9
	A	(5-10)	8.1
39	Bw	(10-25)	4.7
	Bt	(25-57)	3.7
	Bt2	(57-112)	1.9
	bottom	(112-121)	3.9
	A	(5-12)	6.8
40	Bw1	(12-36)	3.6
	Bw2	(36-111)	4.4
	C	(111-121)	4.5

Site	Horizon	Depth Int. (cm)	OM (%)
40	A	(5-12)	10.0
	Bw	(12-30)	4.6
	R	(30-62)	3.8
41	A	(5-17)	13.4
	Bw1	(17-35)	6.2
	Bw2	(35-50)	3.7
	Bw3	(50-92)	2.6
45	BC	(92-121)	2.7
	A	(5-13)	8.6
	Bw1	(13-35)	4.5
	Bw2	(35-66)	3.1
	Bw3	(66-81)	2.5
46	C	(81-115)	5.3
	A	(5-14)	6.4
	Bw1	(14-43)	5.1
	Bw2	(43-55)	3.5
47	R	(55-75)	4.0
	Bw1	(5-40)	5.0
	C	(40-90)	3.4
48	A	(5-10)	10.0
	Bw	(10-39)	5.7
	Bw2	(39-69)	4.0
	Bw3	(69-124)	3.9
50	A	(5-15)	9.1
	Bw1	(15-41)	5.3
	Bw2	(41-53)	2.2
	C	(53-113)	3.0
51	A	(5-11)	14.2
	Bw1	(11-27)	6.4
	Bw2	(27-47)	6.2
	BC	(47-70)	5.3
52	C	(70+)	4.6
	A	(5-9)	10.2
	Bw1	(9-17)	7.3
	Bw2	(17-38)	5.2
	BC	(38-63)	4.3
53	C	(63-116)	4.6
	A	(5-17)	8.1
	Bw1	(17-56)	2.8
	Bw2	(56-90)	2.5
54	C	(90-)	2.4
	A	(5-12)	14.6
	Bw	(12-20)	2.4
55	C	(20-41)	4.0
	A	(5-9)	14.3
	Bw1	(9-23)	2.9
	Bw2	(23-50)	2.7
	Bw3	(50-65)	4.2
	C	(65+)	2.0

Site	Horizon	Depth Int. (cm)	OM (%)
56	A	(5-8)	11.9
	Bw1	(8-28)	6.9
	Bw2	(28-54)	3.5
	Bw3	(54-79)	3.1
60	C	(79-108)	2.7
	A	(5-8)	26.7
	Bw	(8-16)	2.7
	CR	(16+)	3.9
61	A	(5-11)	10.5
	BA	(11-23)	7.4
	Bt1	(23-53)	2.7
	Bt2	(53-75)	6.0
	CB1	(75-88)	3.9
62	CB2	(88+)	2.6
	AE	(5-12)	8.8
	Bt1	(12-30)	4.1
	Bt2	(30-53)	3.5
	Bt3	(53-87)	2.8
	CB1	(87-111)	4.0
63	A	(5-11)	12.7
	Bt1	(11-27)	4.4
	Bt2	(27-50)	3.8
	Bt3	(50-88)	3.8
64	CB1	(88-114)	3.6
	Bt1	(6-48)	4.8
	Bt2	(48-70)	4.0
65	C	(70-121)	3.6
	A	(5-11)	7.6
	Bw1	(11-30)	4.0
	Bw2	(30-47)	2.3
	Bw3	(47-54)	2.2
66	BC	(54-104)	6.7
	C	(104-123)	2.6
	A	(5-11)	10.5
	Bw1	(11-30)	5.0
	Bw2	(30-52)	2.7
67	Bw3	(52-89)	3.1
	BC	(89+)	2.1
	A	(5-11)	11.7
68	CR	(11-40)	6.4
	A	(5-12)	9.2
	Bw1	(12-25)	2.8
	Bw2	(25-37)	4.6
70	C	(37+)	3.0
	A	(5-16)	5.1
	Bw1	(16-37)	4.1
	Bw2	(37-60)	3.2
	Bw3	(60-90)	2.5
	BC	(90-100)	3.0

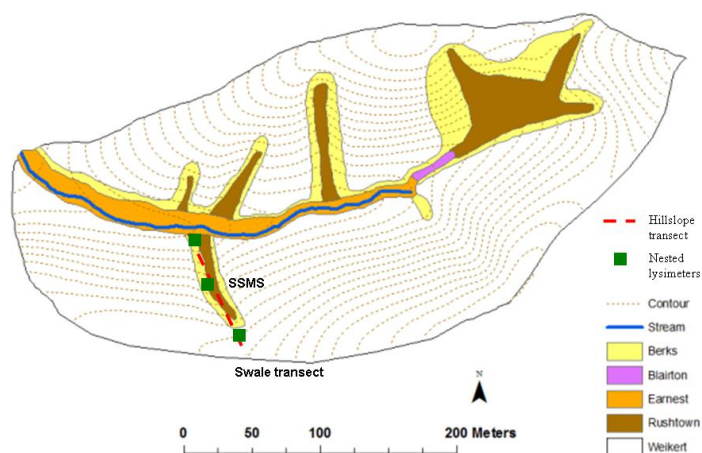
Site	Horizon	Depth Int. (cm)	OM (%)
71	A	(5-10)	3.6
	Bw1	(10-25)	5.2
	Bw2	(25-46)	2.7
	C	(56-95)	3.0
72	A	(5-10)	8.2
	Bw1	(10-16)	4.3
	Bw2	(16-27)	3.4
	Bw3	(27-40)	1.6
	BC	(40-64)	3.1
74	C	(64-114)	2.3
	A	(5-12)	9.0
	Bw1	(12-25)	4.7
	CR	(25-47)	4.3
A1 (2)	A	(5-18)	7.4
	Bw1	(18-38)	3.3
	Bw2	(38-65)	4.3
A1	C	(65-99)	2.6
	A	(5-8)	8.7
	Bw	(8-23)	3.7
A2	CR	(23-63)	2.8
	A	(5-11)	11.8
	Bw	(11-34)	3.5
A3	CR	(24-51)	2.8
	A	(5-9)	10.0
	Bw	(9-23)	4.1
A4	CR	(23-52)	3.5
	A	(5-6)	12.4
	Bw	(6-21)	6.2
A5	CR	(21-41)	3.8
	A	(5-11)	7.6
	Bw	(11-24)	4.4
B1	CR	(24-48)	4.5
	A	(5-11)	10.8
	Bw	(11-42)	4.5
	C	(42-51)	2.8
B2	CR	(51-85)	4.1
	R	(51-127)	3.4
	A	(5-9)	10.0
	Bw1	(9-25)	4.2
	Bw2	(25-51)	3.9
B3	C	(51-95)	4.0
	A	(5-11)	3.4
	Bw1	(11-22)	3.3
	Bw2	(22-42)	3.2
	C	(42-64)	3.8
	R	(64-91)	1.3

Soil pore water DOC (mg/L) data – Swale Ridgetop (SSRT)



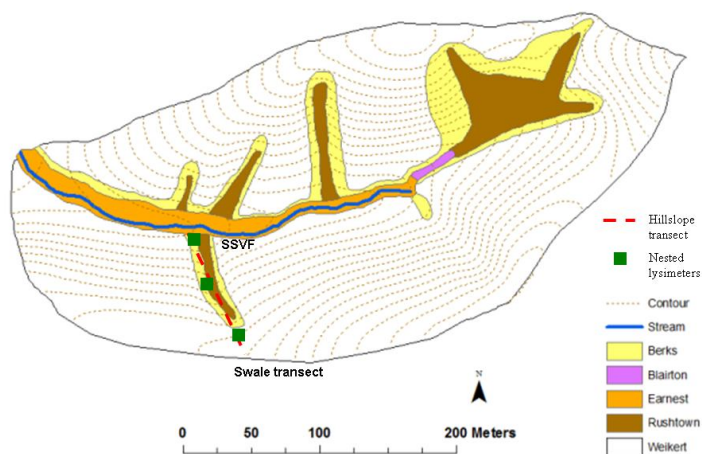
Date	Depth (cm)		
	10	20	30
8/30/07			
11/9/07	21.4	21.7	27.9
11/15/07		6.6	6.0
11/30/07	8.3	5.0	
4/24/08	6.5	4.8	3.2
5/14/08		4.6	4.1
6/5/08	10.5	4.1	3.0
10/3/08	22.6	10.3	4.8
10/10/08	16.2	8.1	3.7
10/17/08	12.6	9.0	4.0
10/31/08	15.7	9.0	4.0
11/8/08	11.4	7.8	8.6
11/21/08			
3/27/09	11.8	8.4	8.4
4/9/09	30.7	10.3	13.0
4/17/09	12.9		5.3
4/24/09	10.8		4.4
5/8/09	13.6	4.3	11.4
5/21/09	12.3	14.3	15.3
6/4/09	10.4	7.9	
6/10/09	12.7	10.4	11.2
6/24/09	16.6	5.4	11.1
7/16/09			
8/12/09	21.1		
10/9/09			
10/19/09	15.9		16.2
10/27/09	15.8		15.8

Soil pore water DOC (mg/L) data – Swale Midslope (SSMS)



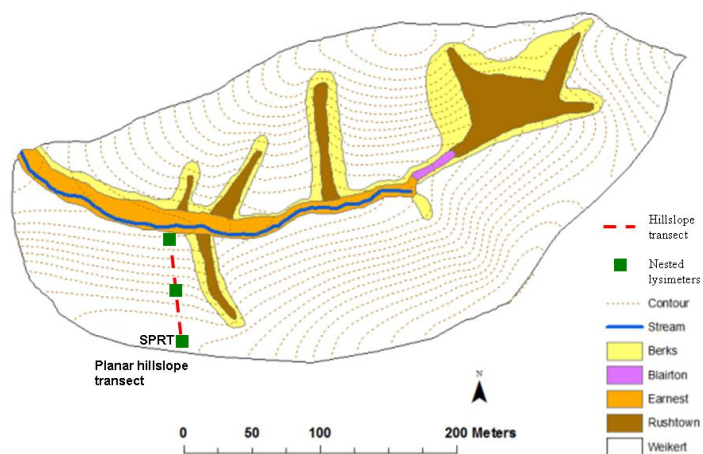
Date	Depth (cm)							
	20	40	60	80	100	120	140	160
8/30/07								
11/9/07	16.2							
11/15/07	5.18				4.99			
11/30/07	3.6		2.9	1.4			1.8	2.5
4/24/08	1.5	5.4	5.2	1.1	2.8	0.9		1.4
5/14/08	1.1	2.5	1.4	0.8	3.2	0.6	0.9	0.8
6/5/08		1.2	2.2	0.7	2.4	0.4	3.3	0.6
10/3/08								
10/10/08								
10/17/08								
10/31/08			13.6					
11/8/08			2.7					
11/21/08	3.9	3.3	2.1					
3/27/09	4.7	3.7		3.5	4.0		3.7	
4/9/09	7.6	15.2	6.4	4.6	3.8	12.3	4.8	5.4
4/17/09		9.6		3.5	2.9		2.9	3.2
4/24/09	5.9	3.9	2.8		2.3	4.6	2.4	
5/8/09	4.5	3.6	4.5	4.4	3.8	5.2	8.5	5.1
5/21/09	7.3	5.6	17.3	5.2	3.2	1.3		8.1
6/4/09	5.9	16.9	5.0	6.4	2.9	5.6	5.8	2.5
6/10/09		3.6		3.3	1.6	4.7	3.4	4.3
6/24/09	5.6	9.3	3.4	2.4	2.8	10.0	2.4	3.5
7/16/09			7.4	7.4	4.9		5.3	6.1
8/12/09			3.9					
10/9/09								
10/19/09	6.2		3.9					
10/27/09	5.8	7.6	6.1	4.3	4.2	5.8	4.2	

Soil pore water DOC (mg/L) data – Swale Valley Floor (SSVF)



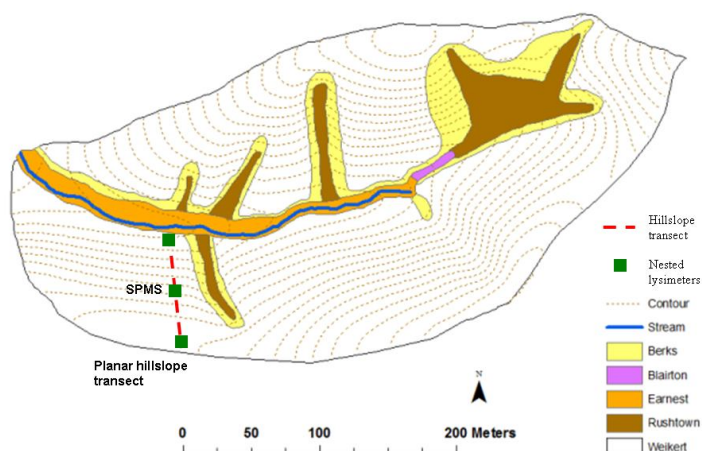
Date	Depth (cm)								
	10	20	30	40	50	60	70	80	90
8/30/07									
11/9/07									
11/15/07		9.4							
11/30/07	12.7	6.9	6.7	4.5	2.2	2.4	1.8		
4/24/08	8.0	4.5		33.6	7.5	1.7	1.3	1.2	1.5
5/14/08		8.2		3.6	1.2	1.6	1.0		1.7
6/5/08		5.0		3.1	0.9	1.5	0.7		
10/3/08									
10/10/08									
10/17/08									
10/31/08									
11/8/08									
11/21/08		8.6		11.8					
3/27/09		10.2		8.7	3.4	8.1	5.3	3.8	5.1
4/9/09		14.5		10.4	3.6	5.5	9.3	26.4	7.4
4/17/09		9.1		11.9	4.4	7.2	7.5	3.8	4.7
4/24/09		8.0		7.4	3.7	10.2	3.0	2.9	3.4
5/8/09		9.4		12.5	4.8	6.4	10.9	5.3	
5/21/09		17.4		16.1	7.1	9.1	5.9	5.6	4.5
6/4/09		12.8		13.9	5.4	6.2	4.2	6.4	5.4
6/10/09	14.3	13.1	16.4	6.8	6.7	4.7		3.3	14.7
6/24/09		11.1		7.6	4.8	4.7	3.3	2.7	4.8
7/16/09					9.8		6.6	4.3	8.0
8/12/09									
10/9/09									
10/19/09	26.4	12.6					13.2		
10/27/09		11.4	13.5	12.7	6.5		6.2	5.9	9.8

Soil pore water DOC (mg/L) data – Planar Ridgetop (SPRT)



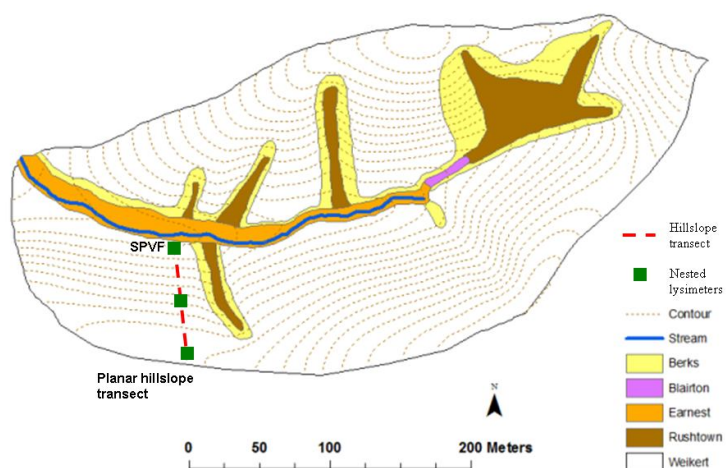
Date	Depth (cm)		
	10	20	30
8/30/07			
11/9/07			
11/15/07		9.5	21.4
11/30/07	17.2		1.8
4/24/08	5.0		1.7
5/14/08	8.1		1.7
6/5/08			
10/3/08		4.0	
10/10/08		3.2	3.6
10/17/08			
10/31/08		4.6	4.2
11/8/08		3.1	4.2
11/21/08	9.0	3.9	4.5
3/27/09	15.2	5.2	6.8
4/9/09	13.0	8.2	11.2
4/17/09	12.6	6.4	6.9
4/24/09	9.2	3.9	5.0
5/8/09	15.5	8.6	
5/21/09	16.6	6.8	9.1
6/4/09		4.8	9.3
6/10/09		5.9	8.4
6/24/09		5.4	6.4
7/16/09			
8/12/09			
10/9/09			
10/19/09		5.8	12.6
10/27/09	14.9	4.9	10.3

Soil pore water DOC (mg/L) data – Planar Midslope (SPMS)



Date	Depth (cm)			
	10	20	40	50
8/30/07				
11/9/07	15.0	12.3		
11/15/07	7.8	5.5	3.3	
11/30/07		2.7	1.5	
4/24/08	1.5		0.5	3.2
5/14/08	7.0		2.7	
6/5/08	1.2		0.5	0.7
10/3/08			2.1	
10/10/08	3.7		1.7	1.3
10/17/08	3.6		1.8	1.5
10/31/08				3.3
11/8/08	3.0		3.6	1.2
11/21/08	4.4	4.0		2.3
3/27/09	5.3			
4/9/09	5.7	7.2	9.2	
4/17/09	4.7			
4/24/09	3.6		2.1	2.1
5/8/09	3.7			4.0
5/21/09	11.0			11.2
6/4/09	4.9		7.9	7.1
6/10/09	7.7		10.0	3.1
6/24/09	5.3		6.3	2.7
7/16/09				4.2
8/12/09				
10/9/09				
10/19/09	7.2		9.5	4.6
10/27/09	5.1	4.1	5.3	3.3

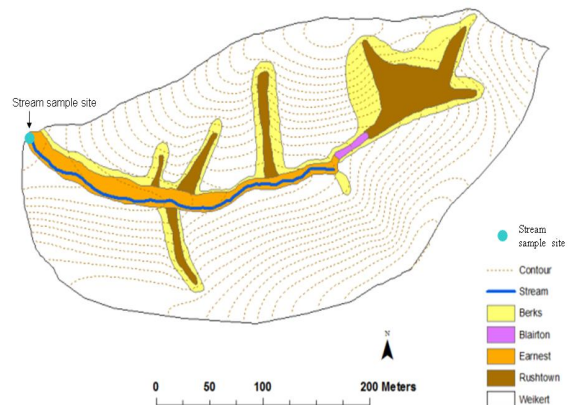
Soil pore water DOC (mg/L) data – Planar Valley Floor (SPVF)



Date	Depth (cm)				
	10	20	30	40	60
8/30/07	4.7		12.2	3.6	3.9
11/9/07					
11/15/07	6.4				
11/30/07	6.0		4.5		1.9
4/24/08	11.4	2.3	3.1		1.3
5/14/08		2.0	3.1		1.5
6/5/08					
10/3/08			13.6		
10/10/08		4.4	7.6	3.7	
10/17/08		4.8			
10/31/08	6.5			13.4	6.6
11/8/08	7.3		6.3	2.7	
11/21/08	6.6	4.9	6.8	3.0	2.5
3/27/09	7.9	4.7	6.9	9.6	5.1
4/9/09	12.5	2.1	8.4	8.4	4.4
4/17/09		6.3	14.6	5.1	4.2
4/24/09	7.2	5.0	6.4	3.0	2.0
5/8/09	7.5		6.3	6.4	4.9
5/21/09	10.4	7.5	11.5	5.3	3.4
6/4/09		7.1	13.9	2.9	4.3
6/10/09	6.9	6.5	12.4	3.6	7.5
6/24/09	8.7	7.4	7.5	4.4	
7/16/09			10.6		5.1
8/12/09			9.3	6.6	
10/9/09	14.1	9.8	17.8	5.9	8.1
10/19/09		6.7	11.1	7.7	4.5
10/27/09		8.4	11.0	6.0	8.4

Daily stream water DOC (mg/L) data from outlet of catchment

Date	DOC (mg/L)	Date	DOC (mg/L)
5/6/08	3.8	3/11/09	4.3
5/7/08	0.9	3/12/09	2.4
5/8/08	13.0	3/13/09	19.1
5/9/08	2.1	3/14/09	4.4
5/10/08	2.4	3/15/09	3.4
5/11/08	0.8	3/16/09	2.3
5/12/08	1.6	3/17/09	3.8
5/16/08	2.2	3/18/09	2.4
5/17/08	1.3	3/19/09	2.3
5/18/08	1.0	3/20/09	1.6
5/19/08	1.2	3/21/09	7.9
5/20/08	1.6	3/22/09	1.9
5/21/08	1.1	3/23/09	5.3
5/22/08	0.7	3/24/09	8.5
5/23/08	0.9	3/25/09	2.7
5/24/08	0.6	3/26/09	2.6
5/25/08	1.3	3/27/09	3.1
5/26/08	0.9	3/28/09	1.9
5/27/08	1.8	3/29/09	16.3
5/28/08	1.0	3/30/09	1.3
5/29/08	0.9	3/31/09	4.1
5/30/08	3.0	4/1/09	1.9
5/31/08	1.2	4/2/09	1.3
6/1/08	1.2	4/3/09	7.1
6/2/08	1.2	4/4/09	27.9
6/3/08	1.0	4/5/09	4.6
7/3/08	4.3	4/6/09	3.7
7/4/08	4.3	4/7/09	4.2
7/5/08	6.4	4/8/09	6.4
7/6/08	7.1	4/9/09	9.8
7/7/08	7.0	4/10/09	1.6
7/8/08	6.4	4/13/09	5.0
7/9/08	6.3	4/14/09	4.4
10/17/08	3.7	4/15/09	4.8
10/18/08	3.7	4/16/09	2.4
10/19/08	3.7	4/17/09	1.5
10/20/08	3.6	4/18/09	6.4
10/21/08	3.7	4/19/09	2.3
10/22/08	3.9	4/20/09	7.3
10/23/08	4.3	4/21/09	1.4
10/24/08	4.3	4/22/09	28.6
10/25/08	14.4	4/23/09	4.1
10/26/08	5.3	4/24/09	2.8
10/27/08	4.4	5/8/09	8.3
10/28/08	4.6	5/9/09	2.4
10/29/08	6.7	5/10/09	4.6
10/30/08	4.5	5/12/09	4.2
10/31/08	6.4	5/13/09	4.7
11/1/08	5.4	5/14/09	6.7
11/2/08	3.4	5/15/09	8.0
11/3/08	4.1	5/16/09	5.9
11/4/08	3.5	5/17/09	9.7
11/5/08	2.7	5/18/09	10.2
11/6/08	4.0	5/19/09	3.1
11/7/08	3.9	5/20/09	3.6
11/8/08	4.2	5/21/09	3.2
11/9/08	3.3	5/22/09	9.6
11/10/08	4.5	5/23/09	3.8
11/11/08	3.2	5/24/09	3.8
11/12/08	3.2	5/25/09	4.9
11/13/08	6.6	5/26/09	6.3
11/14/08	4.2	5/27/09	6.6
11/15/08	5.0	5/28/09	2.9



Date	DOC (mg/L)
5/29/09	5.3
5/30/09	2.4
5/31/09	2.4
6/1/09	3.4
6/2/09	5.7
6/3/09	3.3
6/4/09	3.6
6/6/09	6.4
6/7/09	9.6
6/8/09	4.2
6/9/09	4.0
6/10/09	7.6
6/11/09	1.9
6/12/09	5.5
6/13/09	2.3
6/14/09	4.2
6/15/09	2.0
6/16/09	1.9
6/17/09	5.2
6/18/09	5.1
6/19/09	3.7
6/20/09	4.3
6/21/09	4.1
6/22/09	2.7
6/23/09	2.9
6/24/09	4.8
6/25/09	8.3
6/26/09	4.7
6/27/09	5.1
6/28/09	2.5
6/29/09	2.5
6/30/09	5.4
7/2/09	5.1
7/4/09	4.1
7/6/09	4.4
7/11/09	13.7
7/12/09	13.8
7/14/09	14.7
7/15/09	8.6
7/16/09	16.3
7/17/09	15.6
7/18/09	13.1
7/19/09	17.4
7/20/09	12.2
7/21/09	7.0
7/22/09	6.3
7/23/09	8.3
7/24/09	12.4
7/25/09	7.1
7/26/09	7.8
7/27/09	6.6
7/28/09	6.9
7/29/09	7.8
7/30/09	16.6
7/31/09	19.5
8/1/09	17.6
8/2/09	17.3

Date	DOC (mg/L)
8/3/09	16.1
8/4/09	16.0
8/5/09	16.3
8/6/09	16.4
8/7/09	16.2
8/8/09	19.6
8/9/09	18.6
8/10/09	15.5
8/27/09	12.0
8/28/09	13.0
8/29/09	10.6
9/3/09	21.9
9/4/09	20.7
9/10/09	12.9
9/11/09	11.4
9/12/09	13.9
9/13/09	12.7
9/17/09	11.5
9/18/09	12.2
9/21/09	12.8
9/25/09	12.1
9/26/09	7.4
9/27/09	5.9
9/28/09	10.1
9/29/09	10.5
9/30/09	10.7
10/1/09	13.6
10/2/09	10.1
10/3/09	12.1
10/4/09	12.8
10/5/09	11.7
10/6/09	11.2
10/7/09	11.0
10/8/09	11.8
10/9/09	10.7
10/10/09	10.0
10/12/09	4.5
10/14/09	10.0
10/16/09	10.3
10/18/09	3.8
10/19/09	4.6
10/20/09	3.5
10/22/09	2.6
10/24/09	4.9
10/26/09	4.1
10/27/09	5.1
10/28/09	2.7
10/29/09	4.1
10/31/09	5.8
11/2/09	10.4
11/4/09	0.7
11/6/09	3.4
11/8/09	2.3
11/10/09	2.4
11/12/09	17.3
11/13/09	16.4

Date	DOC (mg/L)
4/10/10	1.2
4/11/10	1.8
4/12/10	2.2
4/13/10	1.3
4/14/10	1.4
4/15/10	1.5
4/16/10	1.7
4/17/10	2.1
4/18/10	1.9
4/19/10	1.6
4/20/10	2.0
4/21/10	2.0
4/22/10	1.9
4/23/10	2.2
4/24/10	1.8
4/25/10	3.1
4/26/10	3.9
4/27/10	4.2
4/28/10	1.3
4/29/10	1.5
4/30/10	1.7
5/1/10	1.4
5/2/10	1.8
5/3/10	5.1
5/4/10	2.6
5/11/10	4.0
5/12/10	14.9
5/13/10	7.5
5/14/10	1.4
5/15/10	1.3
5/16/10	4.9
5/17/10	2.4
5/18/10	2.5

Appendix C

First Approximation of the Carbon Budget for Shale Hills

Carbon budget

The first approximation of the carbon (C) budget for the Shale Hills Critical Zone Observatory was calculated using allometric relationships. These relationships are based on the diameter at breast height (dbh > 20 cm) for the tree species inventoried for the whole catchment. The allometric equations of Jenkins et al. (2003) have been widely used as it captures a wide variety of species (Bailey et al., 2005; Hicke et al., 2007; Chen et al., 2010; Curzon and Keeton, 2010). Aboveground biomass (shoots) was calculated as (Jenkins et al., 2003)

$$bm = \text{Exp}(\beta_0 + \beta_1 \ln dbh),$$

where *bm* is the total aboveground biomass (kg dry weight) and β_0 and β_1 are parameters based on species group, where β_0 and β_1 for maple and birch are -1.912 and 2.365, respectively; mixed hardwood (e.g. ash, poplar, cherry, basswood) are -2.480 and 2.484; oak, hickory and beech are -2.013 and 2.434; hemlock are -2.538 and 2.481; and pine are -2.536 and 2.435 (Jenkins et al., 2003). Live tree biomass was converted to units of Mg C/ha under the assumption that the C fraction of dry biomass is 0.5 (Shoch et al., 2009).

Belowground biomass (roots) was calculated using the following two equations (Li et al., 2003): $RB_s = 0.222AB_s$ and $RB_h = 1.576AB_s^{0.615}$, where *RB* and *AB* are root

and aboveground biomass, respectively, and subscripts s and h are softwood and hardwood species groups, respectively. Values of AB for softwood and hardwood were derived from the equations of Jenkins et al. (2003) as described above. Li et al. (2003) developed these equations based on 340 pairs of aboveground and belowground data for softwood trees and 103 pairs for hardwood trees compiled from temperate and boreal forests, from which the parameter estimates of 0.222, 1.576 and 0.615 in above equations were determined by fitting regression equations between aboveground biomass and belowground biomass.

The gross primary productivity (GPP) was estimated using average yearly precipitation and temperature for this site taken from NOAA (2007) while net primary productivity (NPP) was calculated as 52% of GPP ($NPP = GPP - \text{plant respiration}$) (Chapin III et al., 2002; Fang et al., 2007). Litterfall was estimated according to Raich and Nadelhoffer (1989), while respiration (roots and microbes – CO₂ efflux) was calculated as two and a half times litterfall (Anderson, 1973; Raich and Nadelhoffer, 1989; Davidson et al, 2002). The SOC storage in the soil solum (A and B horizons) were first determined from interpolated maps in ArcGIS 9.1 (Chapter 2), and this was divided by the catchment area (7.9 ha) to obtain the average SOC storage density for the entire catchment. Microbial biomass was calculated as 10% of SOC pool (Wardle, 1998). Wet deposition was calculated as average yearly DOC concentration multiplied by average yearly rainfall flux (e.g. Buckingham et al., 2008).

References

- Anderson, J. M. (1973). Stand structure and litter fall of a coppiced beech *Fagus Sylvatica* and sweet chestnut *Castanea Sativa* woodland. *Oikos* 24: 128-135.
- Bailey, S. W., S. B. Horsley, and R. P. Long. 2005. Thirty years of change in forest soils of the Allegheny Plateau, Pennsylvania. *Soil Science Society of America Journal* 69: 681–690.
- Buckingham, S., E. Tipping, and J. Hamilton-Taylor. 2008. Concentrations and fluxes of dissolved organic carbon in UK topsoils. *Science of the Total Environment* 407: 460-470.
- Chapin III, F. S., P. Matson, and H. A. Mooney (eds). 2002. *Principals of Terrestrial Ecosystem Ecology*. Springer Science + Business Media, New York, USA.
- Chen, J., S. J. Colombo, M. T. Ter-Mikaelian, L. S. Heath. 2010. Carbon budget of Ontario's managed forests and harvested wood products, 2001–2100. *Forest Ecology and Management* 259: 1385–1398.
- Curzon, M. T. and W. S. Keeton. 2010. Spatial characteristics of canopy disturbances in riparian old-growth hemlock – northern hardwood forests, Adirondack Mountains, New York, USA. *Canadian Journal of Forest Research* 40: 13-25.
- Dalva, M. and T. R. Moore. 1991. Sources and sinks of dissolved organic carbon in a forested swamp catchment. *Biogeochemistry* 15 (1): 1-19.
- Davidson, E. A., K. Savage, P. Bolstad, D. A. Clark, P. S. Curtis, D. S. Ellsworth, P. J. Hanson, B. E. Law, Y. Luo, K. S. Pregitzer, J. C. Randolph, and D. Zak. 2002. Belowground carbon allocation in forests estimated from litterfall and IRGA based soil respiration measurements. *Agricultural and Forest Meteorology* 113:

39-51.

- Fang, J., G. Liu, B. Zhu, X. Wang, and S. Liu. 2007. Carbon budgets of three temperate forest ecosystems in Dongling Mt., Beijing, China. *Science in China Series D: Earth Sciences* 50(1): 92-101.
- Hicke, J. A., J. C. Jenkins, D. S. Ojima, and M. Ducey. 2007. Spatial patterns of forested characteristics in the western United States derived from inventories. *Ecological Applications* 17 (8): 2387–2402.
- Jenkins, J.C., D.C. Chojnacky, L.S. Heath, and R.A. Birdsey. 2003. National-scale biomass estimators for the United States tree species. *Forest Science* 49 (1): 12-35.
- Li, Z., W.A. Kurz, M. J. Apps, and S. J. Beukema. 2003. Belowground biomass dynamics in the carbon budget model of the Canadian forest sector: recent improvements and implications for the estimation of NPP and NEP. *Canadian Journal of Forest Research* 33: 126-136.
- National Oceanographic and Atmospheric Administration (NOAA). 2007. U.S. divisional and station climatic data and normals: Asheville, North Carolina, U.S. Department of Commerce, National Oceanic and Atmospheric Administration, National Environmental Satellite Data and Information Service, National Climatic Data Center. <http://cdo.ncdc.noaa.-gov/CDO/cdo>.
- Raich, J. W. and K. J. Nadelhoffer. 1989. Belowground carbon allocation in forest ecosystems: global trends. *Ecology* 70 (5): 1346-1354.
- Shoch, D. T., G. Kaster, A. Hohl, and R. Souter. 2009. Carbon storage of bottomland hardwood afforestation in the lower Mississippi Valley, USA. *Wetlands* 29 (2):

535-542.

Wardle, D. A. 1998. Controls of temporal variability of the soil microbial biomass: a global-scale synthesis. *Soil Biology and Biochemistry* 30 (13): 1627-1637.

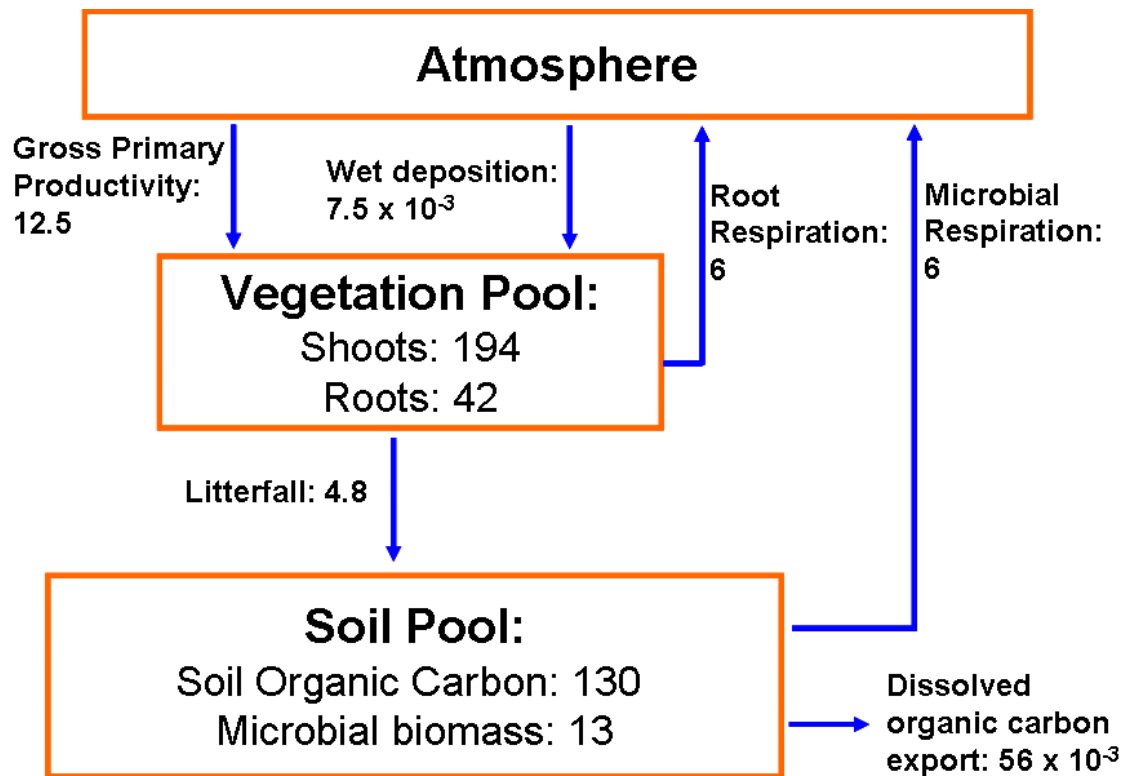


Figure showing carbon budget for the forested Shale Hills CZO. Boxes represent pools (in Mg C/ha) while arrows represent fluxes (in Mg C/ha/yr).

Appendix D

Redox Probes

Redox Probe Construction

Redox sensors were made according to methodology provided by Mike. J.

Vepraskas of NC State University (Dec. 2002).

Materials needed:

- 1/8" diameter brass brazing rod
- 18 gauge platinum wire
- Batterns flux
- 1/4" and 3/16" initial diameter adhesive-lined polyolefin heat-shrink tubing
- Marine-Tex brand waterproof epoxy
- Propane torch with adjustable flame attachment
- 18 gauge copper hook-up
- Sandpaper: 70 grain and 150 grain, 1 pack of each
- Soldering iron and solder

Methodology I: Construction of redox probes (Insulate with Epoxy)

- Cut brass brazing rod to desired length of electrode (~10cm)
- Drill a 1 mm hole 3 mm deep in the end of the brass-brazing rod
- Cut platinum wire into 13 mm lengths

- Brush the drilled end of the brass-brazing rod with the flux and also dip a piece of the platinum wire in the flux
- Insert one end of the platinum wire into the hole on the brass-brazing rod. Hold wire in place with pliers
- While holding the wire in place, direct the tip of the hot blue flame from the propane torch at the area of the rod where the platinum wire was inserted. Continue to heat the rod until it melts, thereby creating a bond between the rod and the platinum. Hold the wire in place until the rod cools. (Note: Rod must be held in a vertical position while performing this procedure to avoid sagging of the molten metal.) Once the rod cools, be sure to check the Platinum/brass interface by tugging on platinum wire with a pair of pliers
- Cut heat shrink tubing approximately 5 cm shorter than the length of the rod. Set aside
- Mix Marine-Tex epoxy according to manufacturer's directions
- Cover the junction between the rod and platinum wire with the Marine-Tex epoxy. Spin the rod so that the entire junction is adequately covered and/or use a Popsicle stick or plastic knife to smooth out the Marine-Tex mixture. Leave at least 5 mm of the tip of the wire uncovered
- Let the Marine-Tex set up until the Marine-Tex can be touched with a latex glove without adhering to the glove. Smooth the Marine-Tex with gloved fingers. Work the Marine-Tex down the rod until at least 5 mm of the Marine-Tex is thin enough

for the heat shrink tubing to slide over. Leave excess Marine-Tex above this thinned area

- After enough time has passed to allow the Marine-Tex epoxy to harden (24 hrs.) You must sand down the epoxied tip to smooth out any rough spots in the epoxy. Starting with a 60 or 70-grain sandpaper, smooth out the larger bumps in the epoxy. Once the larger bumps have been smoothed use the 150-grain sandpaper to give the epoxy a smooth finish. Be sure to leave enough epoxy to allow for a watertight seal around the platinum wire
- Slide a pre-cut piece of heat shrink tubing on the rod from the end without the platinum wire. Shove the tubing over at least 5 mm of the Marine-Tex. Starting with the end of the tubing that is in the Marine-Tex, shrink approximately 5 cm of the tubing
- Slowly continue heating the rest of the tubing. Let harden

Methodology II: Salt Bridge Construction

Salt bridges were constructed to aid redox potential readings. The salt bridges were constructed using 1-inch PVC, Potassium Chloride and Agar.

The salt bridge is composed of:

- (1) 25 – 30 g Agar
- (2) 250 mL of saturated KCL solution
- (3) 1L of boiling deionized water

These ingredients are allowed to cool until a pour able gel forms. This gel is then poured into the 1-inch PVC tubes until they are full and then allowed to cool.

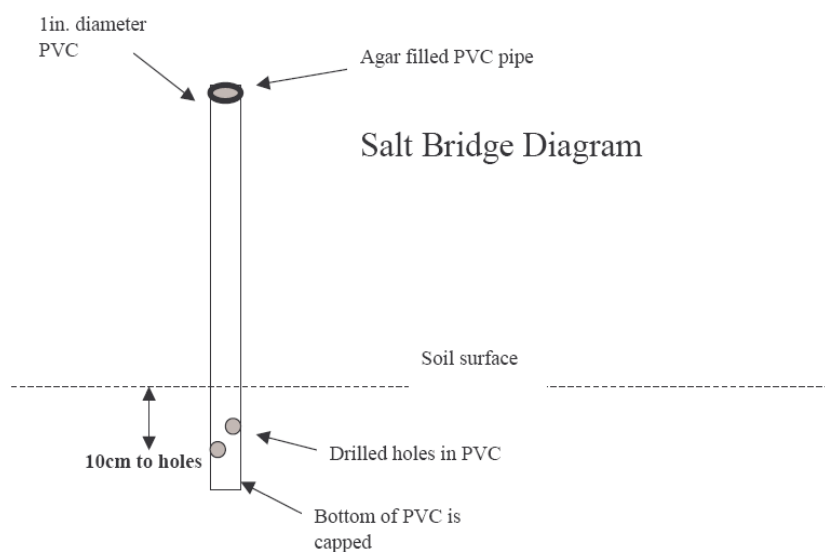


Figure 1: Schematic of a salt bridge (Vepraskas, 2002)

Redox Probe testing in laboratory

Procedure for Making Ferrous-Ferric solution for Redox Potential Measurements and Testing of electrodes

Once constructed the electrodes are checked for accuracy. This is first done using a solution of known and stable redox potential. The solution we have used was described by Light (1972) and is prepared from scratch. The ingredients are shown below.

Composition:	Concentration:
Ferrous ammonium sulfate 39.21 g/l $\text{Fe}(\text{NH}_4)_2(\text{SO}_4)_2 \cdot 6\text{H}_2\text{O}$	0.100M
Ferric ammonium sulfate 48.22 g/l $\text{FeNH}_4(\text{SO}_4)_2 \cdot 12\text{H}_2\text{O}$	0.100M
Sulfuric Acid 56.2 ml/l concentrated H_2SO_4	1.00 M

To test an electrode for accuracy:

First, scratch the platinum tips of each electrode with steel wool. Second, fill a beaker halfway with the ferrous-ferric buffer solution you have made. Fill a second beaker with tap water. Using a Campbell scientific datalogger (Campbell Scientific Inc., Logan, Utah, USA) and an Accumet calomel reference electrode (Fisher Scientific Inc, Pittsburgh, PA, USA), a mV reading of each electrode individually in both the buffer solution and in tap water is made. The buffer solution should read at +476mV (+/- 20 mV). The tap water reading will vary from the buffer reading but should not vary by more than 100 to 150 mV from other electrodes. If an electrode is varying more than 150 mV, there may be something wrong with that electrode. Problems with electrode readout include; electrode not being water tight, platinum not having a good connection to brass rod, and copper wire not being soldered on correctly.

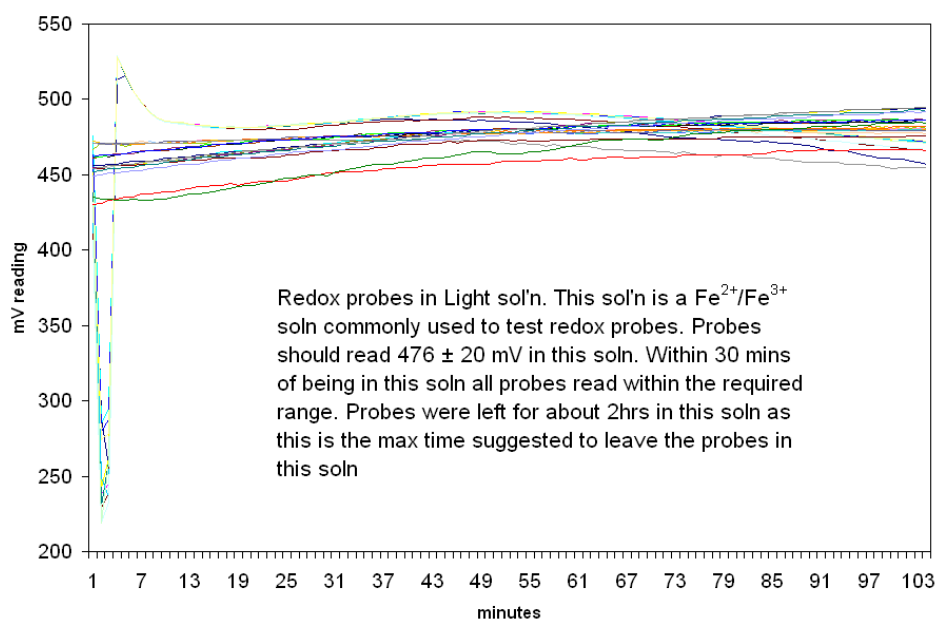


Figure 2: Redox potential data (mV) of probes in Light solution.

Below are figures showing the data collected from lab testing the probes to ensure that they were working properly prior to field installation.

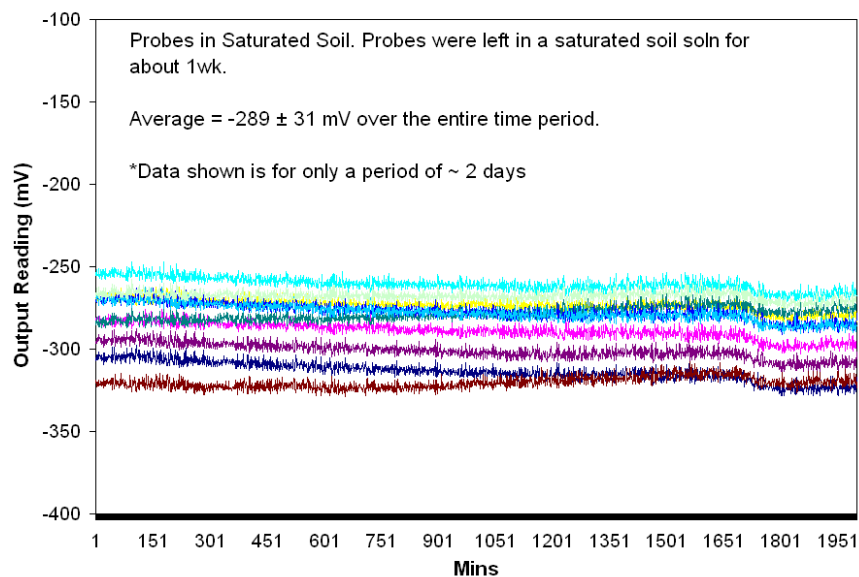


Figure 3: Redox potential data (mV) for probes in saturated soil.

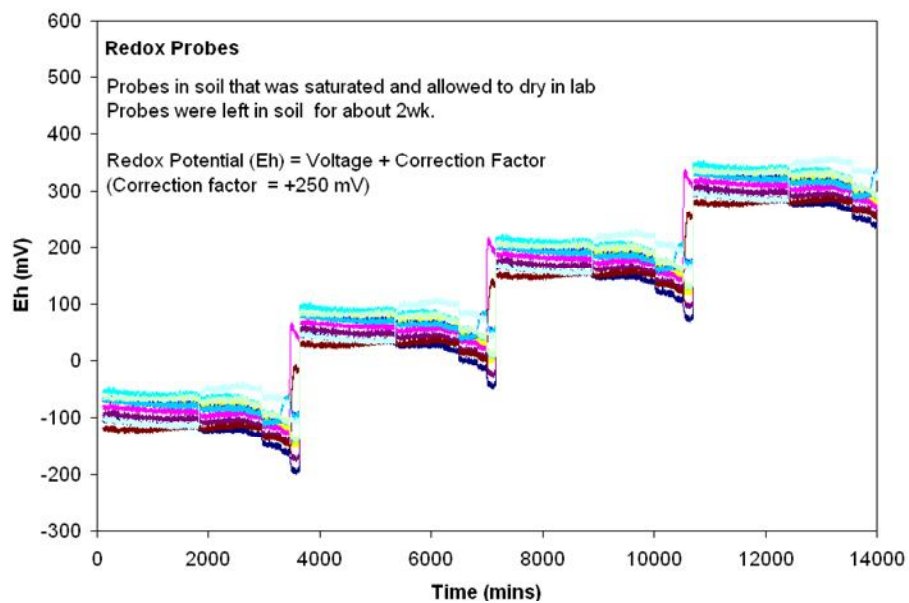


Figure 4: Redox potential data (mV) for probes in drying soil.

Field Installation

After construction and lab testing, redox probes were installed along two transects – a hillslope and a valley floor - in Summer 2009, for a total of seven sites (see Map in Chapter 5, Figure 5-1). Probes were installed in triplicate in the A, B and C horizons at all sites (see Table 5-3). After augering of holes, holes were backfilled with soil slurry and the platinum tips of probes were scraped with glass wool and then the probes were inserted into the slurry. The hole was then completely backfilled. A nearby hole was also augered (~ 60cm except at the ridgetop (~20cm)) and the salt bridge was placed in the hole. The hole was then backfilled. The reference probe was inserted into the salt bridge.

The reference probe and the redox probes (total of 9 per site, except at the ridgetop (6)) were attached to Campbell Scientific dataloggers (Logan, Utah, USA) and data are recorded at 10-min intervals. The salt bridge is checked on a weekly basis and replaced as necessary (every 2-3 months). Redox probes will be pulled up (~ every 12 months) to check for accuracy or drift using the same procedures outlined previously for testing the probes for accuracy. Other researchers have removed installed probes to determine whether they were functioning properly and giving reliable data (e.g. Wafer et al., 2004; Niedermeier and Robinson, 2007). Probes have been removed from soil after a range of 10 - 19 months.

Data Analysis

Data correction

A +250 mV correction factor (Vepraskas, 2002) was added to the field mV measurements: Redox potential = field voltage + 250 mV. Additionally, the readings

were also corrected to pH 7 by adding - 59mV per pH unit (Qualls et al., 2001): pH corrected Redox potential = Redox potential – ((pH7 – soil pH)*59). Variability between the replicates (n=3) were also evaluated (Figure 5).

Table showing pH correction factors

Site ID	Horizon	pH Correction factor)
Ridgetop (site 74)	A	153
	B	160
Shoulder slope (site 53)	A	168
	B	174
	C	175
Midslope (site 51)	A	167
	B	157
	C	177
Valley floor 1 (site 61)	A	145
	B	155
	C	143
Valley floor 2 (site 15)	A	166
	B	110
	C	110
Valley floor 3 (south planar lysimeter transect valley floor)	A	189
	B	173
	C	156
Valley floor 4 (south swale lysimeter transect valley floor)	A	175
	B	139
	C	126

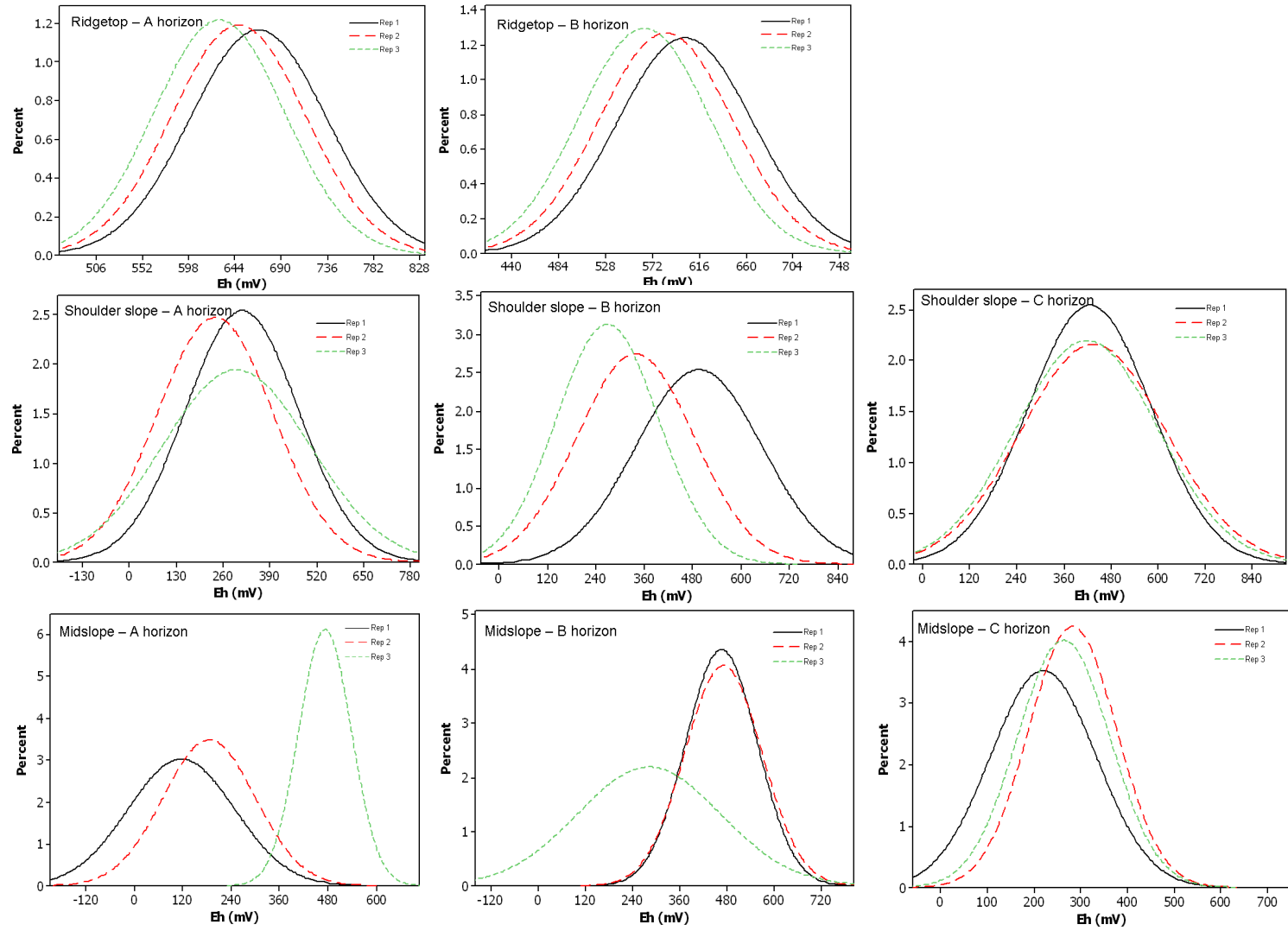


Figure 5: Variability between replicates (n = 3) for each soil depth for each of the seven monitoring sites.

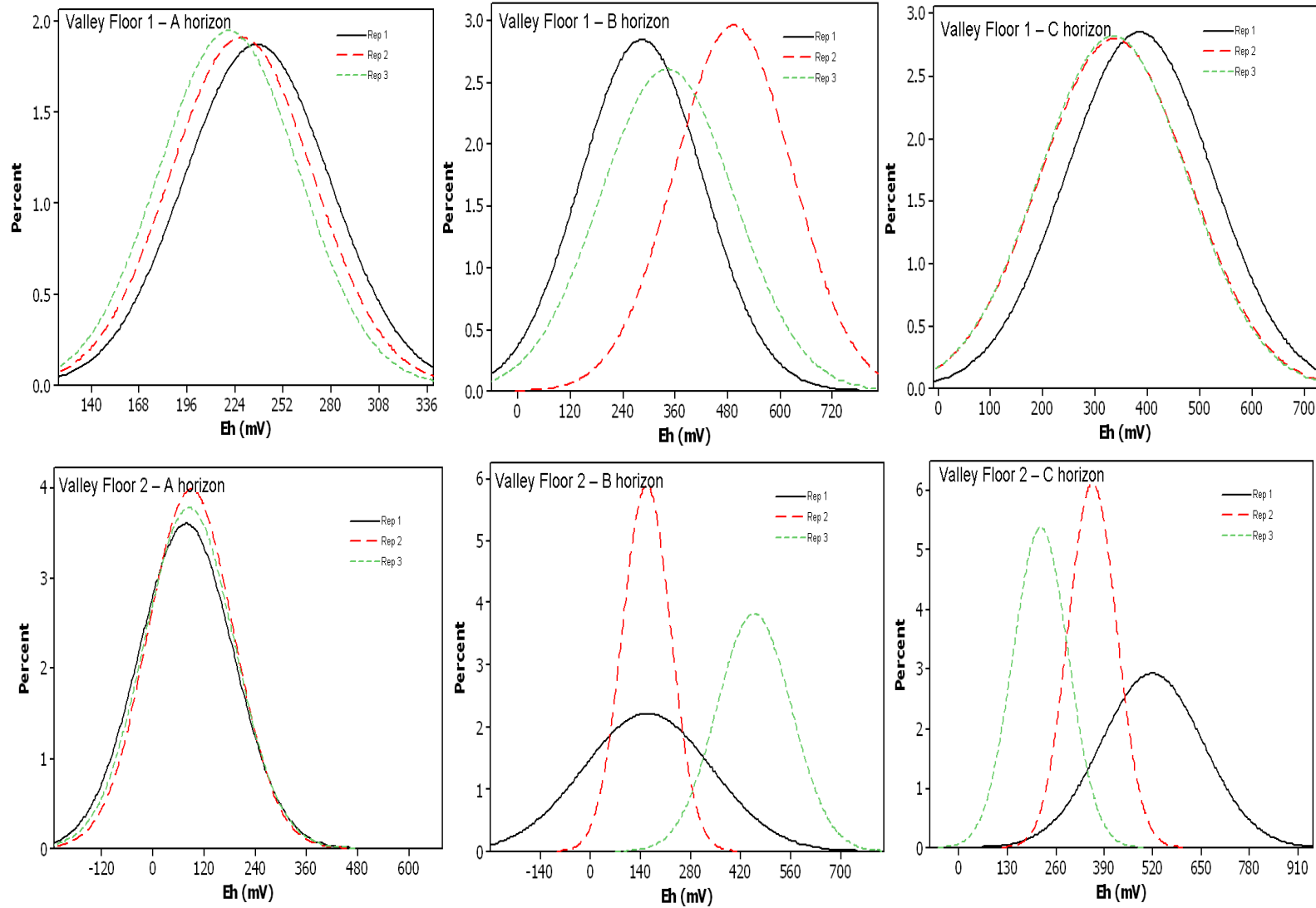


Figure 5 cont'd: Variability between replicates (n = 3) for each soil depth for each of the seven monitoring sites.

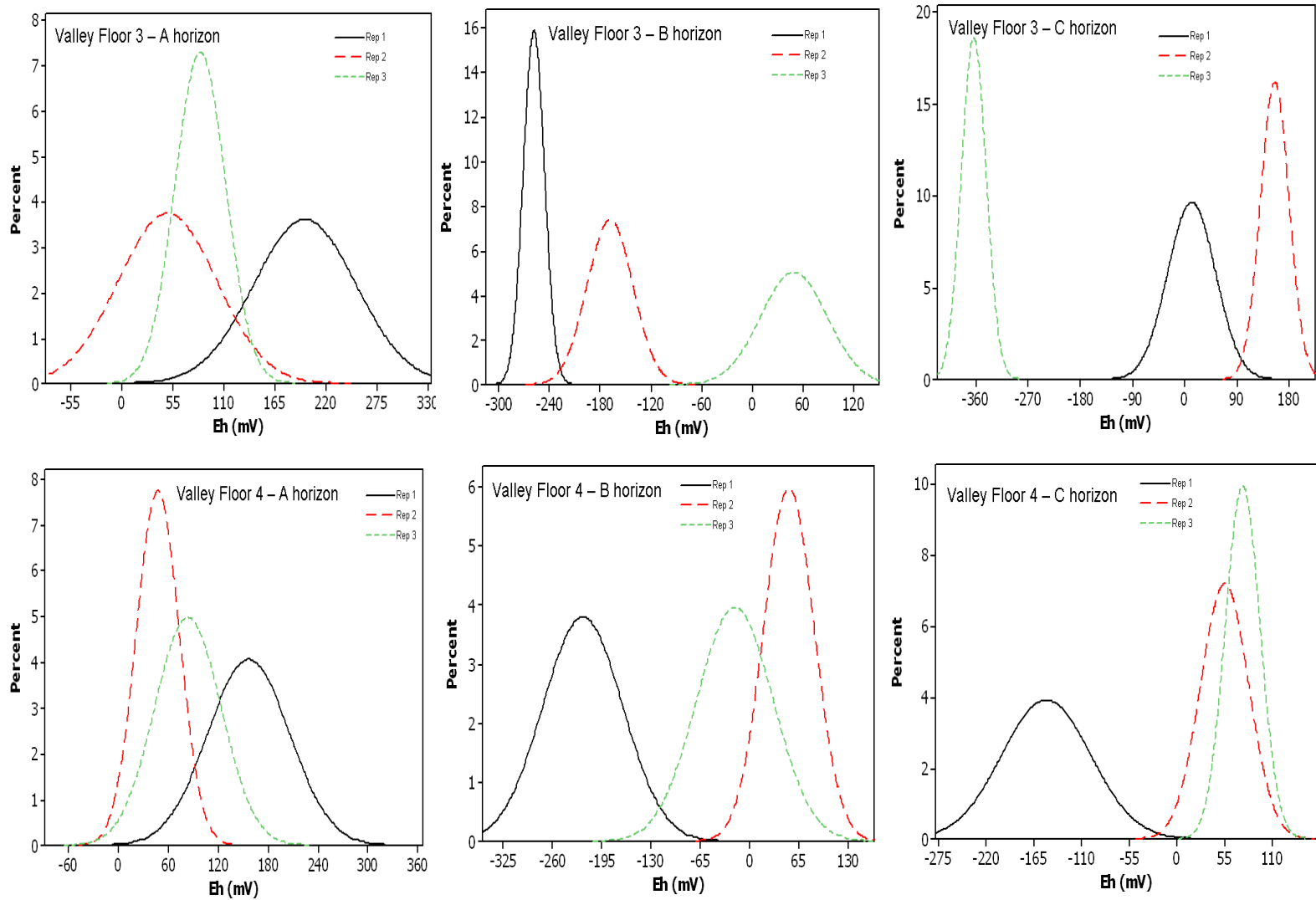


Figure 5 cont'd: Variability between replicates (n = 3) for each soil depth for each of the seven monitoring sites.

The mean Eh (n = 3) was calculated for each landscape position, depth, and date/time of sampling; resulting means were used in all analyses. A 3-hr moving average was also performed on the data for consistency as a couple of the sites produced noisy data (shown below). A moving average is commonly used with time series data to smooth out short-term fluctuations and highlight longer-term trends or cycles.

Errors/noise in data

Time series of mean Eh for each landscape position/each horizon was then plotted. Erroneous data points were deleted upon analysis of time series plots.

1. At the ridgetop, once every hour, every 2 days, there is a 10mV drop in the data. These data points are eliminated.

Date	Time	A	B			Date	Time	A	B
8/1/2010	0:03	585	560			8/1/2010	0:03	585	560
8/1/2010	0:13	575	550			8/1/2010	0:13		
8/1/2010	0:23	585	560			8/1/2010	0:23	585	560
8/1/2010	0:33	585	560			8/1/2010	0:33	585	560
8/1/2010	0:43	585	560			8/1/2010	0:43	585	560
8/1/2010	0:53	585	561			8/1/2010	0:53	585	561
8/1/2010	1:03	585	560			8/1/2010	1:03	585	560
8/1/2010	1:13	585	560			8/1/2010	1:13	585	560
8/1/2010	1:23	585	560			8/1/2010	1:23	585	560
8/1/2010	1:33	585	560			8/1/2010	1:33	585	560
8/1/2010	1:43	585	560			8/1/2010	1:43	585	560
8/1/2010	1:53	585	560			8/1/2010	1:53	585	560
8/1/2010	2:03	575	550			8/1/2010	2:03		
8/1/2010	2:13	585	560			8/1/2010	2:13	585	560
8/1/2010	2:23	585	560			8/1/2010	2:23	585	560
8/1/2010	2:33	585	560			8/1/2010	2:33	585	560
8/1/2010	2:43	585	560			8/1/2010	2:43	585	560
8/1/2010	2:53	585	561			8/1/2010	2:53	585	561
8/1/2010	3:03	585	560			8/1/2010	3:03	585	560
8/1/2010	3:13	586	561			8/1/2010	3:13	586	561
8/1/2010	3:23	585	561			8/1/2010	3:23	585	561
8/1/2010	3:33	585	561			8/1/2010	3:33	585	561
8/1/2010	3:43	585	560			8/1/2010	3:43	585	560
8/1/2010	3:53	575	551			8/1/2010	3:53		
8/1/2010	4:03	586	561			8/1/2010	4:03	586	561
8/1/2010	4:13	585	560			8/1/2010	4:13	585	560
8/1/2010	4:23	585	560			8/1/2010	4:23	585	560
8/1/2010	4:33	585	560			8/1/2010	4:33	585	560
8/1/2010	4:43	585	560			8/1/2010	4:43	585	560
8/1/2010	4:53	585	561			8/1/2010	4:53	585	561
8/1/2010	5:03	586	561			8/1/2010	5:03	586	561

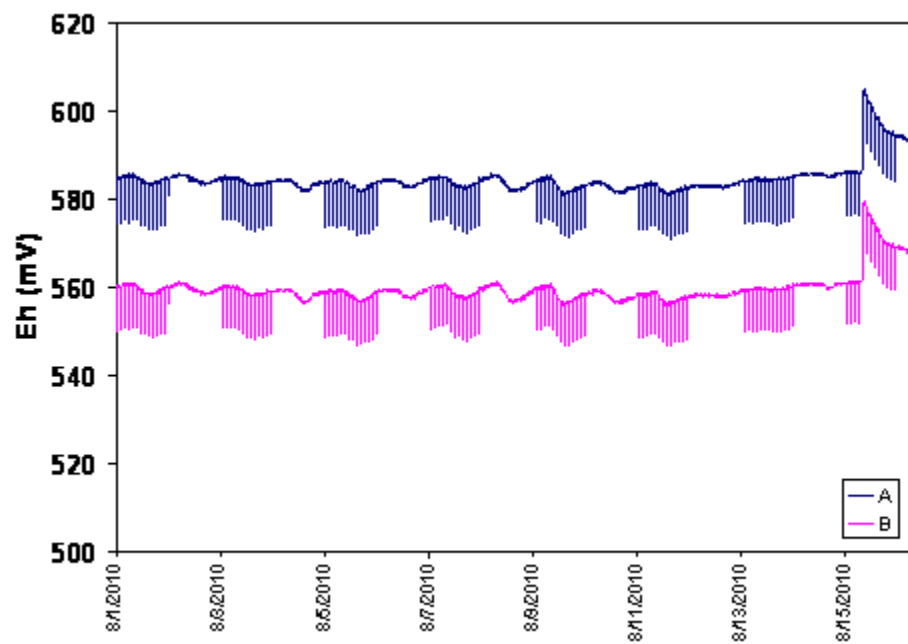


Figure 6a: Prior to removal of data points.

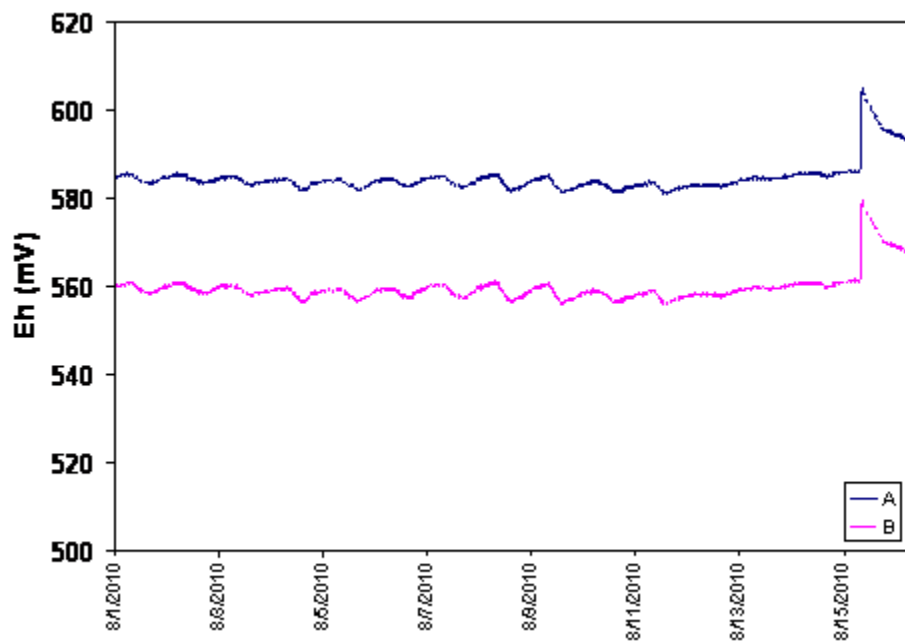


Figure 6b: Post removal of data points.

2. If data were noisy, the data were filtered using a 3-hr moving average.

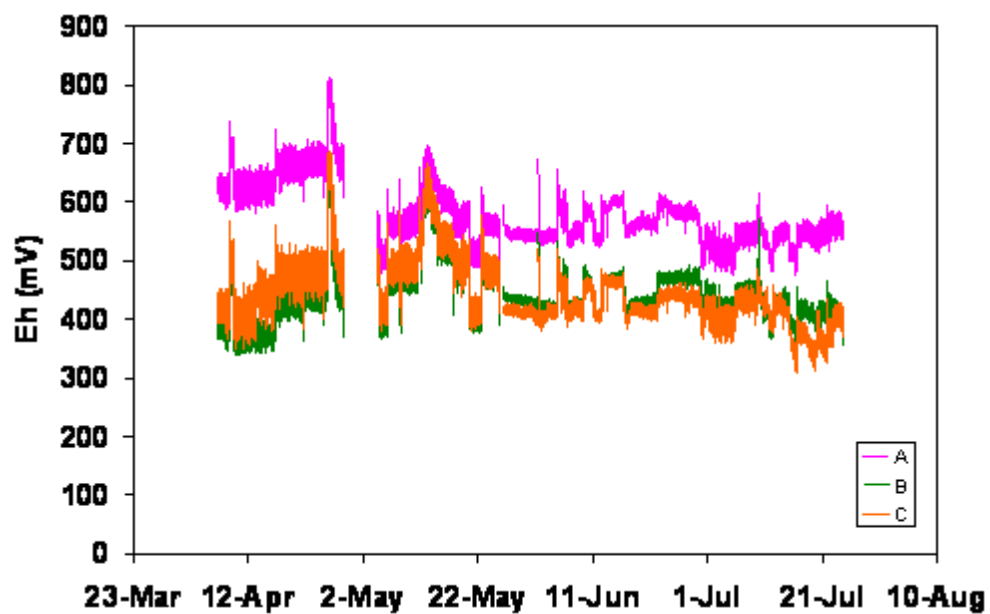


Figure 7a: Prior to moving average.

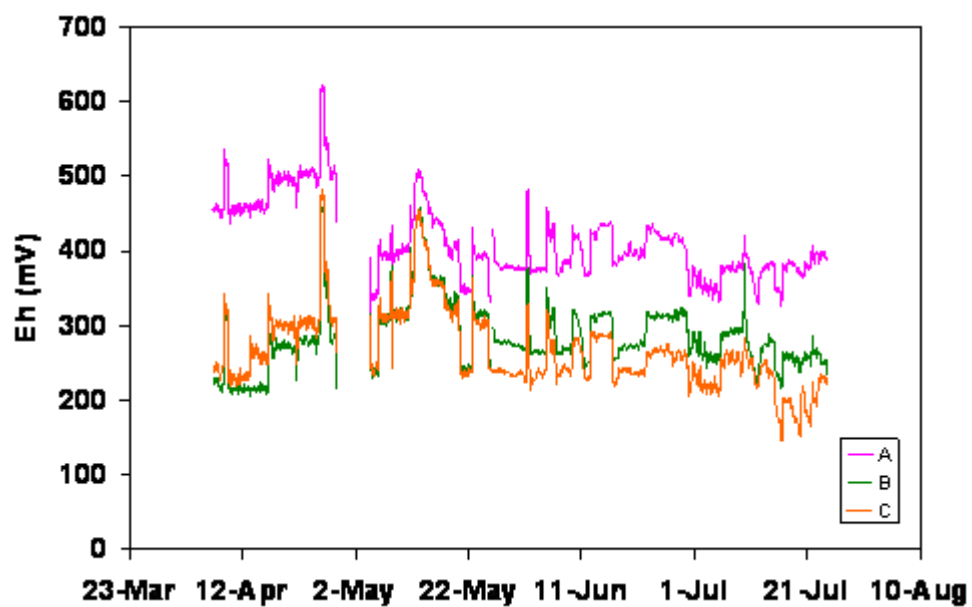


Figure 7b: Post 3-hr moving average.

3. Other errors in data included equipment malfunction. These data points were removed.

Date	Time	A	B	C
8/1/2010	0:03	625	599	478
8/1/2010	0:13	606	609	442
8/1/2010	0:23	627	620	440
8/1/2010	0:33	613	596	472
8/1/2010	0:43	631	627	451
8/1/2010	0:53	597	581	445
8/1/2010	1:03	628	584	430
8/1/2010	1:13	612	585	430
8/1/2010	1:23	643	-6999	475
8/1/2010	1:33	651	-6999	465
8/1/2010	1:43	612	-6999	467
8/1/2010	1:53	598	-6999	444
8/1/2010	2:03	616	-6999	465
8/1/2010	2:13	607	-6999	440
8/1/2010	2:23	599	-6999	440
8/1/2010	2:33	656	-6999	459
8/1/2010	2:43	615	-6999	471
8/1/2010	2:53	640	-6999	433
8/1/2010	3:03	658	-6999	459
8/1/2010	3:13	624	-6999	445
8/1/2010	3:23	622	-6999	450
8/1/2010	3:33	625	-6999	442
8/1/2010	3:43	606	-6999	437
8/1/2010	3:53	633	-6999	461
8/1/2010	4:03	641	-6999	434
8/1/2010	4:13	625	-6999	459
8/1/2010	4:23	600	-6999	436
8/1/2010	4:33	600	581	436
8/1/2010	4:43	605	584	426
8/1/2010	4:53	628	583	421
8/1/2010	5:03	629	565	459

References

- Niedermeier, A. and J. S. Robinson. 2007. Hydrological controls on soil redox dynamics in a peat-based, restored wetland. *Geoderma* 137: 318–326.
- Qualls, R. G., C. J. Richardson, and L. J. Sherwood. 2001. Soil reduction-oxidation potential along a nutrient-enrichment gradient in the everglades. *Wetlands* 21 (3): 403-411.

Veprakas, M. J. 2002. Redox potential measurements (online). Available at

<http://www.soil.ncsu.edu/wetlands/wetlandsoils/RedoxWriteup.pdf>.

Wafer, C. C., J. Barrett Richards, and D. L. Osmond. 2004. Construction of Platinum

Tipped Redox Probes for Determining Soil Redox Potential. *Journal of*

Environmental Quality 33: 2375–2379.

VITA
Danielle M. Andrews

Education:

Ph.D., Soil Science, *The Pennsylvania State University*
M.S., Plant & Soil Science, *University of Kentucky* Summer 2006
B. S., Biology; Chemistry & Env. Sci. minors, Summa cum laude
South Carolina State University Fall 2004

Publications:

1. **D. M. Andrews**, H. Lin, Q. Zhu, L. Jin, and S. L. Brantley. Dissolved organic carbon export and soil carbon storage in the Shale Hills Critical Zone Observatory. *Vadose Zone Journal* (*In review*)
2. Jin, L., **D. M. Andrews**, G. H. Holmes, C. J. Duffy, H. Lin and S. L. Brantley. Water chemistry reflects hydrological controls on weathering in Susquehanna/Shale Hills Critical Zone Observatory (Pennsylvania, USA). *Vadose Zone Journal* (*In review*)
3. **D. M. Andrews**, C. D. Barton, R. K. Kolka, C. C. Rhoades and A. J. Dattilo. 2011. Soil and water characteristics in restored canebrake and forest riparian zones. *Journal of American Water Resources Association* (*In Press*)
4. **D. M. Andrews**, C. D. Barton, S. J. Czapka, and R. K. Kolka. 2010. Influence of tree shelters on seedling success in an afforested riparian zone. *New Forests* 39:157–167
5. C. D. Barton, **D. M. Andrews**, and R. K. Kolka. 2008. Influence of soil physicochemical properties on hydrology and restoration response in Carolina Bay wetlands. *Restoration Ecology* 16 (4): 668–677

Awards:

Soil Science Society of America 2010
Best Paper Award, Forest, Range and Wildland Division

The Pennsylvania State University 2008, 2009, 2010
College of Agricultural Sciences & Dept. of Crop & Soil Sciences Travel Grants

The Pennsylvania State University 2006-2007
Alex and Jesse Black & Robert W. Graham Endowed Graduate Fellowship

University of Kentucky 2004-2006
Research Assistant Fellowship

South Carolina State University 2000-2004
Presidential Scholarship, Gold Medallion Recipient